DE-AC22-91PC91042-F2

PENNSTATE

EFFECTS OF LOW-TEMPERATURE CATALYTIC PRETREATMENTS ON COAL STRUCTURE AND REACTIVITY IN LIQUEFACTION

Final Technical Report - Vol. 2

(Approved by DOE in January 1998)

Vol. 2: Hydrogenative and Hydrothermal Pretreatments and Spectroscopic Characterization Using Pyrolysis-GC-MS, CPMAS ^{13}C NMR and FT-IR

Chunshan Song, Patrick G. Hatcher, Ajay K. Saini, and Kurt A. Wenzel

Fuel Science Program
Department of Materials Science and Engineering
The Pennsylvania State University
University Park, Pennsylvania, PA 16802

January 1998

Prepared for the U.S. Department of Energy
under Contract No.
DE-AC22-91PC91042

DE-AC22-91PC91042-F2

EFFECTS OF LOW-TEMPERATURE CATALYTIC PRETREATMENTS ON COAL STRUCTURE AND REACTIVITY IN LIQUEFACTION

Final Technical Report - Vol. 2

(Approved by DOE in January 1998)

Vol. 2: Hydrogenative and Hydrothermal Pretreatments and Spectroscopic Characterization Using Pyrolysis-GC-MS, CPMAS ^{13}C NMR and FT-IR

Chunshan Song, Patrick G. Hatcher, Ajay K. Saini, and Kurt A. Wenzel

Fuel Science Program
Department of Materials Science and Engineering
The Pennsylvania State University
University Park, Pennsylvania, PA 16802

January 1998

Prepared for the U.S. Department of Energy
under Contract No.
DE-AC22-91PC91042

DISCLAIMER

ACKNOWLEDGEMENTS

This project was supported by the U.S. Department of Energy, Pittsburgh Energy Technology Center, in Advanced Coal Research Program. Dr. M.A. Nowak is DOE/PETC Project Manager; Dr. M. J. Baird was the project manager during the first three quarterly periods. Dr. H.H. Schobert, Dr. C. Song and Dr. P.G. Hatcher are the Co-Principal Investigators at The Pennsylvania State University.

The principal investigators and the authors wish to express their appreciation to U.S. DOE for financial support, to Drs. M.A. Nowak, M. J. Baird, S. Lee, and E. B. Klunder of DOE/PETC for their support and helpful discussion. The authors would also like to thank Dr. A. Davis and Mr. D. Glick of PSU for providing coal samples and data from DOE/Penn State Coal Sample Bank, Mr. J. McConnie for assistance in some liquefaction experiments, Dr. L. Hou for assistance in solid-state NMR analysis, and Mr. R.M. Copenhaver for the fabrication of tubing bomb reactors.

Table of Contents

ABSTRACT

It has been indicated by DOE COLIRN panel that low-temperature catalytic pretreatment is a promising approach to the development of an improved liquefaction process. This work is a fundamental study on effects of pretreatments on coal structure and reactivity in liquefaction. The main objectives of this project are to study the coal structural changes induced by low-temperature catalytic and thermal pretreatments by using spectroscopic techniques; and to clarify the pretreatment-induced changes in reactivity or convertibility of coals.

As the second volume of the final report, here we summarize our work on spectroscopic characterization of four raw coals including two subbituminous coals and two bituminous coals, tetrahydrofuran (THF)-extracted but unreacted coals, the coals (THF-insoluble parts) that have been thermally pretreated in the absence of any solvents and in the presence of either a hydrogen-donor solvent or a non-donor solvent, and the coals (THF-insoluble parts) that have been catalytically pretreated in the presence of a dispersed Mo sulfide catalyst in the absence of any solvents and in the presence of either a hydrogen-donor solvent or a non-donor solvent.

The thermal and catalytic retreatments at or below 300°C have little impact on coal conversion into liquids or THF-soluble materials. At 325°C, catalytic pretreatment using impregnated ammonium tetrathiomolybdate (ATTM) begins to affect coal conversion. At 350°C, catalytic pretreatment can afford substantially increased coal conversion into THF-solubles as compared to the non-catalytic pretreatment. The use of water in the pretreatment (either hydrogenative hydrothermal run under H_2, or hydrous pyrolysis), also has a major impact on coal conversion. Catalytic hydrothermal pretreatment in the presence of H_2 can have dramatic improvement on coal conversion at low temperatures, such as 325-375°C.

We have applied a series of modern analytical techniques to characterize the thermally and catalytically pretreated coals as well as THF-extracted raw coals using cross-polarization magic angle spinning (CPMAS) solid-state ^{13}C NMR, pyrolysis-GC-MS, FT-IR, and dipolar-dephasing magic angle spinning (DDMAS) solid-state ^{13}C NMR.

The analytical results indicate that low-temperature pretreatment does induce subtle structural changes. The combination of the spectroscopic analyses and the conversion data indicated that the catalytic pretreatment at 350°C not only improves coal conversion, but also induces structural changes in the unconverted organic materials, such as a decrease in the content of catechol groups (Py-GC-MS and CPMAS NMR), reduction in ether linkages (FT-IR), and increase in the content of aliphatic groups (FT-IR) such as those in the hydroaromatic unit (DDMAS and CPMAS NMR). Such structural changes are desirable because they could improve the subsequent liquefaction at higher temperatures.

SUMMARY OF MAJOR FINDINGS

This work is a fundamental study on effects of pretreatments on coal structure and reactivity in liquefaction. The main objectives of this project are to study the coal structural changes induced by low-temperature catalytic and thermal pretreatments by using spectroscopic techniques; and to clarify the pretreatment-induced changes in convertibility of coals, as measured by conversion into THF-soluble materials and yields of products.

This report is the second volume of the final technical report on this project. This report deals with thermal and catalytic hydrogenative and hydrothermal pretreatments under different conditions, and spectroscopic characterization of coal structural changes using various modern analytical techniques. In volume 1, we have reported in detail the effects of solvents, catalysts, and temperature program on conversion and structural changes of two lignites and one subbituminous coal. Here in volume 2, we summarize our work on various hydrogenative and hydrothermal pretreatments and spectroscopic characterization of two subbituminous coals, one lignite, and two bituminous coals using pyrolysis-GC-MS, CPMAS ^{13}C NMR and FT-IR.

Chapter 1 discusses the low-temperature pretreatment, with emphasis on the effect of pre-drying and oxidation on the thermal and catalytic pretreatment (low-severity liquefaction) of DECS-8 Wyodak coal at 350°C and liquefaction 425°C. Drying and oxidation of Wyodak subbituminous coal at 100-150°C have been shown to have significant effects on its structure and on its catalytic and non-catalytic low-severity liquefaction (pretreatment) at 350 °C for 30 min under 6.9 MPa H_2. Spectroscopic analyses using solid-state ^{13}C NMR, pyrolysis-GC-MS, and FT-IR revealed that oxidative drying at 100-150°C causes the transformation of phenolics and catechol into other related structures (presumably via condensation) and high-severity air drying at 150°C for 20 h leads to disappearance of catechol-like structures. Increasing air drying time or temperature increases oxidation to form more oxygen functional groups at the expense of aliphatic carbons. For non-catalytic liquefaction at 350°C, raw coal gave higher conversion and oil yield than the dried coals, regardless of the solvent. Compared to the vacuum-dried coal, the coal dried in air at 100 °C gave a better conversion in the presence of either a hydrogen-donor tetralin or a non-donor 1-methylnaphthalene (1-MN) solvent.

Catalytic runs were performed using impregnated ammonium tetrathiomolybdate (ATTM) precursor. In the presence of either tetralin or 1-MN, however, the runs using ATTM

impregnated on air-dried coal (dried at 100°C for 2h) afford better conversions and oil yields than using vacuum-dried coal. Upon drying in air at 150 °C for 20 h, the conversion of air-dried coal decreased to a value significantly lower than that of the vacuum-dried coal both in the thermal and catalytic runs at 350°C. Such a clearly negative impact of severe oxidation is considered to arise from significantly increased oxygen functionality, which enhances the cross-link formation in the early stage of coal liquefaction. Physical, chemical, and surface physicochemical aspects of drying and oxidation and the role of water are also discussed.

We also examined the effects of pre-drying and oxidation of DECS-8 Wyodak coal on its catalytic and non-catalytic liquefaction using 25-mL batch reactors at 425°C for 30 min under an initial (cold) H_2 pressure of 6.9 MPa in the presence of H-donor tetralin solvent. For non-catalytic liquefaction at 425°C in the presence of tetralin solvent, our results indicate that pre-drying has positive effects on the non-catalytic liquefaction of Wyodak coal, and vacuum-drying is better than air-drying in terms of higher coversion and oil yield. Unlike the non-catalytic runs, the catalytic runs at 425°C using ATTM impregnated on the raw and pre-dried coals afforded similar conversions and oil yields. The coal conversion in all the catalytic runs approached 90 wt%. The difference in the physico-chemical properties of the coal samples (prior to ATTM impregnation) caused by pre-drying and oxidation was largely compensated by the catalyst, and to a lesser degree, by H-donor solvent. Therefore, if ATTM is to be impregnated onto Wyodak subbituminous coal from its aqueous solution, whether the coal has been pre-dried or mildly oxidized (weathered) makes no major difference on conversion at 425°C. However, this conclusion does not apply to the catalytic liquefaction using oil-soluble Mo catalyst precursor.

Some interesting observations made during the above-mentioned study on drying effects promoted us to examine the effects of water removal and addition in catalytic pretreatment. Chapter 2 reports on the strong promoting effect of water on catalytic preatment (low-severity catalytic liquefaction). We have observed a strong synergistic effect between added water and a dispersed molybdenum sulfide catalyst for promoting low-severity liquefaction of Wyodak subbituminous coal (DECS-8). Briefly, we found that addition of H_2O to the catalytic run (water/coal = 0.46 wt ratio) can double the coal conversion at 350°C for 30 min under 6.9 MPa H_2, from 29-30 to 66-67 wt% (dmmf). This finding may offer new opportunities for developing novel low-severity liquefaction processes. Such a synergistic effect may be incorporated into liquefaction process either in the pretreatment step or in the first-stage of a two- or multi-stage liquefaction process.

We also used organic solvents including a H-donor and a non-donor. In general, if no water was added, using H-donor affords better coal conversion than non-donor solvent. However, for runs with both water and dispersed Mo catalyst at 350°C, using organic solvents does not offer any advantages in terms of coal conversion. We have also observed the same trends in several sets of experiments using fresh raw DECS-8 coal sample, vacuum-dried coals, as well as air-dried coals. We have analyzed the oils using two-dimensional HPLC with photodiode array detector. The oils from liquefaction with added water contain more phenolic compounds. This suggests that water participates in the reaction leading to phenols.

Chapter 3 is concerned with the effect of thermal pretreatment in H-donor solvent. This Chapter discusses the temperature-programmed liquefaction (TPL) of two low-rank coals in the absence of any catalysts. The TPL was conducted with two objectives. The first is to see if there are any beneficial effects of low-temperature thermal pretreatments. The second is to prepare the relatively well-defined samples from different reactions for subsequent spectroscopic characterization (Chapter 4). Due to the presence of various C-O and C-C bonds in coals, there may be a broad distribution of dissociation energies of bonds connecting the structural units in coals. The temperature-programmed liquefaction (TPL) aims at efficient conversion of low-rank coals by controlling the rate of pyrolytic cleavage of weak bonds and minimizing the retrogressive crosslinking of radicals and thermally sensitive groups.

In the presence of a H-donor tetralin solvent, TPL runs of a Montana subbituminous coal and a Texas lignite using programmed heat-up to 350-425°C afforded considerably higher conversions than the conventional runs under rapid heat-up conditions. Temperature-programming in a non-donor solvent such as naphthalene or 1-methylnaphthalene does not appear to have any significant impact on coal conversion and product distribution. This indicates that beneficial effects of TPL for conversion of low-rank coals in tetralin solvent are probably associated with low-temperature hydrogen transfer during programmed heat-up.

Chapter 4 describes the spectroscopic characterization of the residue samples from temperature-programmed liquefaction (TPL, Chapter 3). Important information on structure and structural transformation during thermal pretreatment and liquefaction reactions of low-rank coals has been derived by applying solid-state CPMAS ^{13}C NMR and flash pyrolysis-GC-MS (Py-GC-MS) for characterization of the macromolecular network of a Montana subbituminous coal and its residues from temperature-programmed and non-programmed liquefaction (TPL and N-PL) at final temperatures ranging from 300 to 425°C in H-donor and non-donor solvents. The results revealed that this coal contains significant quantities of oxygen-bearing structures,

corresponding to about 18 O-bound C per 100 C atoms and one O-bound C per every 5 to 6 aromatic C. The oxygen-bearing components in the coal include catechol-like structures, which seem to disappear from the liquefaction residues above 300°C; carboxyl groups, which almost disappear after 350°C; and phenolic structures, which are most important in the original coal but diminish in concentration with increasing temperature.

These results point to the progressive loss of oxygen functional groups and aliphatic-rich species from the macromolecular network of the coal during programmed heat-up under TPL conditions. The higher conversions in TPL runs in H-donor tetralin (relative to the conventional N-PL runs) suggest that the removal of carboxylic and catechol groups from the coal and the capping of the reactive sites by H-transfer from H-donors during low temperature ($\leq$ 350°C) pretreatments have contributed to minimizing the retrogressive crosslinking at higher temperatures.

Quantitative calculation of NMR data and mathematical correlation were also attempted in this work. For 24 liquefaction residues derived under significantly different conditions, linear correlations between C-distribution and reaction temperature ($\geq$300°C) have been found, which can be expressed by a simple equation, $C_i = \alpha\ f_i + \beta\ T$, where f_i and C_i represent content of aromatic, aliphatic, or oxygen-bound carbons in the original coal and residue, respectively; T stands for the reaction temperature; α and β are constants.

Chapter 5 reports on the chemical transformations of low-rank vitrinite under hydrous pyrolysis conditions, which provided a clue to reactions occurring during pretreatments and liquefaction of low-rank coals in the presence of water. During pretreatments of low-rank coals, water is released from the coal either as tightly bound water or from dehydration/condensation reactions. It is likely that the presence of water has a profound effect on coal at the low temperatures, releasing various hydrocarbons and indicating that chemical degradation of the macromolecular network is occurring. To investigate the effect water has on the chemical structure of coal during pretreatment conditions, we conducted a series of hydrous pyrolysis experiments on a low-rank coal. We selected a sample of pure vitrinite, a piece of coalified wood of lignite rank from Potapsco Formation, because this sample represented a pure maceral which had been previously characterized extensively and because the sample was composed primarily of catechol-like structures which are probably involved in retrogressive reactions during liquefaction due to their reactivity. This sample was heated in tubing bomb reactors in the presence of added water for varying lengths of time at temperatures varying to 300°C. Liquid products were examined by GC-MS and the solid residues were examined by solid-state ^{13}C NMR, elemental

analysis, and flash pyrolysis-GC-MS.

The results show convincingly that the structure of the vitrinite is altered significantly by the low-severity treatment. Perhaps the most significant change observed is the transformation of catechol-like structures to structures based on monohydric phenols. Another change of importance is the cleavage of three-carbon side-chain structures, derived in the original coal from the lignin side-chain. While cleavage of the three-carbon side-chain, probably between the α and β carbons, is is thermodynamically feasible as a pyrolytic process, it is difficult to propose a similar pyrolytic process for dehydroxylation of catechols. More likely, the process is probably a combined dehydration/pyrolysis process. We propose that catechol-like structures in the vitrinite undergo dehydration to diphenyl ethers. Because these ethers are thermally unstable due to the phenolic OH ortho to the ether linked aromatic carbon, there is sufficient energy to induce pyrolytic cleavage of the ether. Consequently, monohydric and dihydric phenolic structures are formed. The dihydric phenol, catechol, can be dehydrated again with another catechol and the reaction proceeds until all the catechols are converted to phenols. In this fashion we can effectively transform the catechols to phenols and explain the observed trends in our residues.

Chapter 6 describes the spectroscopic characterization of the residues of two subbituminous coals from their liquefaction at 300-425°C, using cross-polarization magic-angle-spinning (CPMAS) and dipolar dephasing (DD) solid-state ^{13}C NMR techniques. The DDMAS and CPMAS NMR analysis of a Montana subbituminous coal (DECS-9) indicate that it has 63-64% aromatic carbons among total carbons; 34-35% of the aromatic carbons are protonated carbons, and 23-24% of the aromatic carbons are oxygen-bound carbons, with the remaining 31-33% bound primarily to other carbon atoms. CPMAS ^{13}C NMR spectrum of Wyodak subbituminous coal (DECS-8) is similar to that of Montana subbituminous coal (DECS-9). CPMAS ^{13}C NMR of the residues from DECS-9 coal revealed that catechol-like structures and phenolic structures in the coal are thermally sensitive and diminish gradually with increasing temperature. The carbon aromaticity increased monotonically with increasing reaction temperature, whereas hydrogen aromaticity reached a maximum for residue from a 300°C run and then declines with further increase in temperature. The increase in carbon aromaticity is mainly driven by temperature, rather than by the adduction of aromatic solvents. DDMAS NMR analysis indicates that the degree of protonation of aromatic carbons decreased from 35% (for THF-extracted but unreacted DECS-9 coal) to 13% (for residue from a non-catalytic run) with increasing reaction temperature up to 375°C.

DDMAS ^{13}C NMR of the residues from DECS-8 Wyodak coal revealed that the degree of protonation of aromatic carbons (f_a^{aH}) is lower with the residues from catalytic pretreatment (low-severity liquefaction) at 350°C. These results were surprising, as f_a^{aH} values usually decrease with increasing degree of condensation. However, if this is the case, this decrease should be accompanied by the increase in f_a values. It is possible that, relative to the residues from non-catalytic runs, the lower f_a^{aH} values for residues from catalytic runs were due to hydrogenation of the aromatic rings to form hydroaromatic rings.

Chapter 7 describes the spectroscopic characterization of two bituminous coals and one subbituminous coal by TGA and Py-GC-MS. Thermogravimetric analysis (TGA) of three bituminous coals has revealed the differences in their devolatilization behavior. Py-GC-MS of these coals at different pyrolysis temperatures, ranging from 310 to 610°C, and the Py-GC-MS of thermally pretreated samples (flash pyrolysis at 610°C) provided some new information on their structures and structural transformations. The runs at 310°C showed there was no pyrolytic reactions at this temperature, and Py-GC-MS at 310°C can be viewed as thermal desorption-GC-MS. Major pyrolysis products were detected when pyrolysis temperature was increased to 610°C, where phenols, alkylbenzenes, naphthalenes, and straight and branched alkanes are the main products. However, the products distribution pattern depends on the coal type.

Chapter 8 discusses the liquefaction reactivity of two bituminous coals and one subbituminous coal and the spectroscopic characterization of the oils and residues from the liquefaction. The liquefaction behavior of three bituminous coals with carbon contents ranging from 77% to 85% was evaluated spectroscopically by ^{13}C NMR and pyrolysis/gas chromatograpy/mass spectrometry to delineate the structural changes that occur in the coal during liquefaction. Complementary data include ultimate and proximate analysis, along with optical microscopy for maceral determinations. Even though these are all bituminous coals they exhibit quite different physical and chemical characteristics. The coals vary in rank, ranging from HvC b to HvA b, in petrographic composition, different maceral percentages, and in chemical nature, percent of carbon and of volatiles. It is these variations that govern the products, their distribution, and conversion percentages. Some of the products formed can be traced to a specific maceral group.

Chapter 9 deals with catalytic and thermal low-temperature pretreatments at 300-375°C. Here we describe the spectroscopic characterization of fresh and THF-extracted samples of Wyodak subbituminous coal, its catalytic and thermal low-temperature pretreatments in the absence and presence of hydrogen-donor and non-donor solvents, and the spectroscopic

characterization of thermally and catalytically pretreated coals using cross-polarization magic angle spinning (CPMAS) solid-state ^{13}C NMR, pyrolysis-GC-MS and FT-IR techniques. Characterization of the raw coal revealed that Wyodak coal is rich in oxygen-containing compounds such as phenol and catechol-type compounds. The reactions at 300°C caused little increase in coal conversion, but pyrolysis-GC-MS indicated that pretreatments at 300°C induce some structural changes, particularly in catechol structures, which are not easily detectable by CPMAS ^{13}C NMR and FT-IR. The results of low-temperature pretreatments showed that both dispersed catalyst and solvent affect the coal conversion and product quality at 350°C. The runs at 375°C gave further higher conversion compared to the runs at 350°C.

The combination of the spectroscopic analyses and the conversion data indicated that the catalytic pretreatment at 350°C not only improves coal conversion, but also induces structural changes in the unconverted organic materials, such as decrease in the content of catechol groups (Py-GC-MS and CPMAS NMR), reduction in ether linkages (FT-IR), and increase in the content of aliphatic groups (FT-IR) such as those in the hydroaromatic unit (DDMAS and CPMAS NMR).

CHAPTER 1. Effects of Pre-Drying and Oxidation of Wyodak Subbituminous Coal on Its Thermal and Catalytic Pretreatments (Low-Severity Liquefaction). Spectroscopic Studies of Coal Structural Changes and Products Distribution

Introduction

Low-rank coals, including subbituminous coals and lignites, are characterized by low aromaticities, high oxygen functionalities, and high moisture contents.[1] Because many low-rank coals contain as high as 20-35 wt % of moisture, an extensive amount of fundamental research has been done to develop an understanding of the occurrence of moisture in low-rank coals and their drying behavior.[2-16] Moisture in the coal has been classified[16] into four major forms: 1) superficial free water, 2) capillary condensed water, 3) sorbed water associated with polar groups and cations, and 4) water released only by chemical decomposition of organic or inorganic matter. Wroblewski and Verkade[16] have shown that the differentiation of surface water from pore water is possible by using some reagents in combination with ^{31}P NMR technique. Several methods, including thermal drying under vacuum and in air, microwave drying, chemical drying, or drying under a stream of dry inert gases, have been used and their impacts on coal structure have been studied.[13-21] It has been well established that low-rank coal has a colloidal gel-like structure that can shrink and swell in response to moisture loss and gain.[2,18,19] Suuberg et al.[18] pointed out that water is retained tightly in coal in several forms; coal behaves like a swellable colloid in the presence of water. A drying process, with minimal effect on the reactivity of a coal, is the ultimate goal of several coal conversion studies.[14,19-22] The changes caused by drying could be physical, chemical, or both, depending upon the drying method applied. Vorres et al. studied[13,14] the drying kinetics of Beulah-Zap lignite in detail. They have found that the lignite dehydration follows a unimolecular rate law which is first order in the water in the sample; there are two segments in the dehydration kinetics: the first includes about 80-85% of the water loss and the second covers most of the remaining water. Recently, Vorres[15] also reported that the behavior of a Wyodak subbituminous coal on drying is very similar to that of the Beulah-Zap lignite; there is a transition after about 80 % of moisture loss to a slower unimolecular process.

For thermal liquefaction (i.e., reaction without added catalyst), several groups have examined the effects of drying or oxidation on coal conversion.[14,17,19-22] Some experiences have shown that drying of coal has negative impact on its conversion reactivity,[19-22] while there is also evidence to the contrary in non-catalytic liquefaction.[14] It has been indicated that drying

can cause an irreversible change in the pore structure such as collapse of pores,[13] which could limit accessibility of the reacting components during liquefaction and thus limit the rate of reaction. Oxidative drying of coal has been reported to have very detrimental effect on the coal conversion.[19-22] Atherton[20] pointed out that commercial coal-drying techniques (i.e., thermal) make low-rank coals prone to self-heating and cause a decline in reactivity for subsequent conversion. Neavel[21] reported a significant reduction in the conversion (at 400°C) of a hvC bituminous coal into benzene-soluble products as a result of oxidation. Cronauer et al.[22] found that partial drying of subbituminous coal in a mixture of nitrogen and oxygen or even in nitrogen alone reduced the conversion (at 450°C for 4-30 min) as compared to that of the raw coal. Serio et al.[17] observed that drying has a negative impact on the liquefaction (at 400°C for 30 min) of a lignite and a subbituminous coal but has little impact on the run of a bituminous coal. On the other hand, Vorres et al.[14] recently reported that the oil yield in liquefaction (at 400°C for 4 h) of a lignite sample was highest for the dried sample, lowest for the partially dried and intermediate for the starting material.

For liquefaction of coal with dispersed catalysts, there is little published information about the effects of predrying and mild oxidation. We recognize that, when one considers the overall economics of a coal conversion complex, there may be reasons, other than conversion achieved in liquefaction reactors, to consider drying the coal. Examples of such reasons might be the reduction of coal transportation costs, improvement of process thermal efficiency, lowering of the pressure in the reactors by eliminating the contribution from the partial pressure of water vapor, or reducing the amount of waste water generated. In addition to deliberate drying of the coal carried out as part of a process, some inadvertent drying may occur during storage or transportation. For example, drying and oxidation may occur simultaneously during natural weathering and during transportation. Therefore, it is important to study the effects of predrying and oxidation on catalytic liquefaction process. Fundamental understanding from such studies would provide answer to the question as to how should coals be handled or prepared for a given catalytic liquefaction process.

In the present study we examined the effects of drying of Wyodak subbituminous coal in vacuum (non-oxidative drying) and in air (mild oxidation) on its structure, and thermal (non-catalytic) and catalytic liquefaction. In order to follow the changes in chemical structure and moisture removal caused by drying and oxidation, we used several modern instrumental techniques to characterize the dried coals as well as the raw coal. To monitor the reactivity changes, we used low-severity liquefaction conditions such as 350 °C for 30 min. To detect the difference in physical changes (affecting diffusion) induced by drying under different conditions, we performed the reactions both in the absence of any solvent and in the presence of either a hydrogen donor tetralin or a non-donor 1-methylnaphthalene (1-MN) solvent. We also carried

out both catalytic and non-catalytic liquefaction of DECS-8 Wyodak coal in the 25-mL batch reactors at 425°C for 30 min under an initial (cold) H_2 pressure of 6.9 MPa in the presence of H-donor tetralin solvent.

This Chapter will describe the effects of drying and oxidation of Wyodak coal on 1) its chemical structural features, 2) products distribution in non-catalytic liquefaction, 3) catalytic liquefaction using in-situ generated dispersed molybdenum sulfide, and 4) structural characteristics of the liquefaction residues. Also presented in this report are the physical, chemical, and surface physicochemical considerations of drying and oxidation effects and the role of original moisture.

Experimental

Materials. The coal used was Wyodak subbituminous coal, which is one of the U.S. Department of Energy Coal Samples (DECS-8) in the DOE/Penn State Coal Sample Bank and Data Base. It was collected in June 1990, ground to ≤ 60 mesh (sieve opening: ≤ 250 μm), and stored under argon atmosphere in heat-sealed, argon-filled laminated foil bags consisting of three layers. This coal contains 32.4 % volatile matter, 29.3% fixed carbon, 9.9 % ash and 28.4 % moisture, on as-received basis; 75.8% C, 5.2% H, 1.0% N, 0.5% S and 17.5% O, on dmmf basis. Tetralin and 1-methylnaphthalene (1-MN) were used as hydrogen donor and non-donor reaction solvents, respectively. The solvents were obtained from Aldrich Chemical Company with 98 %+ purity and were used without any further treatment.

Drying Treatment. Both air drying (AD) and vacuum drying (VD) were conducted, in order to distinguish drying from oxidation. The non-oxidative drying was performed by placing a flask containing about 20 g of the coal into an oven which was then evacuated at room temperature (to minimize any possible oxidation due to the presence of air) and gradually heated up within one hour to 100 °C followed an isothermal holding for 2 h and subsequent cooling down in the vacuum oven. The air drying was done by placing a beaker containing about 20 g of the coal into a preheated oven maintained at 100 °C for 2-100 h or at 150 °C for 20 h, with the door partially open to the atmosphere. The temperatures of coal particles during vacuum drying and air drying were measured and found to be similar to each other (within the experimental error range, ±3°C). Fresh as-received coal, with minimum possible exposure to air, was used as the raw coal.

Catalyst Loading. Reagent grade ammonium tetrathiomolybdate (ATTM, from Aldrich Chemical Company with 99.97 % purity) was used as the precursor for the dispersed

molybdenum sulfide catalyst. ATTM [$(NH_4)_2MoS_4$] was dispersed onto the raw coal or dried coal samples by incipient wetness impregnation method from the aqueous solution. The same impregnation method was used in previous studies in this laboratory, but with different solvents.[23] The metal loading was kept at 1 wt % Mo on dmmf coal. Unless otherwise mentioned, the ATTM-impregnated coal was dried in a vacuum oven at 100 °C for 2 h before liquefaction.

Liquefaction and Product Work-up. The liquefaction experiments were carried out in 25 mL microautoclaves with 4 grams of coal at 350 °C (unless otherwise mentioned) for 30 minutes (plus 3 minutes for the reactor heat-up time to attain the reaction temperature). Some tests were conducted at 425°C. When a solvent was used, the ratio of solvent to coal was 1 to 1 by weight. The reactor was purged with H_2 at least three times, and finally pressurized with 6.9 MPa (cold) H_2. A fluidized sandbath was used as heater. After the reaction, the reactor was brought down to temperature below 200 °C by quickly immersing it in cold water and then letting it cool to room temperature in air. The total volume of the gaseous product was measured by the water displacement method and was collected for further analysis. The liquid and solid products were separated by sequential Soxhlet extraction with hexane to obtain oil; with toluene to obtain asphaltene; and with tetrahydrofuran (THF) to obtain preasphaltene.[24] Asphaltene and preasphaltene are solid at room temperature. They were dried at 100 °C for 6 h prior to weighing. Moisture content in the dried products is negligible. The THF-insoluble residues obtained after extraction were washed first with acetone and then with pentane in order to remove all the THF, followed by drying at 110 °C for 6 h under vacuum. The conversion of the coal into soluble products and gases was calculated on the basis of THF-insoluble residues. The water produced from liquefaction reactions would be included in the oil yield, which was determined by difference, as described elsewhere.[25] More experimental details may be found elsewhere.[24,25] All the liquefaction experiments were at least duplicated in order to obtain reliable data. The deviation in conversions and products yields are generally within ± 3 wt%.

The gas analysis was performed using a Perkin Elmer Auto-System gas chromatograph. The yields of CO and CO_2 were determined using a Carboxen-1000, 60/80 mesh column (1.7 mm x 4.5 m) with a thermal conductivity detector. C_1-C_4 hydrocarbon gases were determined using Chemipack C18 column (3.2 mm x 1.8 m) with flame ionization detector. Helium was used as a carrier gas for all the gas analysis. Hydrogen consumption from the gas-phase H_2 was calculated from the difference between the amount of hydrogen initially charged to the reactor and that found after reaction. The amount of H_2 gas left was determined by subtracting the volume of gaseous products [determined by GC using calibrated response factors (CO, CO_2, and hydrocarbon gases)] from the total volume. The dominant component of gases is CO_2, and the

experimental errors for CO_2 yields are usually within ± 0.5 wt% on a dmmf basis. Tetralin and naphthalene present in the spent solvent (mixed with the hexane-soluble fraction) were analyzed using a Hewlett Packard gas chromatograph equipped with Rtx-50 capillary column (0.25 mm i.d. x 30m). The net hydrogen consumption (transfer) from tetralin was calculated from the naphthalene to tetralin ratio after reaction.[24] The experimental errors are usually within ± 0.2 wt% (on a dmmf basis) for net hydrogen consumption from tetralin, and within ± 0.3 wt% for gas-phase H_2 consumption. Most results reported here are average of two or three runs.

Spectroscopic and Thermal Analyses. Thermogravimetric analysis (TGA) of the raw and dried coals and residues was conducted on Mettler TG50MT Analyzer. In a typical run, about 10 mg dried coal was loaded into alumina pan cell, and the furnace temperature was raised at 5 °C/min to 105°C followed by holding at 105°C under N_2 flow (200 mL/min).

Pyrolysis-gas chromatograph-mass spectrometric (Py-GC-MS) analysis of the samples was carried out using Du Pont 490B GC-MS system with DB-17 capillary column coated with phenylmethylpolysiloxane stationary phase. The instrument was interfaced to a Chemical Data Systems Pyroprobe-1000 pyrolyzer. In a typical run, about 0.5-1.0 mg of a sample was loaded into a thin quartz tube, which was then inserted into the horizontal filament coil in the pyroprobe. The pyroprobe was then inserted into an injection port interfaced with the capillary column. The samples were flash (with a heating rate of 5000 °C/s) pyrolyzed at 610 °C for 10 s and the pyrolyzates were cryotrapped at the injection-port end of the column with liquid nitrogen. The GC oven temperature was programmed from 30 °C to 280 °C at a heating rate of 4 °C/min. The data acquisition and processing were controlled by a computer-aided system.

Solid-state ^{13}C NMR spectra were recorded on a Chemagnetics M-100 NMR spectrometer using the cross-polarization magic angle spining (CPMAS) technique. The measurements were carried out at a carbon frequency of 25.1 MHz. For all the samples, 20,000 to 30,000 scans were accumulated, with cross-polarization contact time 1 μs and a pulse delay time 1 s. More details about Py-GC-MS and CPMAS ^{13}C NMR may be found elsewhere.[26]

Fourier transform infrared (FT-IR) spectra of coal and liquefaction residues were recorded on a Digilab FTS-60 spectrometer by co-adding at least 200 scans at a resolution of 2 cm^{-1}. The samples were prepared as KBr pellets. The KBr was dried at 110 °C for over 10 h in a vacuum oven prior to sample preparation. An accurately weighed amount of the predried coal or residue sample (2±0.01 mg) was mixed with a pre-weighed amount of KBr (250-300±0.01 mg) in a Perkin-Elmer Wig-L-Bug Grinder-Mixer for 120 seconds. All the spectra were baseline corrected. The FT-IR difference spectra (I_d) were obtained by subtracting the reference spectra (I_r) from the sample spectra (Is) using equation 1. The subtraction factors (S_f) were determined using equation 2, assuming a constant pellet diameter.

$$I_d = I_s - S_f \times I_r \quad (1)$$

$$S_f = (\text{dmmf organic matter of sample})/(\text{dmmf organic matter of reference}) \quad (2)$$

Results and Discussion

Characterization of Dried Samples. Figure 1.1 shows the TGA profiles for the air-dried and vacuum-dried coals, the ATTM-loaded and vacuum-dried coal as well as the raw DECS-8 coal. Because a slow heating rate (5 °C/min) and a nitrogen flow were used, most of the moisture loss (weight loss) occurred during heat up to 105°C in TGA cell, as can be seen from Figure 1. The amount of weight loss after 10 minutes holding at 105°C was taken as the moisture content. The moisture content value for the raw coal determined from TGA (29 wt%) is in good agreement with the value from the DECS sample bank (28.4 wt%). To get a reliable estimate of errors, we have performed duplicate TGA analyses, which give the following results in regard to moisture contents: 1-2 wt% for vacuum-dried samples; 2-3 wt% for air-dried samples; and 2-3 wt% for ATTM-impregnated and vacuum-dried samples. Relative to air drying, only slightly more water was removed by vacuum drying (Figure 1.1). Therefore, the moisture contents of all the dried samples are considered to be similar to each other.

Figure 1.2 presents the solid-state CPMAS ^{13}C NMR spectra of the coal samples predried under various conditions. In the spectrum of the raw coal, the region between 0 and 80 ppm consists of aliphatic carbons, which may include methoxy carbons, and the second region between 90 and 170 ppm is due to the aromatic carbons, including two shoulders due to catechol-like (at 142 ppm) and phenolic (at 152 ppm) carbons.[26] The carboxylic band appears between 170-190 ppm and carbonyl group between 190-230 ppm. Upon drying coal under vacuum, there is no apparent difference in the NMR spectrum as compared to that of the raw coal.

It appears that, as the coal is dried under oxidative conditions, there is a slight decrease in the intensity of the catechol shoulder, and after air drying at 150°C for 20 h, the catechol shoulder completely disappears from the NMR spectrum. The disappearance of catechol shoulder may be due to the oxidation of catechol type structures to ortho-quinones. The other changes include the broadening of the carboxyl and carbonyl bands. These changes become more apparent after air drying at 150 °C for 20 h, which are also accompanied by a significant decrease in relative intensity of the aliphatic band (Figure 1.2). On the other hand, any other structural changes that might occur under these conditions are too small to be detected by this NMR technique.

Figure 1.3 shows the FT-IR difference spectra of the dried coals obtained by subtracting the spectrum of vacuum-dried coal (100 °C for 2 h) from the spectra of the four air-dried coals. The difference spectra in Figure 1.3 are indicative of the structural changes caused by oxidation. Relative to the vacuum drying at 100°C for 2 h, the changes induced by air drying are the increased intensities in oxygen functional groups (bands in 1500-1800 and 3200-3600 cm^{-1}) and decrease in aliphatic groups (bands around 2920 and 2850 cm^{-1}). The positive band around 3200-3600 cm^{-1} may also includes -OH group in water. The bands around 1550, 1630 and 1700 cm^{-1} can be attributed to carboxylate ions ($Ar\text{-}COO^{-}M^{+}$), highly conjugated ketones (Ar-CO-Ar), and carboxylic acids (Ar-COOH) plus ketones, respectively.[27,28] The shoulder around 1770 cm^{-1} is due to esters. Figure 1.3 indicates that the extent of oxidation increased with increasing severity of air drying, as reflected by the progressive increase in carboxylic band (1700 cm^{-1}) and decrease in the aliphatic bands. As the air drying severity increased to 150°C for 20 h, the formation of etheric C-O becomes apparent, as shown by the small positive band in the 1100-1200 cm^{-1} region in Figure 1.3. It must be noted that this region is interfered by the peaks of minerals (1010, 1035, 1155 cm^{-1}).[29,30] Painter et al.[30] and Liotta et al.[31] also observed the formation of ethers from oxidation of bituminous coals from their FT-IR spectra.

Figure 1.4 presents the Py-GC-MS total ion chromatogram of the raw DECS-8 coal. In this chromatogram there are three major peaks due to phenolic compounds. Other peaks include those of alkylbenzenes, and paraffinic compounds ranging from C_4 to C_{30}, together with small amounts of two- to four-ring aromatic compounds. Also shown in Figure 1.2 are the area ratios of phenolics (phenol, C_1- to C_2-phenols, and catechols) to alkylbenzenes (C_1- to C_3-benzene) of the raw and predried coals, as determined from their Py-GC-MS analysis. This ratio decreased with increasing air drying time at 100°C, from 3.5 after 2 h to 2.3 after 100 h drying, and finally declined to 1.1 after air drying at 150 °C for 20 h. Interestingly, there is a marked catechol peak in the raw coal (Figure 1.4) and vacuum-dried coal, but this peak nearly disappears after air drying at 150°C, which is consistent with the CPMAS ^{13}C NMR data (Figure 1.2).

The information from the above instrumental analysis may be summarized as follows. Combination of FT-IR data (Figure 1.3) with NMR results (Figure 1.2) clearly indicates that the major changes in the coal structure due to oxidative drying are the increase in the carbonyl and carboxyl functionalities at the expense of the aliphatic groups in the coal. More of the increased oxygen functional groups would be expected to occur on the coal surface. Oxidation of aliphatic groups occurs preferrentially during air drying, presumably at the expense of alkyl side-chains attached to aromatic rings. Another interesting chemical effect revealed by NMR and Py-GC-MS is the disappearance of catechol after air drying at 150°C for 20 h. Furthermore, Py-GC-MS data in Figure 1.4 reveal that oxidative drying in air at 100-150°C tends to decrease the relative content of phenolic and catechol compounds in the pyrolyzates.

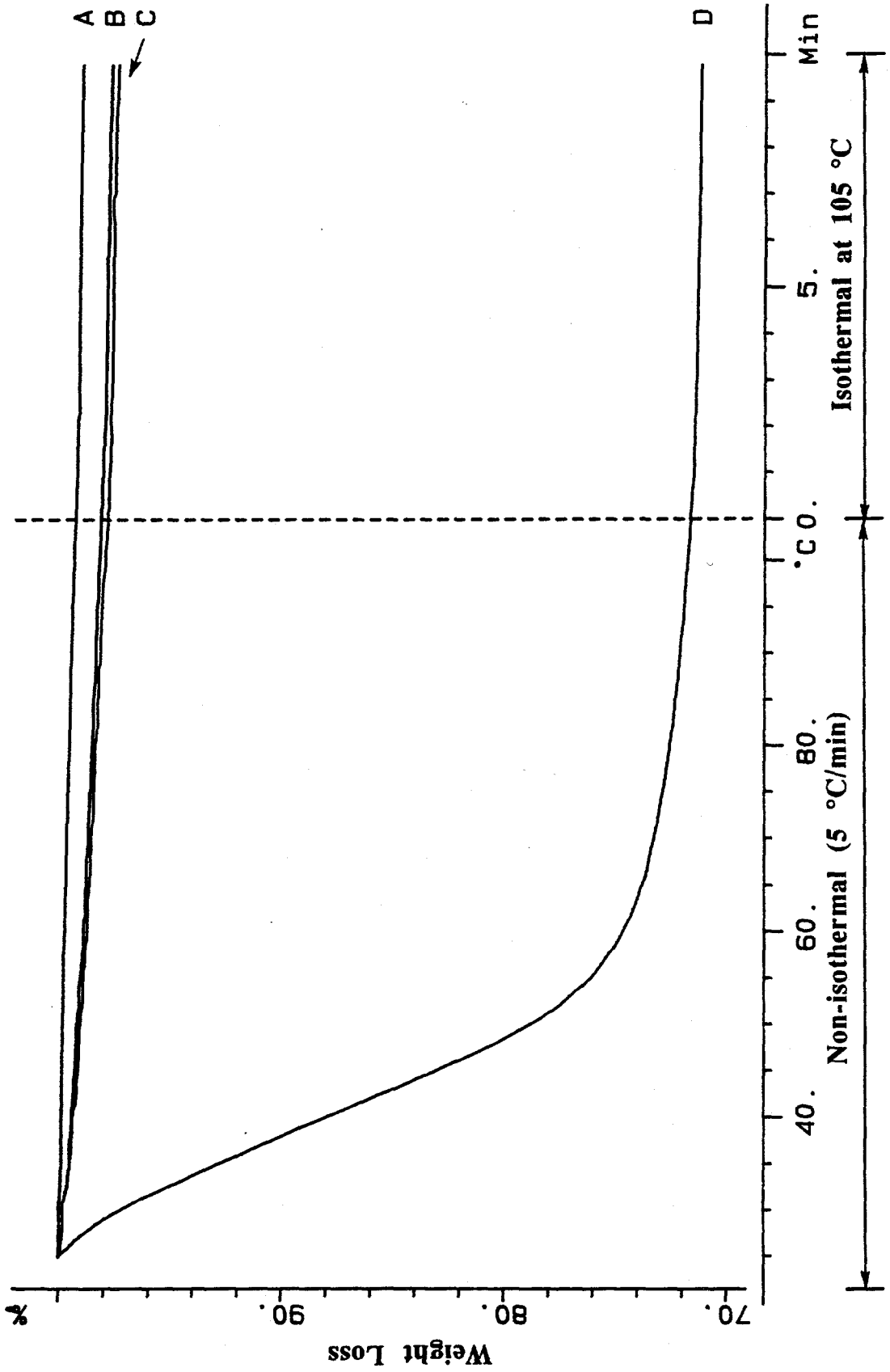

Figure 1.1 Weight loss of predried and raw Wyodak subbituminous coal (DECS-8) during TGA in N_2 flow. **A**: vacuum-dried at 100°C for 2 h; **B**: air-dried at 100°C for 2 h; **C**: raw coal impregnated with ATTM followed by vacuum drying at 100°C for 2 h; **D**: as-received raw coal.

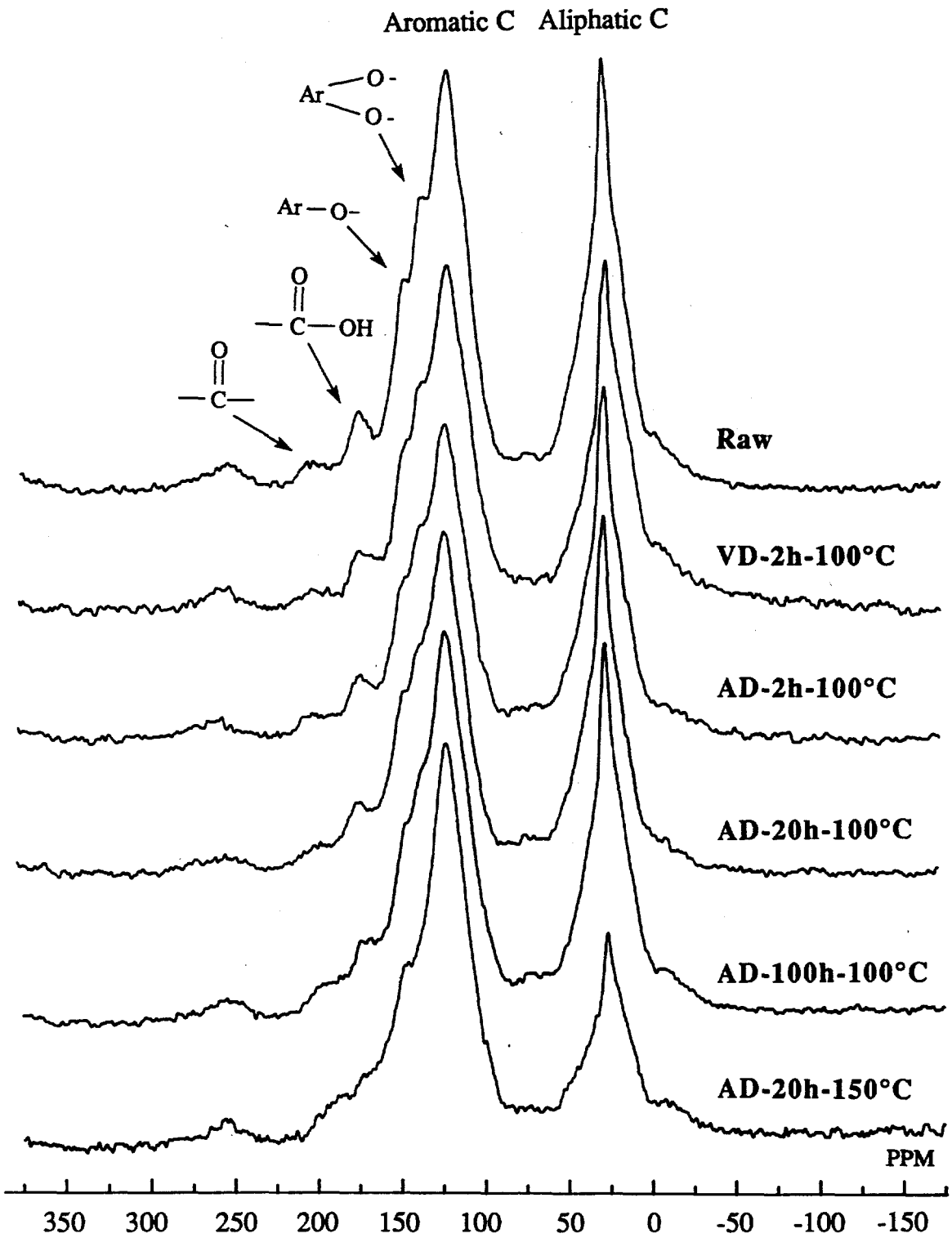

Figure 1.2 CPMAS solid-state ^{13}C NMR spectra of the DECS-8 coal samples predried under various conditions.

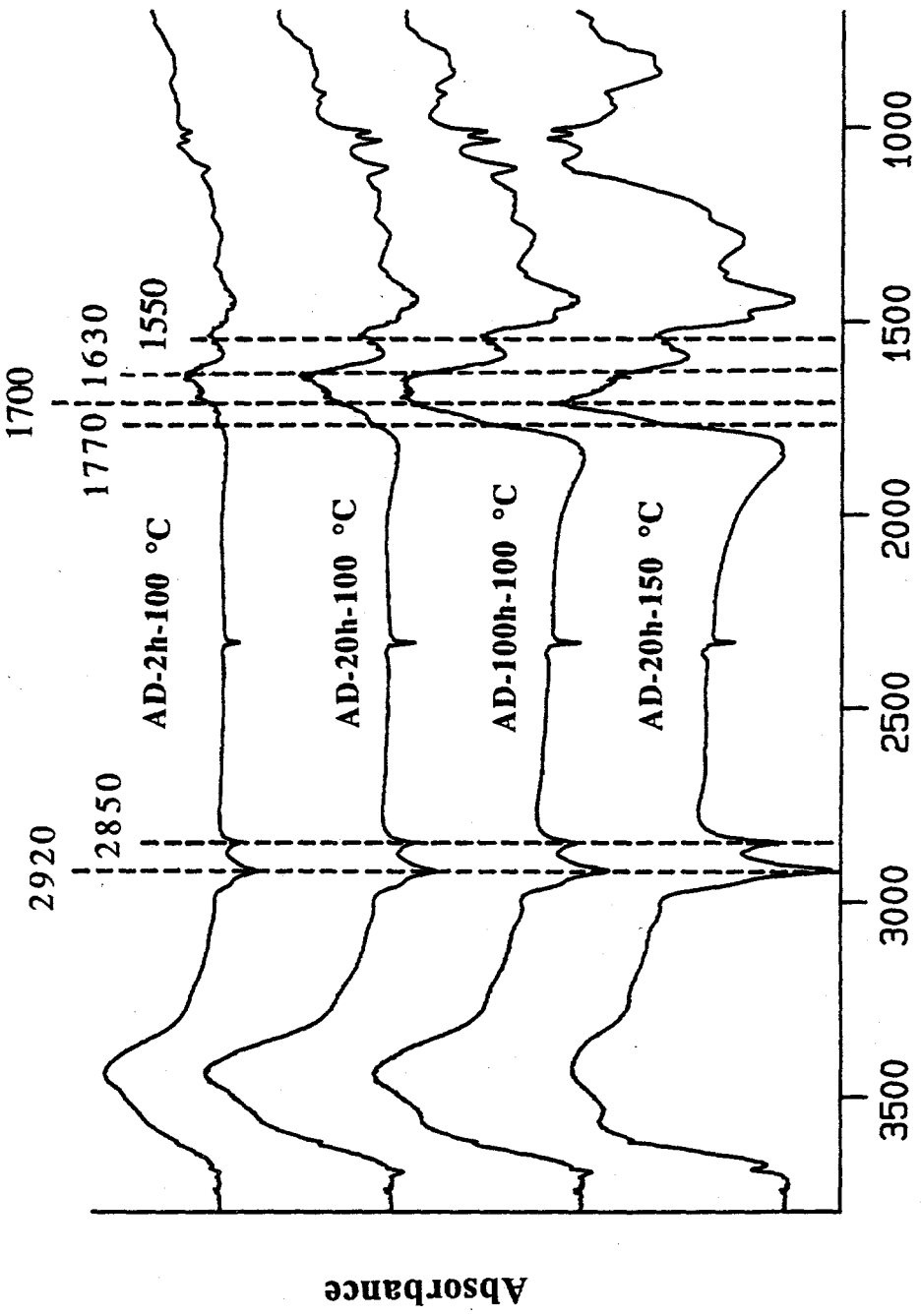

Figure 1.3 FT-IR difference spectra obtained by subtracting the spectrum of vacuum-dried DECS-8 coal (100 °C for 2 h) from the spectra of the four air-dried coals.

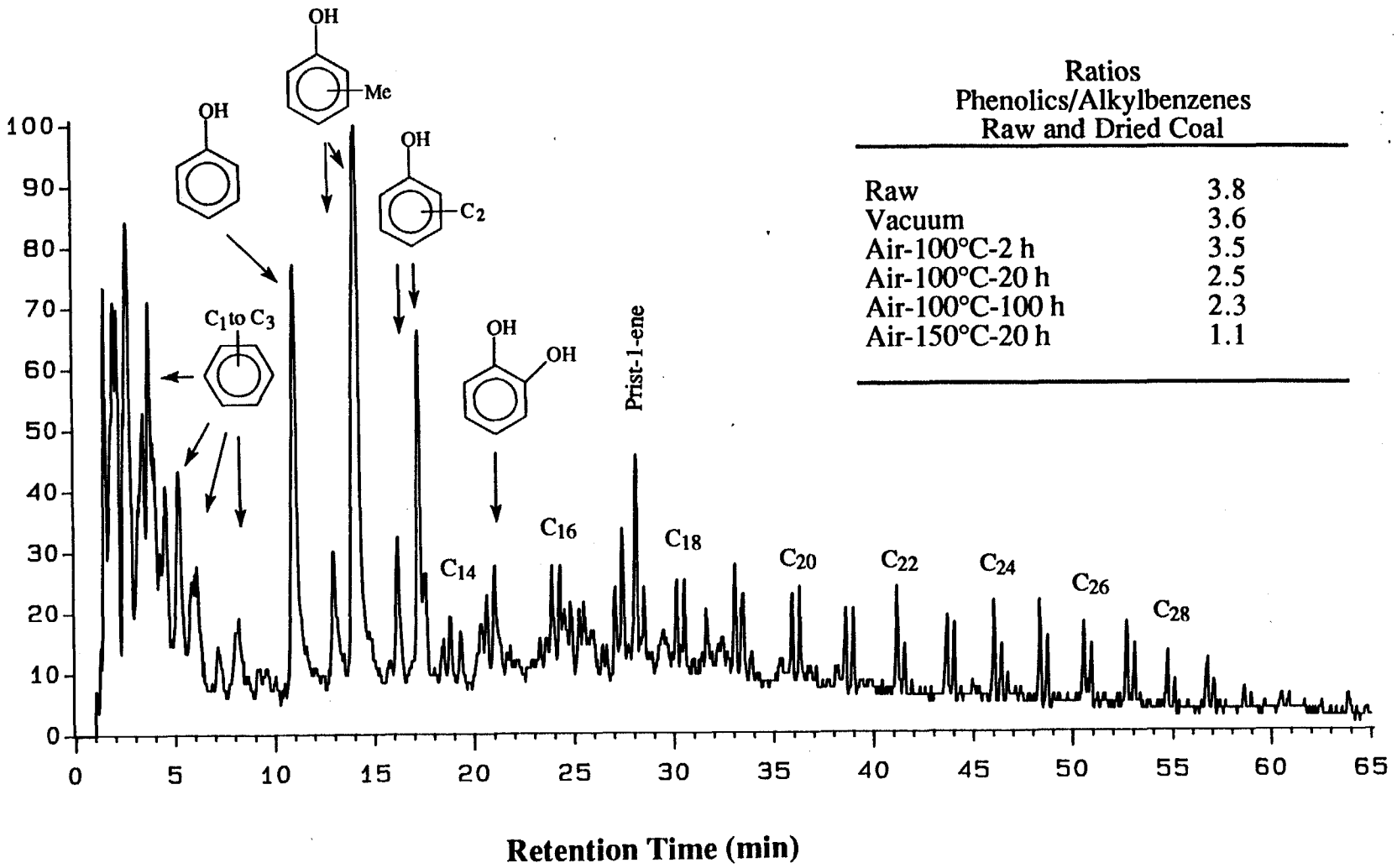

Ratios
Phenolics/Alkylbenzenes
Raw and Dried Coal

Raw	3.8
Vacuum	3.6
Air-100°C-2 h	3.5
Air-100°C-20 h	2.5
Air-100°C-100 h	2.3
Air-150°C-20 h	1.1

Figure 1.4 Py-GC-MS total ion chromatogram of the raw DECS-8 coal, together with the area ratios of phenolic compounds to alkylbenzenes of the predried coals.

Effects of Drying and Oxidation on Non-catalytic Liquefaction. Table 1.1 presents the results for thermal liquefaction (i.e., without added catalyst). Predrying of Wyodak subbituminous DECS-8 coal, whether oxidative (air drying) or non-oxidative (vacuum drying), has a significant effect on the production of gases and liquid products at 350°C both in the absence and the presence of a solvent. Among the gaseous products, CO_2 and CO are the main constituents, and C_1 to C_4 hydrocarbon gases make up the remainder. The effect of drying on gas yields is manifested primarily by the changes in CO_2 yield and secondarily by CO yield. The yields of C_1-C_4 hydrocarbon gases in all the thermal runs were essentially constant; among the C_1-C_4 gases the yields of methane and ethane were always higher than the others.

Figure 1.5 shows the yields of CO and CO_2 from solvent-free liquefaction at 350°C versus predrying conditions. CO_2 yields increased remarkably when air drying severity increased from 100°C-20 h to 100°C-100 h or 150°C-20 h, which corresponds to the considerable increase in intensity of carboxylic band in FT-IR (Figure 1.3). It is considered that decarboxylation and decarbonylation produce CO_2 and CO, respectively. As can be seen from Table 1.1, both solvent-free and solvent-mediated runs of the vacuum-dried coal give lower gas yield compared to those of the raw coal and air-dried coal, due mainly to the lower CO_2 yield from the vacuum-dried coal. Figure 1.5 clearly indicates that increased oxidation of coal has a greater impact on CO_2 production, and a much lesser impact on CO formation. Probably decarboxylation can occur more readily at lower temperature compared to decarbonylation. The severity of drying at 100°C in air does not seem to have any marked effect on the yields of C_1-C_4 gases in thermal reactions at 350°C (Table 1.1).

With respect to the effects of drying on coal conversion, several trends are apparent from Table 1.1. First, using the fresh raw coal always affords the highest conversions and the highest oil yields, regardless of the solvents. Second, predrying the coal under either non-oxidative (vacuum drying) or oxidative (air drying) conditions decreased coal conversion and the yields of oil, asphaltene, and preasphaltene. Third, relative to vacuum drying, air drying at 100 °C for 2 h tends to afford higher coal conversions and oil yields, and this trend becomes more apparent when either a H-donor tetralin or a non-donor 1-MN solvent was used. However, the oil yield in thermal runs drops sharply when the time of predrying at 100 °C in air is increased from 20 to 100 h. Fourth, under the given drying conditions, the coal conversion generally increases in the order of solvent-free < 1-MN < tetralin. Relative to the non-donor 1-MN, the advantage of H-donor tetralin is more apparent for liquefying the coals that have been dried in air at 100 °C for 2-100 h.

Table 1.1 Results of Non-Catalytic Liquefactions of Raw and Dried Wyodak Coal at 350 °C for 30 min with 6.9 MPa H_2

Drying	Reaction	CO	CO_2	C_1-C_4	Oil	Asphal.	Preasp.	Total	**Conversion**
conditions	solvent	dmmf wt%						Liquids[a]	dmmf wt%
Fresh raw coal	none	0.4	8.9	0.2	5.4	2.8	9.1	17.3	25.0
Vacuum, 100°C, 2 h	none	0.2	4.5	0.2	2.1	2.6	4.5	9.2	12.5
Air, 100°C, 2 h	none	0.3	5.9	0.1	3.3	0.7	5.8	9.8	14.8
Air, 100°C, 20 h	none	0.4	6.7	0.2	6.0	0.6	3.2	9.8	15.5
Air, 100°C, 100 h	none	0.7	11.2	0.2	1.2	0.7	3.3	5.2	12.7
Air, 150 °C, 20 h	none	0.8	12.3	0.1	0.6	0.2	0.4	1.1	10.9
Fresh raw coal	Tetralin	0.1	7.4	0.2	15.8	9.3	12.4	37.5	43.3
Vacuum, 100°C, 2 h	Tetralin	0.2	4.1	0.2	4.1	7.6	10.0	21.7	25.9
Air, 100°C, 2 h	Tetralin	0.2	5.9	0.2	11.7	7.4	10.6	29.7	35.1
Air, 100°C, 20 h	Tetralin	0.3	7.5	0.3	11.1	6.5	8.9	26.5	32.4
Air, 100°C, 100 h	Tetralin	0.5	10.9	0.2	6.1	6.3	9.7	22.1	30.8
Air, 150 °C, 20 h	Tetralin	0.6	15.9	0.1	2.1	2.8	3.2	8.1	19.9
Fresh raw coal	1-MN	0.1	7.0	0.2	15.9	6.6	11.4	34.0	39.9
Vacuum, 100°C, 2 h	1-MN	0.2	4.3	0.2	1.1	5.8	7.4	14.3	18.3
Air, 100°C, 2 h	1-MN	0.3	6.2	0.2	4.2	4.0	9.4	17.6	22.7
Air, 100°C, 20 h	1-MN	0.3	7.0	0.2	8.0	5.6	4.7	18.3	24.5
Air, 100°C, 100 h	1-MN	0.5	11.9	0.2	1.7	4.1	6.3	12.1	21.1
Air, 150 °C, 20 h	1-MN	0.7	15.7	0.1	1.8	2.2	2.5	6.6	18.0

a) Sum of yields of oil, asphaltene, and preasphaltene.

Table 1.2 Results for the Low-Severity Catalytic Liquefaction at 350 °C Using ATTM Impregnated on Raw and Dried Coals

Drying conditions	Solvent	CO	CO_2	C_1-C_4	Oil	Asphal.	Preasp.	Total Liquids[a]	**Conversion**
		dmmf wt%							dmmf wt%
Fresh raw coal[b]	none	0.3	4.1	0.5	16.9	9.2	14.9	41.1	43.3
Vacuum, 100°C, 2 h	none	0.2	2.3	0.3	10.0	5.4	11.4	26.8	29.8
Air, 100°C, 2 h	none	0.4	5.2	0.6	12.6	3.2	10.1	25.9	29.2
Air, 100°C, 20 h	none	0.4	5.7	0.7	14.6	3.1	8.7	26.4	31.2
Air, 100°C, 100 h	none	0.7	8.0	0.6	13.3	2.4	5.1	20.8	28.4
Air, 150 °C, 20 h	none	0.9	9.8	0.5	5.1	0.5	1.7	7.3	18.5
Fresh raw coal[b]	Tetralin	0.1	4.5	0.4	16.0	11.5	11.9	39.4	42.2
Vacuum, 100°C, 2 h	Tetralin	0.1	2.6	0.3	10.2	12.9	10.6	33.4	36.4
Air, 100°C, 2 h	Tetralin	0.2	4.8	0.4	15.7	11.1	14.9	41.7	45.6
Air, 100°C, 20 h	Tetralin	0.2	6.9	0.4	18.6	8.6	10.7	37.9	43.5
Air, 100°C, 100 h	Tetralin	0.4	8.8	0.5	16.5	10.8	11.0	38.3	45.0
Air, 150 °C, 20 h	Tetralin	0.4	12.4	0.4	9.6	2.3	5.7	17.6	29.4
Fresh raw coal[b]	1-MN	0.1	4.5	0.3	10.4	10.4	11.9	32.7	35.9
Vacuum, 100°C, 2 h	1-MN	0.1	3.4	0.3	6.1	10.1	12.3	28.5	31.1
Air, 100°C, 2 h	1-MN	0.2	5.2	0.4	10.3	8.1	16.0	34.4	37.4
Air, 100°C, 20 h	1-MN	0.2	9.3	0.5	14.1	8.7	10.5	33.3	39.7
Air, 100°C, 100 h	1-MN	0.3	9.5	0.4	14.4	8.7	11.1	34.2	39.4
Air, 150 °C, 20 h	1-MN	0.3	12.4	0.3	5.3	2.8	4.3	12.4	24.5

a) Sum of yields of oil, asphaltene, and preasphaltene.

b) Raw (fresh as-received) coal was used for catalyst impregnation followed by vacuum drying at 100 °C for 2 h before liquefaction.

Finally, after drying in air under high-severity conditions such as 20 h at 150 °C, conversion of the dried coal decreased to less than 50% of that of the fresh raw coal on a dmmf basis. In this case, the advantage of using a H-donor solvent disappears, as there is no major difference in coal conversions and oil yields between runs with tetralin and 1-MN solvents. However, the runs of the highly oxidized coal using a solvent still gave better conversions (18.0-19.9 wt%) than the solvent-free run (10.9 wt%), as can be seen from Table 1.1.

Effects of Drying and Oxidation on Catalytic Liquefaction. Catalytic runs were conducted using in-situ generated molybdenum sulfide from ATTM impregnated onto raw coal or dried coal samples. ATTM is known to decompose at ≥ 275 °C to form MoS_3 which subsequently transforms to MoS_2; this transformation occurs readily under H_2 pressure.[31] Unlike the thermal reactions which also involve raw coal whose moisture (28.4 wt%) is present in the reaction system, the catalytic reactions discussed below involve only the ATTM-impregnated and dried samples (see curve C in Figure 1.1). The catalytic reaction at 350°C can be considered as low-severity liquefaction or catalytic pretreatment. Table 1.2 presents the data for catalytic runs at 350°C. For solvent-free catalytic runs, using fresh raw coal for impregnation of ATTM afforded significantly higher conversion and higher oil yield, which were also accompanied by higher H_2 consumption (see below), than using the vacuum-dried and air-dried coal. Loading ATTM onto the coals that were predried at 100 °C for 2 h under vacuum and in air gave similar results in the absence of a solvent. However, the coal conversion and oil yield decreased and CO_2 yield increased with further increase in the severity of air drying from 20 to 100 h at 100 °C and from 100 to 150 °C.

Figure 1.6 compares the yields of soluble products, excluding gases, between low-severity catalytic (top, with ATTM) and non-catalytic (bottom) liquefaction of dried coals at 350°C with tetralin solvent. For catalytic runs in the presence of either tetralin or 1-MN solvent, dispersing ATTM on air-dried coal leads to higher conversion and oil yield, especially in tetralin, than loading ATTM on vacuum-dried coal. These results indicate that, relative to the non-oxidative drying, predrying in air at 100°C has some beneficial effect when ATTM is used together with a solvent for runs at 350°C. This may be attributed to the mild oxidation-induced increase in surface functionality and hence increased hydrophilicity, which contributed to increasing catalyst dispersion in the impregnation process. In fact, with a given predrying time of 2 h at 100 °C, the use of air-dried coal in the catalytic runs with either tetralin or 1-MN solvent gave similar or slightly better conversion compared to the case of using the fresh raw coal (Table 1.2). This is in contrast with the trend observed in non-catalytic runs, where using dried coals always gives considerably lower conversion and oil yield at 350°C than using the raw coal (Figure 1.6, Table 1.1).

Similar to the thermal runs, the yields of gases in the catalytic runs also vary significantly due to predrying, which are mainly manifested by the changes of CO_2 yield (Table 1.2). CO_2 yield of catalytic runs increases with increasing severity of air drying. In the runs using ATTM loaded on the raw coal, water was not present during the reaction, but still a higher CO_2 yield was obtained compared to that with ATTM loaded on the vacuum-dried coal (Table 1.2). The presence of a solvent appears to slightly increase CO_2 yield in many cases in the catalytic runs, but has no marked effect on hydrocarbon gas make both in thermal and catalytic runs. In collateral work in this laboratory, it was shown that for a subbituminous coal sample, the gas yields are mainly a function of temperature but are independent of solvent.[32]

As can be seen by comparison of Table 1.2 with Table 1.1, there are some considerable differences in gas composition between thermal and catalytic runs. In general, the total gases yields in the thermal runs of the raw and the dried coal are always higher than those in the corresponding catalytic runs at 350°C. This is due mainly to the lower yields of CO_2 in all the catalytic runs than all the corresponding non-catalytic runs (Figure 1.5). This observation clearly indicates the occurrence of hydrogenation of the oxygen-functional groups in the presence of a dispersed Mo sulfide catalyst at 350 °C. On the other hand, the yields of hydrocarbon gases are always higher in the catalytic runs of the dried coal or the raw coal than in the thermal runs, suggesting that parts of the hydrocarbon gases from catalytic liquefaction resulted from catalytic hydrogenolysis of C-C bond or dealkylation of alkylaromatics. However, the extent of decrease in CO_2 yield due to the use of catalyst at 350 °C is higher than that of the increase in C_1-C_4 gas make.

Effects of Drying on Hydrogen Consumption. Figure 1.7 shows the effect of predrying of the coal on hydrogen consumption from gas-phase H_2 and on net hydrogen transfer from tetralin at 350°C. In the absence of an added catalyst, the runs of the raw coal gave somewhat higher consumptions of gas-phase H_2 than the runs of the coal that has been dried at 100 °C for 2-20 h under vacuum or in air, both in the absence and presence of a solvent (tetralin or 1-MN). This is consistent with the fact that the dried coals gave lower conversions and lower total yields of liquid products (Table 1.1).

Another general trend from the thermal runs is that H_2 consumption and the extent of hydrogen transfer from tetralin increased with increasing severity of oxidative drying from 100°C–20 h to 150°C–20 h. In fact, this parallels qualitatively with the increase in CO_2 formation (Table 1.1). The conversions and the yields of liquid products in the thermal runs of the highly oxidized coal (air dried at 150 °C for 20 h) are the lowest among all the thermal runs. Apparently, higher hydrogen consumptions being observed for runs of the highly oxidized coal This indicates that only a part of the hydrogen consumed in the runs of the highly oxidized coal

is related to the coal conversion or oil formation. The oxidation of coal increases the surface and bulk functionalities, which upon thermolysis can increase the number of free radicals. These considerations point to the conclusion that, relative to the vacuum-dried coal, a significantly higher number of bonds in the highly oxidized coal (air dried at 150 °C for 20 h) are broken during liquefaction at 350 °C, but increased population of such weak bonds contributes to enhanced retrogressive crosslinking, rather than the enhanced dissolution of coal.

The predrying also affects the hydrogen transfer from tetralin during non-catalytic liquefaction (Figure 1.7C). Comparatively, the hydrogen transfer from tetralin in thermal runs of the vacuum- and air-dried coals is slightly higher than that of the raw coal; for the air-dried coal it tends to increase slightly with the severity of air drying. It is very interesting to note from Figure 1.7C that in the thermal run of the raw coal, the consumption of gas-phase H_2 is higher than the amount of hydrogen transferred from tetralin. Generally, radical reactions are dominant at ≥ 350°C and the hydrogen transfer from H-donor tetralin is usually more efficient than that from gas-phase H_2 during non-catalytic conversion. However, if non-radical reaction pathways exist in the presence of moisture (28.4 wt% in raw coal), or water participates in the reaction, then the higher contribution of gas-phase H_2 consumption (relative to the hydrogen transfer from tetralin) in the non-catalytic run of the raw coal compared to those of dried coals at 350°C may not be an unusual phenomenon. Clarification of this issue requires further study.

In the catalytic runs, the consumption of gas-phase H_2 is significantly higher than that for the corresponding thermal runs (Figure 1.7), regardless of the solvent (Figures 1.7B and 1.7C). This clearly shows that, at 350 °C, the dispersed Mo sulfide catalyst facilitates the dissociation of molecular H_2 thus making hydrogen atoms readily available for the free radicals formed during liquefaction, resulting in higher conversion (Table 1.2). It seems possible that the hydrogen atoms from catalytic dissociation of molecular H_2 have also induced bond cleavage to certain extent. This consideration is supported by the facts that using ATTM enhanced C_1-C_4 hydrocarbon gas make as compared to the corresponding thermal runs, but using H-donor solvent had little impact on C_1-C_4 hydrocarbon gas make.

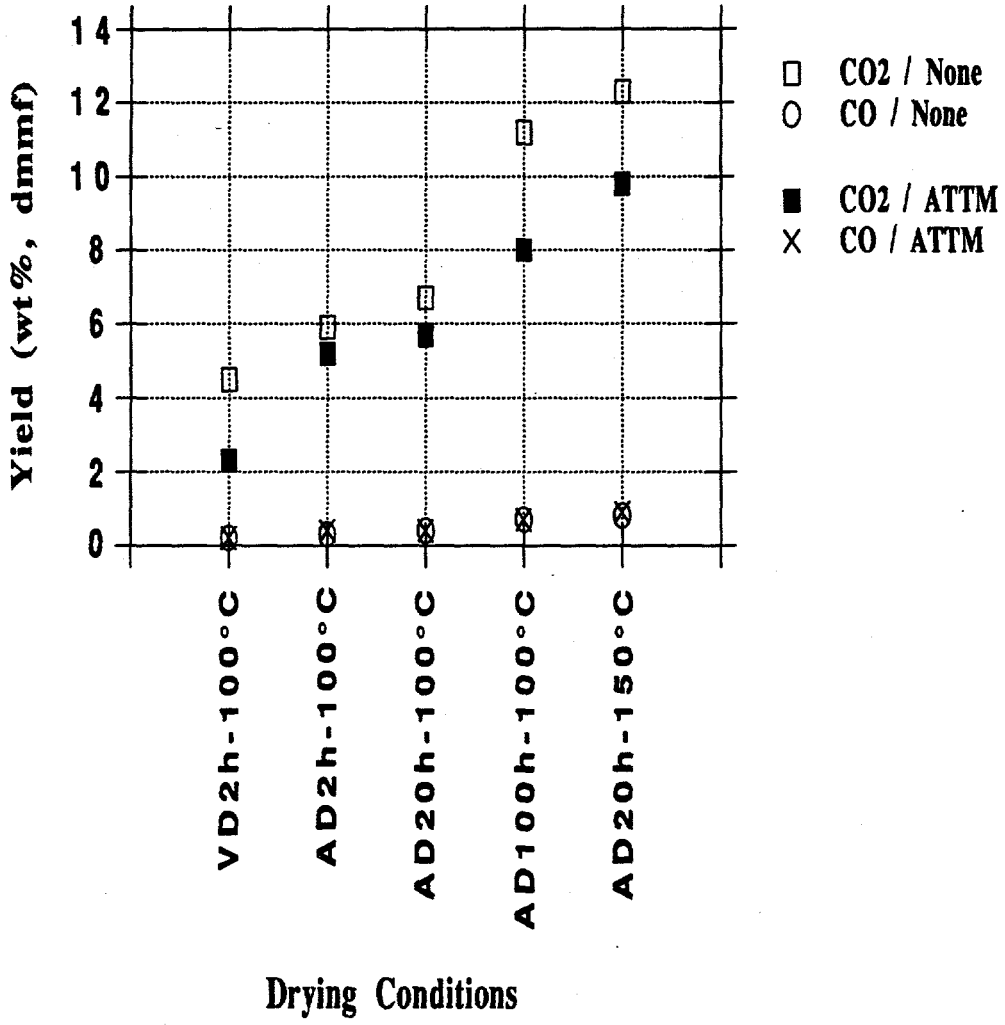

Figure 1.5 Yields of CO and CO_2 from solvent-free non-catalytic and catalytic (ATTM) liquefaction of DECS-8 coal at 350°C versus predrying conditions.

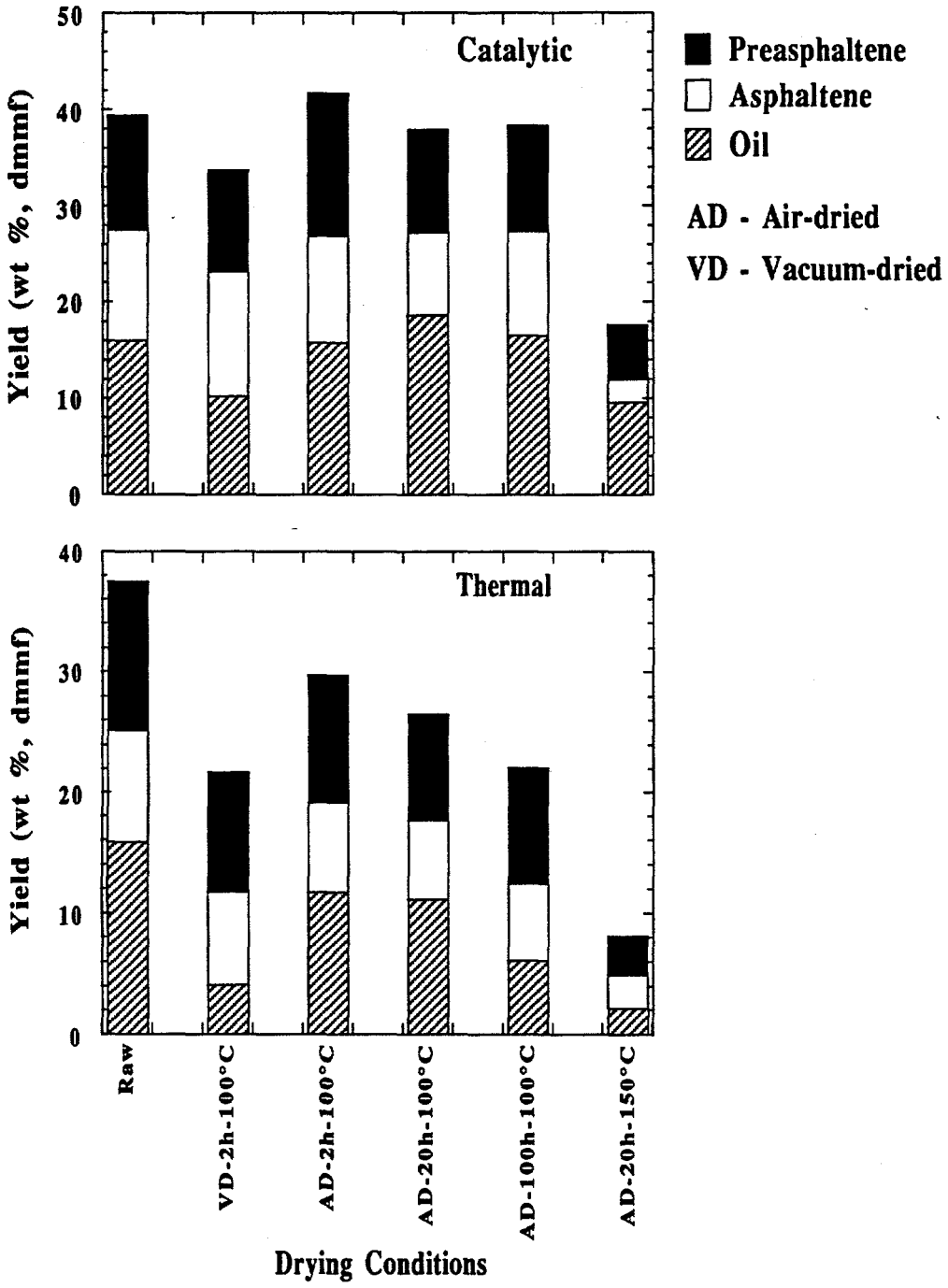

Figure 1.6 Yields of soluble products excluding gases for low-severity catalytic (top, with ATTM) and non-catalytic (bottom) liquefaction with tetralin solvent at 350°C.

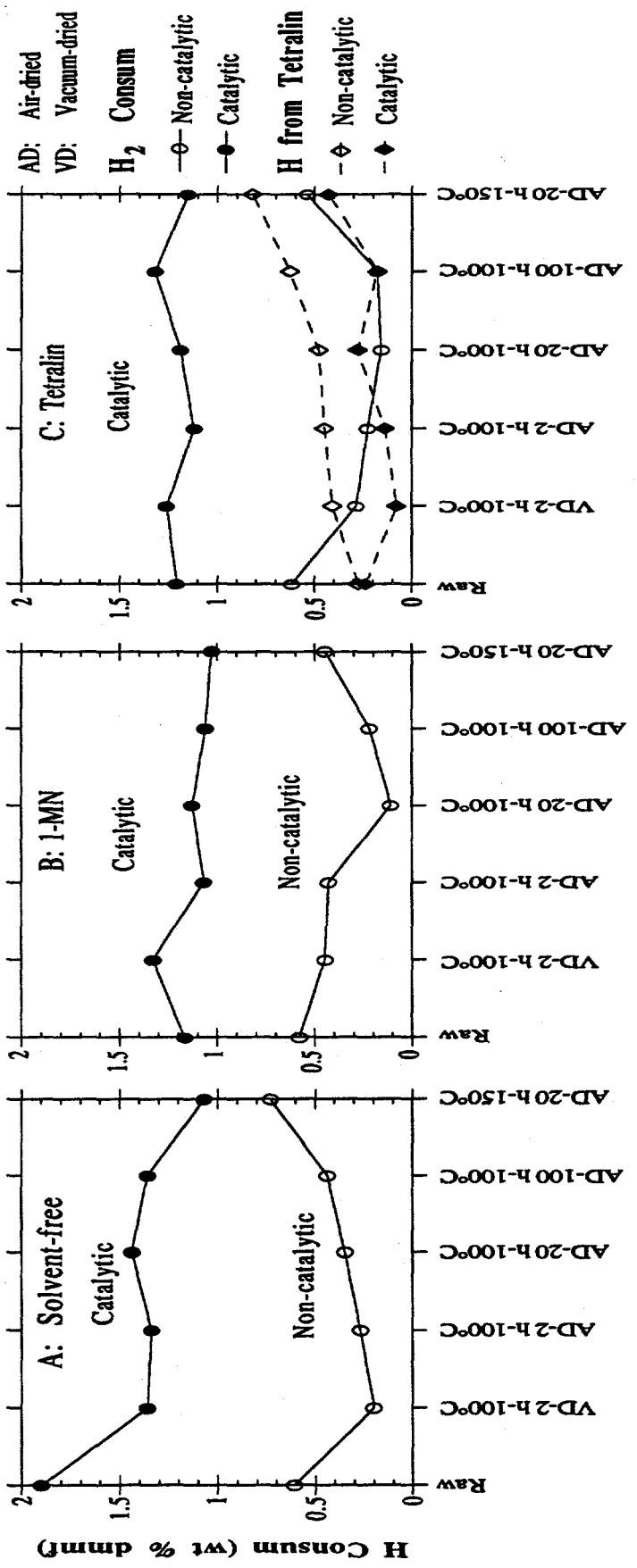

Figure 1.7 Effect of predrying Wyodak subbituminous coal on hydrogen consumption during its liquefaction at 350 °C with 6.9 MPa H_2 (cold).

The maximum H_2 consumption (1.9 wt %, dmmf) is observed in the solvent-free runs with ATTM impregnated on raw coal. When the coal is predried before ATTM impregnation, the catalytic runs consume considerably less hydrogen (in the solvent-free runs). These facts suggest that the water originally present in the coal affects either the catalyst impregnation or the catalyst dispersion, even when aqueous solution is used for ATTM impregnation. As compared to the solvent-free catalytic run with raw coal, the gas-phase H_2 consumption is lower in the catalytic runs at 350°C using either 1-MN (1.2 wt %, dmmf) or tetralin solvent (1.2 wt %, dmmf). It is also clear from Figure 1.3.7C that, except the case with raw coal, using ATTM generally reduces the net hydrogen transfer from tetralin compared to thermal runs. This observation is in good agreement with the earlier findings.[24, 33-35] Both Song et al.[24,33,34] and Artok et al.[35] observed that when an active dispersed[24,33,35] or a supported catalyst[34] is present, the majority of the hydrogen consumed comes from the gas-phase H_2 and only a small part from the H-donor solvent. The mechanisms of hydrogen transfer in catalytic reactions have been discussed elsewhere.[24, 33-35]

Spectroscopic Characterization of Residues. Figure 1.8 presents the 1400-1800 cm^{-1} region of FT-IR difference spectra of residues from solvent-free non-catalytic liquefaction (obtained by subtracting spectrum of residue of the vacuum-dried coal from the spectra of residues of the air-dried coals). It is interesting to note that the effect of oxidation due to air drying is even reflected in the liquefaction residues. Increasing the severity of air drying leads to increased oxygen functionality of the residues from air-dried coals as compared to those of vacuum-dried coal (Figure 1.3.8). The difference spectra between the residues and the predried coals shown in Figure 1.3.9 indicate that higher degree of coal oxidation corresponds to higher extent of decarboxylation (the negative band around 1700 cm^{-1}) during the non-catalytic reaction at 350°C. These results are consistent with the observed CO_2 formation trends (Table 1.1, Figure 1.5).

Figure 1.10 shows the changes of the phenolics/alkylbenzenes ratio determined by Py-GC-MS for predried coals and their residues from solvent-free liquefaction at 350°C versus the drying conditions. Compared to the coals dried at 100°C, the ratios for their liquefaction residues are generally lower. However, the ratio for residues from catalytic runs tends to be higher than that of the corresponding thermal runs. In other words, the relative content of phenollic compounds in the pyrolyzates of residues increases upon the use of dispersed Mo catalyst. It seems that this ratio may have potential to serve as a qualitative measure of extent of crosslinking reactions of phenolics caused by oxidation.

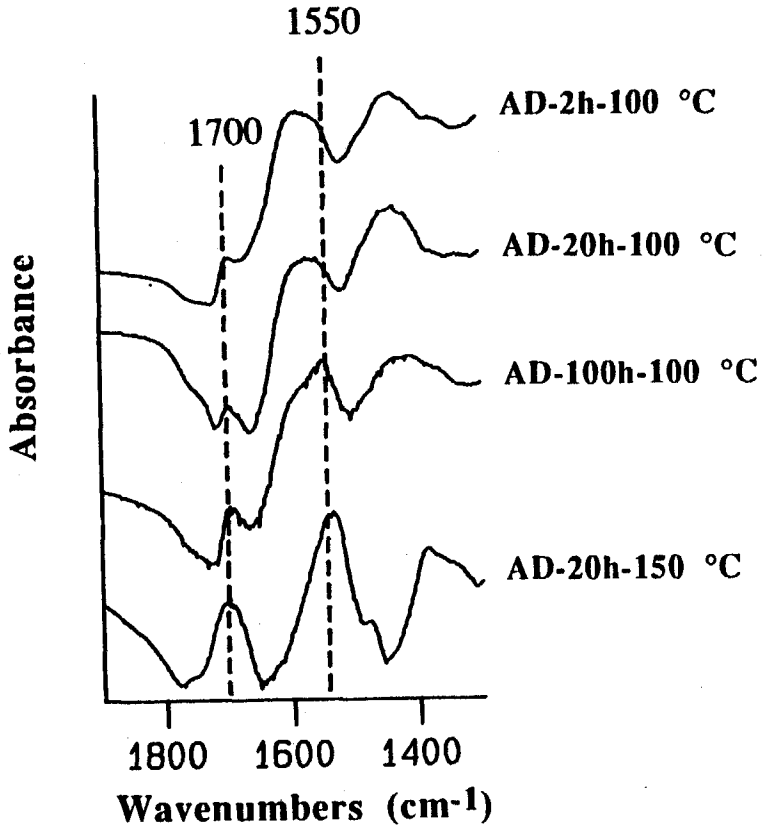

Figure 1.8 FT-IR difference spectra of liquefaction residues (1400-1800 cm^{-1} region: the spectra of residues of the air-dried coals — spectrum of residue of the vacuum-dried coal).

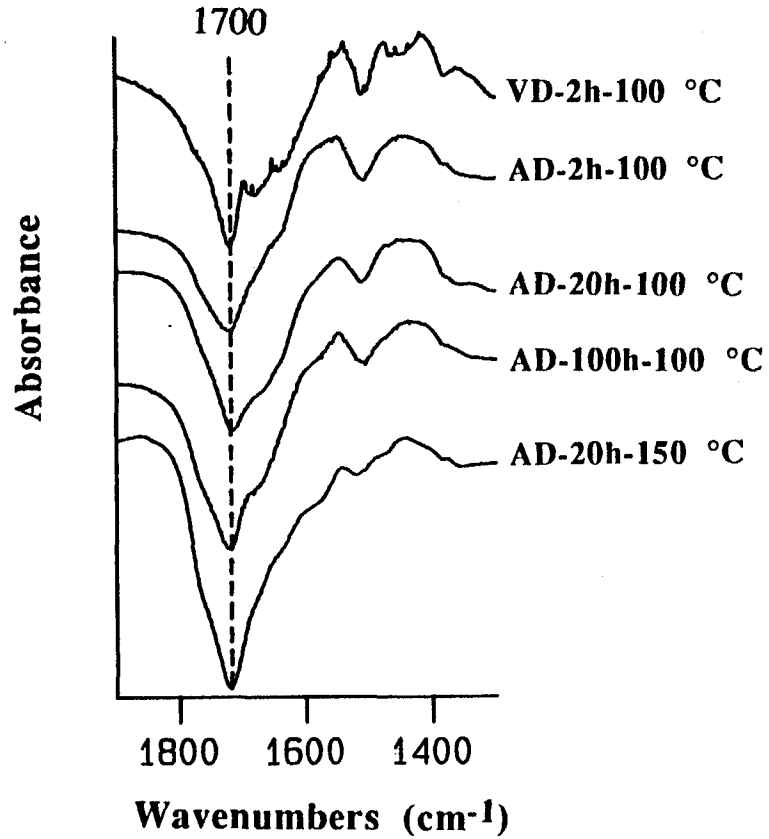

Figure 1.9 FT-IR difference spectra (1400-1800 cm^{-1} region) between liquefaction residues and coals (spectra of liquefaction residues — spectra of the corresponding predried coals).

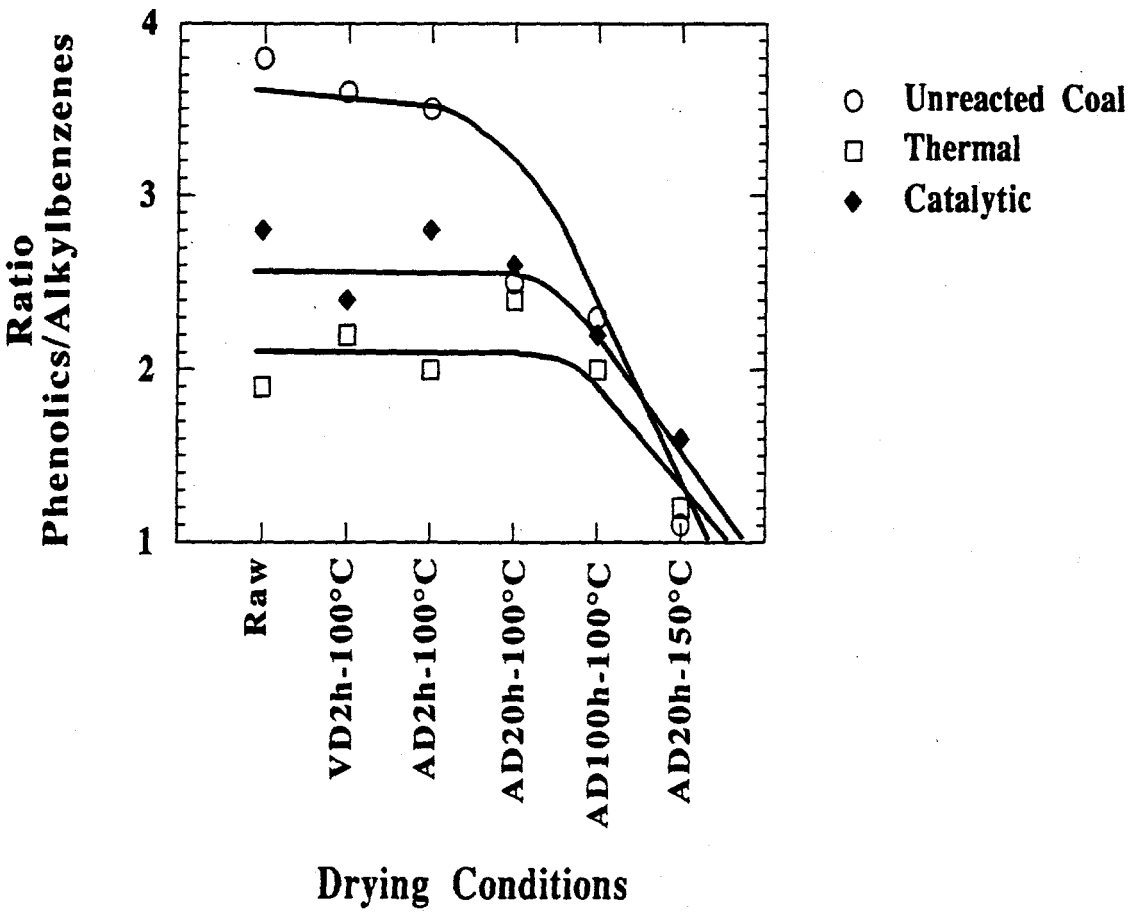

Figure 1.10 Changes in the ratio of phenolics/alkylbenzenes determined by Py-GC-MS for predried coals and their residues from solvent-free thermal and catalytic liquefaction at 350°C.

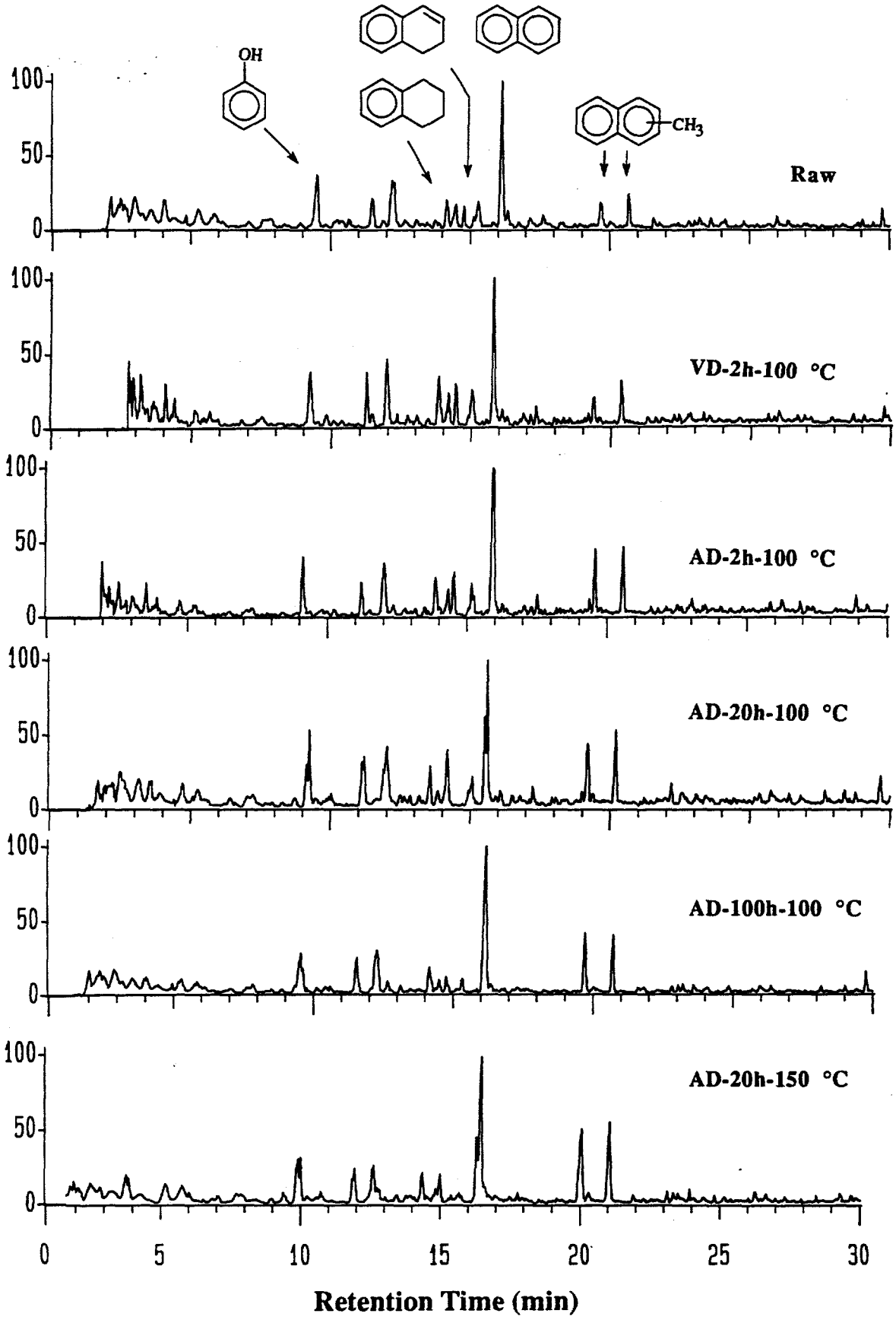

Figure 1.11 Py-GC-MS profiles for residues from non-catalytic liquefaction of raw and dried coals with tetralin solvent at 350°C.

Figure 1.11 shows Py-GC-MS profiles of the residues from non-catalytic liquefaction at 350°C with tetralin solvent. It should be noted that the residues have been extracted by THF for over 24 h, washed by acetone and finally dried at 110°C for over 6 h. Tetralin, dihydronaphthalene, naphthalene, 2- and 1-methylnaphthalene peaks, eluted in that order, are due mainly to the use of tetralin as the reaction solvent.[36] Methylnaphthalene peaks are due mainly to the chemically bound molecular fragments of solvent origin. Apparently, as the severity of oxidative drying increases, the relative intensities of the adducted compounds increases. The adduction of solvent molecules depends on the number of reactive sites (free radicals) created during liquefaction and the inaccessibility of the donatable hydrogen to cap these sites. The solvent molecules can also form free radicals upon hydrogen abstraction by reactive radicals generated from coal. It is clear from Figure 1.11 that the adduction of solvent molecules during liquefaction is enhanced by oxidative drying of the coal, especially air drying at 100°C for 100 h and at 150°C for 20 h. The oxidized coal is richer in oxygen-containing functional groups, which can induce crosslinking reactions upon their thermal decomposition at 350°C.

Physical and Chemical Considerations of Drying Effects. There are at least four physicochemical effects that drying and oxidation may have on coal. The first is the removal of water. The second is the physical changes such as those in pore structure and density that are believed to accompany drying.[14,18] One way by which pore structure can be changed is the shrinkage caused by deswelling due to the removal of water, which is a good swelling solvent for low-rank coal.[18] If this happens, drying before the reaction could also affect the reaction with respect to diffusion of solvents, reactants, and products. The third is the change in surface characteristics such as hydrophobicity induced by drying, as we further describe below. Finally, some chemical reactions may occur during drying such as air drying at 100°C. Obviously, oxidation causes chemical change in oxygen functionality. The effects of these four factors in thermal and catalytic liquefaction are not straightforward, and some of them can exert influence on coal conversion in opposite directions under the same or different conditions.

Apparently, the first effect, the removal of water, was neglected in most previous work on the influence of drying in liquefaction. This is presumably because water was thought to be inert in coal liquefaction. We also examined the effect of water addition.[25] Table 1.3 shows the effect of adding water in the thermal runs of vacuum-dried coal without solvent and with tetralin solvent. Adding a small amount of water equivalent to the original moisture content (28.4 wt%) back to the vacuum-dried coal increased coal conversion from 9.2 to 22.3 wt% in the solvent-free runs, and from 25.9 to 39.9 wt% in the runs with tetralin solvent. In fact, adding water back to the vacuum-dried coal restored over 90 % of the oil yield and conversion of those with the fresh

raw coal in non-catalytic runs at 350 °C both with and without a solvent, as can be seen from Table 1.3.

The above facts suggest that the decrease in conversion in thermal runs at 350°C upon drying is due primarily to the removal of water, and the changes in coal conversion and products distribution caused by drying at 100 °C (except oxidation) seem to be largely reversible upon addition of water. Although the presence of water has significant physical effect (see below), it may also have some impact on the chemical reaction at 350 °C. It has been reported that hydrothermal pretreatment of coal in presence of water is beneficial for improved conversion and better product quality in pyrolysis, liquefaction and coprocessing.[17,37-41] As can be seen from Table 1.1, CO_2 yield is always higher in the runs of raw coal than those of vacuum-dried coal. An increase in the CO_2 yield upon addition of water to vacuum-dried coal has been observed.[25,42] Enhanced CO_2 formation upon water addition was also observed by Lewan[43] in his studies on hydrous pyrolysis of kerogen materials.

The decrease in CO yield upon water addition indicates that water gas shift reaction (equation 3) did occur but this reaction only contributes to a small part of the increased CO_2 yield, as can be seen by comparing the CO and CO_2 yields in Table 1.3 on a molar basis. The majority of increased CO_2 yields upon water addition is probably due to the interaction of water with carbonyl functional groups (equation 4), as also suggested by Petit.[44] This rationalizes the enhanced coal conversion together with increased CO_2 formation upon water addition. Since low-rank coals have high propensity towards retrogressive reactions due to their high oxygen functionalities, the removal of oxygen functional groups in the presence of water at 350 °C can make the coal network less refractory for dissolution and hence higher conversion is achieved.[25] In addition, the effects of water addition to vacuum-dried coal observed in this work has led the way to more efficient low-severity catalytic liquefaction,[25] but further studies are needed to clarify the mechanisms of chemical effects of water.

$$CO + H_2O = CO_2 + H_2 \qquad 3)$$

$$R'COR'' + H_2O = R'H + CO_2 + R''H \qquad 4)$$

From their model compound studies, Tse et al.[41] suggested that water can suppress the retrogressive crosslinking reactions such as those of polyhydroxy groups. On the other hand, according to Siskin et al.,[45] the presence of water during the preconversion step may facilitate depolymerization of the macromolecular structure to give a higher conversion yield by cleavage of ether type crosslinkages. From our data in Tables 1 and 3, it seems that the added water or the original moisture also participated in the chemical reaction at 350°C and acted also as a hydrogen source through some chemical reactions such as that represented by equation 4.

The second effect, physical change such as pore collapse and shrinkage caused by drying, has been discussed quantitatively in a recent paper by Suuberg et al.[18] Their work has demonstrated that water is a good swelling agent for coals ranging from lignites up to high-volatile bituminous coal, and the coals shrink when dried from the as-mined state. They found that shrinkage upon vacuum drying is correlated by equation 5:

$$\text{Volumetric shrinkage (\%)} = 0.863 \times (\text{moisture content, wt\%}) - 0.162 \qquad 5)$$

Applying this relationship would give a 24 % volumetric shrinkage of Wyodak subbituminous coal upon vacuum drying. It is reasonable to consider that drying in vacuum and in air may have somewhat different impacts on the pore collapse, and surface area change, but no data is available for comparison at the present stage.

In regard to surface area change, Vorres et al.[15] have recently observed that the N_2 BET surface areas of low-rank coals decrease on heating above room temperature to 40°C; the areas are relaively constant on heating in vacuum between 40-100°C. Swann et al.[46] reported that vacuum drying of a fresh Yallourn brown coal at 22, 35, and 70°C gives CO_2 surface areas of 290, 262, and 254 m^2/g, respectively. Mahajan and Walker[47] found that for a lignite, CO_2 surface areas following outgassing at 90, 110, 130, and 150°C were 206, 212, 198, and 184 m^2/g, respectively. Following vacuum drying of Yallourn brown coal at 35°C (or 70°C) for 7 days, oxidation by pure molecular oxygen at 35°C (or 70°C) for 45 days further decreased the CO_2 surface areas from 262 to 187 m^2/g (for 70°C vacuum drying followed by oxidation, 254 to 156 m^2/g).[46] On the other hand, these CO_2 surface area values may not be representative of the internal areas accessible by tetralin or 1-MN solvent molecules, which have much larger molecular sizes than CO_2 and N_2.

One of our hypotheses in designing the experiments with different solvents was the following: if drying affects the rate of solvent diffusion into the coal pores or the rate of uptake of solvents by the coal, then the reaction with a H-donor solvent should be more sensitive to the drying conditions than the one with a non-donor solvent. As can be seen from Table 1.1 and Figure 1.6, for thermal runs in the presence of tetralin solvent, considerably higher conversion (35.1 wt%) and higher oil yield (11.7 wt%) were obtained with the air-dried coal (100 °C for 2 h) than with the vacuum-dried coal (25.9 wt% conversion, 4.1 wt% oil yield), and this trend was confirmed by duplicate tests. However, using 1-MN in the thermal runs gave only slightly higher conversion and oil yield for the air-dried coal (100 °C for 2 h) than for the vacuum-dried coal. Neither the oxidation induced by drying in air (Figure 1.3) nor the difference in moisture contents of dried coals (Figure 1.3) can account for these facts. We believe that, for thermal runs in the presence of a H-donor solvent at 350°C, the advantage with air-dried coal (dried at 100 °C

for 2 h) than with vacuum-dried coal is due to the lower mass transport limitations of H-donor molecules (and products) with the former.

The third effect of drying concerns surface characteristics. If drying in different atmosphere or under different conditions affects the surface characteristics of coal, then the dispersion of the catalyst precursor molecules on coal surface may change with drying. It has been shown that removal of the original moisture by drying contributes to increasing the hydrophobicity of coal surface,[48,49] but mild oxidation can convert some hydrophobic sites on coal surface into hydrophilic sites.[50,51] Relative to vacuum-drying, the beneficial effect of predrying in air at 100°C for 2 h in catalytic runs (Table 1.2) may be attributed to the mild oxidation-induced increase in surface oxygen functionality and hence increased hydrophilicity, which could contribute to increasing ATTM dispersion in the impregnation process. As Weller[52] pointed out ten years ago, the degree of dispersion is very important when unsupported Mo catalysts are used for coal liquefaction.

The hydrophobicity is a function of coal rank and maceral composition,[53] but is decreased by prewetting of dried coals.[49] We also performed several tests to see whether prewetting affects the catalyst impregnation, and the results are given in Table 1.4. The vacuum-dried coal was prewetted with a small amount of water which is equivalent to the original moisture (28.4 wt%). The prewetted coal was then impregnated with aqueous ATTM solution either immediately after prewetting or after 24 h storage of the prewetted sample. The results in Table 1.4 show that prewetting the vacuum-dried coal before impregnating ATTM from its aqueous solution has increased coal conversion and enhanced oil formation. The advantage of prewetting the vacuum-dried coal becomes more apparent when tetralin solvent was used for catalytic liquefaction at 350°C, where coal conversion and oil yield increased from 36.4 to 44.6 wt%, and from 10.2 to 18.4 wt%, respectively. Prewetting coal with water decreases hydrophobicity of surface on the one hand, and causes volume expansion due to coal swelling on the other hand. Both these two effects are desirable for better dispersion of ATTM during incipient wetness impregnation. Gorbaty[19] has shown that drying a Wyodak subbituminous coal in vacuum can decrease the amount of a metal salt (nickel sulfate) adsorbed onto coal from its aqueous solution. He attributed the drying-induced changes primarily to pore collapse and secondarily to the replacement of water by gas, namely the volume once occupied by water becomes occupied by the gas present during and after drying.

Table 1.3 Effect of Adding Water Back to the Vacuum-Dried Coal on Its Non-Catalytic Liquefaction at 350 °C

Coal drying conditions	H_2O addition after drying	Reaction solvent	CO	CO_2	C_1-C_4	Oil	Asphal.	Preasp.	**Conversion**
			dmmf wt%						dmmf wt%
Vacuum, 100°C, 2 h	no	none	0.2	4.5	0.2	2.1	2.6	4.5	12.5
Vacuum, 100°C, 2 h	yes	none	0.1	8.2	0.3	5.4	1.9	7.7	22.3
Fresh raw coal	Orig. Moist.	none	0.4	8.9	0.2	5.4	2.8	9.1	25.0
Vacuum, 100°C, 2 h	no	Tetralin	0.2	4.1	0.2	4.1	7.6	10.0	25.9
Vacuum, 100°C, 2 h	yes	Tetralin	0.1	6.9	0.2	14.5	9.2	10.2	39.9
Fresh raw coal	Orig. Moist.	Tetralin	0.1	7.4	0.2	15.8	9.3	12.4	43.3

Table 1.4 Effect of Prewetting of Vacuum-Dried Coal before ATTM Impregnation on Catalytic Liquefaction at 350 °C

Coal drying conditions	Prewetting with H_2O	Reaction solvent	CO	CO_2	C_1-C_4	Oil	Asphal.	Preasp.	**Conversion**
			dmmf wt%						dmmf wt%
Vacuum, 100°C, 2 h	no	none	0.2	2.3	0.3	10.0	5.4	11.4	29.8
Vacuum, 100°C, 2 h	yes[a]	none	0.4	5.6	0.5	16.7	4.2	9.0	34.1
Vacuum, 100°C, 2 h	yes[b]	none	0.3	4.7	0.4	14.0	7.9	8.7	35.0
Fresh raw coal	Orig. Moist.	none	0.3	4.1	0.5	16.9	9.2	14.9	43.3
Vacuum, 100°C, 2 h	no	Tetralin	0.1	2.6	0.4	10.2	12.9	10.6	36.4
Vacuum, 100°C, 2 h	yes[a]	Tetralin	0.1	4.3	0.3	18.4	11.5	11.5	44.6
Fresh raw coal	Orig. Moist.	Tetralin	0.1	4.5	0.4	16.0	11.5	11.9	42.2

a-b) ATTM was impregnated onto the prewetted coal immediately after prewetting (a) or after 24 h storage of the prewetted sample (b), followed by vacuum drying at 100 °C for 2 h before liquefaction.

Table 1.5 Effect of Drying Conditions before and after ATTM Impregnation on Catalytic Liquefaction with Tetralin at 350 °C

Coal drying conditions	Drying after IWI / ATTM	CO	CO_2	C_1-C_4	Oil	Asphal.	Preasp.	**Conversion**
		dmmf wt%						dmmf wt%
Fresh raw coal	Vacuum, 100°C, 2 h	0.1	4.5	0.4	16.0	11.5	11.9	42.2
Fresh raw coal	Air, 100°C, 2 h	0.2	7.4	0.3	18.3	8.8	11.2	43.6
Vacuum, 100°C, 2 h	Vacuum, 100°C, 2 h	0.1	2.6	0.4	10.2	12.9	10.6	36.4
Air, 100°C, 2 h	Vacuum, 100°C, 2 h	0.2	4.8	0.4	15.7	11.1	14.9	45.6

Combination of our results and with those of Gorbaty [19] and Wei et al.[49] suggest that non-oxidative predrying also increases the surface hydrophobicity and reduces the adsorption of metal salt onto the surface of low-rank coals, although water is used to dissolve the metal salt. Prewetting the coal prior to the contact with metal solution, however, decreases the surface hydrophobicity and swells the coal, leading to improved the adsorption and dispersion of metal salt from its aqueous solution (onto more hydrophilic surface).

In this context, relative to vacuum drying, the advantage of predrying coal in air (mild oxidation at 100 °C for 2 h) before ATTM impregnation for the solvent-mediated catalytic runs (Table 1.2) can be rationalized by taking into account the following two factors: 1) mild oxidation (Figure 1.3) converting some hydrophobic sites into hydrophilic sites, which contributes to improved dispersion of the ATTM precursor during its impregnation; and 2) less mass transport limitations of solvent and products are encountered during reactions of air-dried coals at 350°C. In addition, we also examined the effect of drying ATTM-impregnated coal in air, as this may be more practical than vacuum drying for large scale application. ATTM was loaded on the raw coal by incipient wetness impregnation, followed by either vacuum-drying or air drying at 100°C for 2 h. The results given in Table 1.5 reveal that these two methods afford similar coal conversions (44-46 wt%) and oil yields (16-18 wt%) for runs with tetralin solvent at 350°C.

The fourth effect associated with drying is oxidation. It should be noted that, relative to vacuum drying, the advantage of air drying completely diminishes upon increasing the severity to 150°C for 20 h, both in thermal (Table 1.1) and catalytic runs (Table 1.2). In other words, high-severity air drying or oxidation has unambiguously negative impact on catalytic as well as thermal liquefaction of the coal. Such a clearly deleterious effect of severe oxidation on coal liquefaction is considered to arise from significantly increased oxygen functionality, which enhances the cross-link formation in the early stage of coal liquefaction.

Additional Results on Liquefaction at 425°C. We also carried out both catalytic and non-catalytic liquefaction of DECS-8 Wyodak coal in the 25-mL batch reactors at 425°C for 30 min under an initial (cold) H_2 pressure of 6.9 MPa in the presence of H-donor tetralin solvent.

Table 1.6 shows the results of non-catalytic runs at 425°C. Relative to the runs of the raw coal, conversions of the vacuum-dried coal are higher. The oil yields from the latter are also higher than those from the former. The conversions of air-dried coal (runs 187, 201) are also higher than those of raw coal (runs 186, 199), but are lower than those of vacuum-dried coal (runs 189, 200). These results indicate pre-drying has positive effects on the non-catalytic liquefaction of Wyodak coal, and vacuum-drying is better than air-drying in terms of higher comversion and oil yield. Extending the air-drying time from 2 to 20 h decreased oil yield but

increased CO_2 yield, as expected. In the first volume of our final report (section 3.2.2), we also reported the results on the effect of moisture in non-catalytic liquefaction of three low-rank coals (DECS-1, DECS-9, DECS-11) in the absence of any solvent and catalyst. These three coals also contain large amounts of moisture ranging from 25 to 33 wt%. The moisture contents of the three coal samples pre-dried for different duration (2-6 h) can be found in an earlier progress report for this project (TPR-3, Table 8). It was found that, for solvent-free liquefaction at 400°C, vacuum-dried coals gave slightly better or similar conversions compared to the fresh raw coals. However, the product distributions are differeent. The yields of oil are higher with the dried coals than with the raw coals (see Table 3.3 in Vol. 1 of the Final Report). It thus appears that pre-drying is beneficial for a desirable product slate under the conditions employed.

Table 1.6 also lists the hydrogen consumption data for DECS-8 Wyodak coal. In the non-catalytic runs, the amount of hydrogen transferred from tetralin solvent was always higher than that from gas-phase H_2, regardless of the coal type and drying methods. It is apparent from these data that, in the absence of added catalyst, the hydrogen in the hydroaromatic ring of tetralin is more effective for stabilizing thermally derived radicals. In other words, the coal-derived radicals can abstract hydrogen more readily from tetralin than from molecular H_2.

Table 1.7 shows the results of liquefaction using ATTM impregnated on either raw or pre-dried DECS-8 Wyodak coal at 425°C. Unlike the non-catalytic runs, the catalytic runs at 425°C using ATTM impregnated on the raw and pre-dried coals afforded similar conversions and oil yields. The coal conversion in all the catalytic runs approached 90 wt%. This conversion level is very high and close to the upper limit of convertible materials in DECS-8 Wyodak coal, since it contains 78.9 vol% vitrinite (huminite), 11.8 vol% liptinite, and 9.3 vol% inertinite. The difference in the physico-chemical properties of the coal samples (prior to ATTM impregnation) caused by pre-drying and oxidation was largely compensated by the catalyst, and to a lesser degree, by H-donor solvent. It appears that the dispersed Mo sulfide catalyst in situ generated from impregnated ATTM is very active for runs at 425°C. Therefore, whether the coal has been pre-dried or mildly oxidized (weathered) makes no major difference on conversion at 425°C if ATTM is to be impregnated onto Wyodak subbituminous coal from its aqueous solution.

The yields of C_1-C_4 gases from catalytic runs are higher than the corresponding non-catalytic runs, as can be seen from comparing Table 1.7 with Table 1.6. The increased C_1-C_4 gases are due to catalytic hydrogenolysis of C-C bonds, including cleavage of aromatic-alipatic C-C bonds which either connects to the peripheral alkyl groups or bonds to another aromatic ring. In all the catalytic runs, the yields of C_1-C_4 hydrocarbon gases from air-dried coals are consistently lower than those from the vacuum-dried samples. This is an indirect indication that there are relatively less alkyl groups in the air-dried samples (Table 1.7). This observation is consistent with the CPMAS ^{13}C NMR (Figutre 1.2) and FT-IR (Figure 1.3) results.

Table 1.6 Non-Catalytic Liquefaction of Raw and Pre-Dried DECS-8 Wyodak Coal at 425°C for 30 min under 6.9 MPa H_2

Expt No.	Drying conditions	Solvent	CO	CO_2	C_1-C_4	Oil	Asphal.	Preasp.	Tot. Conv.	H from[a]	H from[a]
			dmmf wt%						dmmf wt%	H_2 Gas	Tetralin
186	Fresh raw coal[b]	Tetralin	0.3	22.3	2.3	25.7	14.5	14.7	69.5	0.67	1.26
199	Fresh raw coal[b]	Tetralin	0.3	21.1	2.5	24.1	12.0	14.4	67.6	0.72	1.19
189	Vacuum, 100°C, 2 h	Tetralin	0.4	11.7	2.9	38.9	11.6	22.4	82.2	0.42	1.35
200	Vacuum, 100°C, 2 h	Tetralin	0.5	14.7	2.3	46.2	11.7	13.2	81.8	0.53	1.42
187	Air, 100°C, 2 h	Tetralin	0.6	15.1	2.9	35.7	14.8	14.8	76.6	0.56	1.36
201	Air, 100°C, 2 h	Tetralin	0.6	13.5	2.9	39.1	13.1	13.5	76.7	0.66	1.32
188	Air, 100°C, 20 h	Tetralin	0.6	17.1	3.0	29.9	13.5	24.3	79.5	0.65	1.54

a) H consumption, wt% based on dmmf coal.

b) Raw (fresh, as-received) coal, which contains moisture, was directly used for liquefaction.

Table 1.7 Catalytic Liquefaction at 425 °C Using ATTM Impregnated on Raw and Dried DECS-8 Wyodak Coal

Expt No.	Drying conditions	Solvent	CO	CO_2	C_1-C_4	Oil	Asphal.	Preasp.	Tot. Conv.	H from[a]	H from[a]
			dmmf wt%						dmmf wt%	H_2 Gas	Tetralin
195	Fresh raw coal[b]	Tetralin	0.2	17.8	4.1	53.2	14.5	5.5	84.9	1.57	1.02
202	Fresh raw coal[b]	Tetralin	0.2	15.3	4.1	51.6	16.7	8.3	89.3	1.70	0.97
196	Vacuum, 100°C, 2 h	Tetralin	0.1	12.6	4.0	51.4	7.9	19.4	88.6	1.49	0.96
203	Vacuum, 100°C, 2 h	Tetralin	0.1	12.5	3.9	46.2	8.7	21.4	89.0	1.54	1.01
197	Air, 100°C, 2 h	Tetralin	0.1	11.9	3.2	54.8	11.6	13.7	89.3	1.63	0.74
204	Air, 100°C, 2 h	Tetralin	0.1	12.4	3.1	52.1	8.7	16.9	89.6	1.59	0.87
198	Air, 100°C, 20 h	Tetralin	0.2	12.5	3.3	53.9	7.6	13.3	87.6	1.44	0.73

a) H consumption, wt% based on dmmf coal.

b) Raw (fresh as-received) coal was used for catalyst impregnation followed by vacuum drying at 100 °C for 2 h before liquefaction.

In all the catalytic runs, the consumption of gas-phase H_2 was always higher than the amount of hydrogen transferred from tetralin solvent, regardless of the coal type and drying methods. This trend shows that Mo sulfide catalyst promotes dissociation of molecular H_2 and the transfer of H to coal. It is also interesting to note that the runs using ATTM impregnated on raw coal gave considerably higher CO_2 yields that those using predried coal (Table 1.7), although all the ATTM-loaded samples were vacuum-dried prior to liquefaction.

Additional FT-IR Spectra of Raw, Dried, and THF-extracted DECS-8 Samples and Their Residues. We have discussed some FT-IR difference spectra without showing the original FT-IR spectra in previous sections. For additional information, Figures 1.12 to 1.16 provide the original FT-IR spectra of raw, dried, and THF-extracted DECS-8 coal samples and their residues from non-catalytic and catalytic runs at 350°C.

Additional CPMAS ^{13}C NMR Spectra and Py-GC-MS Profiles of Raw, Dried, and THF-extracted DECS-8 Samples and Their Residues. In previous sections, we only showed the NMR spectra of the dried but un-treated (un-liquefied) samples. There are more NMR data that we have not discussed above. For additional information, Figures 1.17 to 1.20 provide more CPMAS ^{13}C NMR spectra of raw, dried, and THF-extracted DECS-8 coal samples and their residues from non-catalytic and catalytic runs at 350°C. Figure 1.21 gives the selective ion monitoring of long-chain paraffins at m/z 71 from Py-GC-MS profiles of raw and dried DECS-8 samples and their residues from solvent-free non-catalytic pretreatment (low-severity liquefaction) runs at 350°C.

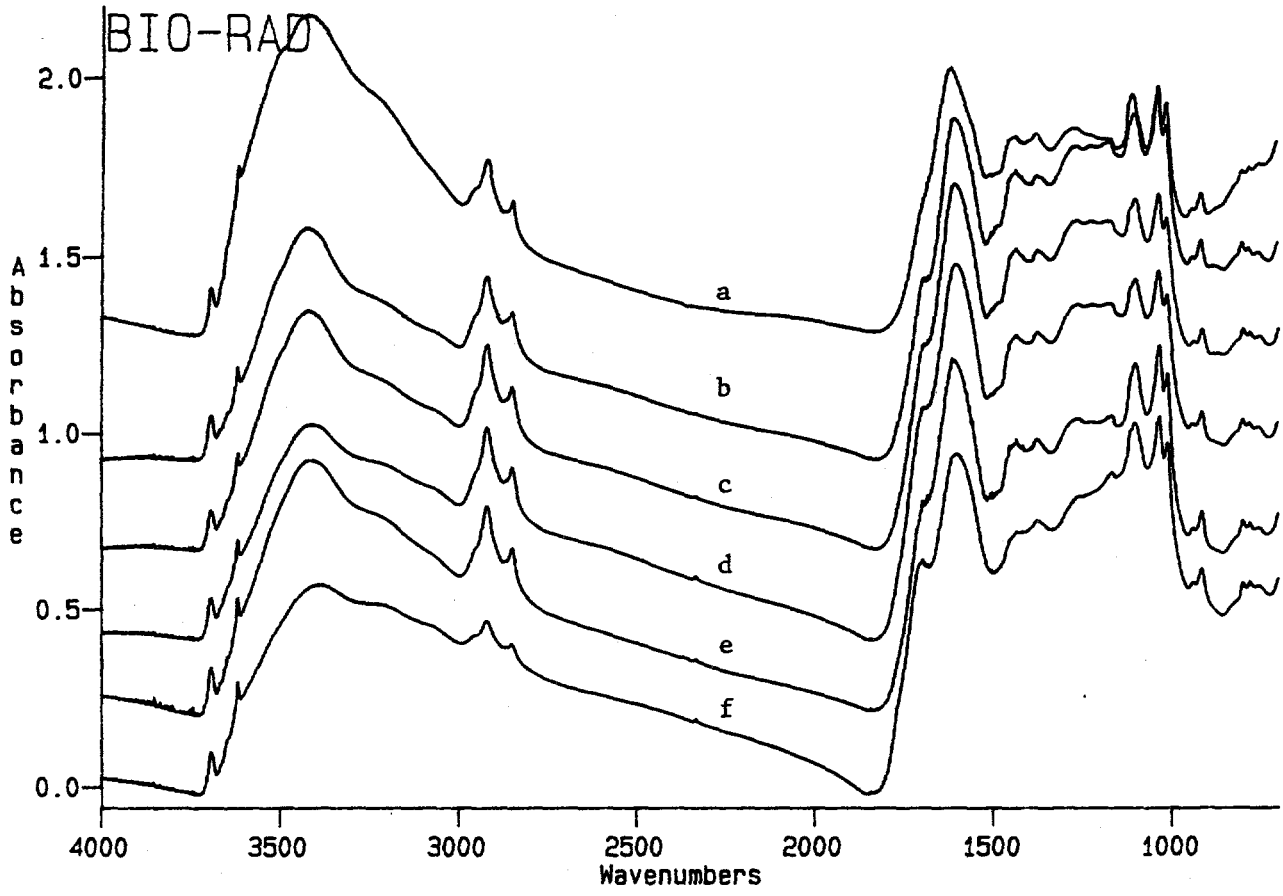

Figure 1.12 FTIR spectra of the DECS-8 raw coal a) as-received; dried in air at 100 °C for b) 2 h; c) 20 h; d) 100 h; e) dried at 125 °C for 20 h; and f) at 150 °C for 20 h.

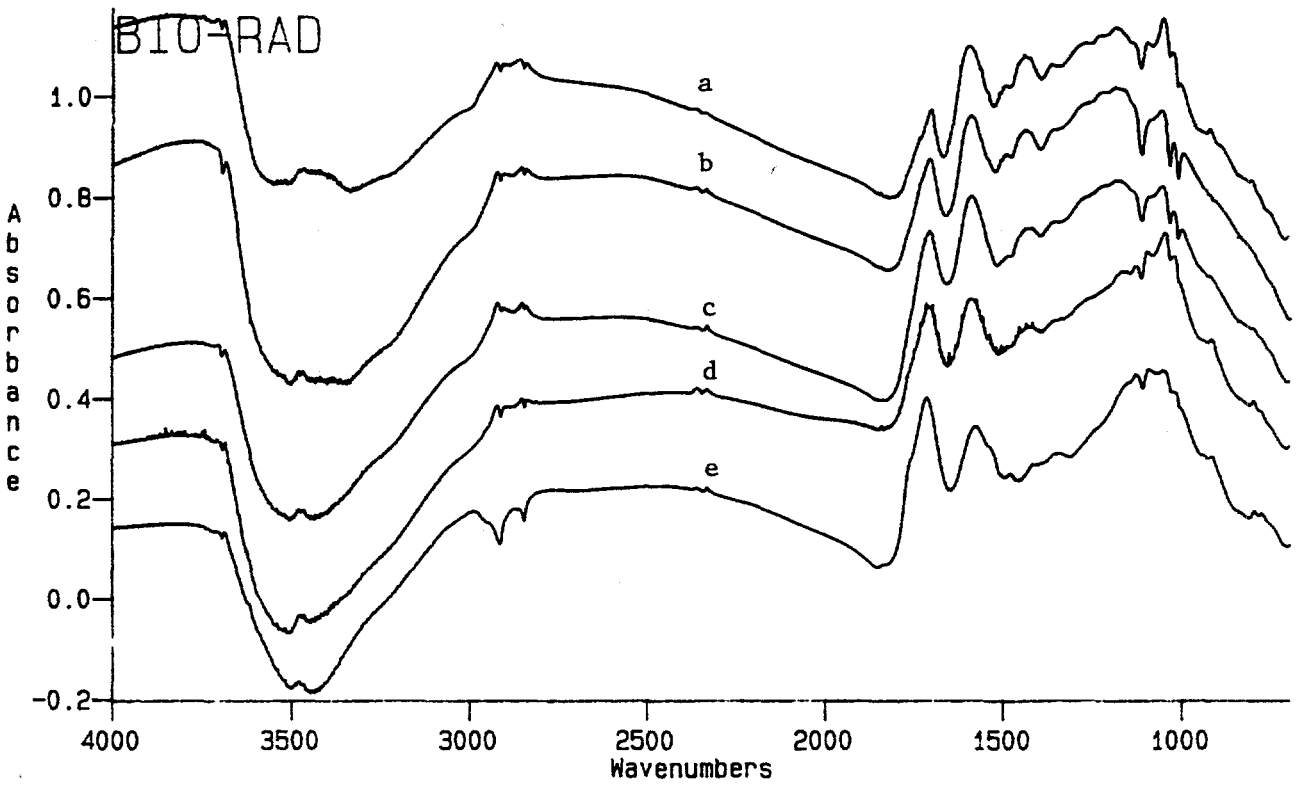

Figure 1.13 FTIR difference spectra after subtracting the FTIR spectrum of the raw coal 'as received' from the FTIR spectra of the coal dried in air at100 °C for a)2 h; b) 20 h; c) 100 h; d) coal dried at 125 °C for 20 h and e) at 150 °C for 20 h.

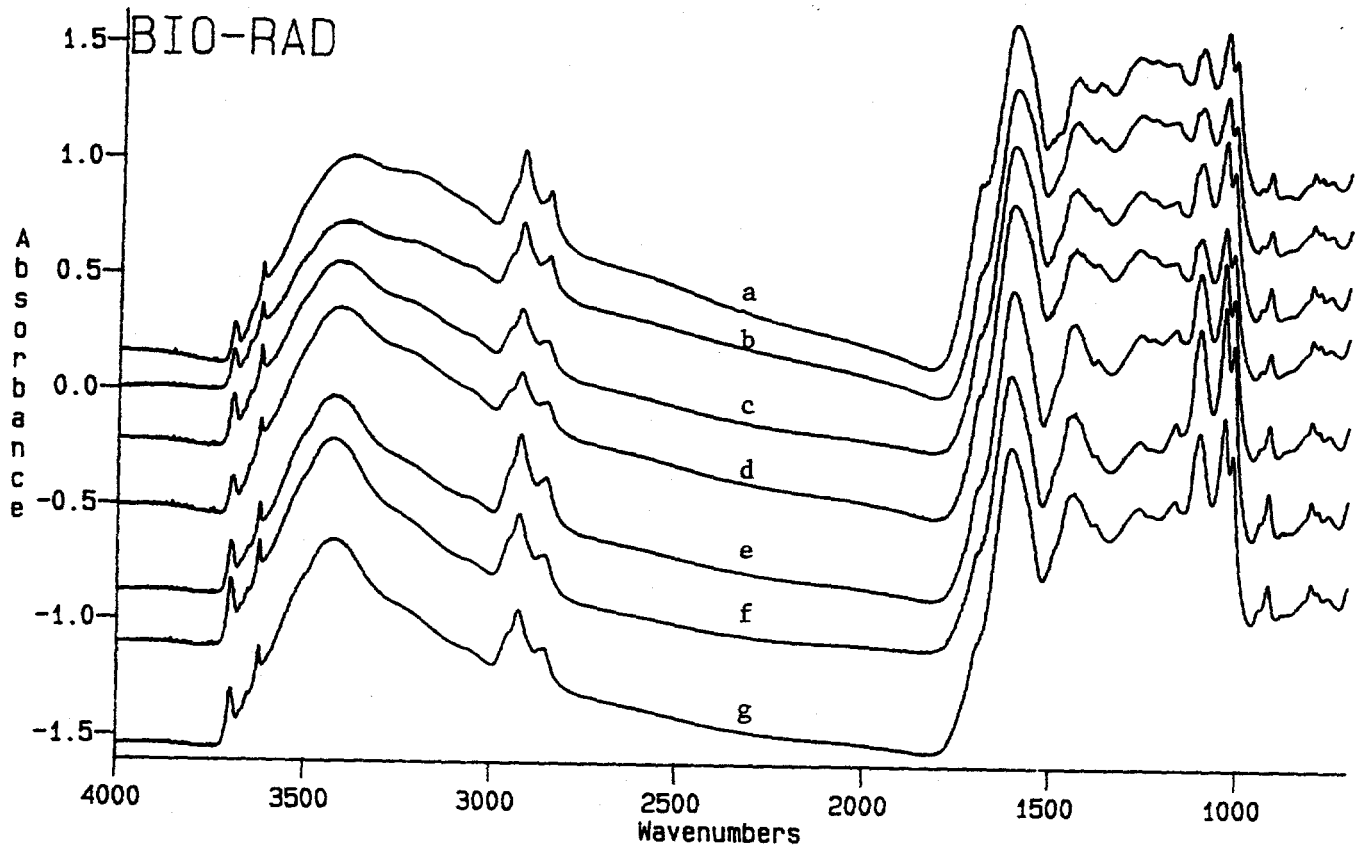

Figure 1.14 FTIR spectra of the THF-extracted coal dried in air for 2 h at 100 °C; a) unreacted; and reacted at 350 °C without catalyst; b) solvent free; c) with tetralin; d) with 1-methylnaphthalene; and in presence of catalyst; e) solvent free; f) with tetralin; g) with 1-methyl-naphthalene.

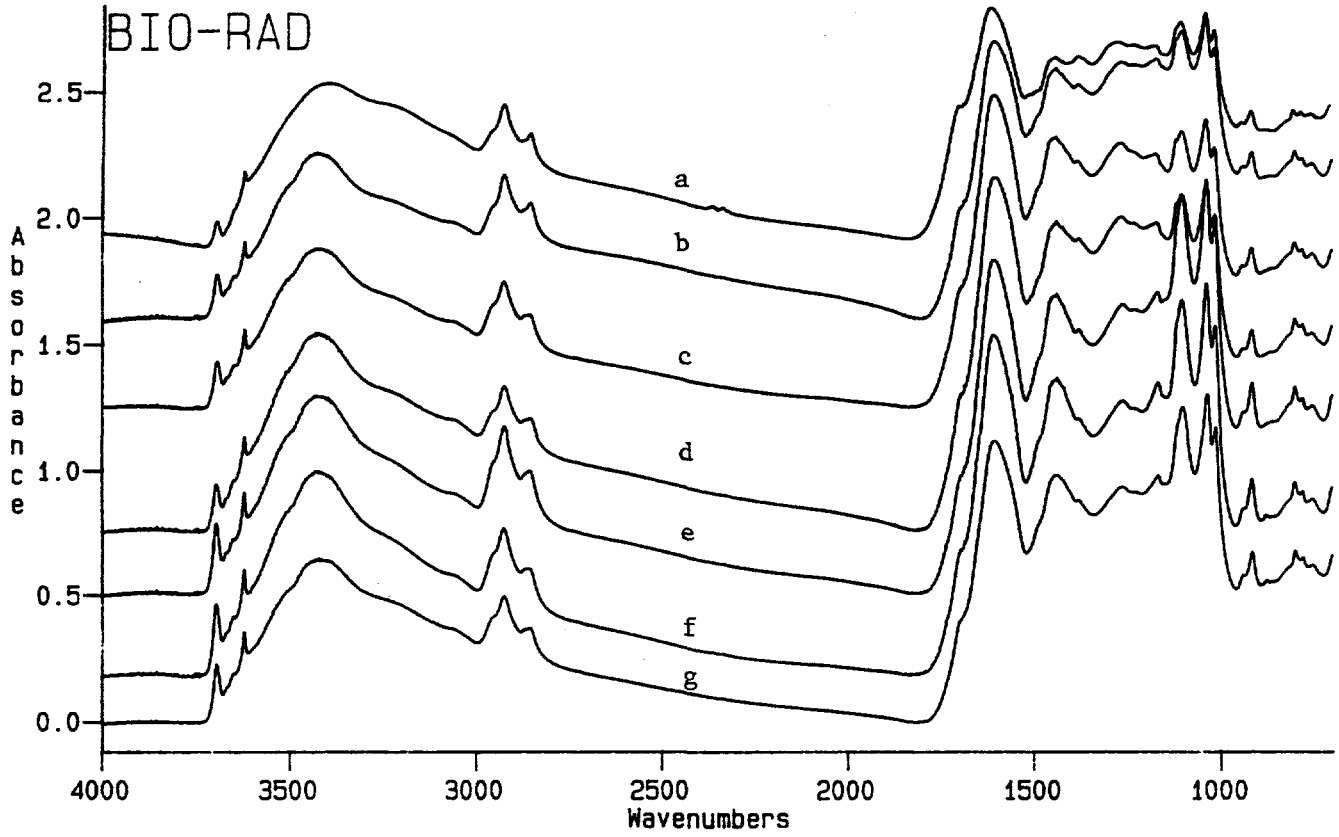

Figure 1.15 FTIR spectra of the THF-extracted coal dried in air for 20 h at 100 °C; a) unreacted; and reacted at 350 °C without catalyst; b) solvent free; c) with tetralin; d) with 1-methylnaphthalene; and in presence of catalyst; e) solvent free; f) with tetralin; g) with 1-methyl-naphthalene.

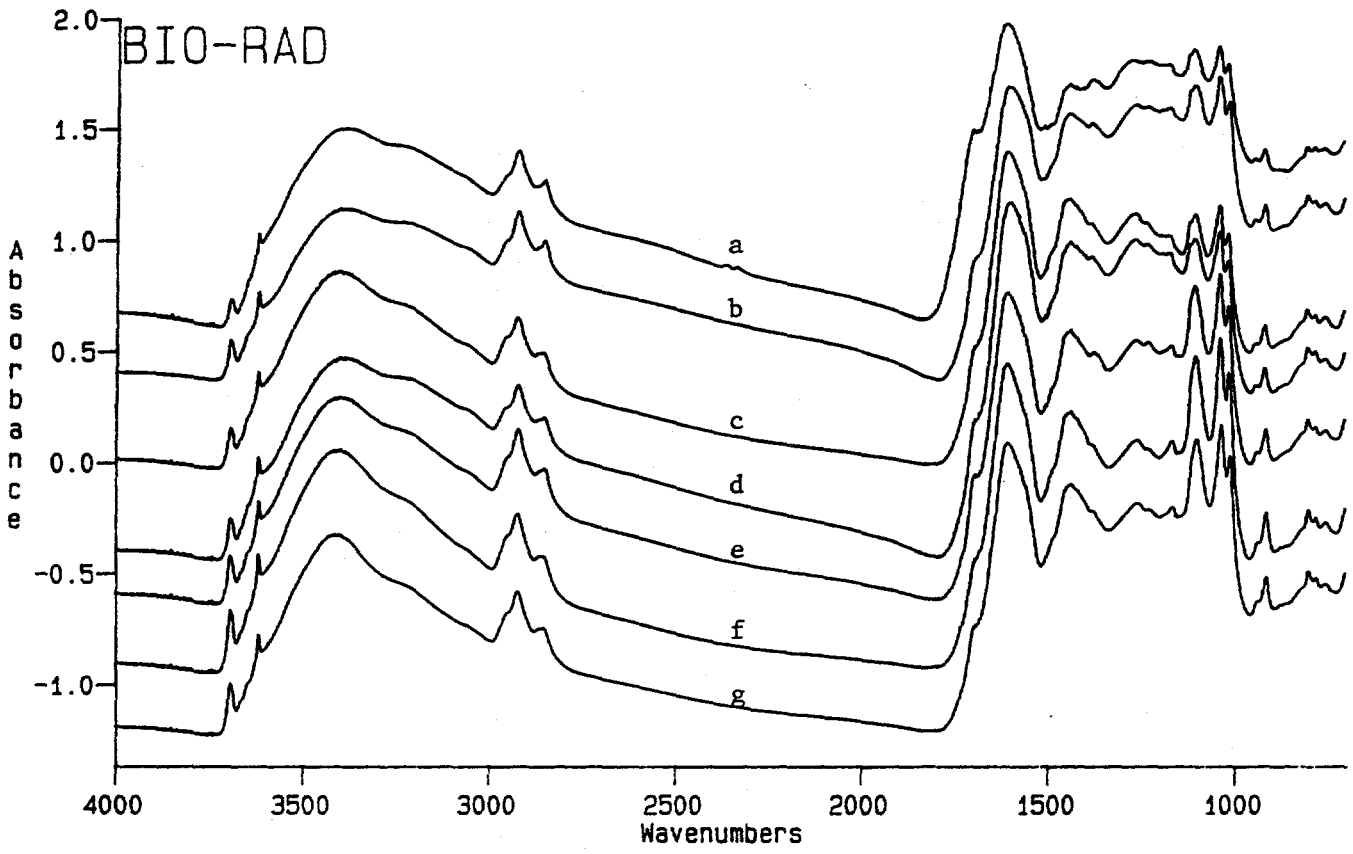

Figure 1.16 FTIR spectra of the THF-extracted coal dried in air for 100 h at 100 °C;a) unreacted; and reacted at 350 °C without catalyst; b) solvent free; c) with tetralin; d) with 1-methylnaphthalene; and in presence of catalyst ; e) solvent free; f) with tetralin; g) with 1-methyl-naphthalene.

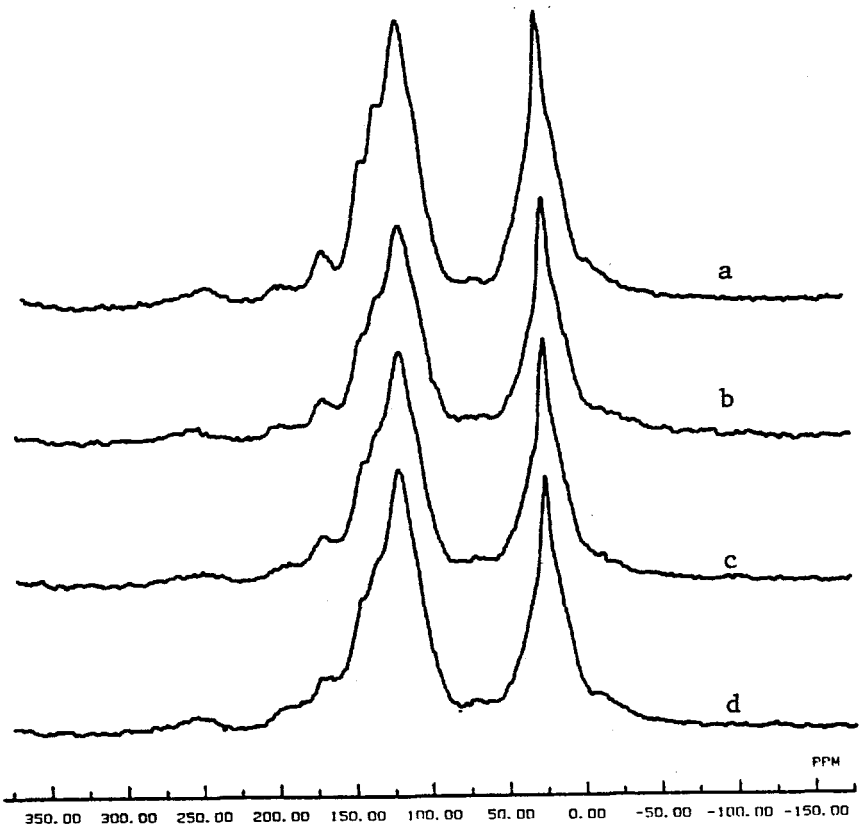

Figure 1.17 CPMAS ^{13}C NMR spectra of the coal a) raw as received; dried in air at 100 °C for; b) 2 h; c) 20 h; d) 100 h.

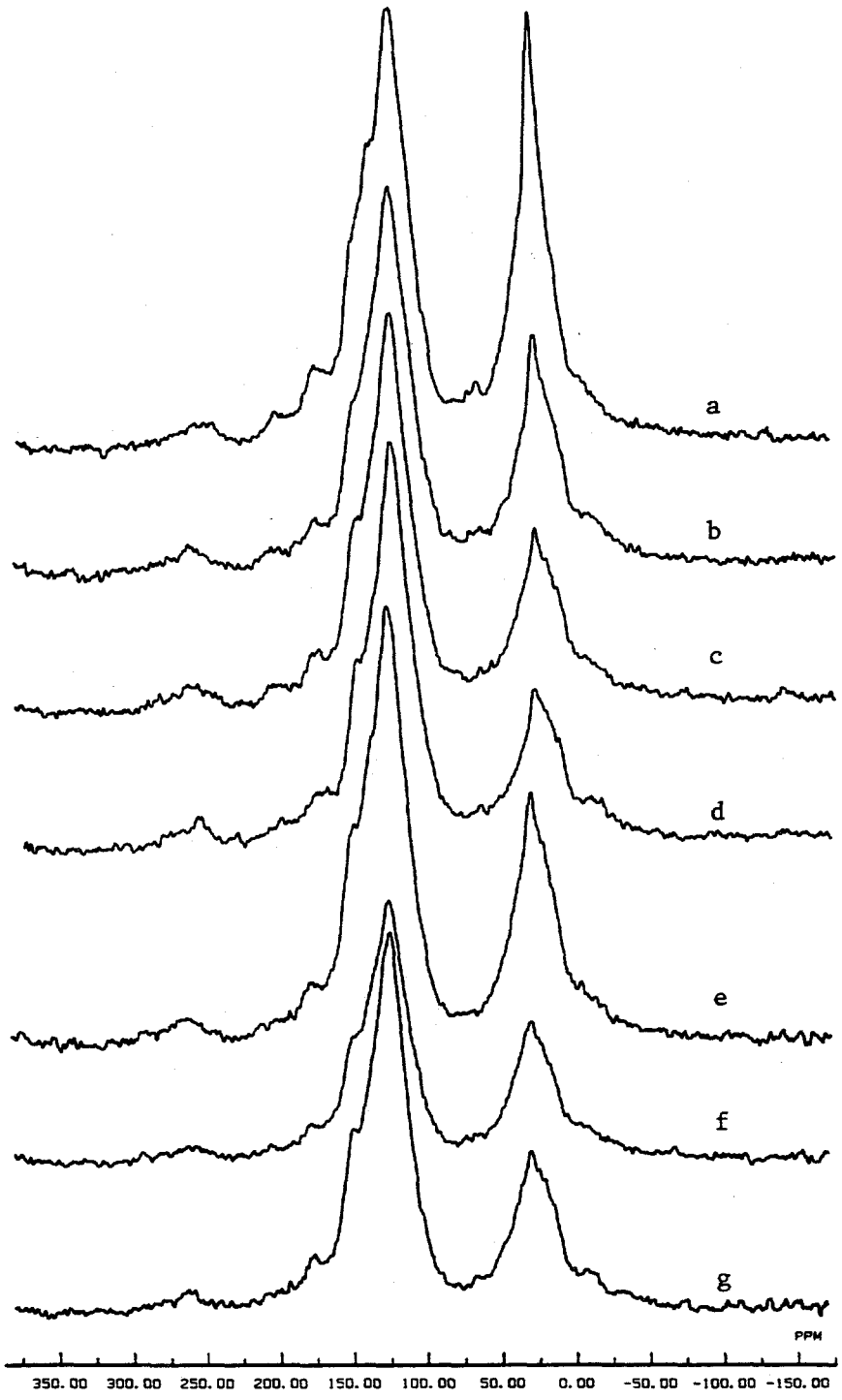

Figure 1.18 CPMAS ^{13}C NMR spectra of the THF-extracted coal dried in air for 2 h at 100 °C; a) unreacted; and reacted at 350 °C without catalyst; b) solvent free; c) with tetralin; d) with 1-methylnaphthalene; and in presence of catalyst; e) solvent free; f) with tetralin; g) with 1-methyl-naphthalene.

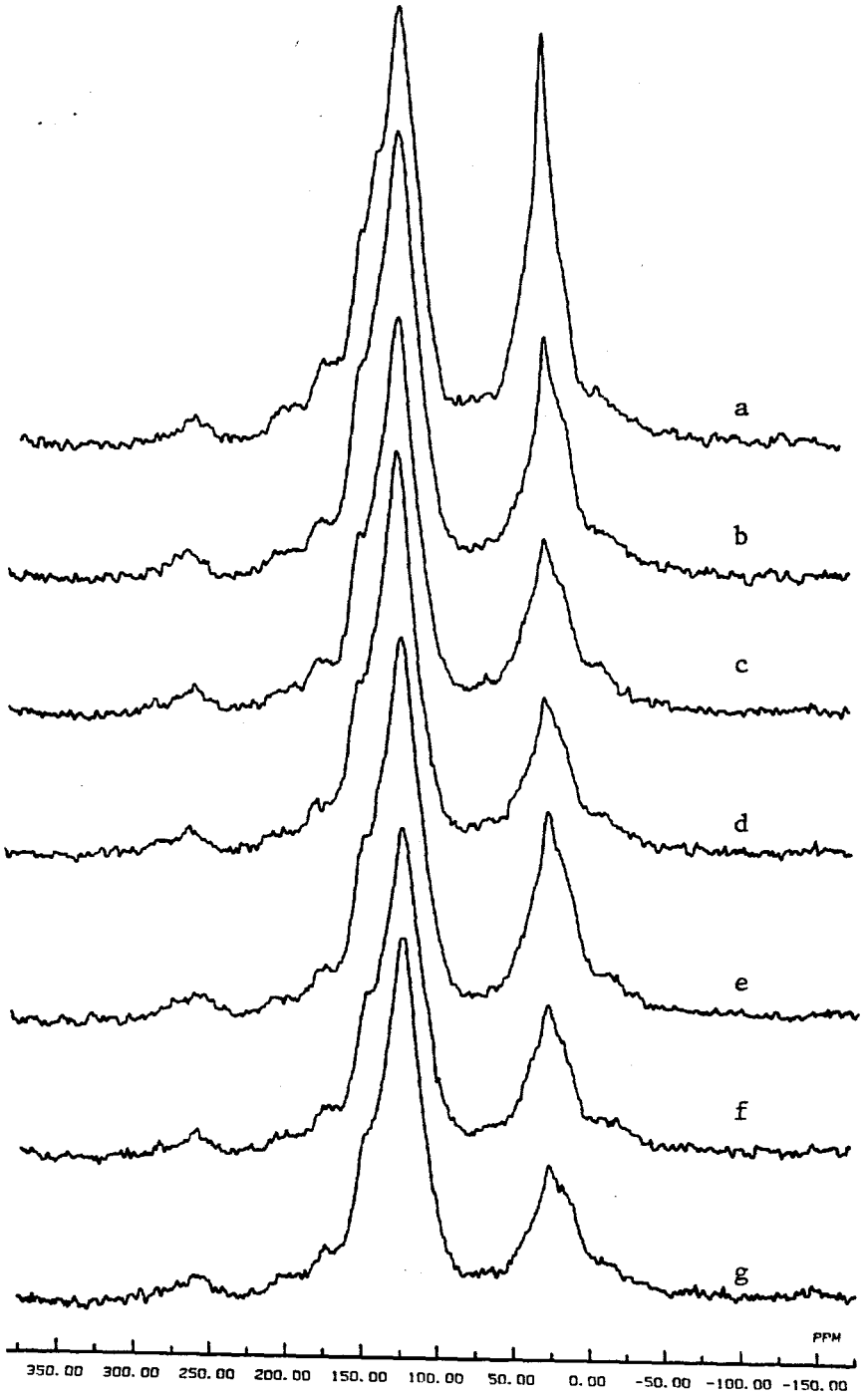

Figure 1.19 CPMAS ^{13}C NMR spectra of the THF-extracted coal dried in air for 20 h at 100 °C; a) unreacted; and reacted at 350 °C without catalyst; b) solvent free; c) with tetralin; d) with 1-methylnaphthalene; and in presence of catalyst; e) solvent free; f) with tetralin; g) with 1-methyl-naphthalene.

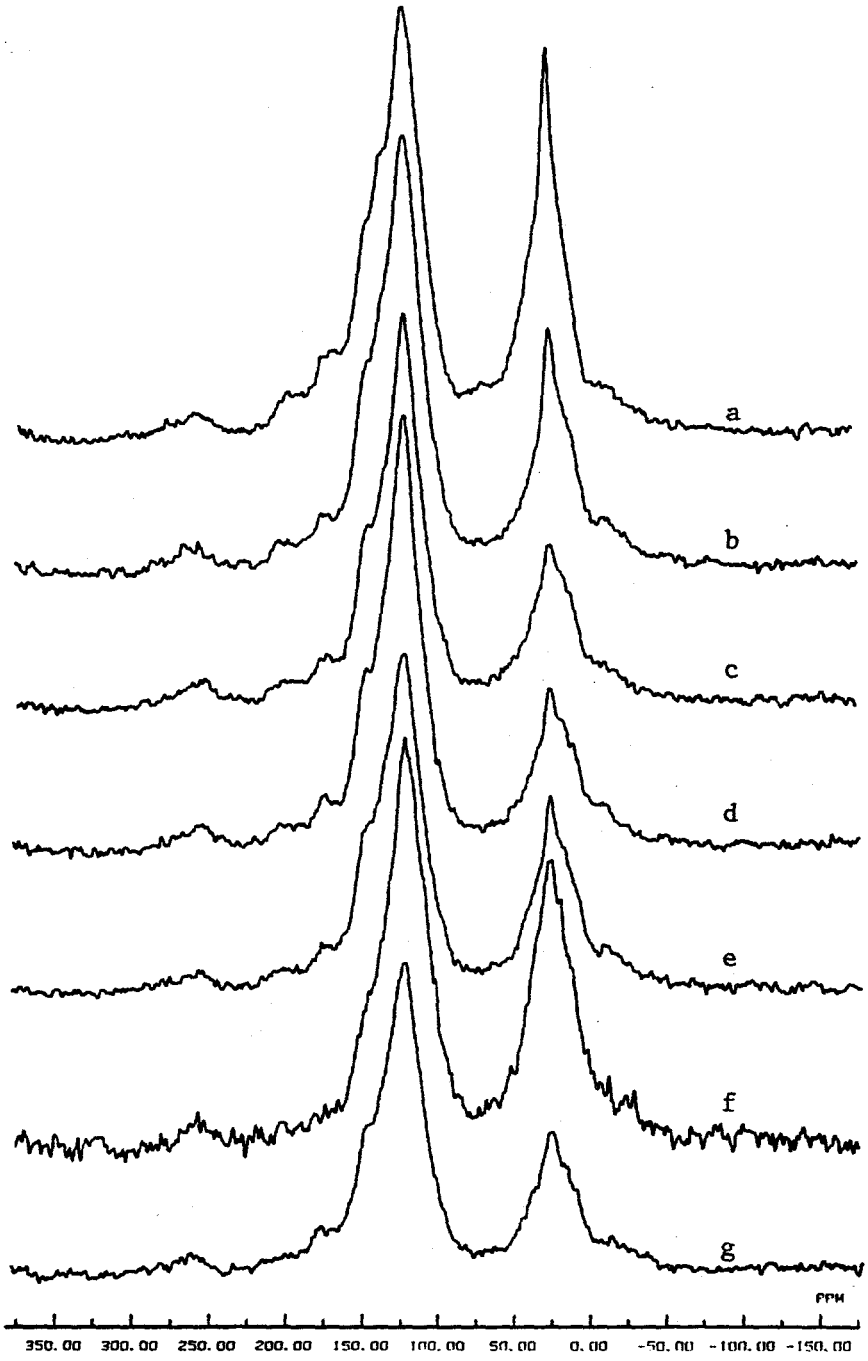

Figure 1.20 CPMAS ^{13}C NMR spectra of the THF-extracted coal dried in air for 100 h at 100 °C; a) unreacted; and reacted at 350 °C without catalyst; b) solvent free; c) with tetralin; d) with 1-methylnaphthalene; and in presence of catalyst; e) solvent free; f) with tetralin; g) with 1-methyl-naphthalene.

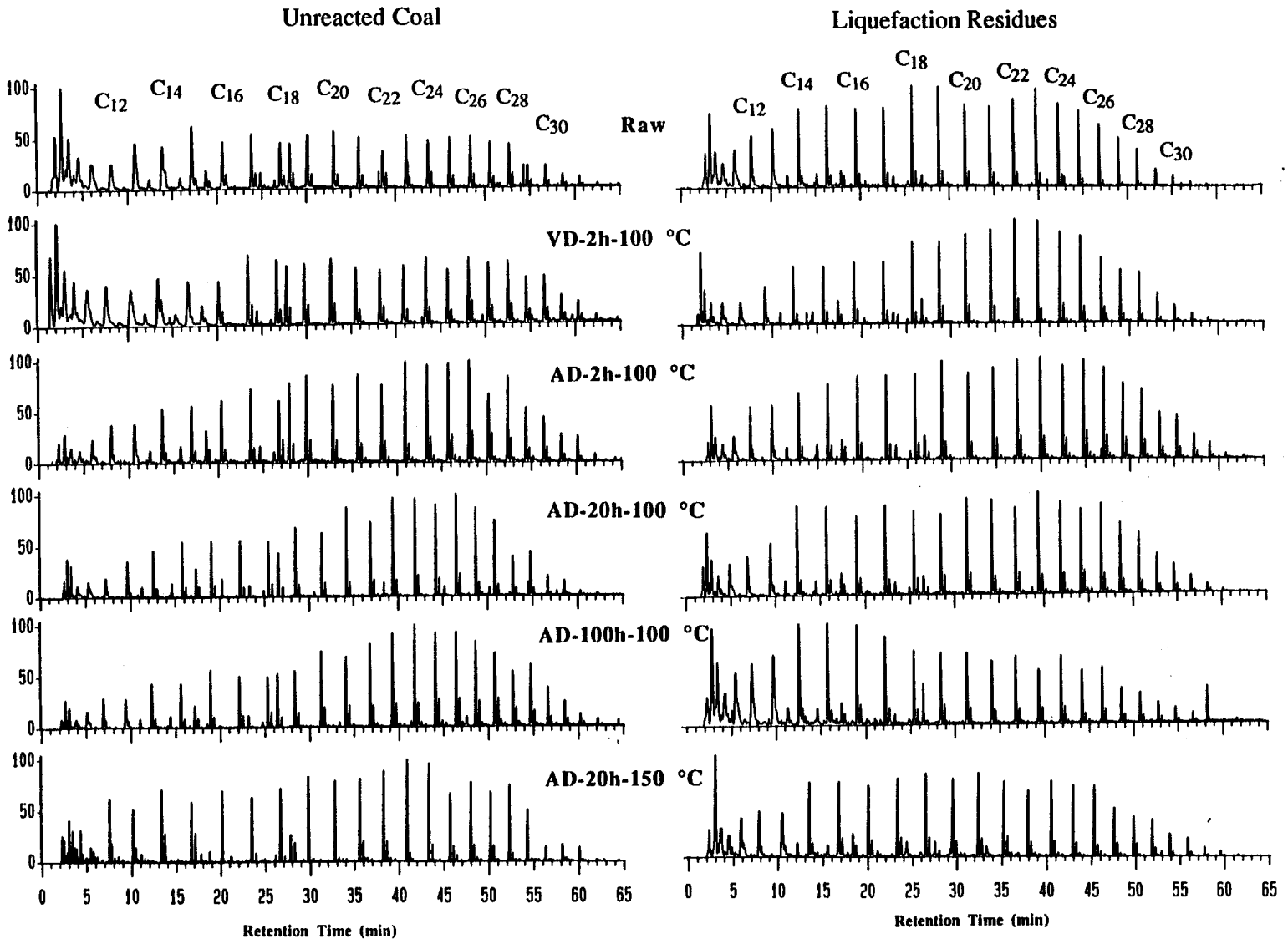

Figure 1.21 Selected ion monitoring of paraffins at m/z 71 from Py-GC-MS profiles of the; A) raw and dried coal at different conditions and; B) their residues from solvent-free non-catalytic liquefactions.

Summary and Conclusions

Drying of Wyodak subbituminous coal (DECS-8), either under vacuum or in air at 100-150°C, can alter its physicochemical properties, which significantly affect its conversion, oil yields, and CO_2 yields both in non-catalytic and catalytic liquefaction at 350 °C.

Spectroscopic characterization using CPMAS ^{13}C NMR, Py-GC-MS, and FT-IR revealed that oxidative drying in air causes oxidation reactions leading to the formation of oxygen functional groups at the expense of aliphatic carbons. Furthermore, Py-GC-MS and NMR data also uncovered that oxidation of coal at 100-150°C can cause the transformation of phenolics and catechol into other related structures (presumably through condensation, or crosslinking), and high-severity air drying at 150°C for 20 h leads to disappearance of catechol from Py-GC-MS and NMR spectra.

For thermal liquefaction runs at 350°C, fresh raw coal gave higher conversion and higher oil yield than the dried coals, regardless of the solvent. In the presence of either H-donor or non-donor solvent, the coal dried in air at 100 °C for 2 h gave a better conversion as compared to the vacuum-dried coal. Runs of raw coal always produces more CO_2 than those of the vacuum-dried coal, both with and without solvent.

For catalytic runs using ATTM impregnated on coal, predrying has negative impacts for solvent-free liquefaction at 350°C. Namely, the runs using ATTM loaded on the raw coal gave higher conversion and higher oil yield than loading ATTM on vacuum- or air-dried coals. In the presence of either tetralin or 1-MN, however, predrying coal in air prior to ATTM impregnation has slightly beneficial effect, at least no apparent negative impact, on coal conversion as compared to the case using raw coal. The runs using ATTM loaded on air-dried coal with either tetralin or 1-MN solvent afford better conversions and oil yields as compared to the runs using vacuum-dried coal. These observations can be rationalized by taking into account the spectroscopic characterization data and the four physicochemical factors associated with drying and oxidation effects mentioned above.

The effect of non-oxidative (vacuum) drying on coal conversion in thermal liquefaction at 350°C is due primarily to the removal of water and secondarily to the physicochemical changes of coal induced by drying. Adding water back to the vacuum-dried coal can restore over 90 % of the conversion of the fresh raw coal in the runs without solvent and with H-donor solvent. For catalytic runs using impregnated ATTM, the effect of predrying is mainly caused by the drying-induced physicochemical changes such as those in pore structure (mass transport) and surface characteristics. If the moisture loss has occurred (due to deliberate or inadvertent drying),

prewetting the dried coal with water before impregnation of the metal salt from its aqueous solution can help to improve the performance of resulting catalyst.

Upon highly oxidative drying coal in air at 150 °C for 20 h, the conversion significantly decreased to a lower value than that of the vacuum-dried coal in the non-catalytic runs. The same trend was observed in the runs of the dried coals loaded with ATTM. Such a clearly negative impact of severe oxidation on coal liquefaction is considered to arise from significantly increased oxygen functionality which enhances the cross-link formation in the early stage of coal liquefaction.

Although mildly oxidative drying at 100°C displayed beneficial effects relative to vacuum drying for liquefaction at 350°C, this advantage may not be valid for liquefaction at higher temperatures such as 400-425°C. The Py-GC-MS results of the dried coals (Figures 4) and the residues (Figures 10, 11) suggest that oxidation can induce more crosslinking at high temperatures, which can lead to lower conversion or poorer products distribution.

For non-catalytic liquefaction at 425°C in the presence of tetralin solvent, our results indicate that pre-drying has positive effects on the non-catalytic liquefaction of Wyodak coal, and vacuum-drying is better than air-drying in terms of higher coversion and oil yield. Unlike the non-catalytic runs, the catalytic runs at 425°C using ATTM impregnated on the raw and pre-dried coals afforded similar conversions and oil yields. The coal conversion in all the catalytic runs approached 90 wt%. The difference in the physico-chemical properties of the coal samples (prior to ATTM impregnation) caused by pre-drying and oxidation was largely compensated by the catalyst, and to a lesser degree, by H-donor solvent. Therefore, if ATTM (water-soluble) is to be impregnated onto Wyodak subbituminous coal from its aqueous solution, whether the coal has been pre-dried or mildly oxidized (weathered) makes no major difference on liquefaction conversion at 425°C. However, this conclusion does not apply to the catalytic liquefaction using oil-soluble Mo catalyst precursor.

References

1. Schobert, H. H. (Ed.) The Chemistry of Low-Rank Coal. ACS Symposium Series 264, American Chemical Society: Washington D.C., **1984**, 305pp.
2. Lavine, I.; Gauger, A. W. *Ind. Eng. Chem.* **1930**, 22, 1226.
3. Larian, M.; Lavine, I.; Mann, C. A.; Gauger, A. W. *Ind. Eng. Chem.* **1930**, 22, 1231
4. Lavine, I.; Gauger, A. W.; Mann, C. A. *Ind. Eng. Chem.* **1930**, 22, 1347.
5. Gordon, M.; Lavine, I.; Harrington, L. C. *Ind. Eng. Chem.* **1932**, 24, 928.
6. Lavine, I. *Ind. Eng. Chem.* **1934**, 26, 154.
7. Goodman, J. B.; Gomez, M.; Parry, V. F.; U. S. Bur. Mines Rept. 4969, **1953**.

8. Hoeppner, J. J.; Fowkes, W. W.; McMurtrie, R. U. S. Bur. Mines Rept. 5215, **1956**.
9. Hube, W. R. *Chem. Eng. Data Ser.* **1957**, 2, 46.
10. Abernathy, R. F.; Tarplay, E. C.; Drogowski, R. A.; U. S. Bur. Mine Rept. 6440, **1964**.
11. Tye, C.; Neumann, R. M.; Schobert, H. H. *Prep. Pap.-Am. Chem. Soc. Div. Fuel Chem.* **1985**, 30(1), 134
12. Schobert, H. H.; Neumann, R. M.; Tye, C.; Bale, H. D.; Hauserman, W. B.; U. S. Dept. Energy Rept. DOE/FE/60181-2096, **1986**.
13. Vorres, K. S.; Kolman, R.; Griswold, T. *Prepr. Pap.-Am. Chem. Soc. Div. Fuel Chem.*, **1988**, 33(2), 333.
14. Vorres, K. S.; Wertz, D. L.; Malhotra, V.; Dang, Y.; Joseph, J. T.; Fisher, R. *Fuel*, **1992**, 71, 1047.
15. Vorres, K. S. *Prepr. Pap.-Am. Chem. Soc. Div. Fuel Chem.* **1993**, 38(2), 587.
16. a) Wroblewski, A. E.; Verkade, J. G. *Energy and Fuels* **1992**, 6, 331; b) Miknis, F. P.; Netzel, D. A.; Turner, T. F. *Prepr. Pap.-Am. Chem. Soc. Div. Fuel Chem.* **1993**, 38 (2), 609.
17. Serio, M. A.; Soloman, P. R.; Kroo, E.; Bassilakis, R.; McMillan, D. *Prepr. Pap.-Am. Chem. Soc., Div. Fuel Chem.* **1990**, 35(1), 61.
18. Suuberg, E. M.; Otake, Y.; Yun, Y.; Deevi, S. C. *Energy and Fuels* **1993**, 7, 384.
19. Gorbaty, M. L. *Fuel* , **1978**, 57, 796.
20. Atherton, L. E. *Proc. Int. Conf. Coal Sci.* **1985**, 553.
21. Neavel, R. *Fuel* **1976**, 55, 237.
22. Cronauer, D.C., Ruberto, R.G., Silver, R.S., Jenkins, R.G., Davis, A., Hoover, D.S. *Fuel*, **1984**, 63, 77.
23. a) Huang, L.; Song, C.; Schobert, H. H. *Prepr. Pap.-Am. Chem. Soc. Div. Fuel Chem.*, **1992**, 37 (1), 223; b) Song, C.; Parfitt, D. S.; Schobert, H. H. *Prepr. Pap.-Am. Chem. Soc. Div. Fuel Chem.*, **1993**, 38 (2), 546.
24. a) Song, C.; Hanaoka, K.; Nomura, M. *Energy and Fuel* **1988**, 2, 639; b) Song, C; Schobert, H.H. *Prepr. Pap.-Am. Chem. Soc. Div. Fuel Chem.* **1992**, 37(2), 976.
25. a) Song, C.; Saini, A. K.; Schobert, H. H. *Prepr. Pap.-Am. Chem. Soc. Div. Fuel Chem.* **1993**, 38 (3), 1031; b) Song, C.; Saini, A.K.; Schobert, H.H. *Proc. 1993 Int. Conf. Coal Sci.*, Banff, Canada, Sept. 12-17, **1993**, Vol. I, p.291
26. a) Song, C.; Hou, L.; Saini, A. K.; Hatcher, P. G.; Schobert, H. H. *Fuel Proc. Technol.* **1993**, 34, 249; b) Hatcher, P. G.; Wilson, M. A.; Vassallo, A.M.; Lerch III, H.E. *Int. J. Coal Geol.* **1989**, 13, 99.
27. Cronauer, D. C.; Ruberto, R. G.; Jenkins, R. G.; Davis, A.; Painter, P. C.; Hoover, D. S.; Starsinic, M. E.; Schlyer, D. *Fuel* **1983**, 62, 1124.

28. Painter, P.; Starsinic, M.; Coleman, M. "Deterimination of Functional Groups in Coal by Fourier Transform Interferometry". in *"Fourier Transform INfrared Spectroscopy"*, J. R. Ferraro and L. J. Basile (Eds.), Academic Press: New York, 1985, Vol. 4, Chap. 5, p.169.

29. a) Painter, P.C.; Coleman, M.M.; Snyder, R.W.; Mahajan, O.; Komatsu, M.; Walker, P. L. Jr. *Appl. Spectroscopy*, **1981**, 35, 106; b) Painter, P.C.; Coleman, M.M.; Jenkins, R. G.; Whang, P.W.; Walker, P. L. Jr. Fuel **1978**, 57, 337.

30. Liotta, R.; Brons, G.; Isaacs, J. *Fuel*, 1983, 62, 781.

31. Artok, L.; Davis, A.; Mitchell, G. D.; Schobert, H. H. *Energy and Fuels* **1993**, 7, 67.

32. Huang, L.; Song,C.; Schobert, H.H. *Prepr. Pap.-Am. Chem. Soc., Div. Fuel Chem.* **1993**, 38 (3), 1093.

33. a) Song, C.; Nomura, M.; Ono, T. *Prepr. Pap. -Am. Chem. Soc., Div. Fuel Chem.* **1991**, 36 (2), 586; b) Song, C.; Parfitt, D. S.; Schobert, H. H. *Energy and Fuel* **1993**, submitted.

34. a) Song, C.; Hanaoka, K.; Nomura, M. *Energy and Fuel* **1992**, 6, 619; b) Song, C.; Nihinmatsu, T.; Nomura, M. Ind. Eng. Chem. Res. **1991**, 30, 1726.

35. a) Artok, L.; Schobert, H. H.; Erbatur, O. *Fuel Proc. Technol.*, **1993**, in press; b) Artok, L.; Davis, A.; Schobert, H. H. *Fuel Proc. Technol*. **1992**, 32, 87;

36. a) Saini, A.K.; Song, C.; Schobert, H.H. *Prepr. Pap. -Am. Chem. Soc., Div. Fuel Chem.* **1993**, 38 (2), 601; b) Saini, A.K.; Song, C.; Schobert, H.H. *Prepr. Pap. -Am. Chem. Soc., Div. Fuel Chem.* **1992**, 37 (3), 1235.

37. Graff, R. A.; Brandes, S. D. *Energy and Fuels* **1987**, 1, 84.

38. Bienkowski, P. R.; Narayan, R.; Greenkorn, R. A.; Chao, K. C. *Ind. Eng. Chem. Res.* **1987**, 26, 202.

39. Ross, D. S.; Loo, B. H.; Tse, D. S.; Hirchon, A. S. *Fuel* **1990**, 70, 289.

40. Pollack, N. R.; Holder, G. D.; Warzinski, R. P. *Prepr. Pap.-Am. Chem. Soc. Div. Fuel. Chem.* **1991**, 36(1), 15.

41. Tse, D. S.; Hirschon, A. S.; Malhotra, R.; McMillen, D. F.; Ross, D. S. *Prepr. Pap.-Am. Chem. Soc. Div. Fuel Chem.* **1991**, 36(1), 23.

42. Serio, M. A.; Kroo, E.; Teng, H. Soloman, P. R. *Prepr. Pap.-Am. Chem. Soc. Div. Fuel Chem.* **1993**, 38(2), 577.

43. Lewan, M. D. *Prepr. Pap.-Am. Chem. Soc., Div. Fuel Chem.* **1992**, 37 (4), 1643.

44. Petit, J. C. *Fuel* **1991**, 70, 1053.

45. a) Siskin, M.; Katritzky, A. R.; Balasubramanian, M. *Energy and Fuel* **1991**, 5, 770; b) Siskin, M.; Bron, G.; Vaughn, S. N.; Katritzky, A. R.; Balasubramanian, M. *Energy and Fuel* **1991**, 4, 488.

46. Swann, P. D.; Allardice, D. J.; Evans, D. G. *Fuel* **1974**, 53, 85.
47. Cited in Mahajan, O. "Coal Porosity" in "Coal Structure", R. A. Meyers (Ed.), Academic Press: New York, **1982**, Chap. 3, p.51.
48. Ramesh, R.; Somasundaran, P. *Coal Preparation*, **1991**, 9, 121.
49. Wei, D.; Chander, S.; Hogg, R. *Coal Preparation*, **1992**, 10, 37.
50. Gutierrez-Rodriguez, J.A.; Aplan, F.F. *Colloids and Surface*, **1984**, 12, 27.
51. Gray, M.L.; Lai, R.W.; Well, A.W. *Prepr. Pap.-Am. Chem. Soc., Div. Fuel Chem.* **1991**, 36(2), 804.
52. Weller, S.W. Coal Liquefaction with Molybdenum Catalysts. in H.F. Barry and P. C. H. (Eds.) "Chemistry and Uses of Molybdenum". Climax Molybdenum Co., Ann Arbor, MI, 1982, pp.179-186.
53. Arnold, B.J.; Aplan, F.F. *Fuel*, **1989**, 651.

CHAPTER 2. Strong Promoting Effect of H_2O on Catalytic Low-Severity Coal Hydroliquefaction (Pretreatment) Using Dispersed Mo Catalyst

Introduction

For coal hydroliquefaction using dispersed catalysts, drying after impregnation of catalyst or precursor salt has been a common procedure since 1950s.[1-9] The advantages of dispersed catalysts for direct coal liquefaction have been reviewed by Weller,[9] and by Derbyshire.[10] It is well known that water or steam deactivates hydrotreating catalysts, such as Mo-based catalysts, under conventional process conditions, and several groups have reported on the negative impacts of water on catalytic hydroliquefaction.[11-13]

The motivation of the present study comes from our recent work (Chapter 1) on the influence of mild pretreatments, drying and oxidation, of Wyodak subbituminous coal on its catalytic pretreatments, low-severity liquefaction.[14] As described in Chapter 1, we found that adding a small amount of water equivalvent to the original moisture content (28.4 wt%) back to the vacuum-dried or air-dried coal restored over 90 % of the conversion of the fresh raw coal in non-catalytic runs at 350 °C with and without solvents. This fact strongly suggests that the negative impact of drying on thermal (uncatalyzed) liquefaction reactions at 350°C is largely due to the removal of water. Another fact that puzzled us in the early stage of that work is that the conversions of fresh raw coal in the non-catalytic runs and catalytic runs with either tetralin or 1-methylnaphthalene (1-MN) solvent are very similar to each other, although the catalytic runs of the vacuum-dried or air-dried coal afforded significantly higher conversions than the corresponding thermal runs. These two facts prompted us to examine the effects of water addition in catalytic coal liquefaction.

This Chapter reports on the dramatic improvement of coal conversion upon addition of a small amount of water in low-severity liquefaction of Wyodak subbituminous coal using a dispersed molybdenum sulfide catalyst at 350 °C for 30 min. We will describe the strong synergistic effect between water and a dispersed mo-lybdenum sulfide catalyst for promoting low-severity liquefaction of Wyodak subbituminous coal. Addition of water to the catalytic run using dispersed Mo catalyst can double the coal conversion at 350°C for 30 min. This finding may offer

new opportunities for developing novel low-severity liquefaction processes.

Experimental

The coal used was a Wyodak subbituminous coal, which is one of the Department of Energy Coal Samples (DECS-8) maintained in the DOE/Penn State Sample Bank. It was collected in June 1990, ground to ≤ 60 mesh, and stored under argon atmosphere in heat-sealed, argon-filled laminated foil bags consisting of three layers. It contains 32.4 % volatile matter, 29.3% fixed carbon, 9.9 % ash and 28.4 % moisture, on as-received basis; 75.8% C, 5.2% H, 1.0% N, 0.5% S and 17.5% O, on dmmf basis. The as-received fresh sample is designated as raw coal. Vacuuum-drying (VD) of the coal was conducted in a vacuum oven at 100 °C for 2 h. Air-drying (AD) was done in an oven maintained at 100 °C for 2-100 h, or at 150 °C for 20 h, with the door partially open.

For the loading of dispersed catalyst, ammonium tetrathiomolybdate (ATTM) was used as precursor, which is expected to generate molybdenum sulfide particles on coal surface upon thermal decomposition at ≥ 325 °C. ATTM was dispersed on to coal (1 wt% Mo on dmmf basis) by incipient wetness impregnation from its aqueous solution. The impregnated coal samples were dried in a vacuum oven at 100 °C for 2 h.

The liquefaction was carried out at 350 or 400 °C for 30 minutes (plus 3 minutes heat-up time) with an initial (cold) H_2 pressure of 7 MPa (1000 psi) in 25 ml tubing bomb microreactor. We conducted three types of reactions including solvent-free runs, the runs in the presence of a hydrogen donor tetralin solvent, and the runs with a non-donor 1-methylnaphthalene solvent, using 4 g of coal and 4 g of solvent, and optionally, added water. The wt ratio of added water to dmmf coal was kept constant (0.46) for both thermal and catalytic runs with added water, unless otherwise mentioned.

After the reaction, the gaseous products were analyzed by GC, with the aid of gas standards for quantitative calibration of GC responses of CO, CO_2, and C_1-C_4 hydrocarbon gases. The liquid and solid products were separated by sequential Soxhlet extraction into oil (hexane soluble), asphaltene (toluene soluble but hexane insoluble), preasphaltene (THF soluble but toluene insoluble), and residue (THF insoluble). The conversions of coal into soluble products were determined from the amount of THF-insoluble residues. More experimental details may be found elsewhere.[14,15] In order to obtain highly reliable data, almost all the experiments were duplicated

or triplicated. The deviations in conversions and product yields are generally within ± 2 wt%.

Results and Discussion

Figure 2.1 shows the effect of water addition on the liquefaction at 350°C. Relative to the non-catalytic run of the dried coal, the addition of water improved coal conversion from 14.5 to 22.5 wt% (dmmf). The use of ATTM increased the coal conversion from 14.5 to 29.8 wt%. On a percentage basis, the use of ATTM and the addition of water improved coal conversion by 106% [(29.8-14.5)/14.5=1.06] and 55%, respectively. When water was added to the catalytic reaction at 350°C, coal conversion increased dramati-cally to 66.5 wt%. This represents a 123% increase from the catalytic run without water, and 359% increase from the non-catalytic run without water. We have confirmed these trends by several sets of experiments. These interesting findings reveal that dispersed molybdenum sulfide catalyst and added water can act in concert to promote coal liquefaction at relatively low temperature, 350°C.

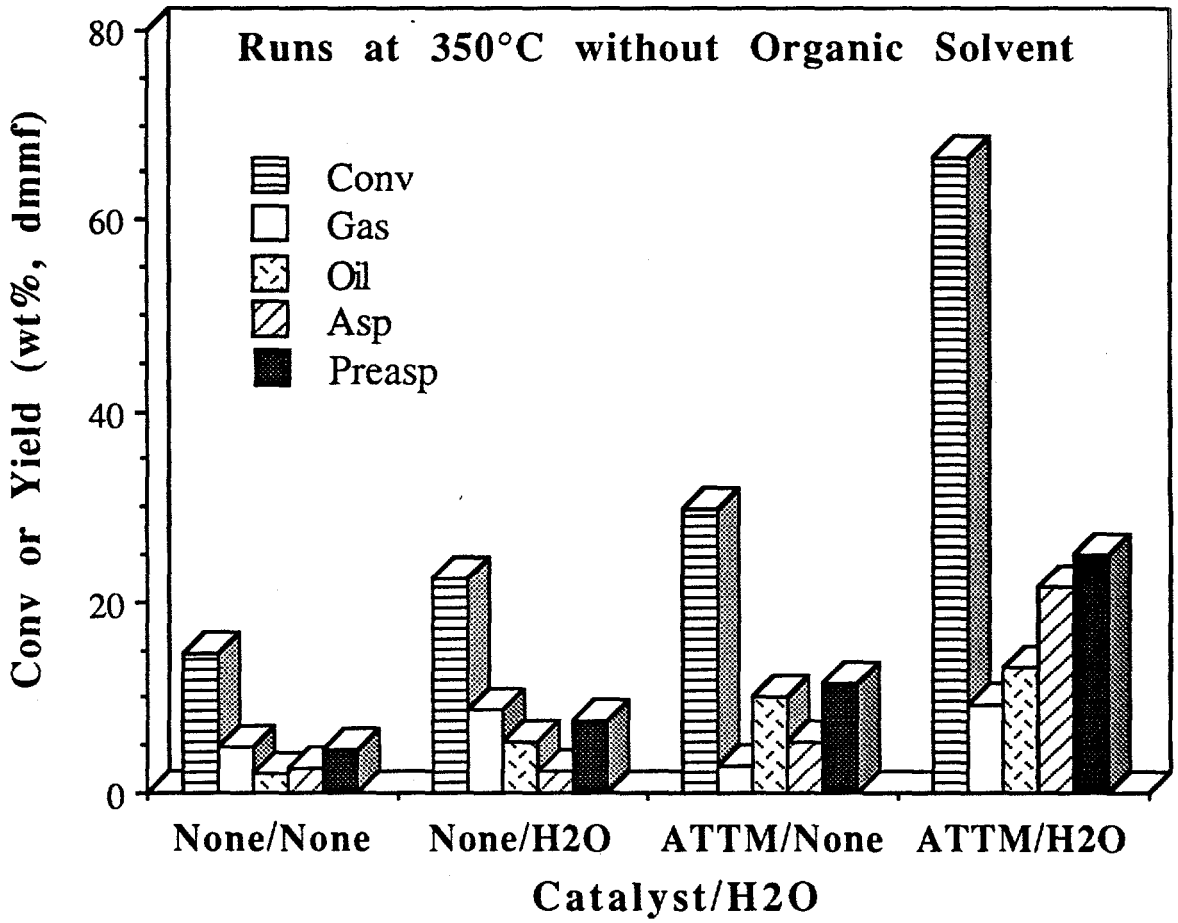

Figure 2.1. Effect of water on catalytic liquefaction of Wyodak coal at 350°C for 30 min.

Figure 2.2 indicates that the addition of water caused substantial increase in gas yields. This is manifested primarily by the increased CO_2 yield. CO yield de-creased upon water addition, indicating the occurrence of water-gas-shift (WGS) reaction. According to the WGS reaction, the increased amount of CO_2 should be 1.57 times the decreased amount of CO (MW ratio: 44/28 = 1.57). However, when water was added to the noncatalytic reaction of vacuum-dried coal, CO_2 yield increased from 4.5 to 8.3 wt% on a dmmf basis, whereas the CO yield decreased from 0.24 to 0.12 wt% (dmmf). Apparently, the majority of enhanced CO_2 yield was caused by chemical interactions between water and the species in coal or coal products, but not by the well-known WGS reaction.

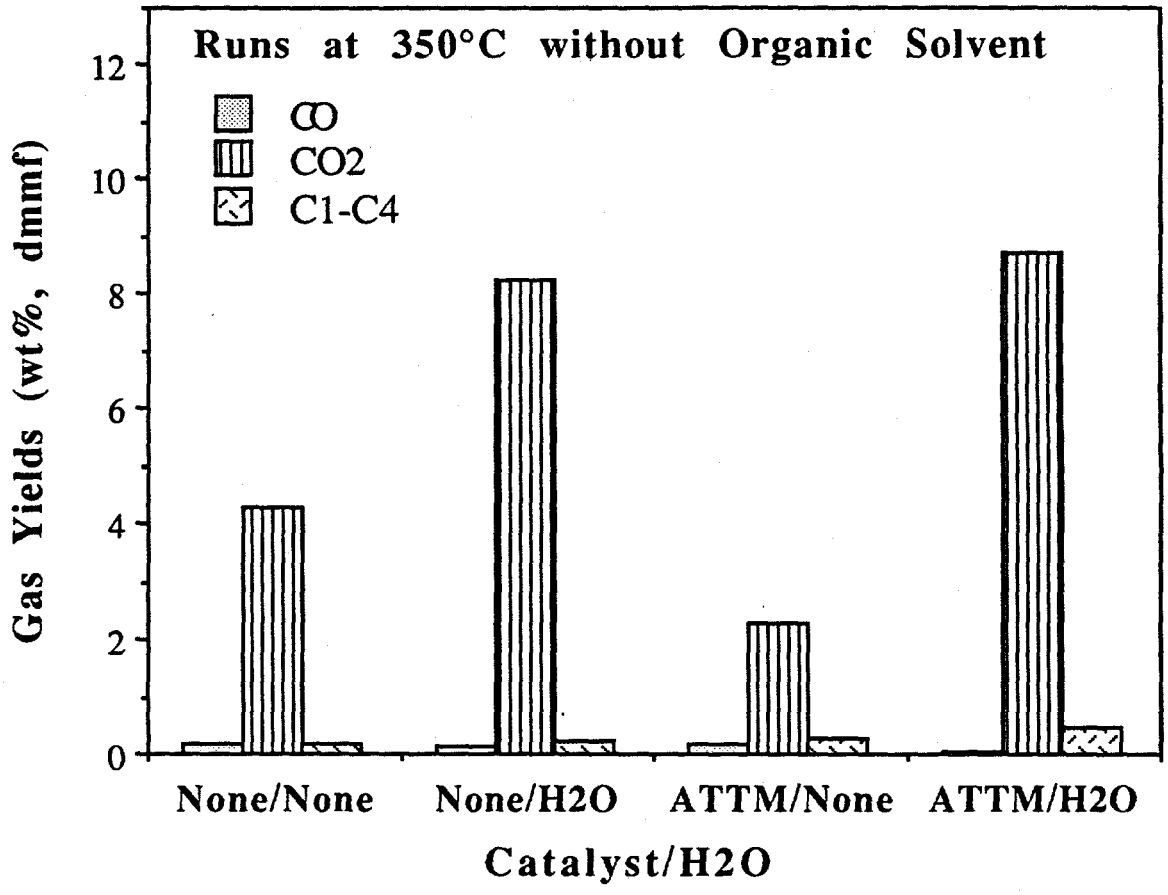

Figure 2.2 Effect of water on gas formation from Wyodak coal at 350°C for 30 min.

It is possible that part of the CO_2 is due to enhanced decarboxylation of carboxylic acids in the presence of H_2O, without causing retrogressive cross-linking(eq. 1).

$$RCOOH + H_2O = RH + CO_2 + H_2O \qquad \text{R, R'= Aryl or Alkyl} \qquad 1)$$

Another possibility is the reaction between water and carbonyl groups in the coal to produce CO_2 (eq. 2). The formation of CO_2 from water and carbonyl groups was also suggested by Lewan[16] for hydrous pyrolysis of shale.

$$RCOR' + H_2O = RH + CO_2 + R'H \qquad \text{R, R'= Aryl or Alkyl} \qquad 2)$$

Two-dimensional HPLC revealed that the oils from liquefaction with added water contain more phenolic compounds.[17] This suggests that water participates in the reaction leading to phenols (eq. 3). Supporting evidence for eq. 3 can also be found in previous studies by Townsend and Klein[18] on hydrothermal reactions of dibenzylether with water at 374°C and by Siskin and Katritzky[19] on diarylether with water at 315°C.

$$ROR' + H_2O = ROH + R'OH \qquad \text{R, R'= Aryl or Alkyl} \qquad 3)$$

The above results were obtained with vacuum-dried coal without any organic solvents. We also performed the tests at 350°C with fresh raw coal as well as air-dried coal samples. The results are shown in Figure 2.3. The general trends observed are substantially enhanced coal conversion upon water addition at 350°C, and enhanced CO_2 formation. From the three sets of experimental results for raw coal, vacuum-dried coal, and air-dried coal, as shown in Figure 2.1 and Figure 2.3, it has now became unambiguous that water can have a dramatic promoting effect on catalytic coal conversion at a relatively low temperature, 350°C.

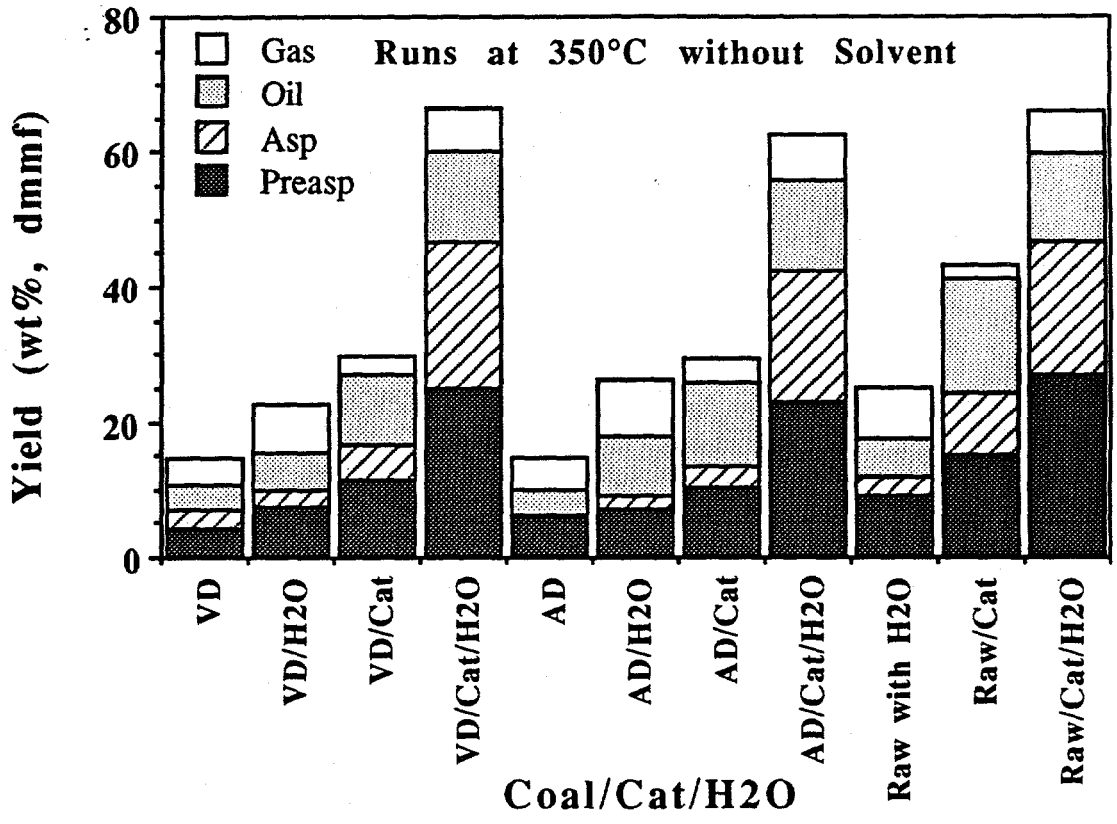

Figure 2.3 Effect of H_2O plus ATTM on conversion of raw and dried Wyodak coal at 350°C.

We also examined the reactions using organic solvents including a H-donor and a non-donor.[15] Figure 2.4 shows that, in the presence of H_2O and Mo catalyst, the use of either a non-donor 1-MN or a H-donor tetralin solvent has no positive impact on coal conversion at 350°C. In general, if no water was added, using H-donor affords better coal conversion than non-donor solvent. However, for runs with both water and dispersed Mo catalyst at 350°C, using orgnaic solvents does not offer any advantages in terms of coal conversion. We have also observed the same trends in several sets of experiments using fresh raw DECS-8 coal sample, vacuum-dried coals, as well as air-dried coals using water-soluble catalyst precursor such as ATTM[15] and oil-soluble Mo catalyst precursor.[27]

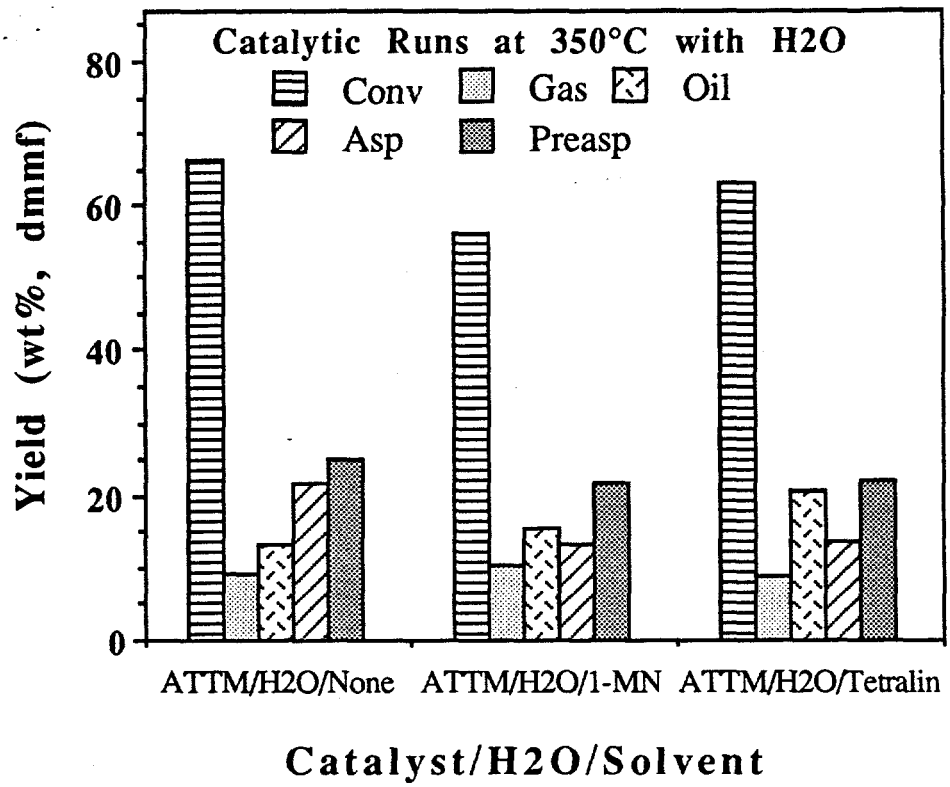

Figure 2.4 Effect of solvent on conversion of Wyodak coal at 350°C using H_2O and ATTM.

Figure 2.5 shows the effect of water on the liquefaction at 400°C. Compared to the runs at 350°C, the positive effect of water addition to the non-catalytic run becomes much less, but the positive impact of using ATTM becomes much more remarkable. The use of ATTM for reaction at 400°C afforded a high coal conversion, 85.4 wt% (dmmf), and a high oil yield, 45.8 wt%. However, addition of water to the catalytic run decreased coal conversion (to 62.1 wt%) and oil yield (to 28.2 wt%). This is in distinct contrast to the trends for corresponding runs at 350°C. An implication from Figure 3 is that the presence of water in the catalytic run at 400°C decreased the catalytic activity level.

We also examined solvent effect for high temperature runs. For runs at 400°C, however, using ATTM without H_2O addition always gives highest conversion, either with or without an organic solvent. An example is shown in Figure 2.6 for runs with 1-MN. It is interesting that adding water can dramatically increase coal conversion in catalytic runs at 350°C, but can decrease conversion in catalytic runs at 400°C.

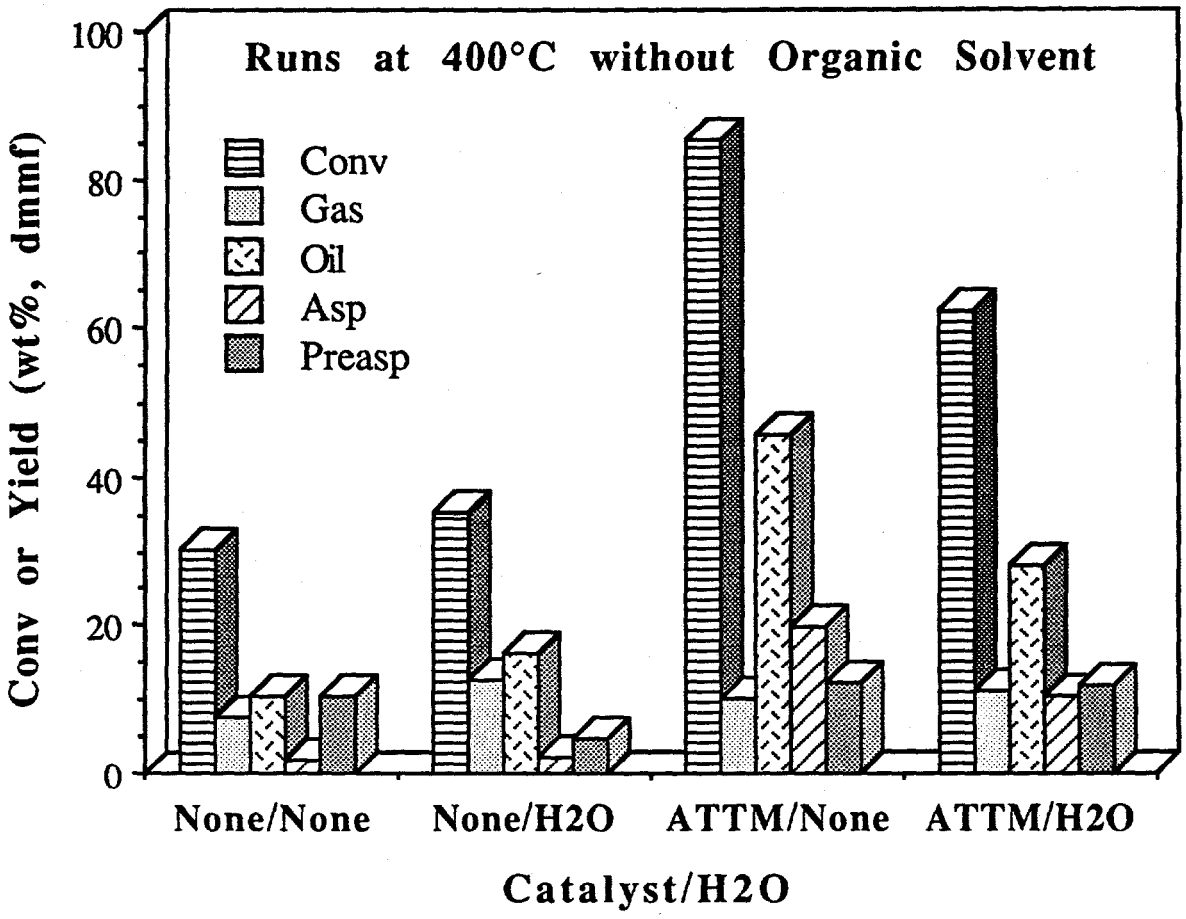

Figure 2.5. Effect of water on solvent-free catalytic liquefaction of Wyodak coal at 400°C.

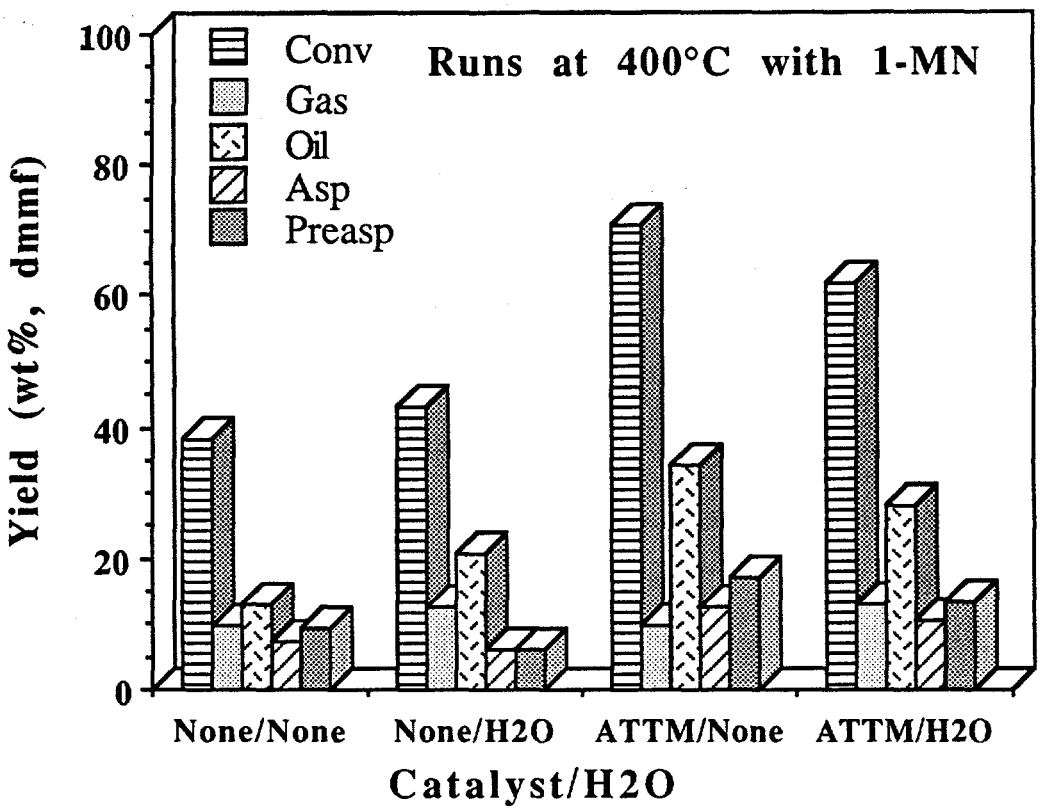

Figure 2.6. Effect of H_2O and ATTM on conversion of Wyodak coal at 400°C in the presence of 1-MN solvent.

The most interesting finding from this work is the strong synergistic effect between water and dispersed Mo sulfide catalyst at 350°C under certain conditions. Bockrath et al..[11] showed that using water as vehicle in the catalytic liquefaction of Illinois No.6 coal (water/coal = 2, wt ratio) at 350°C for 60 min gives much lower conversions than the runs using organic solvents. Ruether et al.[12] examined the effect of water addition in catalytic liquefaction of Illinois No.6 coal at 427°C for 1 h. In the runs using 0.1% dispersed Mo catalyst, highest coal conversions were obtained without added water. Mikita et al.[20] reported on using water and non-donor vehicles for liquefaction of Illinois No.6 coal at 385°C for 30 min. Coal conversion in a non-catalytic run with SRC II solvent and a small amount of water (water/coal=1.7 g/4 g) was similar to a catalytic run with 0.1 wt% Mo and a larger amount of water (water/coal=3.4 g/4 g) (86-88 wt% vs 86-90 wt%). Kamiya et al.[13] have observed that water deactivates the iron catalyst for liquefaction of a brown coal at 400°C and for upgrading of SRC from Wandoan coal at 450°C.

It appears from our results and the above discussion that the reaction temperature and the water/coal and water/catalyst ratios may be important factors. We then systematically examined the

effect of temperature on coal Conversion with H_2O and ATTM over the temperature range of 325-450°C. Figure 2.7 shows the effect of reaction temperature on coal conversion in the catalytic runs with added water (H_2O/dmmf coal = 0.46) but without any solvent. There appears to be a temperature window, within which increasing temperature (325-375°C) significantly increases coal conversion, but beyond which the conversion decreases with increasing temperature (400-450°C). When compared to the catalytic runs without added water (Song et al., 1995), we can see the strong promoting effect of water on low-severity catalytic liquefaction of Wyodak coal in the temperature range of 325-375°C, but an inhibiting effect of water on catalytic runs at 400-450°C. One of the most interesting findings in this work is the strong synergistic effect between water and dispersed molybdenum sulfide catalyst at relatively low temperatures (325-375°C). It should be noted that, even in the low temperature regime, an excessive amount of water may have negative impacts on catalytic coal conversion, as described in our recent paper.[24]

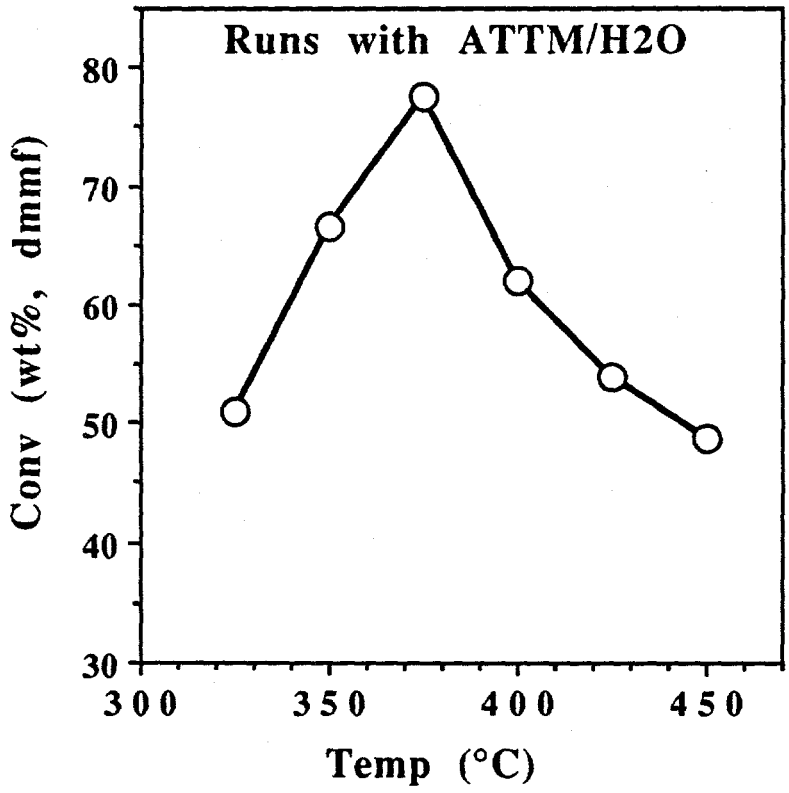

Figure 2.7. Effect of temperature on conversion of Wyodak coal in solvent-free liquefaction.

While the origin of the above-mentioned strong syn-ergism has not been clarified, the promoting effect of water on catalytic liquefaction at 350°C could be partially understood based on literature information on non-catalytic reactions.[19,21-26] Siskin et al.[19] suggested that the presence

of water during coal pretreatment facilitates depolymerization of the macromolecular structure by cleaving important thermally stable covalent cross-links. On the other hand, Tse et al.[24] suggested that hydrothermal pretreatments of low rank coals minimize retrogressive reactions such as crosslink formation from phenolics.

CONCLUSIONS

In summary, we have found that, for liquefaction using dispersed Mo sulfide catalysts from either water-soluble or oil-soluble precursor, adding a proper amount of water can dramatically improve coal conversion at temperatures (325-375°C) that are much lower than those used in conventional processes (400-470°C). The important factors affecting water-promoted catalytic conversion include, but are not limited to, reaction temperature and H_2O/coal ratio.

REFERENCES

(1) Weller, S.; Pelipetz, M.G. Ind. Eng. Chem. 1951, 43, 1243.
(2) Nomura, M.; Miyake, M.; Sakashita, H.; Kikkawa, S. Fuel, 1982, 61, 18.
(3) Derbyshire, F.J.; Davis, A.; Lin, R.; Stansberry, P.G.; Terrer, M. Fuel Process. Technol., 1986, 12, 127.
(4) Song, C.; Nomura, M.; Miyake, M. Fuel, 1986, 65, 922.
(5) Garcia, A.B.; Schobert, H.H. Fuel, 1989, 68, 1613.
(6) Artok, L.; Davis, A.; Mitchell, G.D.; Schobert, H.H. Energy & Fuels, 1993, 7, 67.
(7) Huang, L.; Song,C.; Schobert, H.H. Am. Chem. Soc. Div. Fuel Chem. Prepr., 1993, 38(3), 1093.
(8) Serio, M.; Kroo, E.; Charpenay, S.; Solomon, P.R. Am. Chem. Soc. Div. Fuel Chem. Prepr., 1993, 38 (3), 1021.
(9) Weller, S. Energy & Fuels, 1994, 8, 415.
(10) Derbyshire, F. Chemtech, 1990, 20, 439.
(11) Bockrath, B.C.; Finseth, D.H.; Illig, E.G. Fuel Process. Technol., 1986, 12, 175.
(12) Ruether, J.A.; Mima, J.A.; Kornosky, R.M.; Ha, B.C. Energy & Fuels, 1987, 1, 198.
(13) Kamiya, Y.; Nobusawa, T.; Futamura, S. Fuel Process. Technol., 1988, 18, 1.
(14) Song, C.; Saini, A.K.; Schobert, H. H. Energy & Fuels, 1994, 8, 301.
(15) Song, C.; Saini, A.K.; Schobert, H. H. Am. Chem. Soc. Div. Fuel Chem. Prepr., 1993, 38 (3), 1031.

(16) Lewan, M.D. Am. Chem. Soc. Div. Fuel Chem. Prepr., 1992, 37 (4), 1643.
(17) Song, C.; Saini, A.K. Am. Chem. Soc. Div. Fuel Chem. Prepr., 1994, 39 (4), 1103.
(18) Townsend, S.H.; Klein, M.T. Fuel, 1985, 64, 635.
(19) Siskin, M.; Katritzky, A.R. Science, 1991, 254, 231.
(20) Mikita, M.A.; Bockrath, B.C.; Davis, H.M.; Friedman, S.; Illig, E.G. Energy & Fuels, 1988, 2, 534.
(21) Graff, R.A.; Brandes, S.D. Energy & Fuels, 1987, 1, 84.
(22) Bienkowski, P.R.; Narayan, R.; Greenkorn, R.A.; Chao, K.C. Ind. Eng. Chem. Res., 1987, 26, 202.
(23) Ross, D. Am. Chem. Soc. Div. Fuel Chem. Prepr., 1992, 37 (4), 1555.
(24) Tse, D.S.; Hirschon, A.S.; Malhotra, R.; McMillen, D.F.; Ross, D.S. Am. Chem. Soc. Div. Fuel Chem. Prepr., 1991, 36 (1), 23.
(25) Serio, M.; Kroo, E.; Charpenay, S.; Solomon, P.R. Am. Chem. Soc. Div. Fuel Chem. Prepr., 1992, 37 (4), 1681.
(26) Pollack, N.R.; Holder, G.D.; Warzinski, R.P. Am. Chem. Soc. Div. Fuel Chem. Prepr., 1991, 36 (1), 15.
(27) Song, C.; Saini, A.K.; McConnie J.M. Proc. 8th Int. Conf. Coal Sci., Sept 10-15, Oviedo, Spain, in press.

CHAPTER 3. Temperature-Programmed Liquefaction of Low-Rank Coals in Hydrogen-Donor and Non-Donor Solvents

Introduction

U.S. production of low-rank coals including lignite and subbituminous coals has increased tenfold over the last two decades, and production is poised for a further step increase [1]. Recently there has been increasing interest in finding ways to improve conversion of low-rank coals, which are often less readily liquefied than bituminous coals [2]. In coal liquefaction, the thermally derived reactive fragments (radicals) must be stabilized to achieve molecular weight reduction, otherwise they will promptly recombine or crosslink to form more refractory materials [3]. The rate of thermal fragmentation is mainly determined by coal reactivity, temperature, and time, while its balance with the rate of radical capping by hydrogen-donation is a critical factor [3,4]. It is now recognized that low-rank coals are more reactive than had been thought previously, and their conversion in high-severity processes is accompanied by significant retrogressive reactions [5].

Due to the presence of various C-O and C-C bonds in coals, there may be a relatively broader distribution of dissociation energies of bonds connecting the structural units in low-rank coals, as can be visualized from the dissociation energies of various C-O, C-C and C-H bonds that are believed to be relevant to coal and coal conversion processes [6]. The concept of distribution of bond energies for coals is also supported by the results of temperature-programmed pyrolysis (TPP) of coals ranging from brown to bituminous coals [6,7]. TPP data show that more bonds in low-rank coals are thermally broken at lower temperatures as compared to bituminous coals [6]. The question that arises for liquefying low-rank coals is how to balance the rates of bond cleavage with the rates of hydrogen transfer to the radicals. Of some importance to the present work are several recent reports showing that using relatively slow heating rates [3,4,8] is effective for liquefying low-rank coals. In catalytic liquefaction, temperature-staged conditions have been shown to improve coal conversion and oil yields [9-11], even in the aqueous liquefaction system [12].

For a given reaction system, controlling the conditions is important for maximizing the yield and quality of products and minimizing retrogressive reactions. The retrogressive reactions may include the crosslinking of thermally generated radicals and condensation of thermally sensitive compounds. The temperature-programmed liquefaction (TPL) reported here seeks to efficiently

liquefy low-rank coals by controlling the rate of pyrolytic cleavage of weak bonds while minimizing the retrogressive crosslinking of radicals and thermally sensitive groups. In preliminary communications, we reported that temperature-programming appears to be promising for more efficient conversion of low-rank coals in tetralin [13,14]. This paper reports on the temperature-programmed and non-programmed liquefaction (N-PL) of a subbituminous coal and a lignite in H-donor and non-donor solvents. Reported separately are the solid-state ^{13}C NMR and pyrolysis-GC-MS studies of coal structure and the TPL reactions [15], and catalytic TPL of a low-rank coal using dispersed Mo catalyst [16].

Experimental

The coals used were a Montana subbituminous coal and a Texas lignite obtained from the DOE/Penn State Coal Sample Bank (DECS-9 / PSOC-1546; DECS-1 / PSOC 1538). Table 3.1 shows the characteristics of these coals. The coals were recently collected and stored under argon atmosphere in heat-sealed, argon-filled laminated foil bags consisting of three layers (polyethylene plus aluminum foil plus polyethylene) [17]. The coals were crushed to less than 60 mesh and dried in vacuo at 95°C for 2 h (before use) by placing a flask containing the fresh coal into a preheated vacuum oven. Our preliminary data showed that vacuum dried coal gave similar or slightly higher conversion than the fresh coal. The H-donor vehicle used was tetralin, a known H-donor. As non-donor, naphthalene and 1-methylnaphthalene were used. The products from low temperature runs with naphthalene at ≤350°C were rock-like and difficult to remove from the reactors. However, there were no such experimental problems with 1-methylnaphthalene because it is a liquid.

Liquefaction was carried out in 25 mL microautoclaves using 4 g coal (< 60 mesh) and 4 g solvent under 6.9 MPa H_2 using a given temperature program. The liquid and solid products were separated by sequential Soxhlet extraction with hexane, toluene and THF for about 24 h. The THF-insoluble residues were washed with acetone, then with pentane to remove THF completely, and subsequently dried in a vacuum oven at 100°C for over 6 h before weighing. The conversions of coal into THF-solubles were determined from the amount of THF-insoluble residues and are based on the dmmf basis. The yields of preasphaltene (THF soluble but toluene insoluble) and asphaltene (toluene soluble but hexane insoluble) are given as the yields of recovered products, and the yields of oil plus gases are determined by difference between total conversion and the sum of preasphaltene and asphaltene yields.

Table 3.1. Representative Analyses of DOE / Penn State Coal Samples

Sample No.	DECS-9 or PSOC 1546	DECS-1 or PSOC 1538
Proximate (wt%)		
Volatile Matter	33.5 (47.1)[a]	33.2 (55.5)[a]
Fixed Carbon	37.1 (52.9)[a]	25.8 (44.5)[a]
Moisture	24.6	30.0
Ash	4.8	11.1
Ultimate (wt%, dmmf)		
Carbon	76.1	76.1
Hydrogen	5.1	5.5
Nitrogen	0.9	1.5
Organic Sulfur	0.3	1.1
Oxygen (by diff)	17.6	15.8
Source & Rank		
State	Montana	Texas
County	Bighorn	Freestone
City	Decker	Fairfield
Seam	Dietz	Bottom
Age of Seam	Paleo	Eocene
ASTM Rank	Subbit B	Lig A / Sub C
Sampling Date	6/12/90	12/11/89

a) On a dry, mineral matter free (dmmf) basis.

Results and Discussion

Temperature-Programming

Figure 3.1 shows the reactor heat-up profiles for temperature programmed liquefaction. Although the temperature inside the reactor was not measured, the pressure change of the reactor during the heat-up can gives a direct measure of the temperature change. Figure 3.2 shows the

change of sandbath temperature and pressure of the reactor for a TPL run of DECS-9 in tetralin with 6.9 MPa cold H_2 at final temperature of 400°C. The sandbath temperature was controlled manually such that the heating ramp would be the same for all the runs. It can be seen from Figures 3.1 and 3.2 that the programming was successfully achieved. The t-p profile in Figure 3.2 is typical for a thermal run, but a catalytic run shows a different t-p change pattern [6]. No catalyst was used in the present work. The selected temperature program consisted of a low-temperature soak at 200°C for 15 min, programmed heating to a final temperature at about 7°C/min, followed by a 30 minute hold at the final temperature (300, 350, 375, 400, and 425 °C). We expect few chemical reactions to occur at 200°C. The rationale for selecting such a low temperature for soaking is to allow the solvent molecules to penetrate into the interior of coal particle (diffusion and swelling), before they are needed as hydrogen donors for stabilizing the radicals and thermally labile compounds in the subsequent heat-up period and high temperature stage.

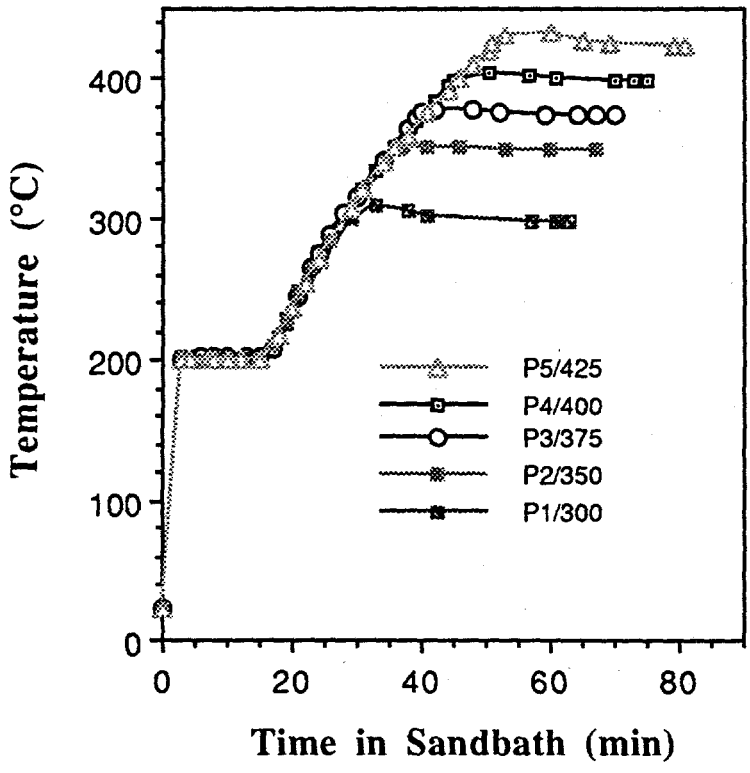

Figure 3.1. Temperature programs examined in TPL of DECS-9 coal.

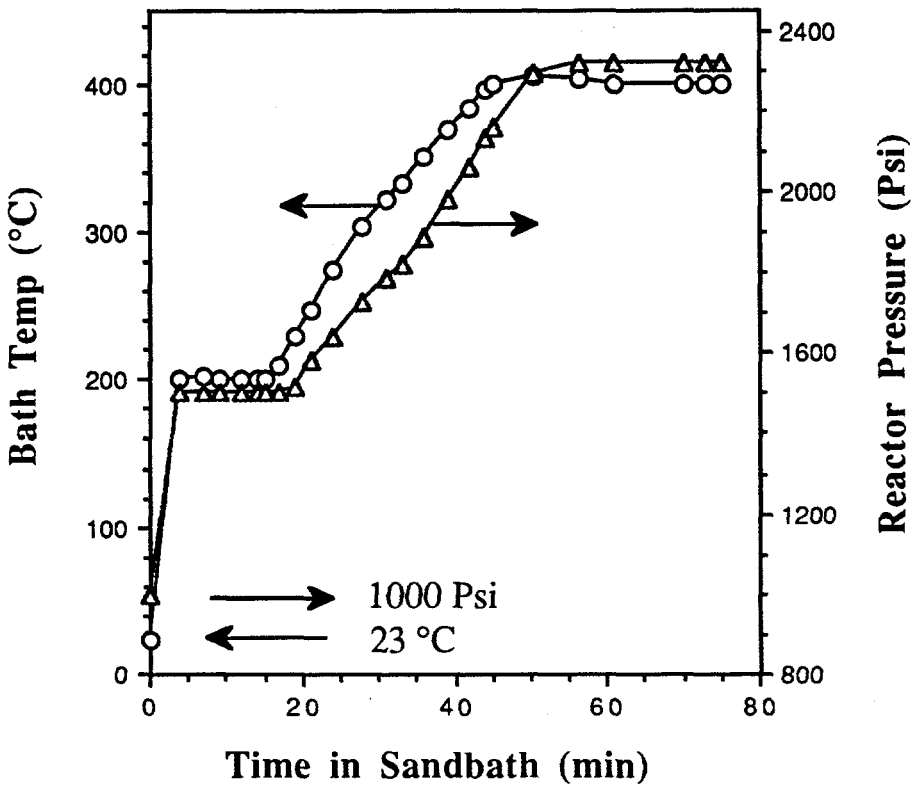

Figure 3.2. Typical temperature-pressure profile during programmed heat-up and holding for non-catalytic TPL of DECS-9 coal in tetralin at a final temperature of 400 °C.

Temperature-Programmed Liquefaction

Figure 3.3 shows the yields of THF-, toluene- and hexane-soluble products plus gas from duplicate runs of Montana coal, as a function of final TPL temperature. At 300°C, the yield of THF-solubles is only slightly higher than that of the original coal. It should be noted that the low temperature TPL did not cause considerable increase in coal conversion, but did result in some desirable change in coal structure. As shown in Figure 3.3, the conversion of coal to THF-solubles increased significantly with increasing final temperature from 300 °C (9%) to 400 °C (about 79%), but rose to a much lesser extent from 400 to 425°C (about 82%). On the other hand, the conversion

to toluene solubles displayed a monotonic increase from 300 to 425 °C.

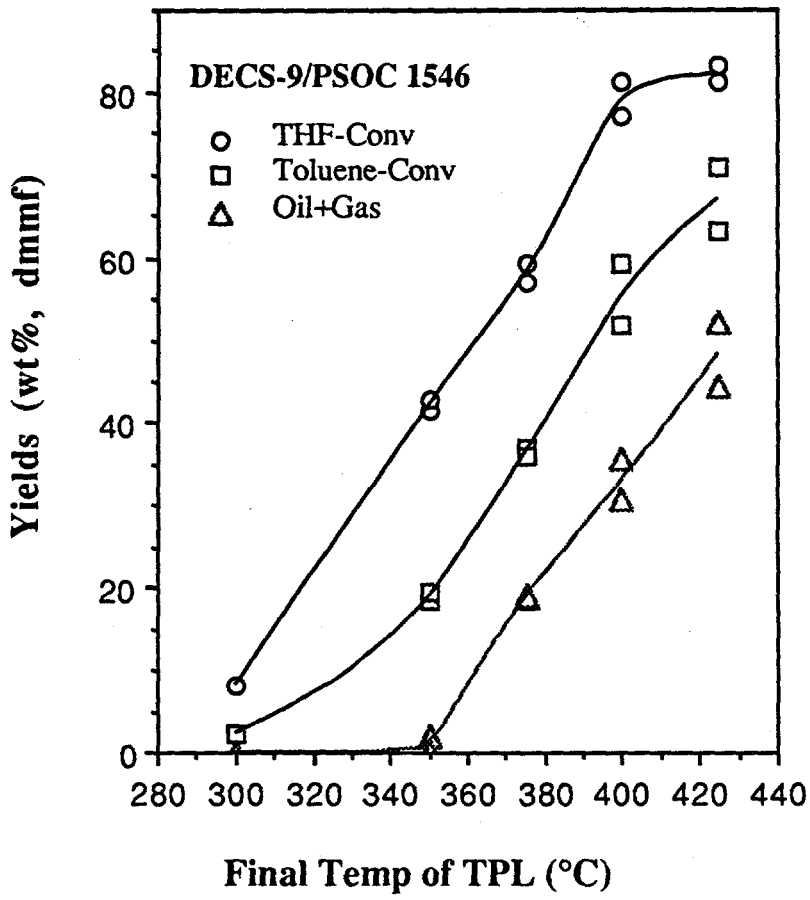

Figure 3.3. Relationship between final temperature of TPL and coal conversion to THF-, toluene- and hexane-solubles plus gases.

Figure 3.4 shows the product distribution from TPL runs in tetralin as a function of final temperature. It is clear from Figure 3.4 that from 300 to 350°C, the increase in conversion was due mainly to gains in preasphaltene and asphaltene yields, while the oil yields rose substantially with increasing temperature from 350 to 425°C. It is likely that under the TPL conditions, increasing temperature up to 350°C contributed to cleavage of the weak bonds that released the larger molecules of asphaltene and preasphaltene classes from macromolecular network; increasing

temperature from 350 to 400 directly promoted the formation of oil from coal; and further increasing temperature from 400 to 425°C further enhanced oil formation from both coal depolymerization and the thermal cracking of preasphaltene and asphaltene.

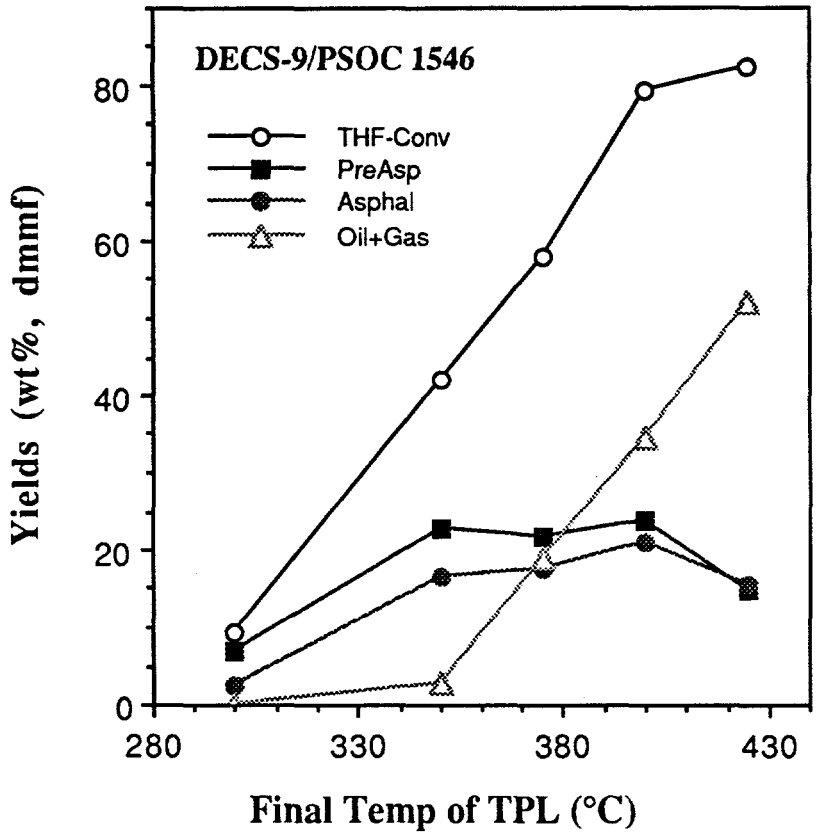

Figure 3.4. Product distribution from TPL of DECS-9 in tetralin at different final temperature.

We also conducted the control runs under the conventional non-programmed (N-PL) conditions (rapid heat-up from 23°C to reaction temperature in 2-3 minutes) at the temperatures of 350-425°C. Figure 3.5 compares the TPL and N-PL data for DECS-9 coal in tetralin. As can be seen from Figure 3.5, relative to N-PL, TPL afforded more preasphaltene at low temperatures between 350-375°C, and more toluene solubles and more oil between 375-425°C. It should be noted that the data in Figure 3.5 are average of duplicate runs for both TPL and N-PL. The raw data from the duplicate runs show the same trend. For example, the THF conversions from duplicate

experiments of N-PL are 70.6 and 72.2% for runs at 400°C, and 75.0, 75.7 and 78.4% for runs at 425°C in tetralin under H_2. A longer N-PL run at 400°C for extended time period (60 min) only increased the THF conversion by about 2-3 % as compared to the 30 min N-PL run. However, the THF conversions from duplicate TPL runs are 77.0 and 81.4% for TPL at 400°C, and 81.4 and 83.1% for TPL at 425°C. In the case of DECS-1 Texas lignite, TPL runs also gave considerably higher conversions than N-PL runs in tetralin. The average values from duplicate runs of DECS-1 in tetralin are shown in Table 3.2.

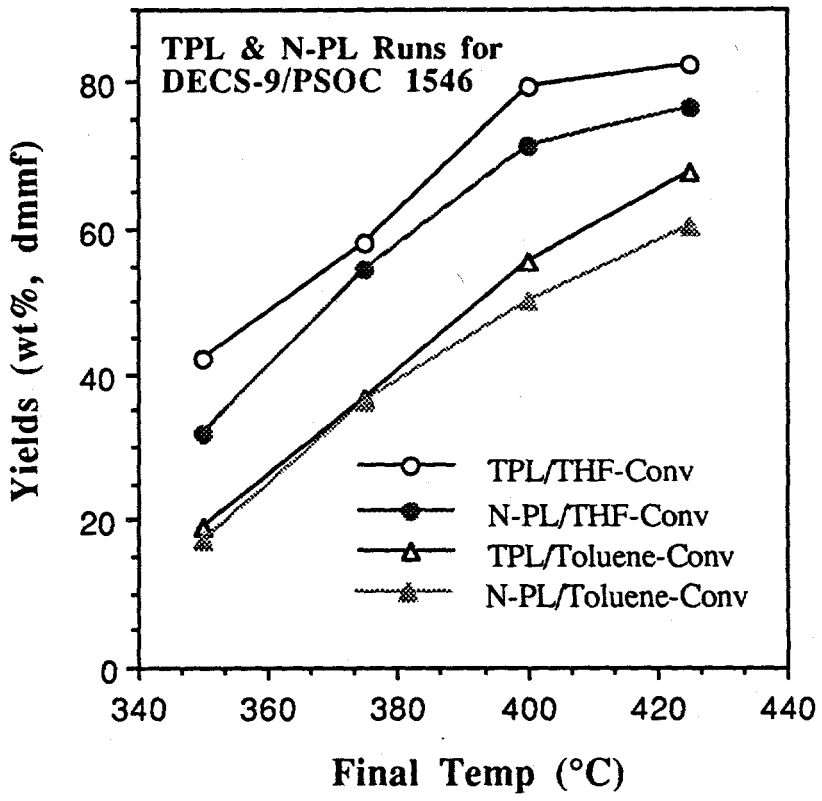

Figure 3.5. Comparison between temperature-programmed (TPL) and non-programmed (N-PL) runs of DECS-9 coal in tetralin solvent. The values shown in this Figure are average of at least two duplicate runs.

In order to understand the beneficial effects of TPL in H-donor tetralin, we also conducted both TPL and N-PL runs in non-donor solvents. The data in Table 3.2 and Table 3.3 shows that

temperature-programming in a non-donor solvent such as naphthalene or 1-methylnaphthalene does not appear to have any significant impact on coal conversion and product distribution. This indicates that beneficial effects of TPL as compared to N-PL in tetralin solvent are closely associated with hydrogen transfer from tetralin.

Table 3.2. Temperature-Programmed (TPL) and Non-programmed Liquefaction (N-PL) with H-Donor Teralin and Non-donor 1-Methylnaphthalene (1-MN) Solvents at 400 °C for 30 min

Coal	DECS-9 Mont Sub	DECS-9 Mont Sub	DECS-1 Texas Lig	DECS-1 Texas Lig	DECS-9 Mont Sub	DECS-9 Mont Sub
Feature	TPL	N-PL	TPL	N-PL	TPL	N-PL
Solvent	Tetralin	Tetralin	Tetralin	Tetralin	1-MN	1-MN
Prod. dmmf wt%						
THF-Conv[a]	79.2	71.4	78.0	69.8	34.1	32.2
Tolue-Conv[b]	55.5	50.1	66.1	58.0	27.1	25.4
Oil + Gas	34.4	29.4	48.5	45.1	18.9	16.0
Asphaltene	21.1	20.6	17.5	12.9	8.2	9.4
Preasphaltene	23.7	21.4	11.9	11.8	7.0	6.8

a-b) Total conversion to a) THF-solubles and b) toluene-solubles plus gas.

Table 3.3. Temperature-Programmed (TPL) and Non-programmed Liquefaction (N-PL) with H-Donor Teralin and Non-donor Naphthalene Solvents at 350 °C for 30 min

	DECS-9	DECS-9	DECS-9	DECS-9
Coal	Mont Sub	Mont Sub	Mont Sub	Mont Sub
Feature	TPL	N-PL	TPL	N-PL
Solvent	Tetralin	Tetralin	Naphthalene	Naphthalene
Prod. dmmf wt%				
THF-Conv[a]	42.0	31.9	21.3	21.4
Tolue-Conv[b]	19.2	17.0	13.7	14.2
Oil + Gas	2.7	4.0	9.3	7.9
Asphaltene	16.5	13.0	4.4	6.3
Preasphaltene	22.8	14.9	7.6	7.2

a-b) Total conversion to a) THF-solubles and b) toluene-solubles plus gas.

The above results demonstrated that in the presence of H-donor solvent, TPL can afford considerably higher conversion than the conventional run at the same or even higher final temperatures. This comparison clearly showed that the programmed heat-up is superior to the rapid heat-up for conversion of the low-rank coals in tetralin under H_2, although it is known that in coal pyrolysis ultrarapid heating increases tar yields [18]. These results indicate that the temperature-programming is a promising approach for converting low-rank coal in H-donor solvent, and further improvement may be achieved by finding the optimum program and by using a catalyst. In fact, we also demonstrated that catalytic TPL of DECS-9 is superior to N-PL in the presence of a dispersed Mo catalyst and a process solvent which has much lower H-donating ability compared to tetralin [16]. Analytical characterization of the residues using CPMAS ^{13}C NMR and pyrolysis-GC-MS [15] points to the progressive loss of oxygen functional groups and aliphatic species from the macromolecular network of the subbituminous coal during its depolymerization in tetralin under TPL conditions. The higher conversions in TPL runs (relative to the conventional runs in tetralin) suggest that the removal of carboxylic and catechol groups from the coal during the programmed heat-up in tetralin may have contributed to minimizing the retrogressive crosslinking at higher temperatures.

Mechanistic Considerations

Comparative examination between the TPL and N-PL runs using different solvents established that the beneficial effects of temperature-programming in tetralin are not due to thermal treatment but are closely associated with low temperature hydrogen-transfer during programmed heat-up. Although H-transfer is a chemical process, both the physical and chemical mechanisms can be responsible for the desirable effects of TPL as compared to N-PL in tetralin. Our initial idea in designing the temperature program was to meet the physical as well as chemical requirements for conversion of coals which are macromolecular in chemical nature but are microporous in physical nature.

The rationale of selecting a low temperature soak is associated with the characteristics of coal pore structure. A large part of pore volume of low-rank coals is located in mesopores (20-500 Å in diameter) and macropores (>500 Å). However, most of the surface area of coals is enclosed in the micropores (<20 Å); hence rates of reaction are limited by rates of diffusion through the micropores [19,20]. Spears et al. [20] reported that the micropore walls contain polar functional groups, and their abundance is higher for low-rank coals. It is considered that soak at 200°C for 15 min will facilitate the diffusion of tetralin into the micropores (< 20 Å) and smaller mesopores (>20 Å). Also, it is likely that tetralin can induce swelling at 200°C which may open up some pores that are solvent-inaccessable at room temperature. However, such physical effects would be smaller for liquefaction of bituminous coals.

The chemically beneficial effect of TPL compared to N-PL in H-donor lies in the programmed heat-up. The H-transfer from H-donor could stabilize the thermally derived radicals and thermally sensitive groups. Because of the bond dissociation energy distribution, one could selectively break certain bonds at certain temperature range by using temperature programming, which would provide time for radical to abstract H from H-donor. Low-rank coals are characterized by low aromaticities and high oxygen functionalities [21]. Suuberg et al. [22], Solomon et al.[18] and Lynch et al.[23] have indicated that during coal pyrolysis, decarboxylation is accompanied by crosslinking reactions and the formation of CO_2. McMillen et al.[24] have provided some insights into the retrogressive reactions involving polyhydroxy structures. It is likely that the retrogressive reactions occurring during liquefaction of low-rank coals under conventional high-severity conditions are, at least in part, associated with the reactions of their oxygen functional groups.

It seems possible from comparative examination of the coal conversion data that the TPL conditions may facilitate the reduction of crosslinking reactions of the thermally sensitive groups such as oxygen-functional groups at low temperatures in H-donor. Both the present and previous results [3,4,8] strongly suggest that very fast heating would result in too fast a thermal fragmentation of low-rank coals at high temperatures to be balanced by H-donation, which consequently leads to enhanced retrogressive reactions.

References

1. Sondreal, E.A., Paper presented at the *Information Transfer Session*, Cooperative Program in Coal Research, The Pennsylvania State University, Nov. 18-19, **1991.**
2. Derbyshire, F.; Davis, A.; Lin, R., *Energy & Fuels* **1989**, 3, 431.
3. Song, C., Hanaoka, K. and Nomura, M. *Fuel* **1989**, 68, 287.
4. Song, C., Nomura, M. and Hanaoka, K. *Coal Sci. Technol.* **1987**, 11, 239.
5. DOE COLIRN Panel, "Coal Liquefaction", Final Report, DOE-ER-0400, Vol. I & II, **1989**
6. Song, C.; Nomura, M.; Ono, T., *Am. Chem. Soc. Div. Fuel Chem. Prepr.* **1991**, 36(2), 586
7. Song, C.; Nomura, M., *Fuel.* **1986**, 65, 922.
8. Masunaga, T and Kageyama Y. *Proc. 1989 Int. Cof. Coal Sci.*, Tokyo, **1989**, 819.
9. Derbyshire, F.J.; Davis, A.; Epstein, M.; Stansberry, P.G. *Fuel* **1986**, 65, 1233
10. Derbyshire, F.J.; Davis, A.; Schobert, H.; Stansberry, P.G. *Am. Chem. Soc. Div. Fuel Chem. Prepr.* **1990**, 35, 51.
11. Burgess, C.E. and Schobert, H. *Am. Chem. Soc. Div. Fuel Chem. Prepr.* **1990**, 35, 31.
12. Stenberg, V.I., Gutenkurt, V., Nowok, J. and Sweeny P.G. *Fuel* **1989**, 68, 133.
13. Song, C.; Schobert, H.H.; Hatcher, P.G., *Proc. 1991 Int. Conf. Coal Sci.*, **1991**, UK, p.664.
14. Song, C.; Schobert, H.H.; Hatcher, P.G., *Energy & Fuels* **1992**, in press.
15. Song, C.; Schobert, H.H.; Hatcher, P.G., *Am. Chem. Soc. Div. Fuel Chem. Prepr.* **1992**, 37, in press.
16. Huang, L.; Song, C.; Schobert, H.H., *Am. Chem. Soc. Div. Fuel Chem. Prepr.* **1992**, 37, in press.

17. Davis, A.; Glick, D.C.; Mitchell, G.D., Proceedings of DOE Liquefaction Contractors' Review Meeting, Sept. 3-5, **1991**, Pittsburgh, p.398-410.
18. Solomon, P.R.; Serio, M.A.; Despande, G.V.; Kroo, E. *Energy & Fuels* **1990**, 4, 42.
19. Mahajan, O.P.; "Porosity of Coals and Coal Products", in *Analytical Methods for Coal and Coal Products, Vol.1*, C. Karr, Ed., Academic Press, New York, **1978**, p.125-162.
20. Spears, D.R.; Sady, W.; Kispert, L.D., *Am. Chem. Soc. Div. Fuel Chem. Prepr.* **1991**, 36 (2), 1277.
21. Schobert, H.H., *Resources, Conservation and Recycling* **1990**, 3, 111.
22. Suuberg, E.M.; Unger, P.E.; Larsen, J.W. *Energy & Fuels* **1987**, 1, 305.
23. Lynch, L.J.; Sakurovs *Proc. 1991 Int. Cof. Coal Sci.*, Newcastle upon Tyne, **1991**, 592.
24. McMillen, D.F.; Chang, S.; Nigenda, S.E.; Malhotra, R. *Proc. 1985 Int. Cof. Coal Sci.*, Sydney, **1985**, 153.

CHAPTER 4. CPMAS ^{13}C NMR and Pyrolysis-GC-MS Studies of Structure and Liquefaction Reactions of Montana Subbituminous Coal

INTRODUCTION

Modern solid state ^{13}C nuclear magnetic resonance (NMR) spectroscopy originated in the 1970's when cross-polarization (CP) and magic angle spinning (MAS) techniques were developed and combined (CPMAS) [1-4]. Since the first paper on ^{13}C NMR of coals was published by VanderHart and Retcofsky in 1976 [5], solid-state NMR has been applied extensively in characterization of coals. The techniques of CPMAS and dipolar dephasing MAS (DDMAS) ^{13}C NMR can provide useful structural information on insoluble organic solids. In recent years, solid-state NMR has rapidly become one of the most important non-destructive techniques for studying the structure of solid coal, coal macerals, coal-derived products, geochemical samples, and other organic solids [6-14]. As long as one recognizes the important experimental variables necessary for quantitative measurements, it can make a major contribution to the structural characterization of insoluble carbonaceous materials [15-18].

Flash pyrolysis-gas chromatography-mass spectrometry (Py-GC-MS) is also an important analytical technique for structural study of polymeric materials [19-23]. Py-GC-MS is relatively simple in theory, and can be viewed as a combination of the well known MS techniques with pyrolysis-GC [24-27]. While these techniques have been applied in many investigations, very few applications have been made in coal liquefaction studies. Yoshida et al. [10,11] analyzed several different coals by using CPMAS ^{13}C NMR and attempted correlating their liquefaction reactivity with structural characteristics. Franco et al. [28] characterized the structural changes of two coals before and after chemical treatments using CPMAS ^{13}C NMR. Fatemi-Badi et al. [29] examined a lignite and its liquefaction residues using solid state NMR and IR. Recently, Song et al. [30,31] and Saini et al. [32] reported preliminary studies of coal structure, pretreatments and liquefaction using CPMAS ^{13}C NMR, pyrolysis-GC-MS and FT-IR.

The present work is a part of our research program to examine the structure and temperature-programmed liquefaction of low-rank coals, and involves the spectroscopic study of coals and their residues from liquefaction at different temperatures by using the combination of CPMAS ^{13}C NMR and Py-GC-MS techniques [30-34]. The NMR technique has an advantage of providing the information related to the type and distribution of aromatic and aliphatic carbons in a non-destructive and quantitative fashion. Its disadvantage is that the information from NMR does

not provide a direct picture of the molecular components and their environments. This is partly because the coal organic matrix is a complex mixture, whose individual components can not be resolved by NMR. Py-GC-MS is a very useful technique for studying the molecular components or structural units of polymeric organic solids. However, the major drawback to Py-GC-MS is that the proportion of coal that can be volatilized and analyzed by GC-MS is relatively small. For many coals more than half of the organic material remains as a residue. Since each technique has advantages and disadvantages, we can make complementary use of these techniques by using them in tandem. The combined use of solid state NMR and Py-GC-MS has the potential to provide both average structural information and specific molecular components, and when applied to properly selected samples, can provide insights into the major and minor changes in coal structures and structural transformations involved in coal liquefaction processes [30-34].

The objectives of the present work are 1) to characterize the structural features and structural components of a subbituminous coal, 2) to delineate the chemical reactions occurring during coal liquefaction by characterizing the resultant structural changes in coal macromolecular network using CPMAS ^{13}C NMR and Py-GC-MS, and 3) to make quantitative evaluation of changes in carbon distribution of coal macromolecular network as a function of reaction temperature. Mathematical correlation of CPMAS ^{13}C NMR data with reaction temperature was also attempted in the present work, and the results are described in this report.

EXPERIMENTAL

Sample Preparation

The coal used was a Montana subbituminous coal obtained from the DOE/Penn State Coal Sample Bank (DECS-9 or PSOC-1546). This sample was collected from Dietz seam in Bighorn County in June 1990, and it was stored in a multi-layer laminated bag under argon atmosphere. The proximate and ultimate analysis of this coal are as follows: 33.5% volatile matter, 37.1% fixed carbon, 4.8% ash, 24.6% moisture, on a raw coal basis; 76.1% C, 5.1% H, 0.9% N, 0.3% organic S, and 17.5% O, on a dmmf basis. The coal was dried in a vacuum oven at 95°C for 2 h before use. The liquefaction vehicles used were tetralin, a known H-donor, and non-donors such as 1-methylnaphthalene and naphthalene as well as process solvent, which is a middle distillate fraction from two-stage catalytic liquefaction of Pittsburgh #8 bituminous coal at the Advanced Coal Liquefaction Research and Development Facility in Wilsonville in Run 259E (WI-MD) [35]. Liquefaction was carried out in 25 mL microautoclaves using 4 g coal (< 60 mesh) and 4 g solvent under 6.9 MPa (cold) H_2. After the reaction, the liquid and solid products were separated by sequential extraction with hexane, toluene and tetrahydrofuran (THF). More details about

liquefaction experiments may be found elsewhere [33].

In order to derive structural information related to the macromolecular network, the low molecular weight species in the coal and coal liquefaction products were removed by THF extraction, and the THF-insoluble residues were analyzed by CPMAS ^{13}C NMR and Py-GC-MS. Our preliminary tests showed that a trace amount of THF remains in the residue even after vacuum drying at 100 °C for over 6 h, which significantly interferes with the characterization using Py-GC-MS and NMR [31]. Therefore, prior to analyses, all the THF-insoluble residues were washed first by using acetone and then n-pentane, followed by vacuum drying at 100°C for 6 h. This procedure was found to be very effective for removing trace amounts of THF, as confirmed by NMR and Py-GC-MS.

CPMAS ^{13}C NMR Spectroscopy

The NMR spectra were acquired on a Chemagnetics M-100 NMR spectrometer by using the combined high power proton decoupling, cross-polarization and magic-angle-spinning (CPMAS) techniques. The measurements were carried out at a carbon frequency of 25.1 MHz. About 0.4-0.6 g of a sample was packed in a 0.4 mL bullet-type rotor made of polychlorotrifluoroethylene (Kel-F); the spinning speed of the rotor was about 3.5 kHz. The experimental conditions for all the samples are as follows: a cross-polarization contact time of 1 ms and a pulse delay time of 1 s. An instrumental calibration test was performed with the rotor containing hexamethylbenzene, which was adjusted to the magic angle (54.7°) to give the correct chemical shifts. To assure good spectra with high signal-to-noise ratios, the number of pulses accumulated for obtaining a spectrum was at least 10,000, and most of the spectra were obtained with numbers of scans between 20,000 to 35,000. Other details concerning solid state NMR may be found elsewhere [9].

For quantitative evaluation, the NMR spectra were input into computer as graphs by using an automated digitizing system UN-PLOT-IT software developed by Silk Scientific, Inc. in 1990. Further data processing was performed by using LAB CALC software developed by Galactic Industries Co. in 1990. The peak separation and quantitative calculation of specific NMR bands were carried out by using the curve-fitting program of LAB CALC.

Pyrolysis-GC-MS

Py-GC-MS analysis was performed on a Du Pont 490B GC-MS system fitted with a 30 m x 0.25 mm i.d. DB-17 capillary column coated with 50% phenylmethylsilicone stationary phase with a film thickness of 0.25 μm, and interfaced to a Chemical Data Systems Pyroprobe-1000 pyrolyzer. Helium was used as a carrier gas. The data acquisition and processing were controlled through a computer-aided system. In a typical run, about 0.6-1.0 mg of a sample was loaded into a thin quartz tube, which was then inserted into the horizontal filament coil in the pyroprobe. The

pyroprobe is then interfaced directly to the capillary GC inlet. Prior to the start of data acquisition, the sample was flash-pyrolyzed (with a nominal heating rate of 5000°C/second) at 610°C for 10 seconds, during which the pyrolyzates (pyrolysis products) were cryotrapped in the close-to-inlet part of the capillary column by cooling with liquid nitrogen. The column temperature was programmed from 30°C to 280°C at a heating rate of 4°C/min. The mass spectrometer was operated in the electron impact mode at 70 eV. It should be noted that our preliminary Py-GC-MS data were obtained by using an old capillary column [31,34]. A new DB-17 column was installed for the Py-GC-MS runs reported here, which exhibited better sensitivity and resolution, especially for catechol and methylcatechol peaks.

RESULTS AND DISCUSSION

CPMAS ^{13}C NMR of DECS-9 Montana Subbituminous Coal

Figure 4.1 shows the CPMAS ^{13}C NMR spectra of the fresh Montana subbituminous coal and the unreacted but THF-extracted coal. It is interesting to note that the THF-extracted coal, which lost about 8 % THF-soluble materials, gave a spectrum similar to that of the raw coal in terms of the aromaticity and functionality (see below). Integration of the spectra gives only a slightly higher aromaticity (fa) value for the THF-extracted coal than for the raw coal. It should be noted that, for some coals, the THF-extracted samples may display substantially different spectra.

A general observation is that these NMR spectra are relatively poorly resolved, as compared to the spectra of pure materials, primarily because of the presence of a large number of different molecular species that have only slightly different chemical shifts. The representative carbon types are also marked in Figure 4.1. In general, there two major spectral bands, an aromatic band from 90 to 170 ppm and an aliphatic band from 0 to 90 ppm. Among the aliphatic carbons, methyl groups appear at 0-25 ppm, methylene carbons resonate between 25-50 ppm, methoxyl groups around 50-65 ppm and ether group between 70-80 ppm [10,28,31]. The aromatic region also includes two shoulders which are likely due to catechol-like carbons and phenolic carbons, respectively. There are some other bands with lower intensities, including carboxyl groups at 170-190 ppm and carbonyl groups between 190-230 ppm.

Py-GC-MS of Montana Coal

Figure 4.2 shows the retention time (RT) window (0-40 min) of the total ion chromatogram (TIC) obtained from Py-GC-MS of the THF-extracted raw coal. With the aid of computer-based data processing, it is now possible to perform a compound type analysis of coal pyrolysis products by using the selective ion monitoring technique in Py-GC-MS, as has been used for hydrocarbon

type analysis of liquid fuels by GC-MS [36]. Low-rank coals are known to have high oxygen functionalities [37]. We have examined the oxygen compounds in the pyrolyzates by using the characteristic ion masses for phenol (m/z 94), cresol (m/z 108), xylenol and ethylphenol (m/z 122), catechol (m/z 110) and methylcatechol (m/z 124). Within the RT range of 9-16 min in the TIC, there are five dominant peaks, and all of them are phenolic compounds. Also found in this sample are catechol and methylcatechol between RT of 17-21 min, in relatively high intensities. The relative retention order of 3- and 4-methylcatechol in Figure 4.2 was determined based on the results of Bergen et al. [38].

There are many other small peaks appearing over the whole RT region, and selective ion monitoring at m/z 71 indicates that many of them are long-chain alkanes and alkenes. Figure 4.3 shows the whole TIC and selected SICs at ion masses characteristic of alkanes (m/z 71) and alkylbenzenes (m/z 91). In the SIC at m/z 71 there are a number of alkanes ranging from C_4 to C_{31} (the carbon-number indicates the even-numbered alkanes). Several hydrocarbon peaks which appeared as unresolved peaks between RT of 2-3 min in this SIC are C_4-C_6 alkanes plus alkenes. It is interesting to note that this sample still contains long-chain aliphatic components up to n-C_{31} although it was pre-extracted by THF for over 24 h. Prist-1-ene was also found in this sample, as marked between n-C_{17} and n-C_{18} in the SIC at m/z 71. Both pristane and prist-1-ene are known fossil fuel biomarkers [20]. The presence of prist-1-ene but absence of pristane in the pyrolyzates may suggest that pristane is chemically bound into the coal structure. In the SIC for m/z 91, there are only three major peaks. The two relatively large peaks around RT of 4 min and 5 min are toluene and p- and o-xylene, in that order. Another peak appearing around RT of 35 min is n-dodecylbenzene. We also performed Py-GC-MS of the raw coal (undried and unextracted). The Py-GC-MS TIC is similar to that in Figure 4.3 in that one can found identical peaks in both, but the relative intensities of the peaks eluting before RT of 3 min are higher for the raw coal, which is expected. Overall, the above results show that the DECS-9 coal contains significant amounts of oxygen-containing structural units such as phenol, alkylphenols, catechol (1,2-benzenediol), and methylcatechol, together with small amounts of alkylbenzenes, alkylnaphthalenes and paraffins.

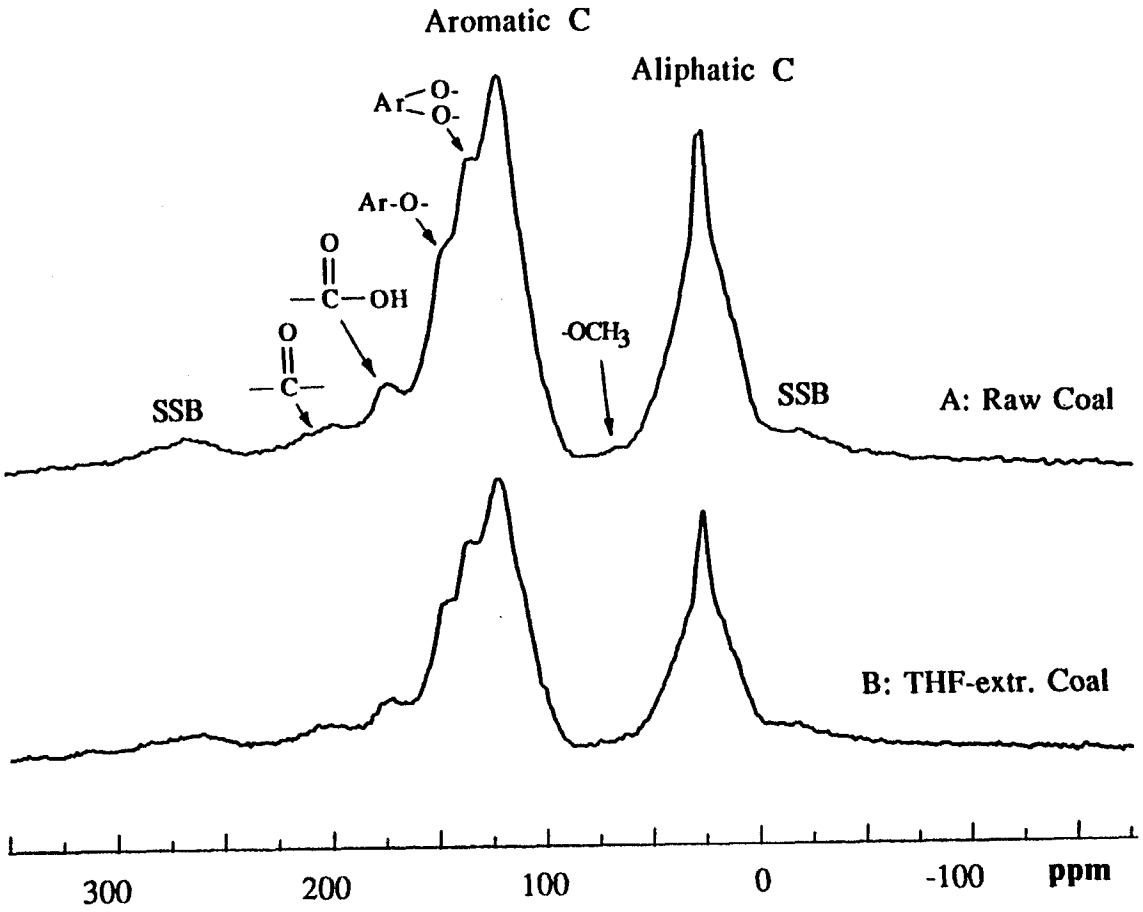

Figure 4.1 CPMAS ^{13}C NMR spectra of DECS-9 Montana subbituminous coal (A) and the THF-extracted coal (B).

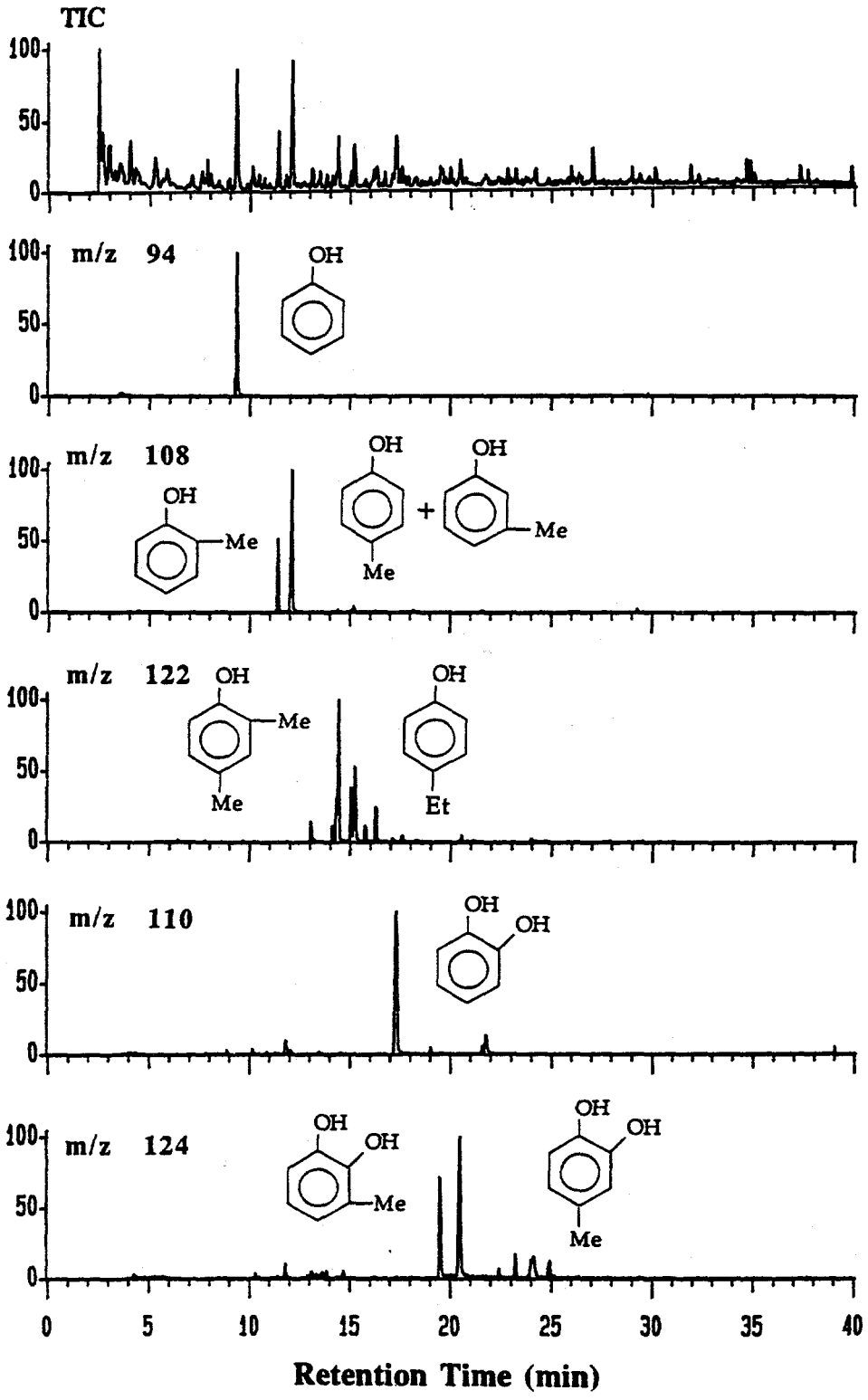

Figure 4.2 Retention time window (0-40 min) of totoal ion chromatogram (TIC) from pyrolysis-GC-MS of THF-extracted DECS-9 coal, and specific ion chromatograms (SIC) at ion masses characteristic of O-containing compounds.

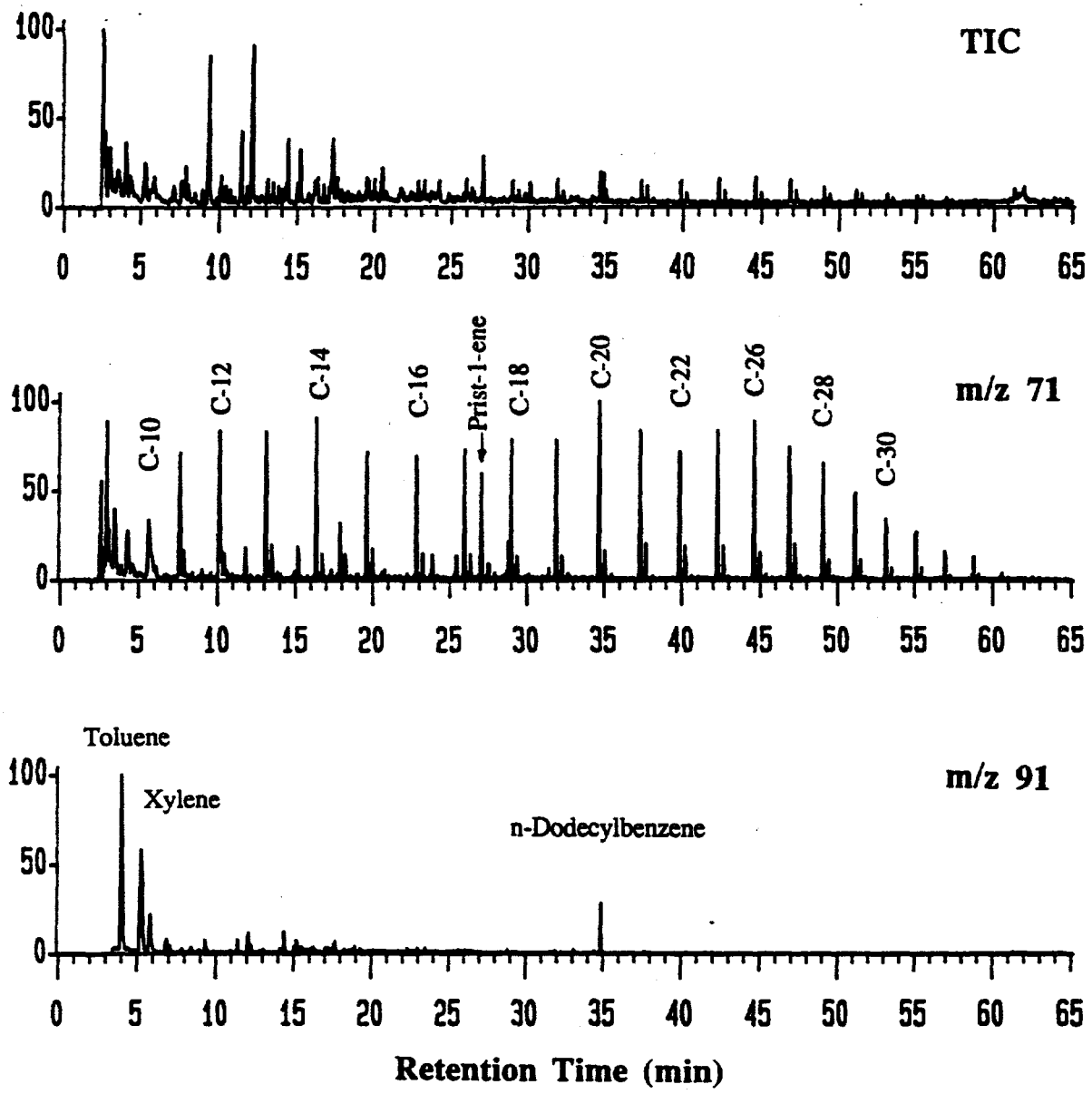

Figure 4.3 Py-GC-MS TIC of THF-extracted DECS-9 coal, and SIC at ions characteristic of long-chain paraffins (m/z 71) and alkylbenzenes (m/z 91).

Table 4.1. Identified Peaks in TIC from Py-GC-MS of DECS-9 Montana Subbituminous Coal

Peak No.	MW	Identified Compounds	Peak No.	MW	Identified Compounds
1	100 + 98	Heptane + Heptene	40	156	Dimethylnaphthalene
2	78	Benzene	41	240	n-Heptadecane (n-C_{17})
3	114 + 112	Octane + Octene	42	238	1-Heptadecene
4	92	Toluene	43	266	Prist-1-ene
5	128 + 126	Nonane + Nonene	44	170	C_3-naphthalene
6	106	p- & m-Xylene	45	254	n-Octadecane (n-C_{18})
7	106	o-Xylene	46	252	1-Octadecene
8	120	C_3-benzene	47	144	2-Naphthol
9	120	C_3-benzene	48	170	C_3-naphthalene
10	120	C_3-benzene	49	144	1-Naphthol
11	94	Phenol	50	268	n-Nonadecane (n-C_{19})
12	118	Indane	51	266	1-Nonadecene
13	170	n-Dodecane (n-C_{12})	52	282	n-Eicosane (n-C_{20})
14	168	1-Dodecene	53	246	n-Dodecylbenzene
15	116	Indene	53*	246	Dodecylbenzene
16	108	o-Cresol	54	280	1-Eicosene
17	108	p- & m-Cresol	55	296	n-Heneicosane (n-C21)
18	184	n-Tridecane (n-C_{13})	56	294	1-Heneicosene
19	182	1-Tridecene	57	178	Phenanthrene
20	130	Methylindene	58	310	n-Docosane (n-C_{22})
21	132	Tetralin	59	308	1-Docosene
22	122	2,4-Dimethylphenol	60	324	n-Tricosane (n-C_{23})
23	130	1,2-Dihydronaphthalene	61	322	1-Tricosene
24	122	4-Ethylphenol	62	338	n-Tetracosane (n-C_{24})
25	128	Naphthalene	63	336	1-Tetracosene
26	146	Methyltetralin	64	352	n-Pentacosane (n-C_{25})
27	198	n-Tetradecane (n-C_{14})	65	350	1-Pentacosene
28	146	Methyltetralin	66	366	n-Hexacosane (n-C_{26})
29	196	1-Tetradecene	67	364	1-Hexacosene
30	110	Catechol (Pyrocatechol)	68	380	n-Heptacosane (n-C_{27})
31	136 + 144	C_3-phenol + C_2-indene	69	378	1-Heptacosene
32	124	3-Methylcatechol	70	394	n-Octacosane (n-C_{28})
33	212	n-Pentadecane (n-C_{15})	71	392	1-Octacosene
34	142	2-Methylnaphthalene	72	408	n-Nonacosane (n-C_{29})
35	210	1-Pentadecene	73	406	1-Nonacosene
36	124	4-Methylcatechol	74	422	n-Triacotane (n-C_{30})
37	142	1-Methylnaphthalene	75	420	1-Triacotene
38	226	n-Hexadecane (n-C_{16})	76	436	n-Hentriacotane (n-C_{31})
39	174 + 160	C_3-tetralin + C_2-tetralin	77	434	1-Hentriacotene

C. Song's sample S-915 / File: D:\Dataaq\Ajay\S915 / Py-GC-MS Run at 5°C/ms to 610°C for 10 s

Liquefaction of DECS-9 Montana Subbituminous Coal.

The temperature-programmed liquefaction (TPL) and non-programmed liquefaction (N-PL) of DECS-9 Montana subbituminous coal in various solvents were carried out at final temperatures ranging from 300 to 425°C. The selected temperature program consisted of rapid heat-up to a low temperature of 200°C, subsequent soaking at 200°C for 15 min, programmed heating at about 7°C/min to a final temperature, followed by a 30 min hold. The importance of controlling the heat-up step in coal liquefaction has been discussed in previous reports [30,33,39]. For the sake of comparing the amount of organic materials in the THF-insoluble residues, Figure 4.4 shows the conversions of DECS-9 coal into THF-soluble products plus gas from duplicate runs of DECS-9 coal, as a function of final temperature of TPL or N-PL in tetralin and in WI-MD. It has been found that TPL gives higher conversion of low-rank coals in H-donor solvents such as tetralin and WI-MD than non-programmed liquefaction (N-PL, rapid heat-up to reaction temperature in about 3 min followed by a 30 min hold). On the other hand, TPL in non-donor solvents such as naphthalene or methylnaphthalene gave only slightly higher or similar conversions as compared to N-PL runs. However, under comparable conditions (either TPL or N-PL), the coal conversions decreased as the solvent quality decreased: none < naphthalene < methylnaphthalene < WI-MD < tetralin. Detailed TPL results may be found elsewhere [33,34].

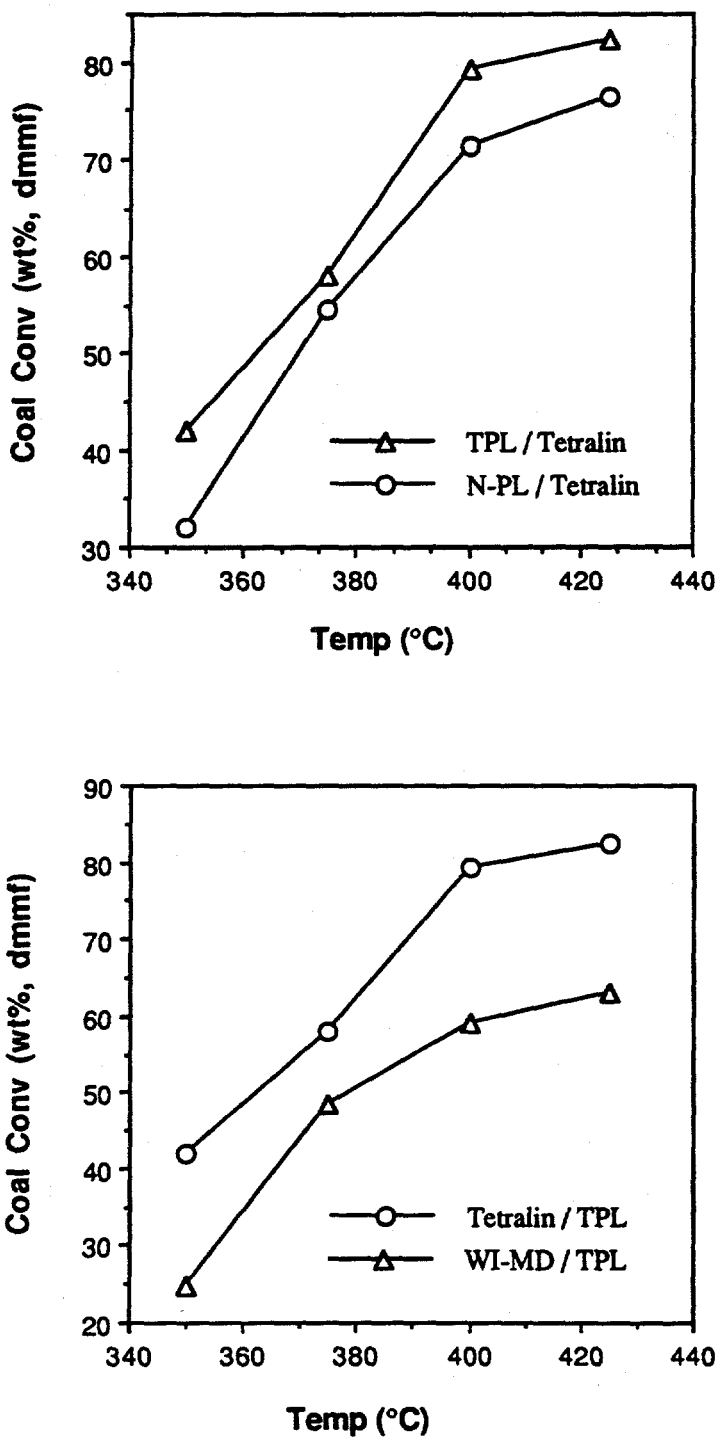

Figure 4.4 Conversion of DECS-9 coal to THF-solubles versus liquefaction temperature for TPL and N-PL in tetralin and for TPL in WI-MD.

CPMAS ^{13}C NMR of Liquefaction Residues.

Figure 4.5 presents the NMR spectra of the THF-insoluble residues from TPL runs with tetralin. The spectrum of THF-extracted unreacted coal serves as a baseline. The THF-insoluble residue from TPL at final temperature of 300°C has a spectrum (Figure 4.5B) similar to that of the THF-extracted coal (Figure 4.5A). In this spectrum, an intense peak is present for aliphatic carbons (0-60 ppm) which may also include trace amounts of aliphatic ether (-C-O-X). This aliphatic peak becomes progressively smaller with increasing severity of liquefaction. The aromatic region has three peaks: an intense peak around 130 ppm (aromatic C), and two shoulders, one at about 142 ppm (possibly catechol-like C), and another at 152 ppm (phenolic or aromatic ether C). A peak at 181 ppm (carboxyl C), and a broad band around 212 ppm (ketone or aldehyde C) define the rest of the spectrum. The peaks at 142 and 212 ppm almost disappear after TPL at 350°C, and the peak at 181 also diminishes after TPL at 375°C. A decrease in intensity of the peak at 152 ppm is only observed after 375°C, and this is accompanied by further loss in aliphatic carbons. Concomitant with the decrease in total aliphatic carbons, the relative contribution from methyl carbons (0-25 ppm) increases. Figure 4.6 gives the NMR spectra of residues from TPL runs with a process solvent, WI-MD. The trends observed from Figures 5 and 6 are similar to each other. In general, the intensity of the aliphatic region (0-60 ppm) decreases, and the aromaticity increases with an increase in severity of TPL. The half-width of the aromatic peak decreased and hence the peak became narrower and sharper with increasing temperature, indicating that the aromatic carbons in the residue from a run at higher temperature tend to become more similar to each other (or less diverse).

Pyrolysis-GC-MS of Liquefaction Residues.

Figure 4.7 shows the 0-32 min RT window of the Py-GC-MS profiles for the residue from TPL in tetralin at 300°C and THF-extracted raw coal, the major peaks of which are numbered and identified in Table 4.1. Phenol, alkylphenols, alkylbenzenes, catechols as well as alkanes and alkenes are formed from flash pyrolysis of the THF-extracted raw coal. Relative to this sample, there is apparent change in the Py-GC-MS profile of the residue from TPL at 300°C. The disappearance of catechol (peak No. 30) and methylcatechol (No.36) and appearance of a major peak for naphthalene (No.25) differentiate the latter from the former. This is especially interesting, since the NMR spectra of these two samples (Figure 4.5) and the corresponding yields of THF-solubles (7-9%) are very similar to each other [30,33]. From these results, it is clear that the reaction at 300°C did cause some structural change. Repeated Py-GC-MS runs have confirmed the disappearance of catechol and methylcatechol peaks. The naphthalene peak in Figure 4.7 is due

mainly to the use of tetralin as solvent, because this peak was found to be very small with other solvents or without solvent. Since the residue has been extracted by THF for over 24 h, washed by acetone and pentane (to remove THF completely) several times and then dried in a vacuum oven at 90-100°C for 6 h, the naphthalene/tetralin remained in the residue must be either chemically bound to other species or physically entrapped in solvent-inaccessible micropores or closed pores which can not be removed by solvent extraction. From these results, it appears that Py-GC-MS can detect some subtle differences in coal structure which are not easily detectable by CPMAS ^{13}C NMR.

Figure 4.8 presents the Py-GC-MS profiles of residues from TPL in tetralin at 375°C and 400°C. The numbers attached to the main peaks correspond to those shown in Table 4.1 for identification. It is clear that even after liquefaction at 375°C for 30 min, the residue still contains significant amounts of structures whose pyrolytic cleavage gives rise to phenol and cresols. The intensities of naphthalene and methylnaphthalene in the pyrolyzates became much higher as compared to the residue from run at 300°C shown in Figure 4.7. Although in this case part of the naphthalene peak also comes from the tetralin solvent as mentioned above, the ratio of methylnaphthalenes to phenols clearly increased significantly as TPL temperature rose from 300 to 375°C (Figures 7B and 8A). Even higher intensity of naphthalene and methylnaphthalene (relative to the phenols) is seen for the pyrolyzates of residue from TPL at 400°C (Figure 4.8B).

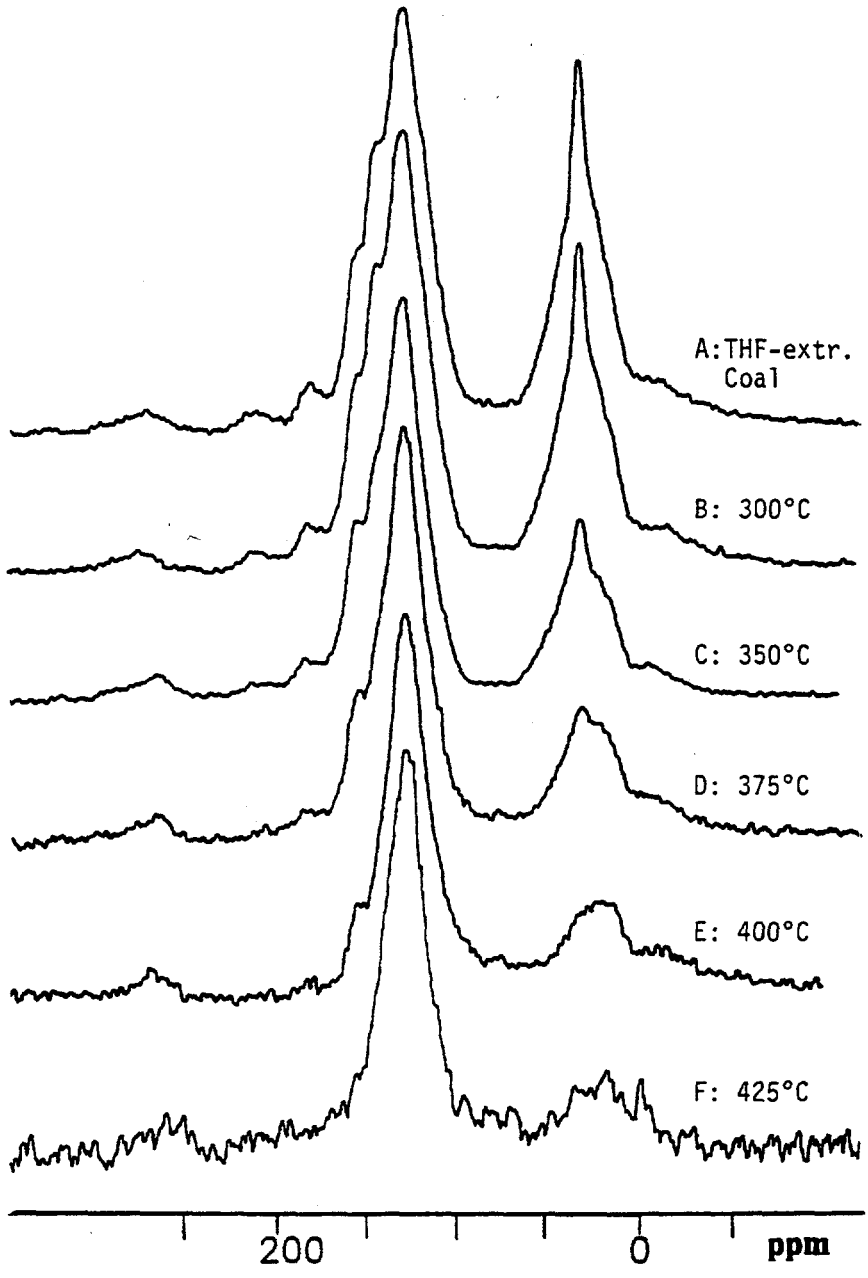

Figure 4.5 CPMAS ^{13}C NMR spectra of THF-insoluble residues from TPL of DECS-9 coal in tetralin at different final temperatures from 300 to 425°C.

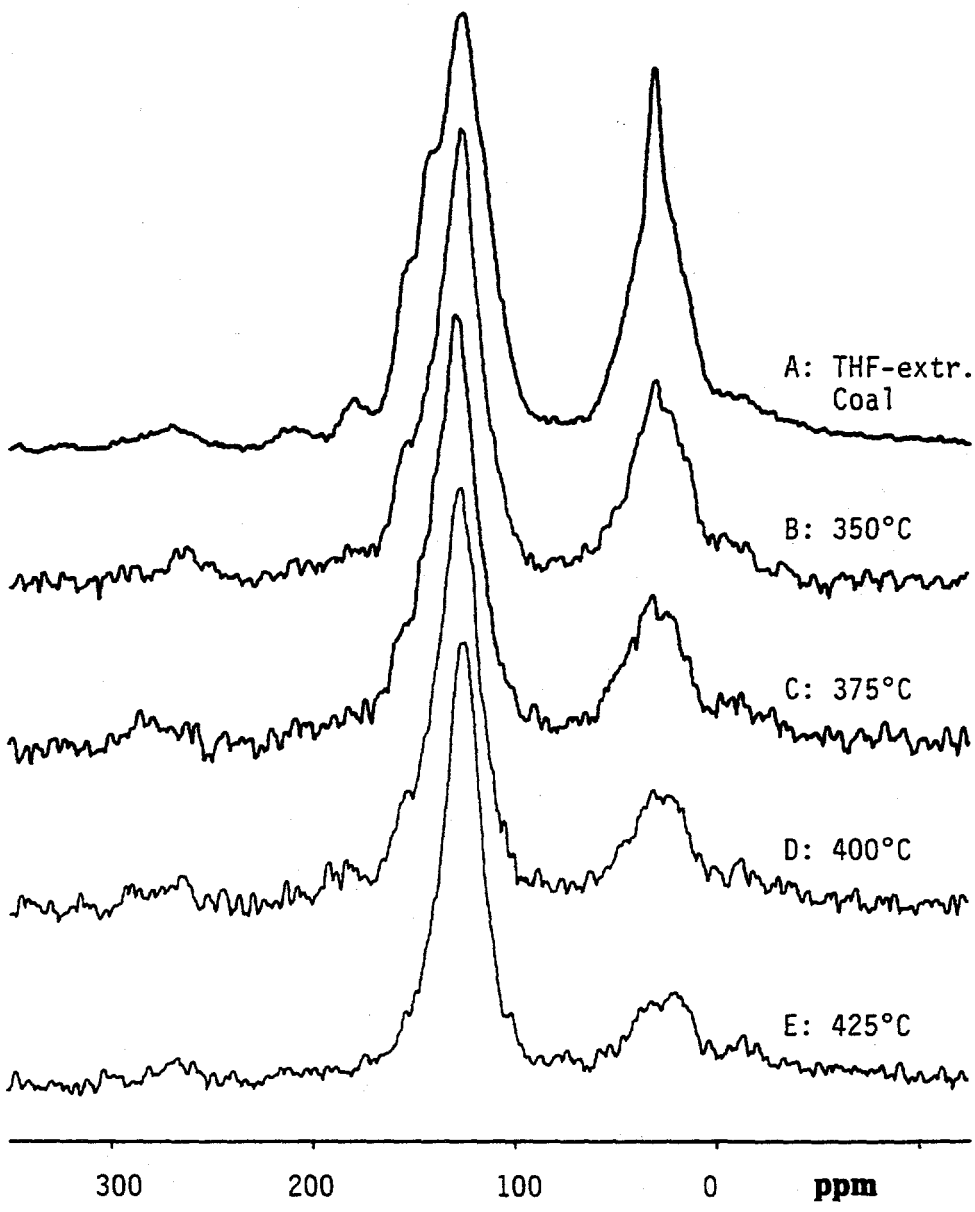

Figure 4.6 CPMAS ^{13}C NMR spectra of THF-insoluble residues from TPL of DECS-9 coal in WI-MD at different final temperatures from 350 to 425°C.

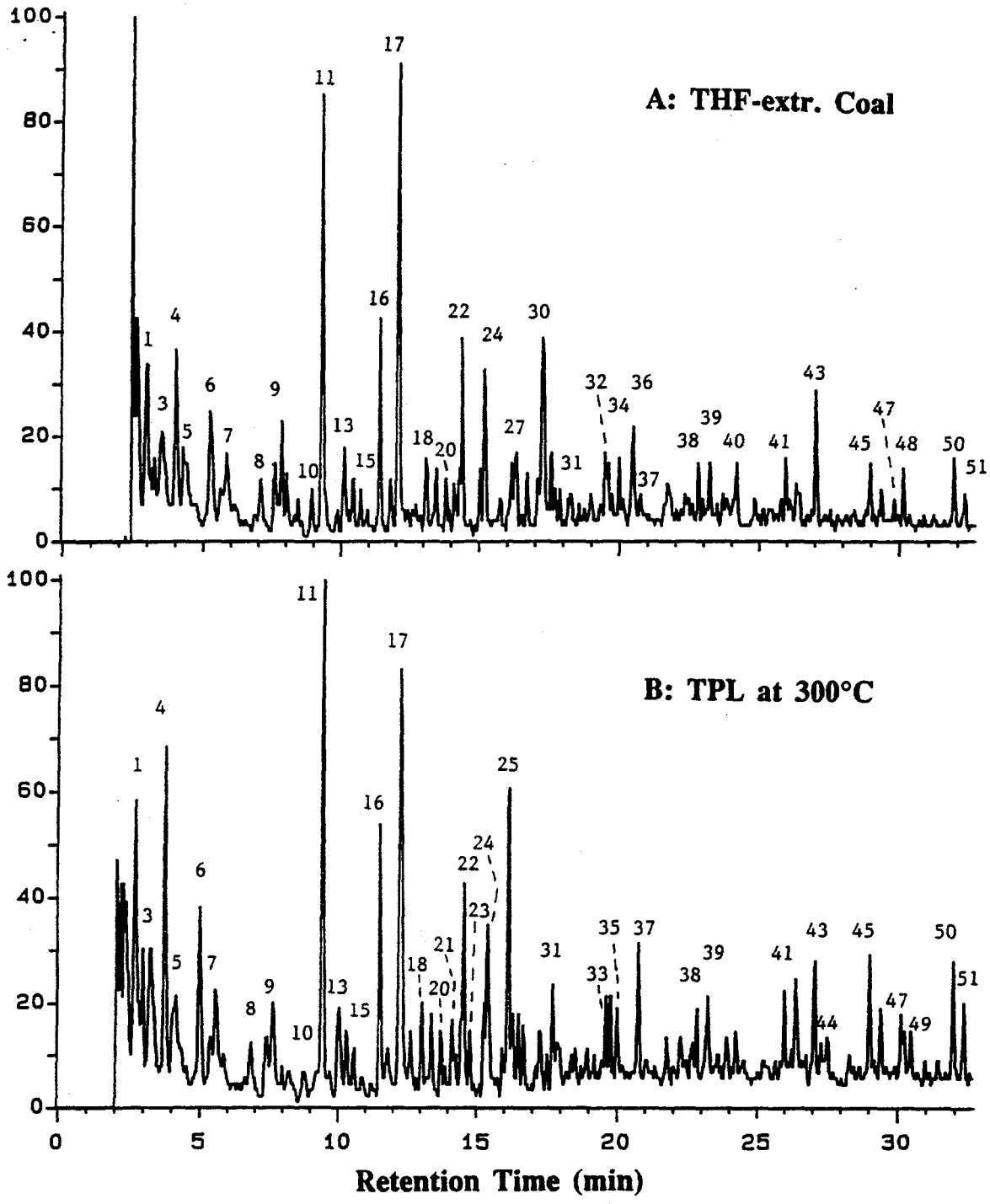

Figure 4.7 Py-GC-MS profiles of THF-extracted unreacted DECS-9 coal (A) and the residue (B) from TPL in tetralin at 300°C.

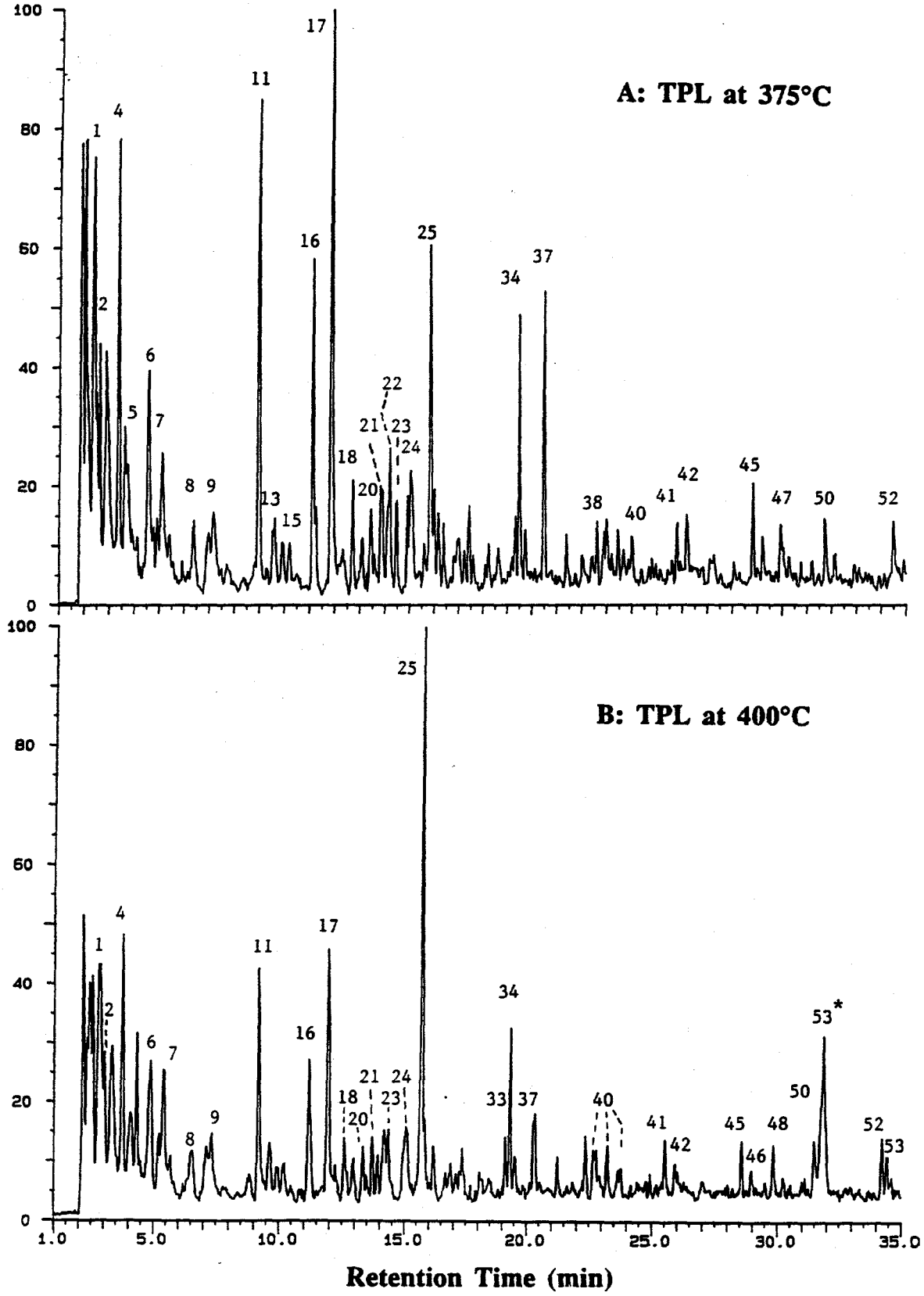

Figure 4.8 Py-GC-MS profiles of the residues from TPL in tetralin at 375°C (A) and 400°C (B).

We have made several replicate Py-GC-MS runs of this sample as well as some other samples. In general the reproducibility was good and distribution patterns of major peaks remained unchanged, although considerable deviations occur sometime with the intensities of the very light C_4-C_6 molecules relative to the other major peaks, presumably due to differences in the amount of liquid nitrogen and time used for cooling capillary column to trap pyrolysis products. In any Py-GC-MS runs of this sample, naphthalene was the most predominant peak. These results indicate higher contents of naphthalene and alkylnaphthalene structures in the residues from runs at higher temperatures, being consistent with the aromaticity increase with increasing temperature as can be seen from Figures 5 and 6.

Quantitative CPMAS ^{13}C NMR for C-Distribution

The progressive changes observed in NMR spectra shown in Figures 5 and 6 prompted us to make quantitative evaluation of coal structural change during liquefaction by curve-fitting the NMR spectra of the residues. Figure 4.9 shows an example of peak separation of NMR spectrum by using the curve-fitting program in LAB CALC software. Table 4.2 gives the results of quantitative calculation for the raw and THF-extracted DECS-9 coal. The oxygen-containing peaks are grouped into oxygen-bound aromatic C-O and aliphatic C-O. The calculated carbon distribution shows that aromaticity of raw DECS-9 coal is about 63 % and this coal contains 18 oxygen-bound carbons per 100 carbon atoms. An interesting result is that most of the oxygen is bound to aromatic carbon: 15 aromatic C versus 3 aliphatic C per 100 C. This means that about 84% of all the oxygens are bound to aromatic rings and nearly 20% of the aromatic carbons are bound to oxygen, pointing to one O-bound C every 5-6 aromatic C. Table 4.2 also indicates that the total number of O/100 C from NMR data is very similar to that from independent, elemental analysis.

Figure 4.10 shows the change of aromaticity as well as coal conversion as a function of final temperature of TPL in tetralin. There appears to be a linear relation between aromaticity of the residue and the reaction temperature above 300°C. It is also clear from Figure 4.10 that higher coal conversion corresponds to higher aromaticity of the residue. A similar trend for aromaticity change with coal conversion was also observed by Fatemi-Badi et al. [29]. Figure 4.11 shows the carbon distribution of THF-insoluble residues versus temperature of TPL in tetralin. Increasing temperature below 300°C had little impact but further increase up to 425°C resulted in almost linear decrease of aliphatic carbons and O-bound carbons and increase of aromatic carbons.

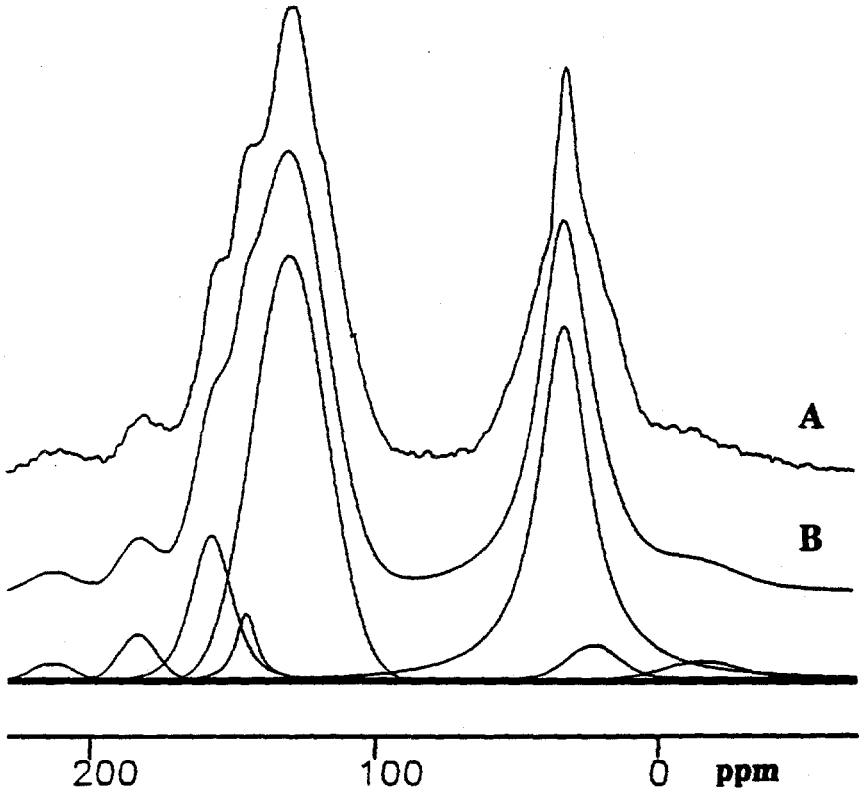

Figure 4.9A Peak separation of NMR bands of THF-extracted raw DECS-9 coal using curve-fitting program. A: real spectrum, B: simulated spectrum.

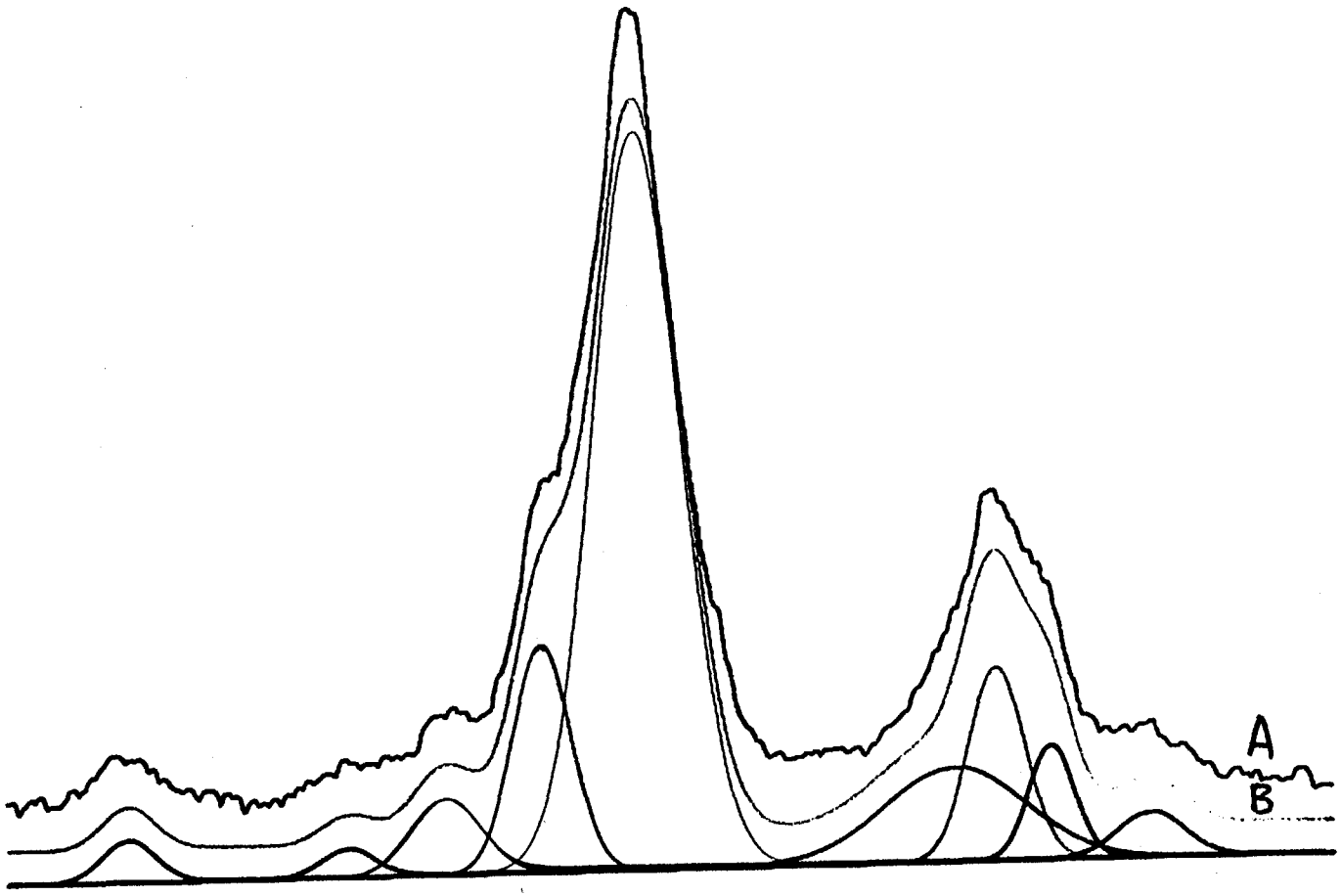

Curve Fitting on NMR Spectrum of Residue from TPL-350°C

Figure 4.9B Peak separation of NMR bands of residue from TPL of DECS-9 coal in tetralin at 375°C using curve-fitting program. A: real spectrum, B: simulated spectrum.

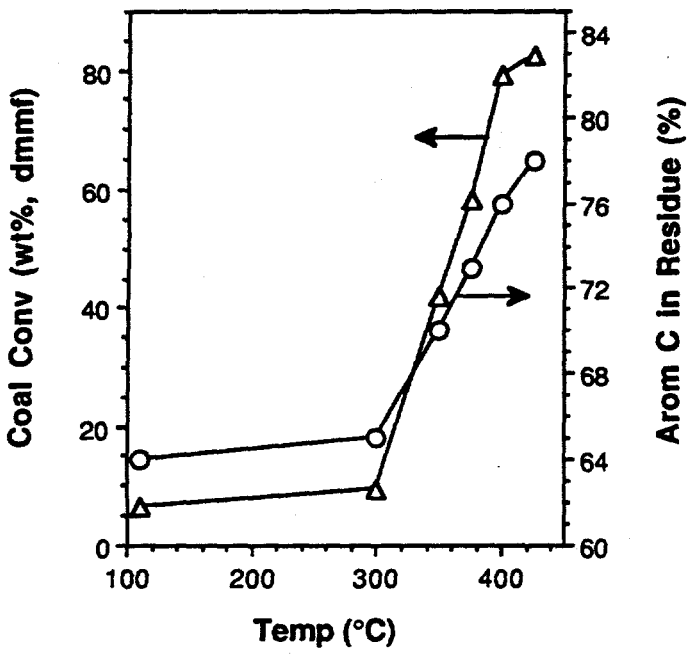

Figure 4.10 Changes of aromaticity of the residues and the coal conversion versus final temperature of TPL in tetralin.

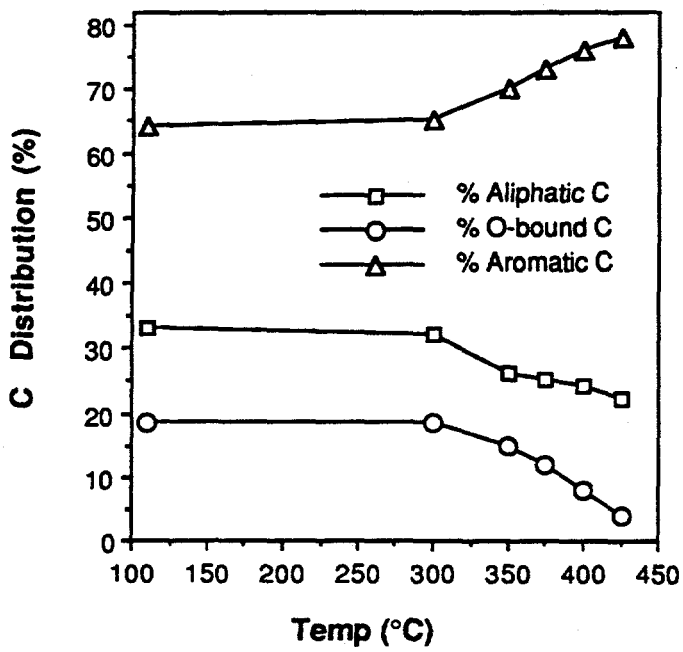

Figure 4.11 Changes of carbon distribution in the residues versus temperature of TPL in tetralin.

In a previous work, the increased aromatics in residues from liquefaction of subbituminous coals with naphthalene solvent was attributed by Solomon et al. [40] to naphthalene adduction. We have examined the residues from runs with different solvents (tetralin, naphthalene, methylnaphthalene, WI-MD) and without solvent by using solid state NMR and Py-GC-MS. Figures 4.12 and 4.13 shows the NMR spectra of residues from TPL of DECS-9 coal with different solvents at 350°C and 400°C, respectively. For comparison, Figure 4.14 presents the NMR spectra of residues from TPL and N-PL runs with tetralin at temperatures ranging from 350-425°C. Taking the significant differences in coal conversion into account, the differences between the ^{13}C NMR spectra of residues from runs at the same final temperatures but using different solvents (Figures 4.12 and 4.13) or different heat-up program (Figure 4.14) are relatively small. Table 4.3 gives some results of quantitative calculation of NMR data. The data in Figures 4.5, 4.6, 4.11-4.14 and Table 4.3 show that aromaticity increase is mainly dependent on reaction temperature; the use of different solvents and different conditions did not cause substantial differences in the aromaticity of the residue, although the coal conversions can vary significantly in different solvents or under different conditions (Figure 4.4). These results reveal that the final reaction temperature is most important in determining carbon distribution and structural transformation.

Table 4.2. C-Distribution & O-Functionality of DECS-9 Subbituminous Coal

	Total Oxygen		Carbon Distribution (%)[a]			
Samples	O/100 C	O/100 C	Aromatic C	Aliphatic C	Aliphatic C-O	Aromatic C-O
	^{13}C NMR	Elemental	95-160 ppm	0-60 ppm	170-230	Shoulders[b]
Raw DECS-9	18	17.4	63	35	3	15
THF-extr. DECS-9	18		64	33	3	15

a) The absolute deviations for the carbon distribution calculations are about ± 2 %.

b) Include phenolic carbons around 156 ppm and catechol-like carbons around 145 ppm.

Table 4.3. C-Distribution of Liquefaction Residues from DECS-9 Subbituminous Coal

Conditions			Carbon Distribution (%)[a]		
Temperature	Solvent	Program	Aromatic C	Aliphatic C	O-bound C[b]
350	Tetralin	TPL	70	26	15
350	Tetralin	N-PL	70	25	16
350	Naphthalene	TPL	70	28	13
400	Tetralin	TPL	76	24	8
400	Tetralin	N-PL	74	26	7
400	WI-MD	TPL	74	26	7
400	WI-MD	N-PL	75	25	7
400	1-MN	N-PL	78	22	6
400	Naphthalene	N-PL	76	24	5
400	None	N-PL	75	24	6

a) The absolute deviations for the carbon distribution calculations are about ± 2 %.

b) Include phenolic carbons around 156 ppm and catechol-like carbons around 145 ppm.

Figure 4.15 indicates that both total and aromatic O-bound carbons decrease with increasing temperature from 300 up to 425°C. The progressive changes of O-containing compounds can be clearly seen from the gradual decrease of catechol-like and subsequently phenolic peaks in the expanded aromatic region of the NMR spectra of these residues, as shown in Figure 4.16. However, the peak shapes of Figures 16E and 16F indicate that there still exist O-bound aromatic carbons even after reaction at 400 and 425°C. This observation is also supported strongly by the observed phenolic components in the pyrolyzates as shown in the Py-GC-MS TIC in Figure 4.8. It also appears from the expanded region that increasing the temperature from 400 to 425°C caused a decrease in protonated aromatic-C (93-129 ppm) and an increase in bridgehead-C and substituted-C (130-150 ppm), indicating increased degree of condensation.

Effect of Solvent on NMR of Residues from TPL at 350°C

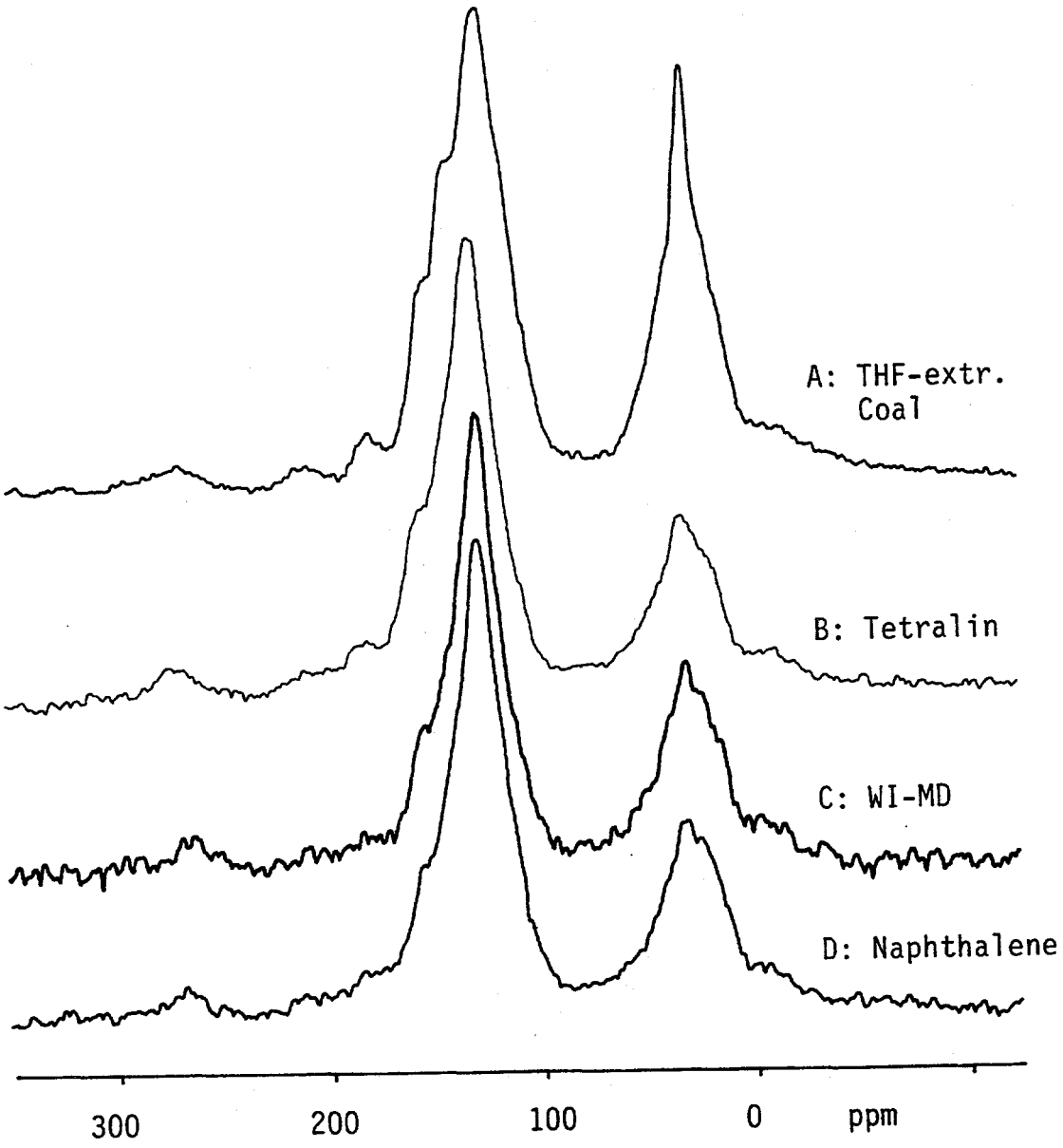

Figure 4.12 CPMAS ^{13}C NMR spectra of residues from TPL of DECS-9 coal at final temperature of 350°C (A, THF-extracted raw coal; B, tetralin; C, WI-MD; D, naphthalene).

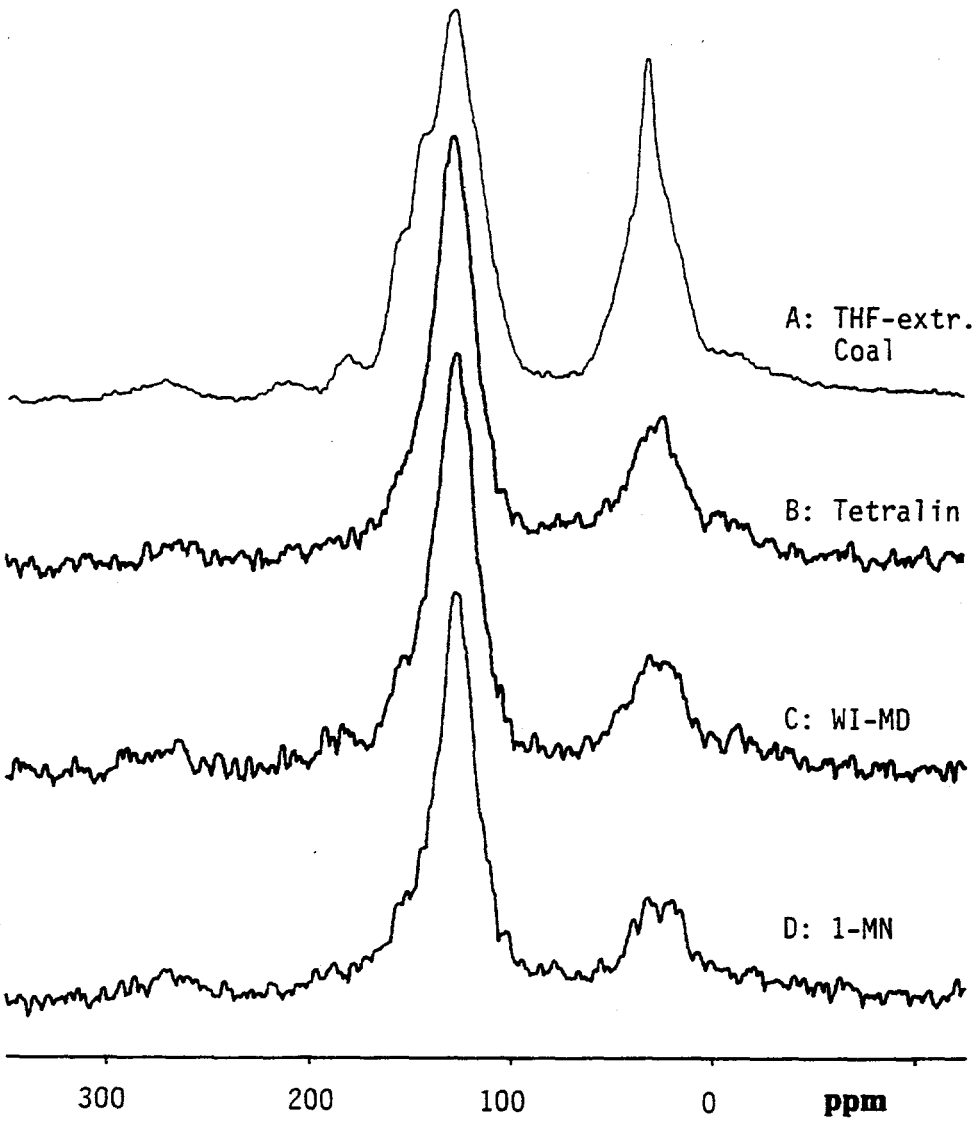

Figure 4.13 CPMAS ^{13}C NMR spectra of residues from TPL of DECS-9 coal at final temperature of 400°C (A, THF-extracted raw coal; B, tetralin; C, WI-MD; D, 1-methylnaphthalene).

CPMAS ^{13}C NMR of Residues from TPL & N-PL with H-donor Tetralin

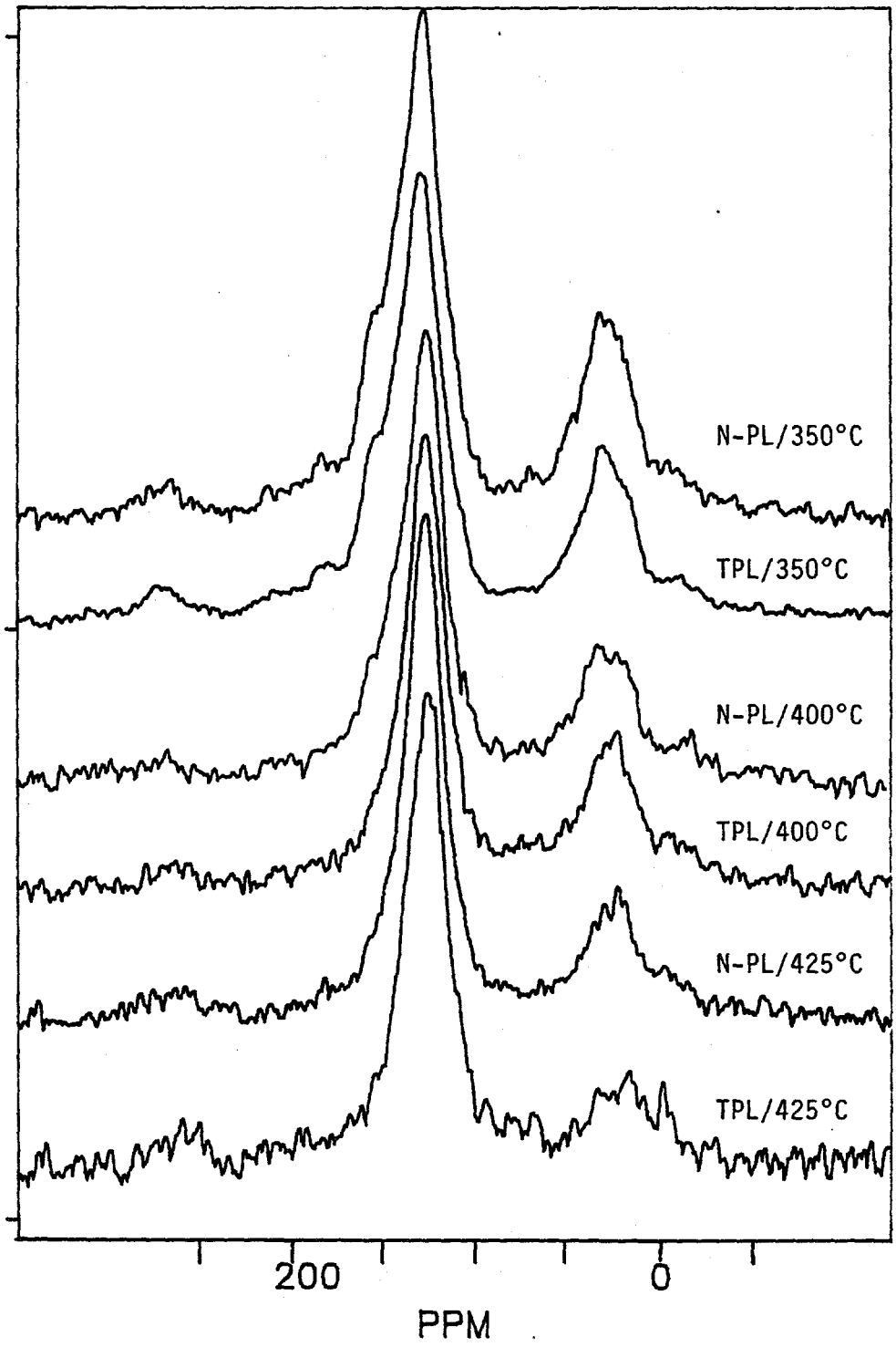

Figure 4.14 CPMAS ^{13}C NMR spectra of residues from TPL and N-PL of DECS-9 coal with tetralin at final temperatures ranging from 350 to 425°C.

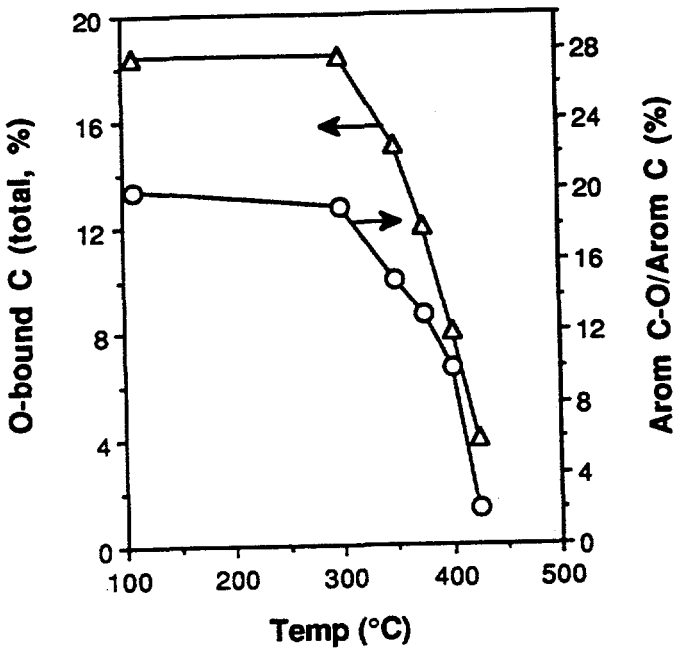

Figure 4.15 Changes of total oxygen-bound C and aromatic O-bound C versus final temperature of TPL in tetralin.

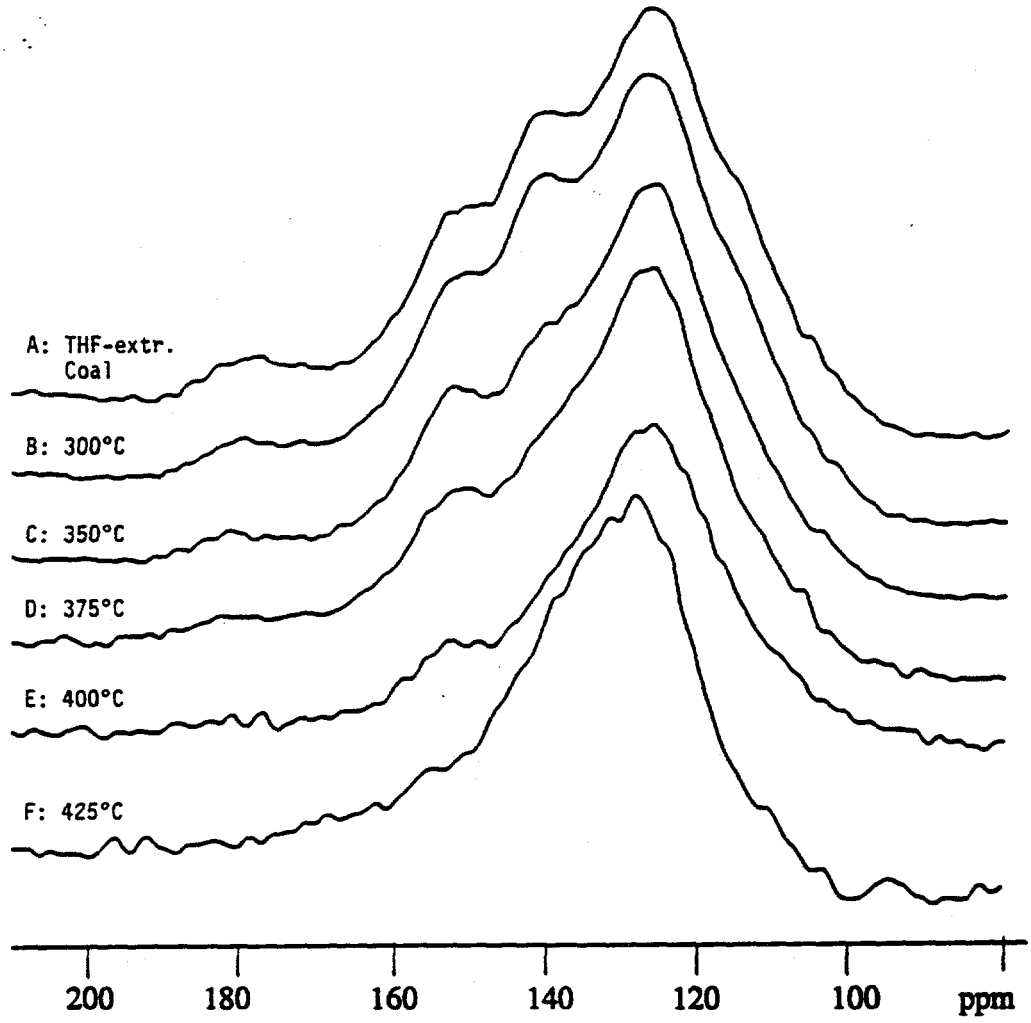

Figure 4.16 Expanded aromatic region of ^{13}C NMR spectra of residues from TPL in tetralin.

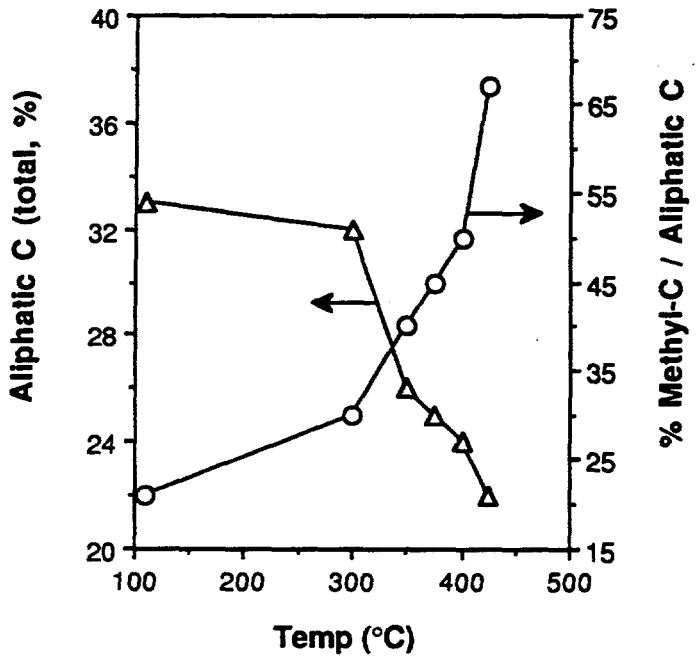

Figure 4.17 Changes of total aliphatic carbons and methyl carbons in the residues versus final temperature of TPL in tetralin.

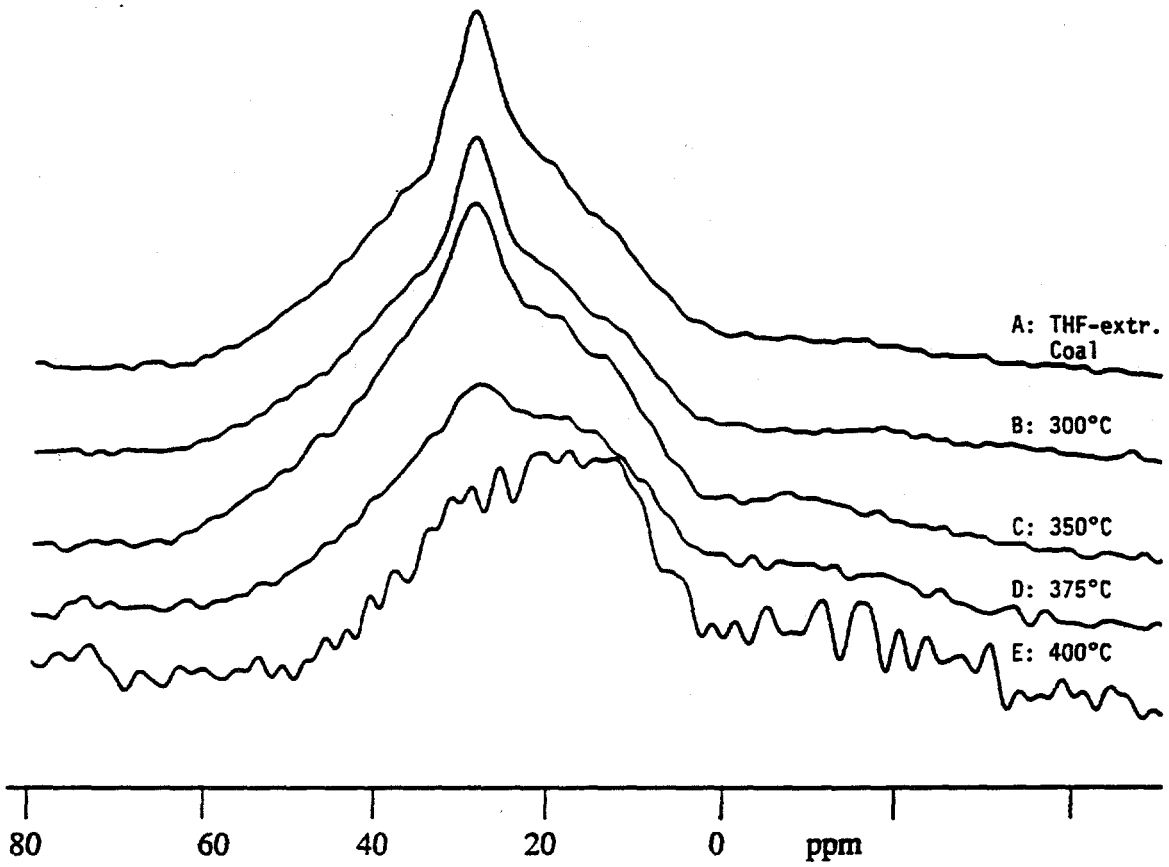

Figure 4.18 Expanded aliphatic region of ^{13}C NMR spectra of residues from TPL in tetralin.

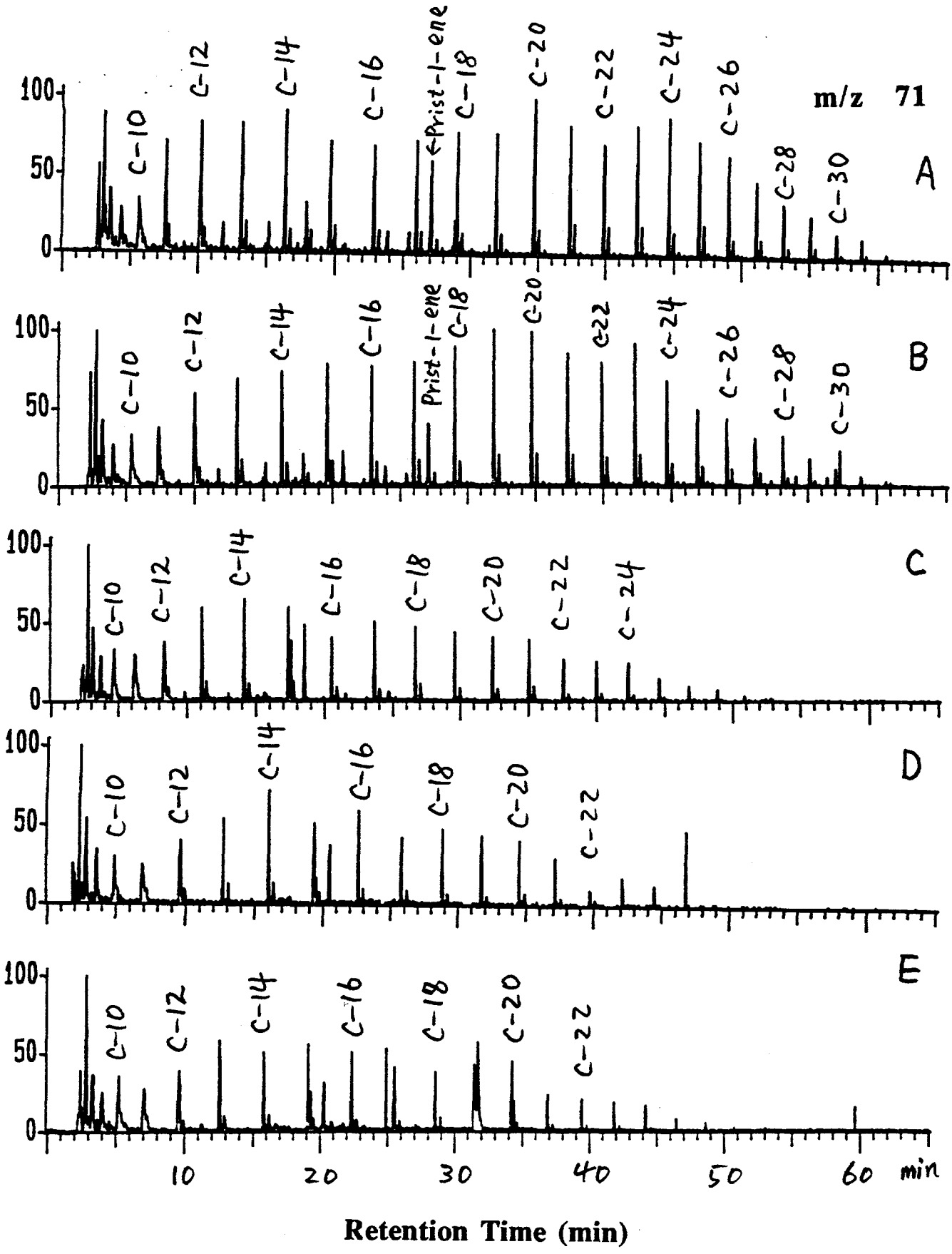

Figure 4.19 Selective ion monitoring of long-chain paraffins at m/z 71 from Py-GC-MS profiles of residues from TPL in tetralin at 300 °C (A), 375°C (B) and 400°C (C).

While the total aliphatic carbons decreased, Figure 4.17 shows that the percentage of methyl carbons relative to total aliphatic carbons increased with increasing reaction temperature. This can be due either to the increase or formation of methyl carbons or the decrease in methylene carbons. However, the expanded aliphatic region of NMR spectra, as shown in Figure 4.18, unambiguously show that the trend observed from Figure 4.16 is due mainly to the decrease or removal of methylene carbons from the coal during the reaction. Selective ion monitoring using SIC at m/z 71 provided additional evidence from Py-GC-MS data. As shown in Figure 4.19, the contents of long-chain paraffins in the pyrolyzates decreased with increasing temperature above 300°C, and this is at least partially responsible for the decrease in aliphatic methylene carbon observed from ^{13}C NMR. The above results also demonstrate the potential and importance of combining CPMAS ^{13}C NMR and Py-GC-MS.

Mathematical Correlation of CPMAS ^{13}C NMR Data

On the basis of above-mentioned NMR data, there exist good correlations between carbon distribution in the residues and the reaction temperature above 300°C. This presents a unique opportunity for us to attempt mathematical correlation. Little or no work has been reported in literature on mathematical correlation of CPMAS ^{13}C NMR data with reaction temperature. We have found that the changes in distributions of aromatic, aliphatic, and oxygen-bound carbons in the residues can be correlated with reaction temperature by equations 1, 2 and 3, respectively,

$$C_{arm} = \alpha_1 f_{arm} + \beta_1 T \qquad \text{For aromatic carbon or aromaticity} \qquad 1)$$

$$C_{alip} = \alpha_2 f_{alip} + \beta_2 T \qquad \text{For aliphatic carbons} \qquad 2)$$

$$C_{O\text{-}C} = \alpha_3 f_{O\text{-}C} + \beta_3 T \qquad \text{For oxygen-bound carbons} \qquad 3)$$

where f_{arm}, f_{alip} and $f_{o\text{-}c}$ and C_{arm}, C_{alip}, and $C_{o\text{-}c}$ represent the contents of aromatic, aliphatic, and oxygen-bound carbons in the original coal and in the residues, respectively; T stands for reaction temperature in degree Celsius; α and β are constants whose values depend on the samples and reaction conditions. A general expression of these correlations can be written as equation 4.

$$C_i = \alpha f_i + \beta T \qquad \text{For specific carbon type i} \qquad 4)$$

Figure 4.20 presents the plots and the linear correlations for residues from TPL in tetralin. A least-squares analysis of the data in Figure 4.20 was made in order to obtain a best fit. Table 4.4 lists the values of α and β and correlation coefficients. As can be seen from Figure 4.20 and Table

4.4, the mathematical correlations provide a very good fit of the CPMAS ^{13}C NMR data.

Table 4.4. Mathematical Correlation of ^{13}C NMR Data of Residues with Reaction Temperature

Carbon Type		$C_i = \alpha f_i + \beta T$ $T \geq 300°C$		Correlation Coefficient
C_i in Residue	f_i of Orig. Coal	α	β	
For TPL in Tetralin				
Aromatic C	63	0.5204	0.10696	0.997
Aliphatic C	35	1.5429	-0.0762	0.946
O-bound C	18[a]	3.0111	-0.1155	0.959
For All the Runs[b]				
Aromatic C	63	0.5431	0.1026	0.961
Aliphatic C	35	1.4747	-0.0684	0.826
O-bound C	18[a]	3.038	-0.1191	0.900

a) Including both aromatic O-bound C and aliphatic O-bound C.

b) For all the TPL and N-PL runs using different solvents including H-donor tetralin, non-donor naphthalene and methylnaphthalene, and process solvent WI-MD as well as a solvent-free run at 400°C.

In fact, we have processed the NMR spectra of 24 residue samples from TPL and N-PL runs of the coal in different solvents including tetralin, WI-MD, 1-methylnaphthalene and naphthalene, and one residue from solvent-free run at 400°C. Figure 4.21 presents the NMR data and the mathematical correlation by a linear fit for all of the samples. In fact, the % C values for runs at the same final temperature but using different solvents or under different conditions, are so close that many of them overlapped in Figure 4.21. The correlation coefficient associated with a least-squares analysis for aromatic C is 0.961, indicating a good fit of the data by a straight line even though the samples were derived from considerably different conditions.

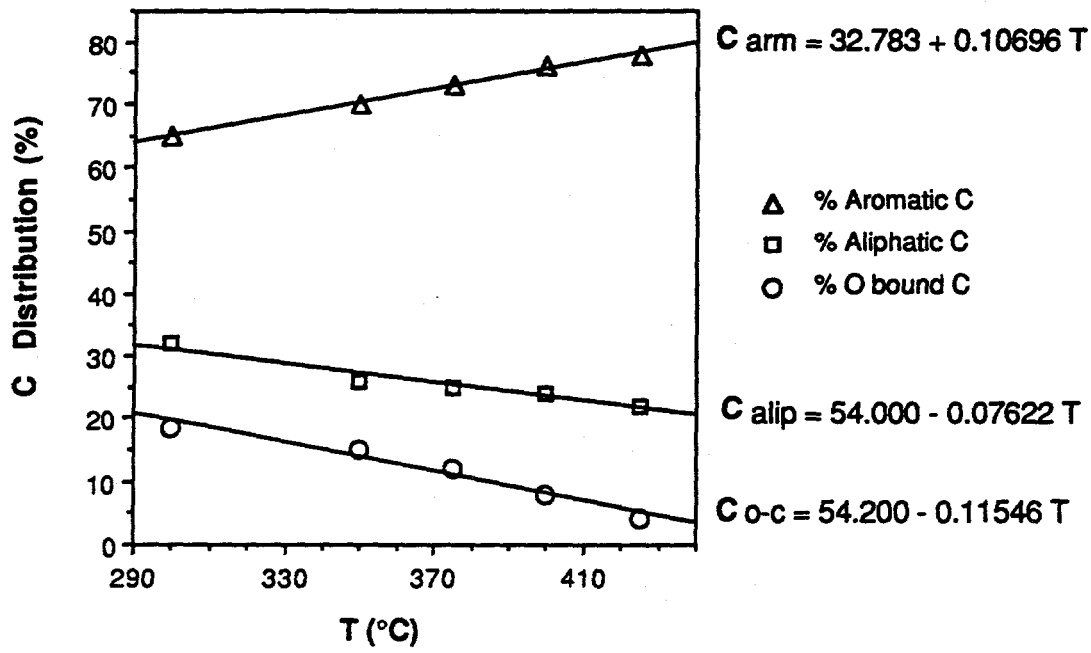

Figure 4.20 Correlation of C-distribution of residues with TPL temperature in tetralin (T≥ 300°C).

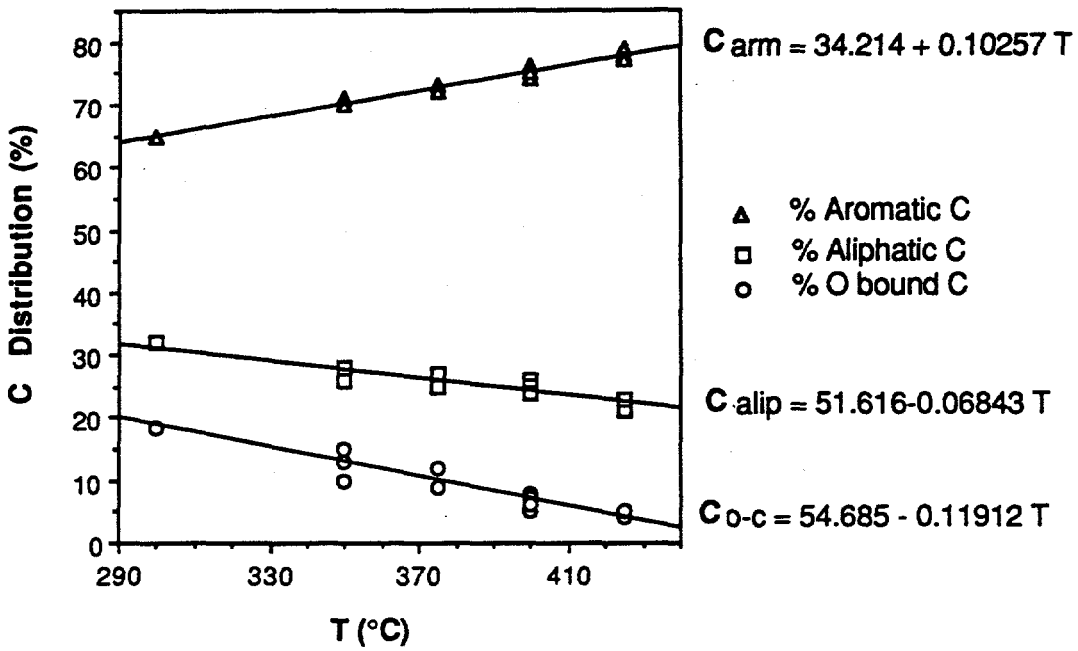

Figure 4.21 Linear correlation of C-distribution with final temperature for residues from TPL and N-PL runs using different solvents including tetralin, WI-MD, naphthalene and methylnaphthalene ($T \geq 300°C$).

These results revealed that the change of carbon distribution, especially aromaticity, is strongly dependent on the final reaction temperature and only slightly on the nature of the solvents and heat-up program, even though using different solvents and different heat-up programs caused significant differences in the coal conversions and remaining amounts of organic materials in the residues. There is also a good correlation of C distribution of residues with coal conversion in TPL in tetralin or WI-MD, because the coal conversion is dependent upon the reaction temperature. These results also show that prediction of the changes of carbon distribution of coals versus reaction temperature is possible in practice by using the methodology developed here.

Structural Characteristics and Liquefaction Reactions of Low-Rank Coals

Combination of the NMR and Py-GC-MS data suggests that the original DECS-9 coal contains significant quantities of oxygen-containing structures, which include catechol, methylcatechols, phenols, alkylphenols, and carboxylic and carbonyl groups, chemically bound to its macromolecular network, corresponding to about 18 O-bound C per 100 C atoms (Figures 5 and 6, Table 4.2). It is very interesting to note that curve-fitting and subsequent calculation of CPMAS ^{13}C NMR spectra of both raw and THF-extracted coal point to the presence of approximately one O-bound carbon in every 5-6 aromatic carbon atoms. Py-GC-MS data revealed that phenol, cresols, C_2-phenols, catechol and methylcatechols are the major components in the pyrolyzates of these samples (Figures 4.2 and 4.7, Table 4.1), being in excellent agreement with the CPMAS ^{13}C NMR data.

Characterization of residues from TPL revealed that liquefaction of the coal involves the considerable changes of the oxygen-containing structures including catechol-like structures, which seem to disappear in the liquefaction residues above 300°C; carboxyl groups, which almost disappear after 350°C; and phenolic structures which are most abundant in the original coal but diminish in concentration with increasing temperature. The analytical results point to the progressive loss of oxygen functional groups (Figures 4.13 and 4.14) and aliphatic species (Figures 4.17 and 4.18) from the macromolecular network of the subbituminous coal during its liquefaction under TPL conditions. Relative to the conventional N-PL runs, the higher conversions from TPL runs in tetralin (Figure 4.4) suggest that the removal of carboxylic and catechol groups from the coal during the programmed heat-up ($\leq$ 350°C) in H-donor vehicle has contributed to minimizing the retrogressive crosslinking at higher temperatures. In other words, the reactive sites generated by the removal of carboxyl and catechol groups, which could happen at low temperatures, can be effectively stabilized by H-transfer from tetralin at lower temperatures during programmed heat-up.

Low-rank coals are characterized by low aromaticities and high oxygen functionalities, which can also be seen clearly from data in Figures 4.1 and 4.2 and Table 4.2. Recently there has

been increasing interest in finding ways to improve conversion of low-rank coals, which are often less readily liquefied than bituminous coals [33,39,41,42]. This is considered to relate to the propensity for low-rank coals to form crosslinks upon heating, which render the coal less amenable to liquefaction [41,42]. It is now recognized that low-rank coals are more reactive than had been thought previously, and their conversion in high-severity processes is accompanied by significant retrogressive reactions [33, 39-46]. For example, Suuberg et al. [43] reported that a lignite starts to cross-link at much lower pyrolysis temperature than bituminous coals. Solomon et al. [40,45] and Lynch et al. [46] have suggested that low-temperature cross-linking is related to decarboxylation. Manion et al. found that it is difficult to establish coupling reactions resulting from decarboxylation of monomeric benzoid acid compounds under homogeneous reaction conditions [47], while our preliminary data suggest that crosslinking could be caused by decarboxylation reactions involving "immobilized molecular fragments" in low-rank coals. In regard to retrogressive reactions of other functional groups, McMillen et al. [44] and Tse et al. [48] have provided some evidence on the condensation of polyhydroxy structures in model compound studies. The present work has revealed progressive and important changes in oxygen-functionalities of a low-rank coal during its liquefaction at different temperatures.

The term crosslinking used in this report refers to chemical linking of molecular fragments (e.g., reactive radicals from coal thermal decomposition, or thermally unstable compounds, etc) to coal through covalent bonds, which leads to increased crosslinks (usually with stronger bonding) in coal macromolecular network. It should be noted that the definition of the term used here is different from that used in polymer science, where crosslinking means the linking of polymer chains through covalent or ionic bonds to form a network.

Our ^{13}C NMR and Py-GC-MS in combination with liquefaction data suggest that if one removes the catechol and carboxyl groups from coal macromolecular network under hydrogen-transferring conditions (e.g., with H-donor) at low temperatures ($\leq$ 350°C), the reactive sites generated from their reactions (such as decarboxylation) can be effectively stabilized by H-donor. It has been indicated [39] that, for low-rank coals, using very fast heat-up to high temperatures would lead to extremely rapid formation of reactive radicals that exceed the capacity or rate of H-donation, resulting in significant retrogressive reactions. Therefore, programmed heat-up in H-donor in low temperature regime could significantly reduce retrogressive crosslinking (at the reactive sites) at high temperatures.

Probably the reactions responsible for retrogressive crosslinking during initial stage of liquefaction of low-rank coals in conventional high-severity processes are associated with their oxygen functional groups, such as crosslinking caused by reactions of catechols and phenollic compounds and decomposition of carboxlic groups. Comparative examination of our coal conversion data and Py-GC-MS and NMR spectroscopic data suggests that the TPL conditions in

H-donor vehicle facilitate the reduction of crosslinking reactions of the thermally sensitive groups such as oxygen-functional groups at low temperatures.

Py-GC-MS also revealed the incorporation of the reaction solvents such as tetralin into coal structure during liquefaction at both low and high temperatures, but CPMAS ^{13}C NMR was not sensitive with respect to this. When tetralin was used as the solvent, naphthalene and small amounts of tetralin and dihydronaphthalene were also detected in the pyrolyzates of the residues from TPL at 300-400°C, as can be seen from Figures 7 and 8 and Table 4.1. Comparative examination of Py-GC-MS profiles indicated that for runs at low temperatures such as 300°C, most of the naphthalene in the pyrolyzates of the residue came from the reaction solvent, presumably by physical imbibition which could not be removed by THF extraction, and in part by chemical binding; but in the residue from TPL at higher temperatures such as 400°C, the naphthalene peak also came from pyrolysis of the residue, because even the residues from solvent-free runs at 400°C can produce considerable amounts of naphthalene and methylnaphthalenes. It is considered that the aromaticity increase in the residues with temperature is due mainly to structural transformation, rather than solvent incorporation.

CONCLUSIONS

This work has clearly demonstrated that, by the combined use of the CPMAS ^{13}C NMR and Py-GC-MS techniques on properly prepared samples, it is possible to characterize both the structural features and molecular/structural components in coal macromolecular network, and to follow changes in functionalities and carbon distribution during coal liquefaction [Song et al., 1992c]. The present results indicate that DECS-9 Montana subbituminous coal contains considerable quantities of oxygen-containing structures, corresponding to about 18 O-bound C per 100 C atoms and one O-bound C every 5 to 6 aromatic C. The oxygen-bearing components in the coal include phenolic structures, catechol-like structures, and carboxyl groups. Py-GC-MS in combination with ^{13}C NMR revealed that some dominant structures in the coal exist in a fashion such that they will produce phenol, alkylphenols, catechol, methylcatechols, toluene, and xylene upon flash pyrolysis.

The analytical results of liquefaction residues point to the progressive loss of oxygen functional groups and aliphatic species from the macromolecular network of the coal during its depolymerization in tetralin under TPL conditions. The progressive changes for the oxygen-bearing components are characterized by disappearance of the catechol-like structures from the liquefaction residues at ≥300°C, disappearance of carboxyl groups after 350°C, and gradual decrease of phenolic structures with increasing reaction temperature. The higher conversions in TPL runs (relative to the conventional non-programmed runs) in tetralin suggest that the removal of catechol and carboxylic

groups from the coal macromolecular network and the stabilization of the reactive sites (generated from the reactions of catechols, carboxyl groups, etc.) by H-transfer from H-donor at $\leq 350°C$ have contributed to minimizing the retrogressive crosslinking at higher temperatures.

Quantitative calculation of NMR data and mathematical correlation were also attempted in this work, and the results, though preliminary, appear to be very promising. For a relatively large number of experimental samples (24 residues) derived under significantly different conditions, quantitative and linear correlations between C-distribution and reaction temperature have been found, which can be expressed by a simple equation, $C_i = \alpha f_i + \beta T$, where f_i and C_i represent content of aromatic, aliphatic, or oxygen-bound carbons in the original coal and residue, respectively; T stands for the reaction temperature; α and β are constants.

REFERENCES

1 Pines, A.; Gibby, M.G.; Waugh, J.S., 1972. J. Chem. Phys., 56: 1776.

2 Pines, A.; Gibby, M.G.; Waugh, J.S., 1973. J. Chem. Phys., 59: 569.

3 Schaefer, J.; Stejskal, E.O., 1976. J. Am. Chem. Soc., 98:1031

4 Yannoni, C.S., 1982. Acc. Chem. Res., 15: 201

5 VanderHart, D.L.; Retcofsky, H.L., 1976. Fuel, 55: 202

6 Alemany, L.B.; Grant, D.M.; Pugmire, R.J.; Alger, T.D.; Zilm, K.W., 1983. J. Am. Chem. Soc., 105: 2142.

7 Wilson, M.A.; Pugmire, R.J.; Karas, J.; Alemany, L.B.; Woolfenden, W.R.; Grant, D.M., 1984. Anal. Chem., 56: 933-943.

8. Dennis, L.W.; Maciel, G.E.; Hatcher, P.G., 1982. Geochimica et Cosmochimica Acta, 46, 901-907

9 Hatcher, P.G., Wilson, M.A., Vassallo, A.M. and Lerch III, H.E., 1989. Int. J. Coal Geol., 13, 99.

10. Yoshida, T.; Maekawa, Y., 1987. Fuel Processing Technol., 15, 385-395.

11. Yoshida, T., 1992. Sekiyu Gakkaishi, 35 (1): 1-13.

12. Solum, M.S.; Pugmire, R.J.; Grant, D.M., 1989. Energy & Fuels, 3: 187-193.

13. Botto, R.E.; Wilson, R.; Winans, R.E., 1987. Energy & Fuels, 1: 173.

14. Supaluknari, S.; Larkins, F.P.; Redlich, P.; Jackson, W.R., 1989. Fuel Processing Technology 23: 47-61.

15 Davidson, R.M., 1980. Molecular Structure of Coal, ICTIS/TR08, IEA Coal Research, London, 86 pp.

16 Davidson, R.M., 1986. Nuclear Resonance Studies of Coal, ICTIS/TR32, IEA Coal Research, London.

17 Snape, C.E., Axelson, D.E., Botto, R.E., Delpuech, J.J., Tekely, P., Gerstein, B.C., Pruski, M., Maciel, G.E. and Wilson, M.A., 1989. Fuel, 68: 547.

18 Meiler, W. and Meusinger, R. 1990. NMR of Coals and Coal Products, Annual Reports of NMR Spectroscopy, Vol.23, Academic Press, New York, pp.375-410.

19. Nip, N.; de Leeuw, J.W.; Schenck, P.H.; Meuzelaar, H.L.; Stout, S.A.; Given, P.H.; Boon, J.J., 1985. J. Anal. Appl. Pyrol., 8: 221-240.

20 Philp, R.P., 1985. Fossil Fuel Biomarkers, Elsevier, Amsterdam, 294 pp.

21. Saiz-Jimenez, C.; De Leeuw, J.E., 1986. J. Anal. Appl. Pyrol., 9: 99-119.

22. Hatcher, P.G.; Lerch, H.E.; Kotra, R.K.; Verheyen, T.V., 1988. Fuel, 67: 1069-1075.

23 Nomura, M., Ida, T., Miyake, M., Kikukawa, T. and Shimono, T., 1989. Chem. Lett., 1989: 645-648.

24 Gallegos, E.J., 1979. "Pyrolysis Gas Chromatography", in "Chromatography in Petroleum Analysis", K.H. Altgelt and T.H. Gouw Eds., Marcel Dekker, New York, pp.163-184.

25 Meuzelaar, H.L.C.; Haverkamp, J.; Hileman, F.D., 1982. "Pyrolysis Mass Spectrometry of Recent and Fossil Biomaterials", Elsevier, Amsterdam, 287pp.

26 Maswadeh, W.S., Fu, Y., Dubow, J., Meuzelar, H.L.C., 1992. Am. Chem. Soc. Div. Fuel Chem. Prepr., 37 (2) : 699-706.

27 Winans, R.E. , Melnikov, P.E. and McBeth, R.L., 1992. Am. Chem. Soc. Div. Fuel Chem. Prepr., 37 (2) : 693-698.

28 Franco, D.V., Gelan, J.M., Martens, H.J. and Vanderzande, D. J.-M., 1991. Fuel, 70: 811-817.

29 Fatemi-Badi, S.M., Swanson, A.J., Sethi, N.K. and Roginski, R.T., 1991. Am. Chem. Soc. Div. Fuel Chem. Prepr., 36 (2) : 470-480.

30. Song, C.; Schobert, H.H.; Hatcher, P.G., 1991. Proc. 1991 Int. Conf. Coal Sci. U.K., 1991, pp.664-667.

31 Song, C.; Schobert, H.H.; Hatcher, P.G., 1992. Am. Chem. Soc. Div. Fuel Chem. Prepr., 37 (2) : 638-645.

32 Saini, A.K., Song, C., Schobert, H.H., Hatcher, P.G., 1992. Am. Chem. Soc. Div. Fuel Chem. Prepr., 37 (3) : 1235-1242.

33. Song, C.; Schobert, H.H., 1992. Am. Chem. Soc. Div. Fuel Chem. Prepr., 37 (2) : 976-983.

34. Song, C.; Schobert, H.H.; Hatcher, P.G., 1992. Energy & Fuels, 6: 326-328.

35 Gollakota, S.V., Davies, O.L., Vimalchand, P., Lee, J.M. and Cantrell, C.E., 1990. Proceedings of U.S. DOE Direct Liquefaction Contractors' Review Meeting, Sept. 24-26, Pittsburgh, pp.129-158.

36. Song, C.; Hatcher, P.G., 1992. Am. Chem. Soc. Div. Petrol. Chem. Prepr., 37 (2) : 529-

539.

37. Schobert, H.H., 1990. Resources, Conservation and Recycling, 3: 111-123.

38 van Bergen, P.F., Collinson, M.E., Damste, S.S. and de Leeuw J. W., 1991. Am. Chem. Soc. Div. Fuel Chem. Prepr., 36 (2): 698-701.

39 Song, C., Hanaoka, K. and Nomura, M., 1989. Fuel, 68: 287-292.

40 Solomon, P.R.; Serio, M.A.; Despande, G.V.; Kroo, E., Schobert, H.H., Burgess, C., 1991. Am. Chem. Soc. Sym. Ser., 461: 193-212.

41 DOE COLIRN Panel, 1989. "Coal Liquefaction", Final Report, DOE-ER-0400.

42 Derbyshire, F.; Davis, A.; Lin, R., 1989. Energy & Fuels, 3: 431-437.

43 Suuberg, E.M.; Unger, P.E.; Larsen, J.W., 1987. Energy & Fuels, 1: 305-308.

44 McMillen, D.F.; Chang, S.; Nigenda, S.E.; Malhotra, R., 1985. Am. Chem. Soc. Div. Fuel Chem. Prepr., 30 (4): 414-426.

45 Solomon, P.R.; Serio, M.A.; Despande, G.V.; Kroo, E., 1990. Energy & Fuels, 4: 42-54.

46 Lynch, L.J.; Sakurovs, 1991. Proc. 1991 Int. Cof. Coal Sci., Newcastle upon Tyne, Sept. 16-20, **1991**, pp. 592-595.

47 Manion, J.A., McMillen, D.F. and Malhotra, R., 1992. Am. Chem. Soc. Div. Fuel Chem. Prepr., 37 (4): 1720-1726.

48 Tse, D.S., Hirschon, A.S., Malhotra, R., McMillen, D.F. and Ross, D.S., 1991. Am. Chem. Soc. Div. Fuel Chem. Prepr., 36 (1): 23-28.

CHAPTER 5. Hydrous Pyrolysis of Vitrinite Derived from Coalified Wood: A Clue to Reactions of Low-Severity Pretreatment during Liquefaction

Introduction

Low-severity pretreatments in liquefaction strategies often involve either a temperature programmed or two stage thermal pretreatment to induce an opening up of the coal network prior to a more thermally intense treatment (*1*). Apparently, the pretreatment changes the structure of the coal such that retrogressive reactions are minimized in subsequent more severe thermal treatments. During the pretreatment, water is released from the coal either as tightly bound water or water from dehydration/condensation reactions. It is likely that the presence of water has a profound effect on coal at the low pretreatment temperatures, releasing various hydrocarbons and indicating that chemical degradation of the macromolecular network is occurring(*2*). To investigate the effect water has on the chemical structure of coal during pretreatment conditions, we conducted a series of hydrous pyrolysis experiments on a low-rank coal. We selected a sample of pure vitrinite, a piece of coalified wood of lignite rank from the Patapsco Formation, because this sample represented a pure maceral which had been previously characterized extensively and because the sample was composed primarily of catechol-like structures which probably are involved in retrogressive reactions during liquefaction due to their reactivity.

Recently, Siskin and Katritzky (*2*) have demonstrated that many of the reactions which typify coalification and may play an important role in liquefaction are facilitated, if not completely initiated, by the presence of water. From their study of an enormous number of reactions with model compounds, several mechanisms with direct bearing on the chemical structural evolution of coal during thermal stressing are clear. The demethylation of methoxybenzene, for example, has been shown to be acid catalyzed yielding phenol as the predominant product (*3*). The mechanism by which the alkyl-aryl ether linkage (known as the ß-0-4 linkage) of the modified lignin is rearranged to the ß-C-5 linkage as proposed by Hatcher (*4*) to explain coalification of lignin under the influence of natural thermal stresses may reasonably be expected to parallel the mechanism that Siskin et al.(*5*) demonstrated for their model compound study of the hydrous pyrolysis of benzylphenylether. They observed a significant yield of 2 benzyl phenol; this product is a perfect analog for the rearrangement necessary to yield the ß-C-5 linkage found to be important in lignin subjected to natural heating during coalification.

In a recent study of the temperature programmed liquefaction of a low rank coal, we have noted that some significant alteration of the lignin-derived dihydric phenols (catechols) occurs (*6*). Principally, we observe disappearance of catechol-like structures in the coal with subsequent conversion to structures composed mostly of monohydric phenols. Currently, there is no mechanism proposed for the conversion of catechol-like structures to phenol-like structures during thermal stressing. However, this transformation appears to be a principal means by which the oxygen content of coal is reduced during temperature-programmed liquefaction and during the natural coalification of wood to the subbituminous range (*4*). Although Siskin and Katritzky (*2*) have not investigated the chemistry of catechols specifically, they did study 4-phenoxyphenol. It appears reasonable to assume that the reactions involving condensed catechols, as might be found in coal liquefaction residues, may follow a similar reaction chemistry.

The present paper sets out to investigate this possibility as well as to investigate the role of hydrous pyrolysis on a lignitic coalified log. By comparing the chemical structural evolution of the lignitic log, which has been subjected to hydrous pyrolysis, to the results from previous studies of coal liquefaction, it should be possible to derive the most probable mechanism for the catechol reduction pathway.

Experimental

A crushed sample of a coalified gymnospermous wood described previously as the Patapsco lignite (*7*) was heated under hydrous conditions in a 22 mL autoclave reactor described in a previous report (*8*). The reactor was charged under nitrogen with approximately 1 gram of coal and 7 milliliters of deionized, deoxygenated water following a procedure similar to that of Siskin et al. (*5*). The tubing bomb reactor was consecutively pressurized to 1000 psi and depressurized with nitrogen three times to ensure all the oxygen was removed from the reactor. Finally it was depressurized to atmospheric pressure before heating. The bomb was inserted into a heated fluidized sand bath for different reaction periods at various temperatures. Experiments were run for 10 days at 100° C, 30 minutes to 48 hours at 300° C, and 3 hours, 6 hours and 3 days at 350° C. After the elapsed heating times the reactor was removed and immediately quenched in water and then allowed to cool to room temperature. The gases, the liquids and the solids were collected and analyzed. Only trace amounts of gases were detected. An entire series of hydrous pyrolysis experiments were repeated at 300°C with more water added to the reactor than many of the previous experiments. This was done to ensure that water would remain in the liquid state throughout the experiment and would not be in the vapor state.

The bombs were opened and the liquid content pipetted off. The organic matter dissolved in the water was separated by extraction with diethylether, and the data will be reported at a later date. The residual lignite was extracted in a 50:50 mixture of benzene and methanol. The residue was then treated first with acetone and then with pentane to remove any benzene:methanol from the altered coal. The coal was then dried in a vacuum oven at 45° C for twenty four hours, and weighed.

Both the original lignite and the solid residues from the reactors were analyzed by flash pyrolysis and by solid state ^{13}C NMR. The flash pyrolysis technique used was that published by Hatcher et al. (*9*). Using a Chemical Data System Pyroprobe 1000, approximately one milligram of sample was loaded into a quartz capillary tube, and this tube was placed inside the coils of the pyroprobe. The probe and sample were then inserted into the injection port (temperature maintained at 280°C) of a Varian 2700 gas chromatograph and the sample pyrolyzed. The residue was first thermally desorbed at 300°C for thirty seconds. The samples were then pyrolyzed. Flash pyrolysis conditions were as follows: temperature, 610°C for 10 s with a heating rate 5°C/msec. The pyrolyzate was cryotrapped with liquid nitrogen prior to being chromatographed on a 25 m x 0.25 mm i.d. J & W DB-17 capillary column. The GC was temperature programmed from 30° to 280°C at 4°C/min. The effluent was swept into the source of a DuPont 490B mass spectrometer fitted with a Technivent Vector 1 data system for detection and compound identification. Compounds were identified by a combination of methods which included comparison of mass spectra to the NBS/Wiley library, to published mass spectra, and to authentic standards whenever possible.

Solid-state ^{13}C NMR spectra were obtained by the method of cross polarization and magic angle spinning (CPMAS) using the conditions previously given (*7*). The spectrometer was a Chemagnetics Inc. M-100 spectrometer operating at 25.2 MHz carbon frequency. Cycle times of 1sec and contact times of 1msec were chosen as the optimal conditions for quantitative spectroscopy.

Results

Elemental analyses and product yields. The hydrous pyrolysis of the Patapsco lignitic wood induced pronounced alteration of the sample as depicted by the elemental compositions and product yields for some of the experiments shown in Tables 6.1 and 6.2, respectively. Elemental compositions are only available for the original unaltered sample and three

of the hydrous pyrolysis residues. The data indicate a general loss of hydrogen, relative increase in carbon and loss of oxygen as a function of increasing thermal severity that are all consistent in only a general way with trends during increased thermal degradation. Product yields measured as the loss of sample weight during hydrous pyrolysis vary from a low of 8.4% to a high of 40%, with the products being mostly water soluble phenols and catechols (Wenzel and Hatcher, unpublished data).

Table 5.1. Elemental data and vitrinite reflectance for the Patapsco log and its residues obtained from hydrous pyrolysis.

sample	rank	R_0	%C	%H	%N	%O	H/C	O/C
Patapsco lignite	lignite	0.269	65.5	4.8	.34	28.4	0.873	0.326
residue 10 days 100° C	lignite*	0.296	69.2	4.4	.33	26.0	0.758	0.282
residue 0.5 hr 300° C	subbit.*	0.496	73.2	4.3	.22	22.3	0.700	0.229
residue 2 hr 300° C	HvC bit.*	na	76.9	3.4	.01	19.7	0.527	0.192
residue 3 hr 350° C	Mv. bit.*	1.37	na	na	na	na	na	na

*= rank obtained due to thermal alteration

na = data not available

R_0 = vitrinite reflectance, mean maximum

Table 5.2. Hydrous pyrolysis yields at various temperatures.

time, hrs	temperature, °C	+conversion %
240	100	29.3
.5	300	29.8(8.4)*
2	300	30.6(22.9)
3	300	(22.9)
5	300	(22.4)
8	300	(29.9)
3	350	39.7

*values in parenthesis are for samples to which more water was added to ensure hydrous pyrolysis

+refers to the yield of non-residue

^{13}C NMR. The NMR spectra of Patapsco lignite and its hydrous pyrolysis residues at different temperatures and heating times are shown in Figure 5.1. The unaltered Patapsco lignitic wood has an NMR spectrum dominated by aromatic carbons with a major peak at 145 ppm that is assigned to aryl-O carbons in catechol-like structures. The aliphatic region (0-85 ppm) shows peaks assigned to alkyl-C carbons(0-50 ppm), methoxyl carbons (56 ppm), and alkyl-O carbons (60-80 ppm). A small and broad peak at 170- 200 ppm is assigned to carboxyl and carbonyl carbons. The most obvious change due to severity of hydrous pyrolysis is the diminution of the catechol peak at 145 ppm. The most severely altered residue shown in Figure 5.1, 300°C for 48 hrs, shows a nearly complete loss of this peak; the peak of significance that emerges is the one at 155 ppm, that of phenolic carbon. This trend is analogous to that observe in studies of temperature-programmed liquefaction of a Montana subbituminous coal (*6*).

The other major change occurring with increasing hydrous pyrolysis severity is the loss of aliphatic carbons relative to the aromatic carbons, again analogous to previous studies (*6*). Accordingly, the carbon aromaticity, f_a, in Table 5.3 shows this trend as f_a increases from 0.68 to 0.88. The diminution of aliphatic carbons (Figure 5.1) involves loss of methoxyl, alkyl-O, and alkyl-C carbons. The methoxyl carbons decrease rapidly but appear to persist at 300°C. The alkyl-O carbons are lost at low thermal severity. It is clear that a temperature of at least 350°C is required to reduce the methoxyl carbons to below detection. The alkyl-C carbons show resonances distributed over a large chemical shift range with an apparent shift in the intensity maximum from about 30 ppm to about 20 ppm. This is consistent with the conclusion that methyl carbons, which resonate at lower chemical shifts, are dominant in the thermally stressed lignitic wood. Perhaps the residual aliphatic carbons are simply methyl carbons.

The NMR data for samples subjected to hydrous pyrolysis at 300°C for intervals varying from 0.5 to 48 hrs and with additional water in the reactor are shown in Table 5.3. The overall trends in this data are similar to those described above. Carbon aromaticity is observed to increase steadily over the course of 48 hrs of heating. Inverse trends are observed for aryl-O carbons (140-160 ppm), aryl-O/ aryl (aryl-O carbons normalized to total aromatic carbons), and aliphatic carbons (0-50 ppm). These trends are consistent with what was noted above-that hydrous pyrolysis induces loss of catechols and aliphatic structures. The precipitous loss of aryl-O carbons at the long heating time indicates additional loss of oxygenated functional groups, perhaps representing the condensation of phenols which may be involved in retrogressive reactions during liquefaction (*10*).

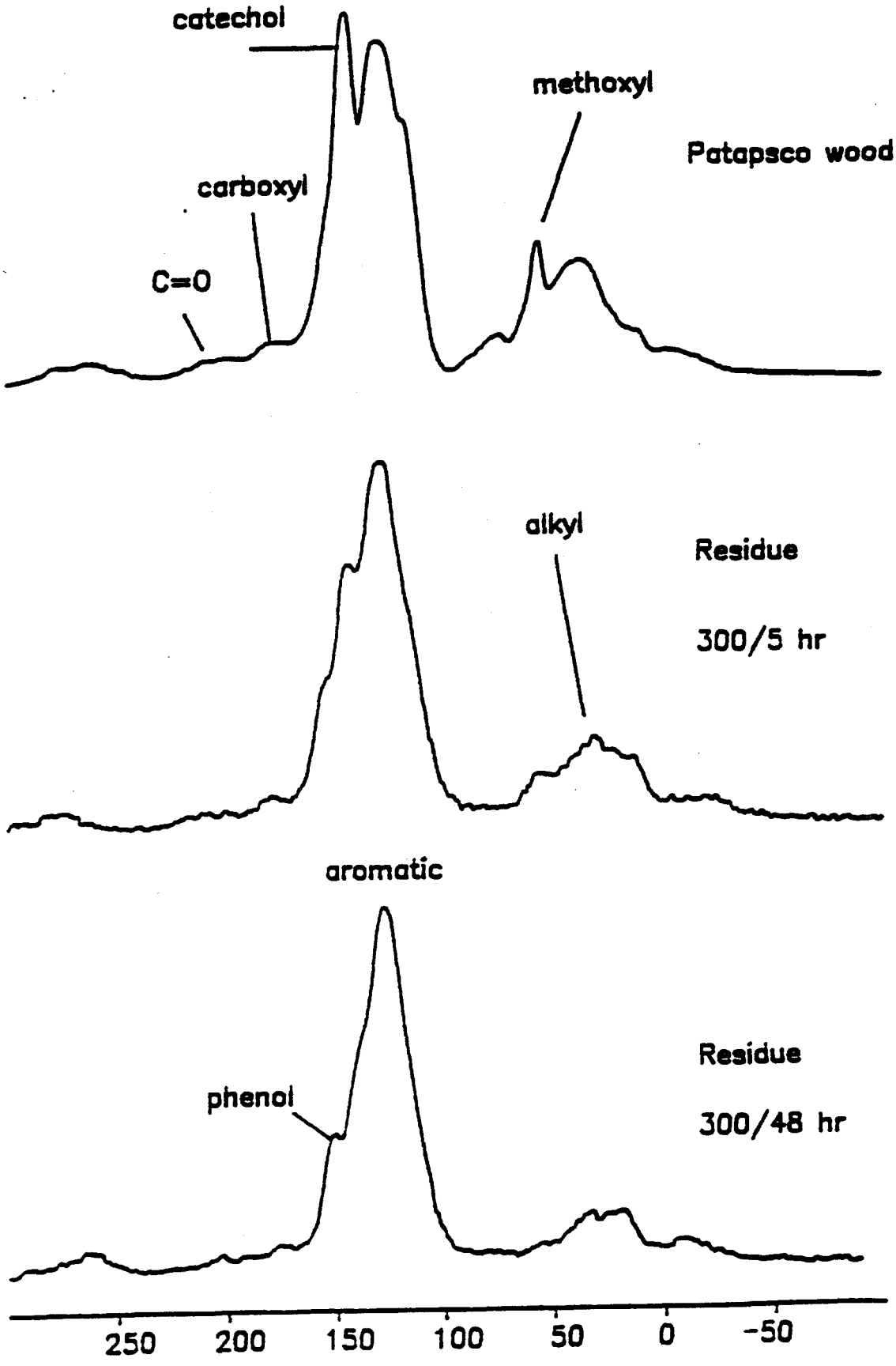

Figure 5.1. Solid-state ^{13}C NMR spectra of unaltered Patapsco lignitic wood and a few representative spectra of its hydrous pyrolysis residues heated at the various temperatures and times indicated.

Table 5.3. NMR parameters for the Patapsco lignitic wood and hydrous pyrolysis residues measured by integration of the spectra.

Sample	f_a	Aryl-O/Aryl	#C=O	#COOH	$f_a^{a,H}$
Patapsco lignitic wood	0.68	0.40	2.6	3.2	0.41
residues/exp. 1:					
300°C/0.5hr	0.75	0.35	2.0	2.5	
300°C/2hr	0.75	0.25	1.7	1.7	
300°C/ 3hr	0.80	0.12	2.7	2.9	NA
350°C/3hr	0.83	0.16	<0.5	2.4	0.27
350°C/72hr	0.88	0.12	<0.5	<0.5	NA
°residues/ exp. 2:					
300°C/5hr	0.74	0.30	3.1	2.1	
300°C/8hr	0.77	0.26	1.8	2.0	
300°C/12hr	0.75	0.28	1.4	1.8	
300°C/36hr	0.80	0.27	1.8	1.8	
300°C/48hr	0.81	0.13	1.3	3.0	

°in these experiments more water was added to reactor and temperature was kept constant at 300°C

values are % of total carbon

f_a carbon aromaticity

$f_a^{a,H}$ fraction of aromatic carbons which are protonated

Dipolar dephasing of the unaltered Patapsco lignite (7) indicates that approximately 3.5 substituents are attached to the aromatic ring ($f_a^{a,H}$, or the fraction of protonated aromatic carbons, is 0.41). The value of $f_a^{a,H}$ for the residue stressed at 350°C for 3 hours is 0.27, significantly less than that of the original sample. This decrease in $f_a^{a,H}$ is indicative of increased aromatic substitution resulting from thermal stress.

PY/GC/MS

Flash pyrolysis GC/MS was preformed on the Patapsco lignite and the residues generated from the hydrous pyrolysis experiments in an effort to characterize the chemical changes that occured during low-severity thermal alteration of the coalified wood. The changes in the lignite are best represented by comparing the pyrograms of the raw lignite (Figure 5.2) and of the series of altered residues from hydrous pyrolysis (Figure 5.3). The pyrograms are normalized to the highest peak. Major peaks are identified by number. See Table 5.4 for the complete list of identified compounds for all the pyrograms.

Table 5.4. Peak assignments for the pyrograms in Figures 2 and 3.

Peak #	assignment
1	toluene
2	xylene
3	xylene
4	phenol
5	*ortho*-cresol
6	*meta and para*-cresol
7	guaiacol
8	2,4-dimethylphenol
9	4-ethylphenol
10	4-methylguaiacol
11	catechol
12	C_2-guaiacol
13	3-methylcatechol
14	4-methylcatechol
15	C_4-guaiacol
16	C_2-catechol
17	ethylcatechol
18	C_2-naphthalene
19	C_5-naphthalene

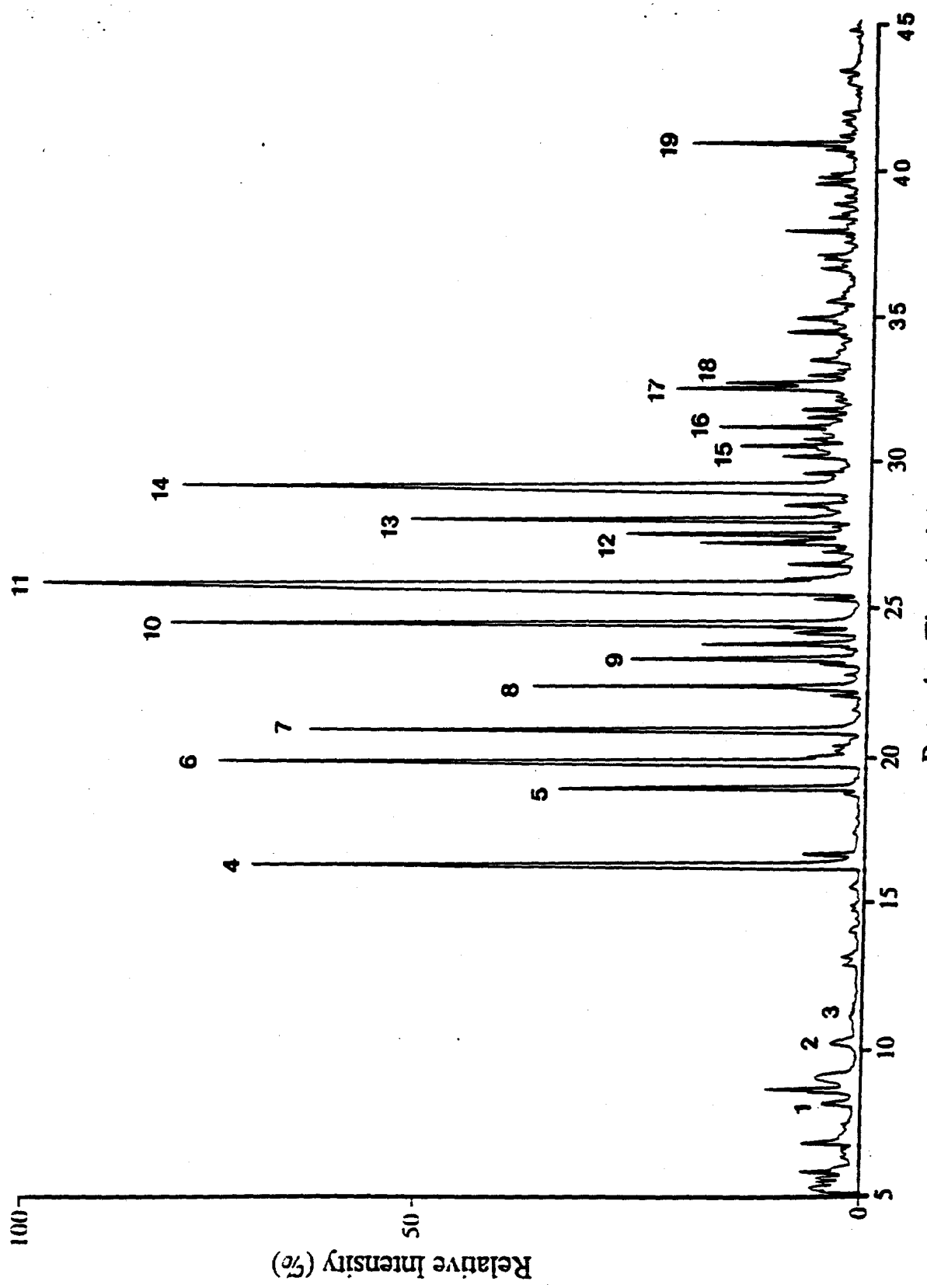

Figure 5.2. Flash pyrolysis/gc/ms trace of the unaltered Patapsco lignitic wood sample with identifications for major numbered peaks listed in Table IV.

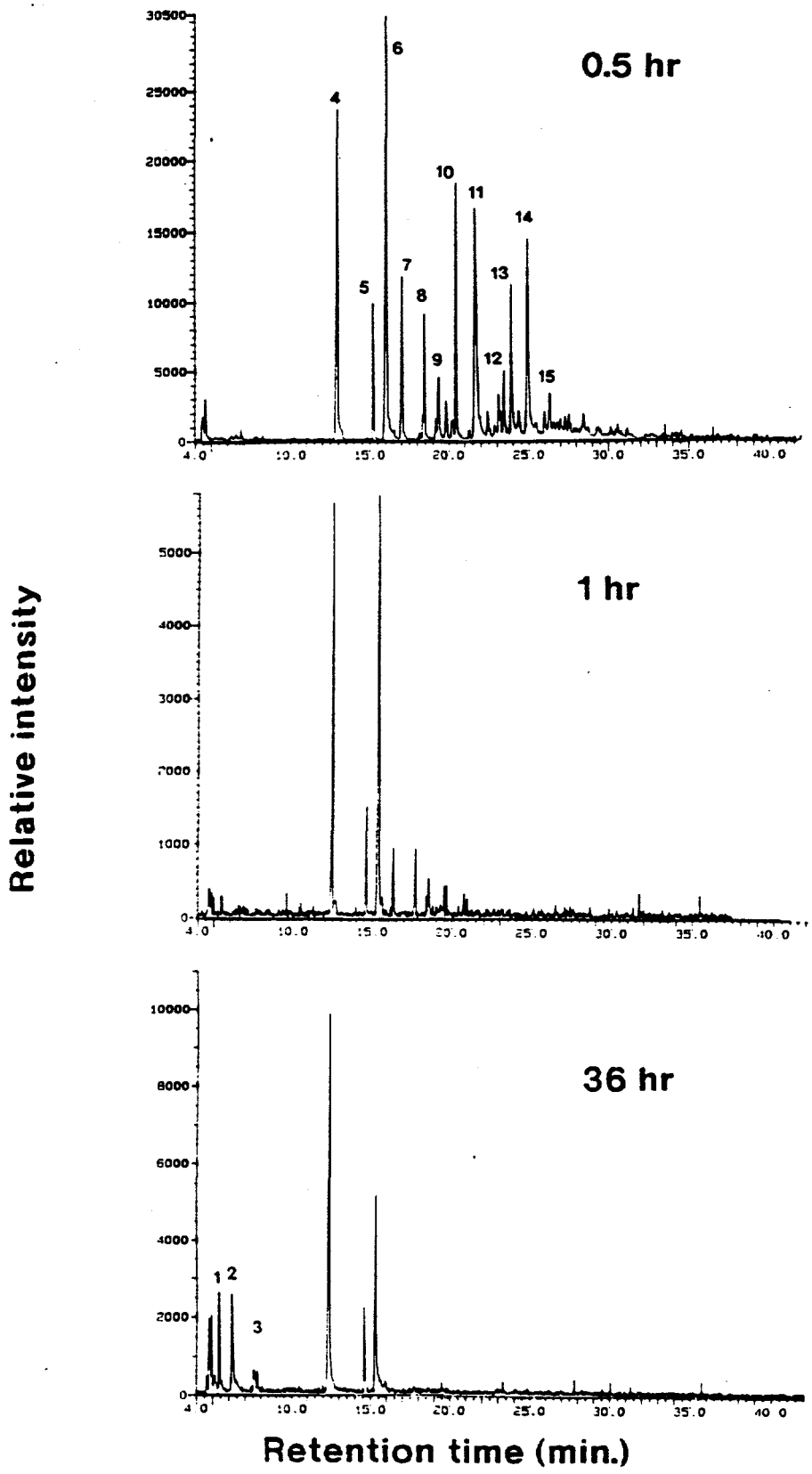

Figure 5.3. Flash pyrolysis/gc/ms trace of hydrous pyrolysis residues of the Patapsco lignitic wood heated for the various times indicated at 300°C. The numbered peaks are identified in Table IV.

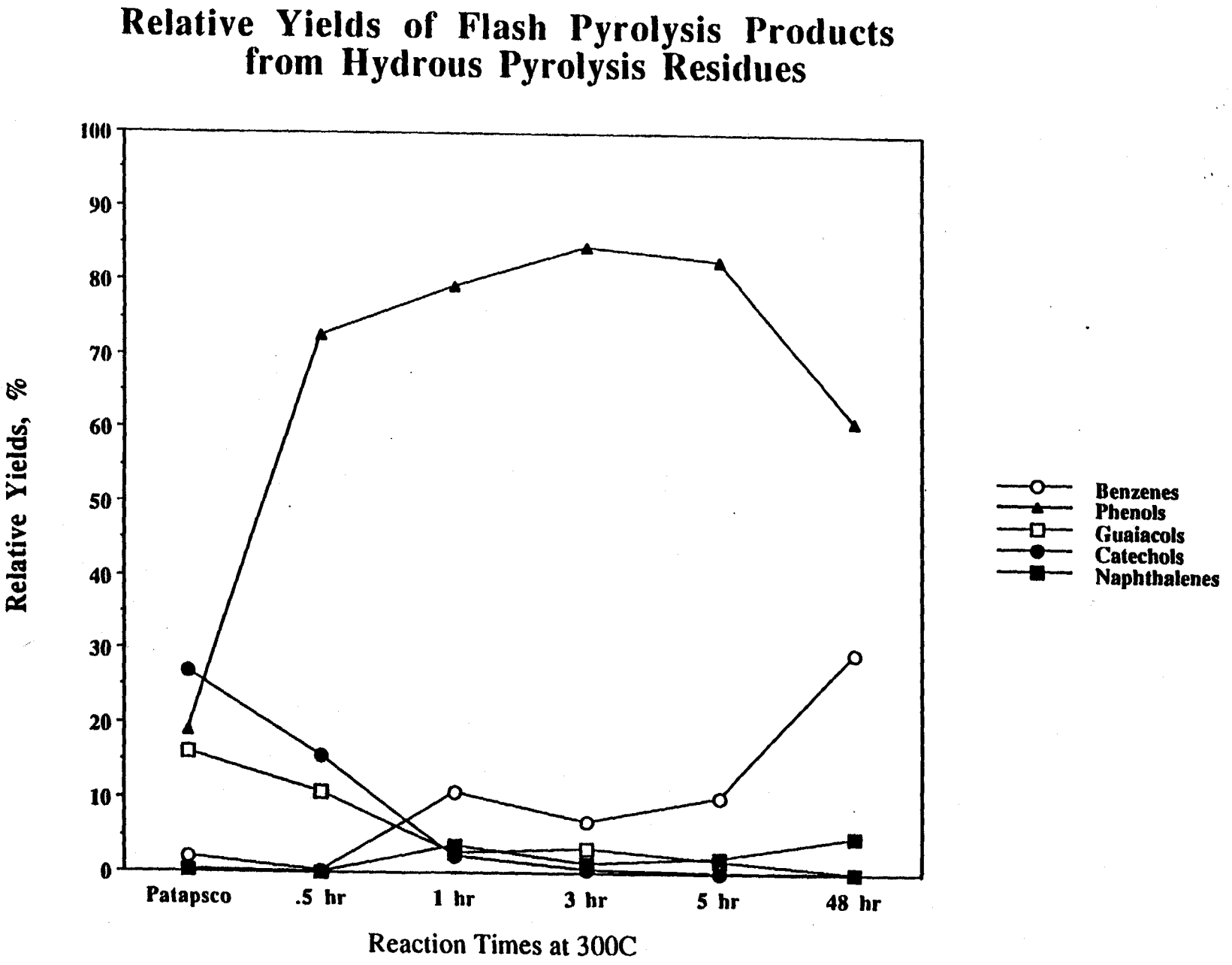

Figure 5.4. Relative yields of individual compounds from flash pyrolysis/gc/ms of hydrous pyrolysis residues obtained at 300°C plotted as a function of heating time (hrs). The compounds are grouped into compound classes and include all the various alkylated isomers of each class.

The pyrolyzate of the Patapsco coalified wood is dominated by peaks attributable to residual lignin structures as indicated by the presence of guaiacol, methylguaiacol, ethylguaiacol, and other methoxyphenols. The intense signals for catechol and alkylcatechols confirms the existence of a predominantly catechol-like structure for this sample. Phenol and alkylated phenols are present but in lesser amounts. Some of the phenols derive from thermal decomposition of catechol-like structures and lignin-like structures.

Pyrograms for the samples subjected to hydrous pyrolysis are distinctly different from those of the unaltered lignitic wood. With increasing hydrous pyrolysis severity, a significant diminution of catechols and lignin phenols (guaiacols) is observed. The pyrograms become dominated by phenol and its alkylated homologs, in much the same way which occurs naturally during coalification of wood. However, the major difference compared to naturally coalified wood is the general lack of significant quantities of the alkylated phenolic homologs. The pyrolysis of the residues yields mostly phenol and cresol isomers. Other alkylated phenols, the C_2 and C_3 phenols, are not as abundant relative to phenol and cresols as are the C_2 and C_3 phenols in the pyrolysis of the original Patapsco lignite or in coalified wood from a natural coalification series (*10*). The relative depletion of C_2 and C_3 alkylphenols in the artificial series is probably related to the fact that alkyl substitutents are not abundant in the residue and the alkyl substituents are probably mostly methyl substituents as was deduced from NMR data.

Figure 5.4 shows the trends in the compound yields from the flash pyrolysis products of hydrous pyrolysis residues heated at 300°C for varying periods of time. Compounds are grouped according to five major groups. The groups of compounds are benzene, phenol, guaiacol, catechol and naphthalene and their alkylated derivatives. The loss of catechol-like structures is documented with a significant loss of catechols in the pyrolyzate of the altered residues. With the loss of catechols, phenols and alkyl phenols become the dominant products in the pyrolyzate, as noted above.

Discussion

Hydrous pyrolysis of the Patapsco lignite was conceived as a means to examine reactions which might occur during low-severity pretreatment prior to liquefaction. Accordingly, our goal was to examine the residues before and after thermal treatment and to infer reactions pathways from this treatment, pathways which may shed light on various liquefaction strategies. It is important to note that there appeared to be a loss of mass during thermolysis. This mass loss probably reflects low molecular weight products formed, water, and partial solubilization of lignitic

structures originally of low molecular weight. The GC/MS analysis of the water soluble materials (Hatcher and Wenzel, unpublished results) indicates the presence of lignin phenols and catechols, all of which are components of the lignite prior to thermolysis. Cleavage of a few bonds on the macromolecule could conceivably produce a catechol or methoxyphenol which would be soluble in water. Another water soluble product identified was acetic acid. This product is most likely derived from hydrolysis of the side-chain carbons associated with the original lignin and coalified lignin in the sample. The content of evolved gases was not quantified because the amount of gas evolved was negligible.

The NMR data of the thermolysis residues indicates clearly the evolutionary path during thermolysis . Comparing the NMR data for the residues (Figure 5.1, Table 5.3) with the original lignite and with gymnospermous wood coalified to higher rank (7) there appear to be several changes which describe the average chemical alteration. First, the most obvious change is the loss of aryl-O carbons having a chemical shift at 145 ppm. From previous studies (7) this peak has been assigned to aryl-O carbons in catechol-like structures in the coalified wood, based on chemical shift assignments and pyrolysis data. These are thought to be originally derived from demethylation of lignin during coalification. The NMR spectrum of the hydrous pyrolysis residue has clearly lost most of the intensity at 145 ppm but now shows a peak at 155 ppm which is related to aryl-O carbons in monohydric phenols. It is obvious that the catechol-like structures of the lignitic wood have been tranformed to phenol-like structures somewhat similar to those in higher rank coal or residues from low-severity liquefaction of low-rank coal. Thus, the hydrous pyrolysis has reproduced, to some degree, the reactions acting on aromatic centers during such thermal stress.

The second most apparent change to occur during hydrous pyrolysis is the loss of aliphatic structures, a phenomenon observed in studies of the liquefaction of low-rank coal. The methoxyl groups at 56 ppm are lost from the lignitic wood as are the other alkyl-O carbons at 74 ppm. However, the loss of alkyl-C carbons (those aliphatic carbons not substituted by oxygen) is the most significant change in the aliphatic region in the hydrous pyrolysis residue. It is important to note that the alkyl-C carbons in the hydrous pyrolysis residues become dominated by methyl carbons with increasing thermal stress.

The pyrolysis data provide confirmation for the average changes in structure observed by NMR. The loss of catechol-like structures is documented with the significant diminution of catechols in the pyrolyzate of the hydrous pyrolysis residue compared to that of the original lignitic wood. This loss of catechols is the singular most significant change in pyrolysis products. The

pyrolyzate of the residue appears to be dominated by phenol and alkylphenols. Another difference between hydrous pyrolysis residues and the original lignitic wood is in the abundance of methoxyphenols derived from lignin-like structures. The hydrous pyrolysis has apparently reduced the relative yields significantly, consistent with the NMR data showing loss of methoxyl carbons. Some of the methoxyphenols may have been transformed to water soluble phenols and washed out of the residue in the aqueous phase; others may have undergone demethylation reactions, converted to catechols and then transformed to phenols.The pyrolysis of the residues yield mostly phenol and the cresol isomers; other alkylated phenols, the C_2 and C_3 phenols, are not as abundant relative to phenol and cresols as the C_2 and C_3 phenols are in the pyrolysis of original lignite. This is probably related to the fact that alkyl substituents are not as abundant in the residue and the alkyl substituents are probably mostly methyl substituents as was deduced from the NMR data.

By noting the changes in the NMR and pyrolysis data when lignitic wood is subjected to hydrous pyrolysis and a generalized schematic of the transformation pathway may be deduced. It is clear that the catechol-like structures are being transformed to phenolic structures. From previous studies on the lignitic wood, catechol-like structures are thought to be the dominant structural element, similar to the one depicted in structure **1**. Thermolysis can easily induce dehydration or condensation (2) to form an ether link between two catechols as shown in structure **2**. Hydrolysis of the ether can reverse the reaction to regenerate the catechols, but thermolysis can also induce homolytic cleavage of the ether to generate a phenoxy radical (**3**) and a catechol radical (**4**). If we assume that sufficient hydrogen transfer occurs under the high temperature regime to cap the radicals, then the products **3** and **4** would be tranformed to a phenol (**5**) and a catechol (**1**). It is also possible that radicals are capped by methyl or alkyl radicals formed from other thermolytic reactions elsewhere in the coal structure (e.g., the side chain sites). In such cases methoxy or alkoxyphenols (**6**) could be formed. Such reactions could explain why methoxyphenols persist in pyrolyzates of the residues during hydrous pyrolysis. It is also possible that the alkyl radicals could attack the aromatic ring sites and induce alkylation (**7**). This would lead to increased substitution of the rings, consistent with the dipolar dephasing NMR data which show an increase in the average number of aromatic substituents with increased hydrous pyrolysis.

Recently, Siskin et al.(5) demonstrated that hydrous pyrolysis at 343°C will induce cleavage of 4-phenoxyphenol (**8**) to form phenol instead of hydroquinone (1,4-dihydroxybenzene); the detailed pathway being presumably unknown. This compound has some similarity to structure **2** found in the lignitic wood.

Thus we can expect the above mechanism proposed for catechol to be analogous to that

shown for 4-phenoxyphenol. In fact, we might expect the reaction to proceed at a much faster rate due to the fact that additional phenol substituents at *orto* or *para* positions to the ether linkage can activate the reaction.

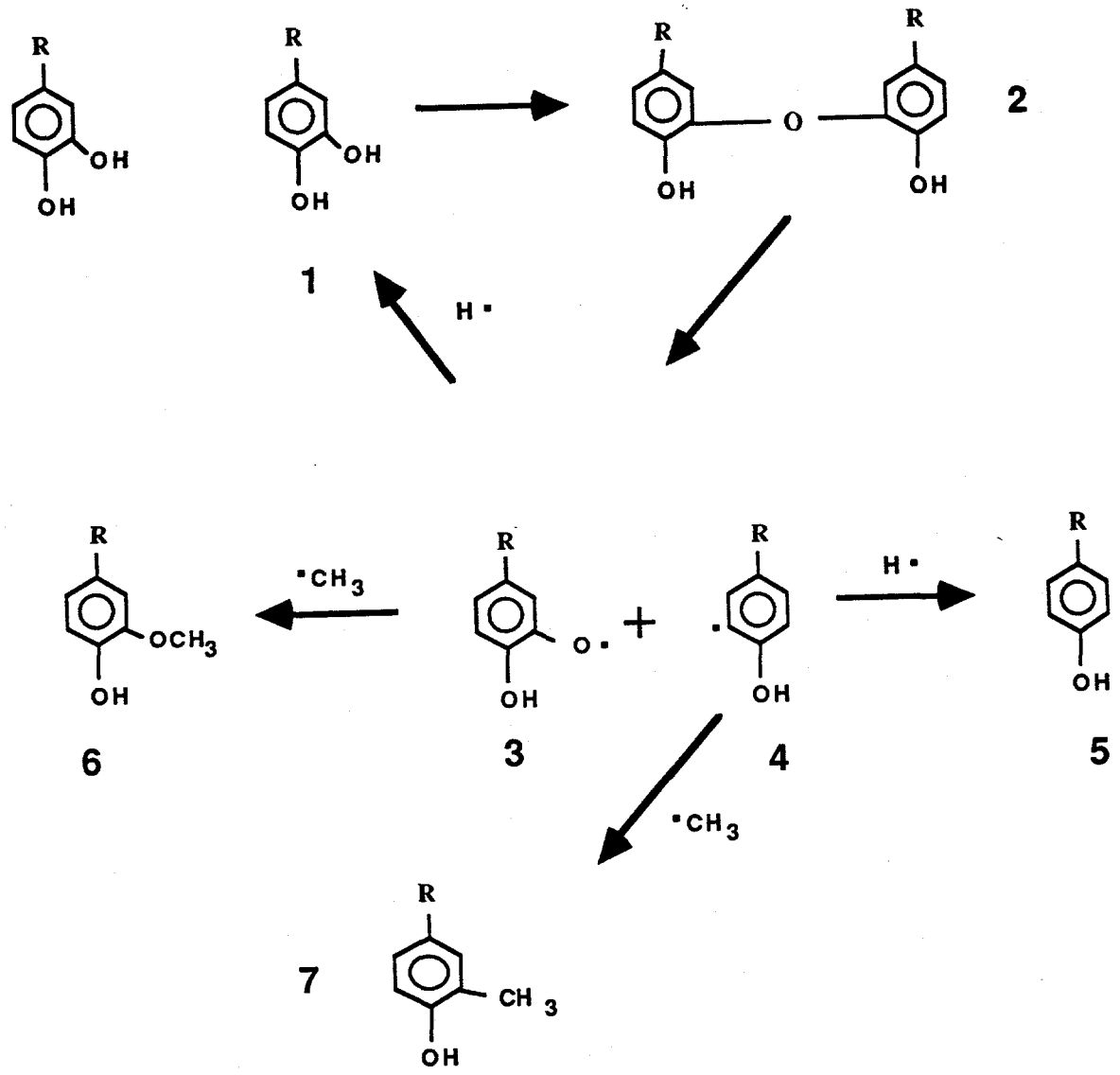

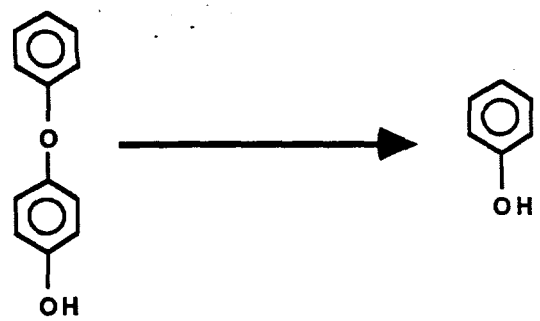

8

Literature Cited

1.Song, C.; Saini, A.; Huang, K.; Wenzel, K.; Hatcher, P. G.; Schobert, H. H. *Quarterly Technical Progress Report, Department of Energy, Pittsburgh Energy Technology Center,* DE-AC22-91PC91042, TPR-1, January, 1992, 90pp.

2. Siskin, M.; Katritzky, A.K. *Science* **1991**,*254*, p.231.

3. Katrikzky, A.K.; Murugan, R.; Balasubramanian, M.; Siskin,M.; *Energy Fuels* **1990**,*4*, p. 543.

4. Hatcher, P. G. *Org.Geochem.* **1990,** *16,* p. 959.

5. Siskin, M.; Brons, G.;Vaughn, S.N.;Katritzky, A.K.;Balasubramanian, M.;*Energy Fuels* **1990**, *4*, p. 488.

6. Song, C.; Schobert, H. H.; Hatcher, P. G. *Energy & Fuels* **1992**,*6*, p. 326.

7. Hatcher, P.G. *Energy Fuels* **1988,** 2, 4p. 8.

8. Wenzel, K. A.; Hatcher, P. G.; Cody, G. D.; Song, C., Preprints, American Chemical Society Fuel Division **1992,** *38,* p. 571.

9. Hatcher, P. G.; Lerch, H. E.; Kotra, P.K.; Verheyen, T. V.; *Fuel* **1988,** *67*, p. 106.

10. Hatcher, P. G.; Faulon, J.-L.; Wenzel, K. A. ; Cody, G. D. *Energy Fuels* **1992,** *6,* p. 813.

CHAPTER 6. CPMAS and DDMAS ^{13}C NMR Analysis of Two THF-Extracted Subbituminous Coals and Their Liquefaction Residues

INTRODUCTION

As described in previous Chapters, we have shown that spectroscopic analyses of liquefaction residues (by NMR, pyrolysis-GC-MS, and FT-IR) can provide important structural information which can be used for elucidating the chemical reactions of liquefaction (Song et al., 1992, 1993, 1994) as well as the effects of dispersed catalysts (Saini et al., 1992; Huang et al., 1993; Song et al., 1994). The work reported in this Chapter involves solid-state ^{13}C NMR studies of residues of two subbituminous coals from their liquefaction at 300-425°C, using cross-polarization (CP), dipolar dephasing (DD) and magic-angle-spinning (MAS) techniques. A preliminary survey of some CPMAS ^{13}C NMR results for one of the two coals was presented previously (Song et al., 1993). In a companion paper, we report on the analysis of oils from liquefaction of these coals by two-dimensional HPLC and GC-MS (Saini and Song, 1994).

EXPERIMENTAL

Sample Preparation

Three types of samples were examined in this study. The first set of samples are THF-insoluble residues from temperature-programmed liquefaction (TPL) of a Montana subbituminous coal (DECS-9) in tetralin solvent at a final temperature ranging from 300°C to 425°C for 30 min (Song et al., 1992). The second set of samples are THF-insoluble residues from liquefaction of a Wyodak subbituminous coal (DECS-8) at 350°C with and without a solvent in the absence and presence of a dispersed molybdenum sulfide catalyst (Song et al., 1994). The coals were predried in vacuum at about 100°C for 2 h prior to liquefaction. The third set of samples are the fresh raw coals (DECS-8, DECS-9) and THF-extracted but unreacted coals. Our experience shows that trace amounts of THF always remain in the THF-extracted residues even after vacuum drying at 100°C for over 6 h, which interferes with spectroscopic analysis. We have solved the problem by washing the residue first with acetone, then with

pentane, followed by vacuum drying at 100°C for 6 h prior to spectroscopic analysis. The residue samples were also subjected to elemental analysis.

Solid-State ^{13}C NMR

NMR spectra were acquired on a Chemagnetics M-100 spectrometer. The measurements were carried out at a carbon frequency of 25.035 MHz. The spectrometer performance was checked with a standard sample of hexamethylbenzene to assure the Hartman-Hahn match. In a *typical* analysis, about 0.4-0.6 g of a sample was packed in a 0.4 mL bullet-type rotor made of polychlorotrifluoroethylene (Kel-F). Kel-F does not have a CPMAS ^{13}C signal. The MAS speed of the rotor was about 3.5 kHz.

The CPMAS ^{13}C NMR spectra were obtained by using the combined high power proton decoupling, cross-polarization, and magic angle spinning techniques. The experimental conditions for all the samples are as follows: a cross-polarization contact time of 1 msec, a pulse delay time of 1 sec, 50 kHz of proton decoupling, sweep width of 14 kHz, and 20-30 Hz line broadening. Carbon aromaticity was determined by integrating the peaks between 95 and 165 ppm (ppm relative to tetramethylsilane). Spinning sideband intensity was distributed for aromatic carbons. Other details concerning CPMAS maybe found elsewhere (Hatcher , 1987, Song et al., 1993).

Dipolar-dephasing ^{13}C NMR spectra (DDMAS) were acquired by using the pulse sequence described by Alemany et al. (1983) and Wilson et al. (1984). After the protons are spin-locked and cross-polarization is induced, a variable dephasing time T_{dd} is inserted, during which the high-power decoupler is turned off. During this period, which lasts from 5 to 180 μsec, carbon magnetization becomes influenced and diminished (dephased) by the strong dipolar interactions between ^{13}C and ^{1}H spins. Carbons directly bonded to hydrogens (protonated carbons) dephase much more rapidly than those without attached hydrogens (non-protonated carbons). More details about the theory and procedures of dipolar dephasing may be found elsewhere (Hatcher, 1987, 1988; Pan and Maciel, 1993). In general, protonated carbons dephase within the first 60 μsec (T_{dd}), and the signals remain after 60 μsec are due to non-protonated carbons.

RESULTS AND DISCUSSION

Structural Characteristics of THF-extracted Coals

Figure 6.1 shows the CPMAS and DDMAS ^{13}C NMR spectra of THF-extracted but unreacted Montana subbituminous coal (DECS-9). In the CPMAS spectrum, there are two major bands, an aromatic bands from 95 to 165 ppm and an aliphatic band from 0 to 80 ppm. Among the aliphatic bands, methyl carbons appear at 0-25 ppm, methylene carbons resonate between 25-51 ppm, methoxyl groups around 51-67 ppm and ether groups between 67-93 ppm (Yoshida et al., 1987). The aromatic region includes two shoulders which may be attributed to catechol-like oxygen-bound carbons (centered around 142-144 ppm) and phenolic carbons (centered around 152-154 ppm). There are two other bands with lower intensities, including carboxyl groups between 170-190 ppm and ketonic carbonyl groups between 190-230 ppm.

DDMAS ^{13}C NMR was used to examine the degree of protonation of carbons. Protonated carbons decay at a rate that is dependent on T_{dd}^2 and is often referred to as the Gaussian component of signal decay; non-protonated carbons decay at a much slower rate that is exponential with respect to T_{dd} (Alemany et al., 1983). Compared to the CPMAS spectrum , signal decay in the 95-165 ppm region was due mainly to protonated aromatic carbons (95-130 ppm). The signal intensity remaining in the aromatic region in the DDMAS spectrum in Figure 6.1 can be attributed to bridgehead and substituted aromatic carbons (130-148 ppm) and oxygen-bound aromatic carbons (140-165). Apparently, the shoulders that we identified as catecholic (structure I) and phenolic (structure II) carbons remain in the DDMAS structure and are clearly non-protonated carbons.

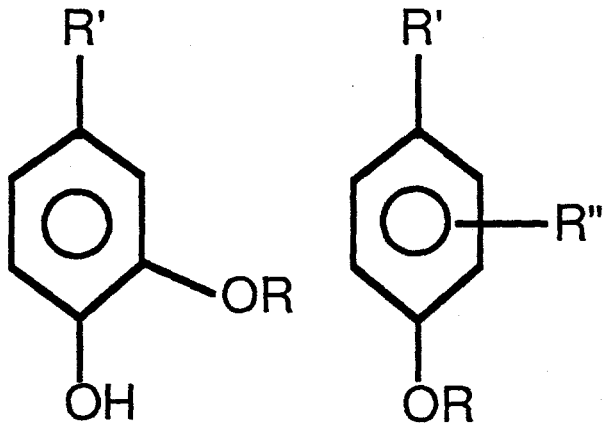

Str. I Str. II

Our assignment of the peak centred at 142-144 ppm in the DDMAS spectra is different from that of Pan and Maciel (1993). They assigned the 144 ppm peak for Beulah-Zap lignite (801) to an aniline-type aromatic carbon. We have assigned this peak to the catecholic oxygen-bound aromatic carbon (shown in structure I). This is based on the NMR spectra of lignin-related model compounds and lignin (Hatcher, 1987) and the combined CPMAS NMR and pyrolysis-GC-MS studies of low-rank coals, including DECS-9 (Song et al., 1993) and DECS-8 (Saini et al., 1992) coals used in this work, as well as a lignite (Wenzel et al., 1993).

Flash pyrolysis GC-MS of lignites (Hatcher et al., 1988; Wenzel et al, 1993), DECS-9 Montana coal (Song et al., 1993), and DECS-8 Wyodak coal (Saini et al., 1992) revealed that catechol and phenol as well as their homologs are important components in the pyrolyzates of low-rank coals. Another important evidence is that as catechol observed in the pyrolysis-GC-MS diminishes, so does the catecholic peak in the CPMAS ^{13}C NMR spectra (Hatcher et al., 1988; Song et al., 1993; Wenzel et al., 1993).

Quantitative CPMAS NMR analysis of Montana coal was performed by means of curve-fitting, as described in our recent paper (Song et al., 1993). This coal has 63-64% aromatic carbons among total carbons. Combination of DDMAS and CPMAS NMR data reveals that about 34-35% of the aromatic carbons are protonated carbons; 23-24% of aromatic carbons are chemically bound to oxygen atoms; the remaining 31-33% aromatic carbons are bound primarily to other carbon atoms and secondarily to nitrogen and sulfur. The above spectroscopic results suggest that the Montana coal contains approximately two or three protonated carbons, one or two oxygen-bound carbons, and two substituted or bridgehead carbons per aromatic ring.

Compared to the Montana coal, THF-extracted Wyodak subbituminous coal (DECS-8) has a lower aromaticity (57%). However, it also has all the characteristic peaks (aliphatic, aromatic, carboxyl, carbonyl) and shoulders (phenolic, catecholic) that DECS-9 Montana coal possess (Figure 6.1). The DDMAS ^{13}C NMR data indicate that about 29% of the aromatic carbons in the THF-extracted Wyodak coal (DECS-8) are protonated carbons. Peak separation of NMR spectrum of THF-extracted DECS-8 gives 34.9% aliphatic carbon (0.60 ppm), 57% aromatic carbon (95-165 ppm), and 8.3% carboxyl and carbonyl carbon (170-230 ppm). There are 15.3% oxygen-bound aromatic carbons, which means about 25% of the aromatic carbons are chemically bonded to oxygen.

On an average, per 100 carbon atoms in THF-extracted DECS-8, there are about seven (7) catecholic carbons (Str. I), and eight (8) phenolic carbons (Str. II). The contents of O-bound carbons in DECS-9 coal is relatively ssmaller. Per 100 carbon atoms in THF-extracted DECS-9, there are about five (5) catecholic carbons (Str. I), and ten (10) phenolic carbons (Str. II). Combination of DDMAS and CPMAS data indicates that about 25% of the aromatic carbons in the THF-extracted Wyodak coal (DECS-8) are bonded to oxygen, 29% of the aromatic carbons are bonded to hydrogen, and the remaining 54% are bonded to carbon. These results point to a picture that there are about 1 to 2 oxygen atoms in every six aromatic carbons. In other words, most of the aromatic rings are of phenolic and catecholic types.

Characterization of Residues from Non-Catalytic Liquefaction

Table 6.1 shows the carbon aromaticities of unreacted coal and residues from DECS-9 Montana coal determined by CPMAS ^{13}C NMR, and the degree of protonation of aromatic carbons determined by DDMAS ^{13}C NMR. Figure 6.2 presents the CPMAS and DDMAS ^{13}C NMR spectra of THF-insoluble residue from non-catalytic TPL of a Montana subbituminous coal (DECS-9) in the presence of tetralin solvent at a final temperature of 350°C for 30 min. Details of TPL procedures and results may be found elsewhere (Song and Schobert, 1992). Comparative examination of DDMAS data indicates at least three trends. First, relative to the THF-extracted unreacted coal, non-protonated carbons contribute more to the aromatic band in the residue from 350°C run. Second, the catecholic peak almost disappeared after 30 min at 350°C. Third, phenolic peak does not diminish as much as the catecholic peak upon reaction at 350°C, as can be seen by comparing the two DDMAS spectra (Figures 6.1 and 6.2).

Table 1. NMR-Derived Carbon Aromaticity (f_a) and Degree of Protonation of Aromatic Carbons (f_a^{aH}) of THF-insoluble Residues from Temperature-Programmed Liquefaction (TPL) of DECS-9 Montana Coal at Final Temperature of 300-425°C for 30 min under 6.9 MPa (cold) H_2 Pressure

Sample	Temp, °C	Solvent	CPMAS NMR f_a	DDMAS NMR f_a^{aH}
Raw coal			0.63	0.33
THF-extracted but unreacted coal			0.64	0.35
Residue	200°C-15 min 300°C-30 min	Tetralin	0.65	0.34
Residue	200°C-15 min 350°C-30 min	Tetralin	0.70	0.24
Residue	200°C-15 min 375°C-30 min	Tetralin	0.73	0.13
Residue	200°C-15 min 400°C-30 min	Tetralin	0.76	0.11
Residue	200°C-15 min 425°C-30 min	Tetralin	0.78	

Figure 6.3 shows the CPMAS and DDMAS ^{13}C NMR spectra of THF-insoluble residue from non-catalytic reaction of a vacuum-dried Wyodak subbituminous coal (DECS-8) in the absence of any solvent at 350°C for 30 min under 6.9 MPa H_2. Since no donor solvent or catalyst was used, the coal conversion is very low, only about 12.5 wt%. More liquefaction results of this coal are described elsewhere (Song et al., 1994). The characteristics of both CPMAS and DDMAS spectra of this sample resemble those of the corresponding spectra for residue from Montana coal (Figure 6.2), although the two samples were derived from different coals under different conditions.

The reaction temperature has the most significant impact on the spectral characteristics of the liquefaction residues. We have performed both DDMAS and CPMAS ^{13}C NMR analysis of the THF-insoluble residues from TPL reactions of Montana coal (DECS-9) at 300, 350°C, 375, 400 and 425°C for 30 min. Catechol-like structures were found to be thermally sensitive and diminish gradually with increasing temperature up to 350°C. The catecholic shoulder at 142-144 ppm disappears from the residue of 375°C run. Carboxyl (165-190 ppm) and carbonyl (190-230) peaks diminish significantly after 375°C and they disappear in the spectrum of residue from 400°C run. Phenolic structures diminish with increasing temperature up to 425°C. These results clearly indicate that there are thermally reactive oxygen functional groups in coal and their reactions can take place at temperatures as low as 300-375°C.

As shown in Figure 6.4, the carbon aromaticity of residues increased monotonically with increasing reaction temperature after 300°C. Comparison of the curve for H/C atomic ratio and that for carbon aromaticity indicates that THF extraction of unreacted coal and that reacted at 300°C, removed more aliphatic materials. However, the conversion level at 300°C in tetralin is below 10 wt% (dmmf). The H/C ratio of the residues decreased significantly with increasing temperature up to 425°C. The aromaticity of the residues increased with increasing coal conversion, being consistent with the observations by two other groups on residues from liquefaction (Fatemi-Badi et al., 1991; Franco et al., 1991). The increase in carbon aromaticity is driven primarily by temperature, and secondarily by the adduction of aromatic solvent molecules (Song et al., 1993, 1994). Another interesting observation is that, while the total aliphatic carbons decrease, the percentage methyl carbons relative to total aliphatic carbons increases with increasing temperature up to 425°C.

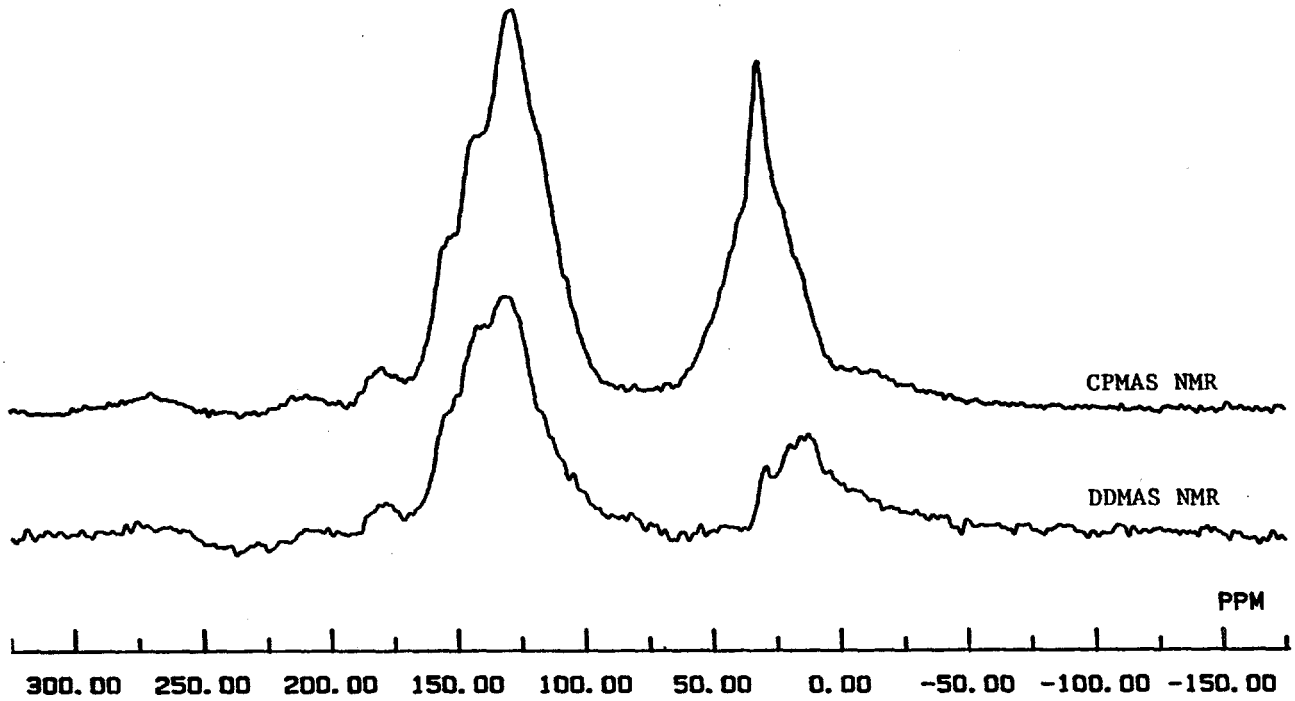

Figure 6.1. CPMAS and DDMAS ^{13}C NMR spectra of THF-extracted but unreacted Montana subbituminous coal (DECS-9). For DDMAS, Tdd = 60 μs.

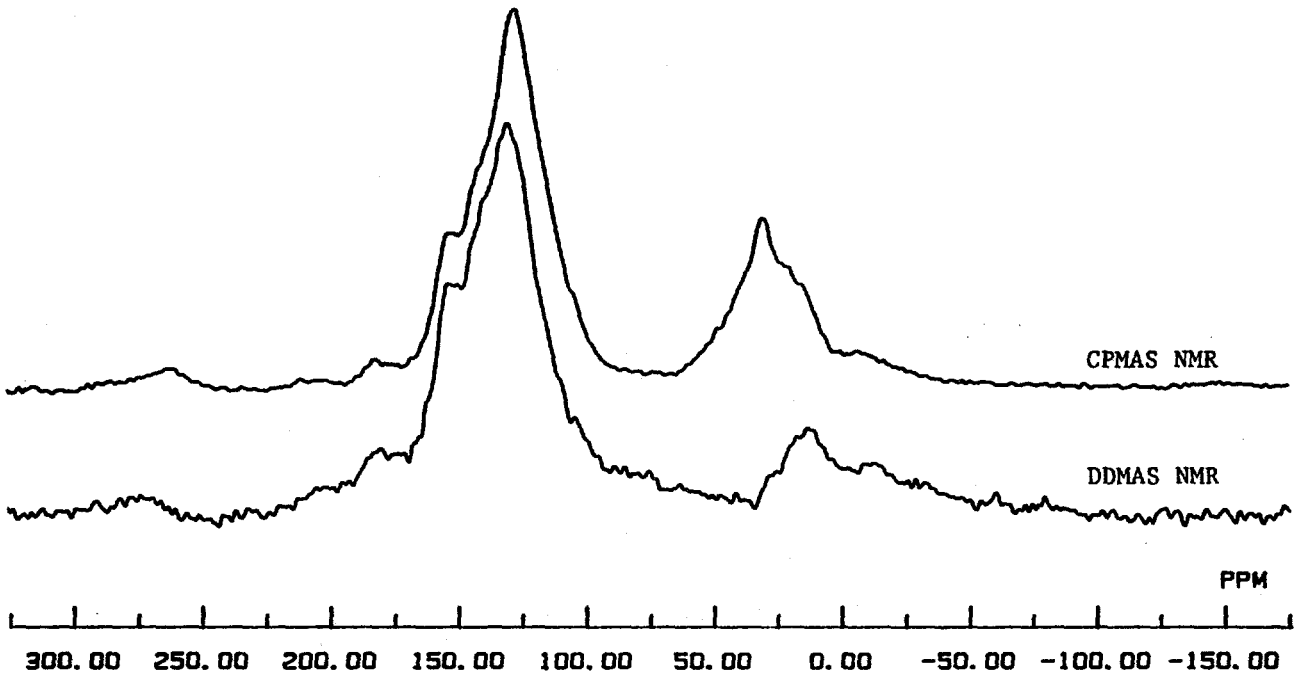

Figure 6.2. CPMAS and DDMAS ^{13}C NMR spectra of residue from TPL of Montana coal in the presence of tetralin at a final temperature of 350°C for 30 min. For DDMAS, Tdd = 60 μs.

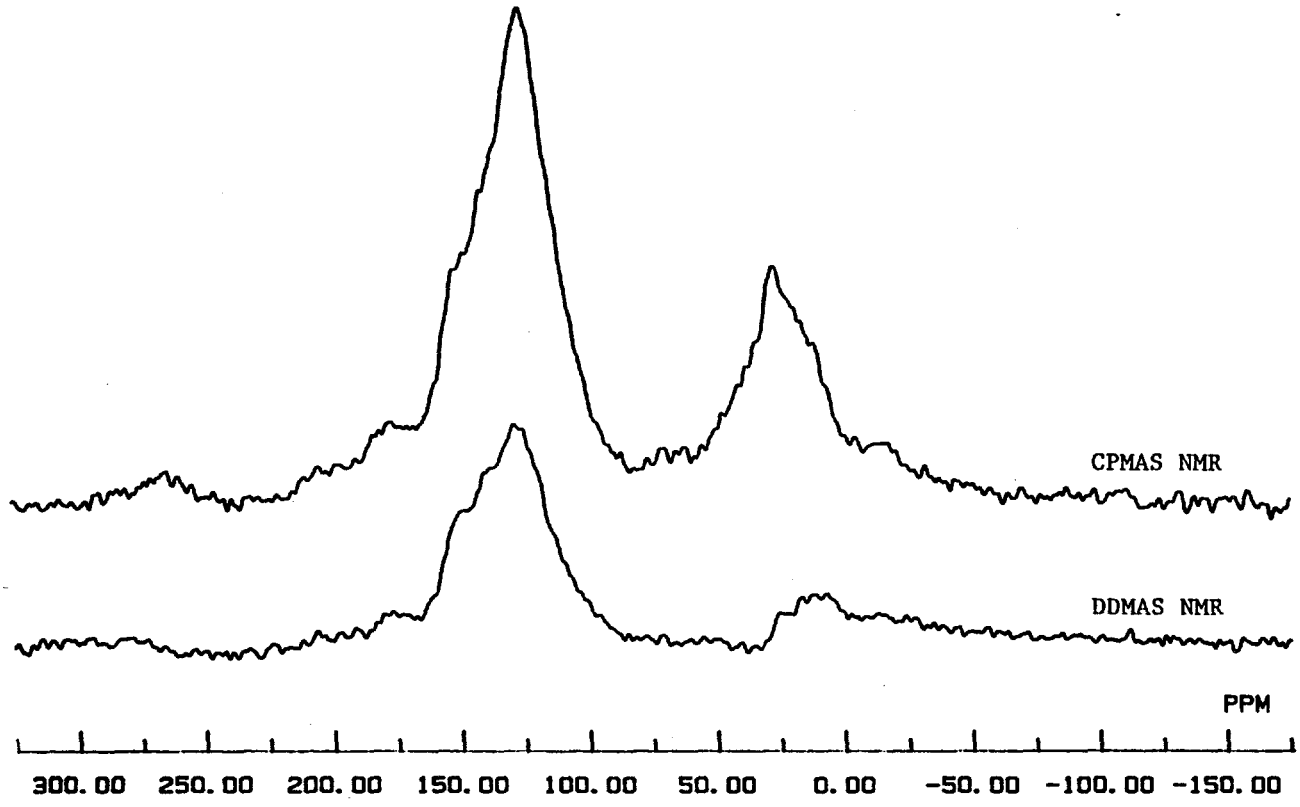

Figure 6.3. CPMAS and DDMAS ^{13}C NMR spectra of residue from liquefaction of Wyodak coal (DECS-8. vacuum-dried) without anv solvent at 350°C for 30 min. For DDMAS. Tdd = 60 us.

DDMAS analysis (Figure 6.5) shows that the degree of protonation of aromatic carbons in the residues decreased from 35% (for THF-extracted but unreacted Montana coal) to 13% for residue from the non-catalytic run at final reaction temperature of 375°C. General trends observed from DDMAS experiments for residues from DECS-9 are as follows. The degree of protonation of aromatic carbons in the residue decreases with increasing coal conversion. In other words, the higher the coal conversion into THF-soluble products, the more non-protonated aromatic carbons in the THF-insoluble residues. The higher content of non-protonated carbons among total aromatic carbons could originate from either higher degree of condensation or higher extent of substitution. Since the aromaticity increases and atomic H/C ratio decreases with increasing temperature, the decrease in the relative content of protonated aromatic carbon (or the increase of non-protonated aromatic carbons) is due mainly to the increased degree of condensation. This means that there are more bridgehead aromatic carbons or more condensed-ring aromatic structures in the residues from runs at higher temperatures.

As discussed above, there exists good correlation between carbon distribution and reaction temperature above 300°C. We have attempted mathematical correlation of the NMR data for the residue with reaction temperature (Song et al., 1993). Figure 6 shows that the changes in the aromatic, aliphatic, and oxygen-bound carbons of the residues can be related to the liquefaction temperature by a linear correlation. A general expression is given below:

$$C_i = \alpha f_i + \beta T \qquad \text{for specific carbon type } i \qquad (1)$$

where T is reaction temperature (°C), f_i and C_i represent the content of specific carbons (%) in the original coal and residue, respectively, and α and β are constants. The specific correlations for aromatic C (C_{ar}), aliphatic C (C_{ali}), and oxygen-bound carbons ($C_{O\text{-}C}$) are given in Figure 6. We have quantitatively analyzed the NMR spectra of 26 residues from liquefaction of DECS-9 coal under various conditions with and without solvents (Song et al., 1993). The results show that equation 1 holds for all the cases with good linear correlation.

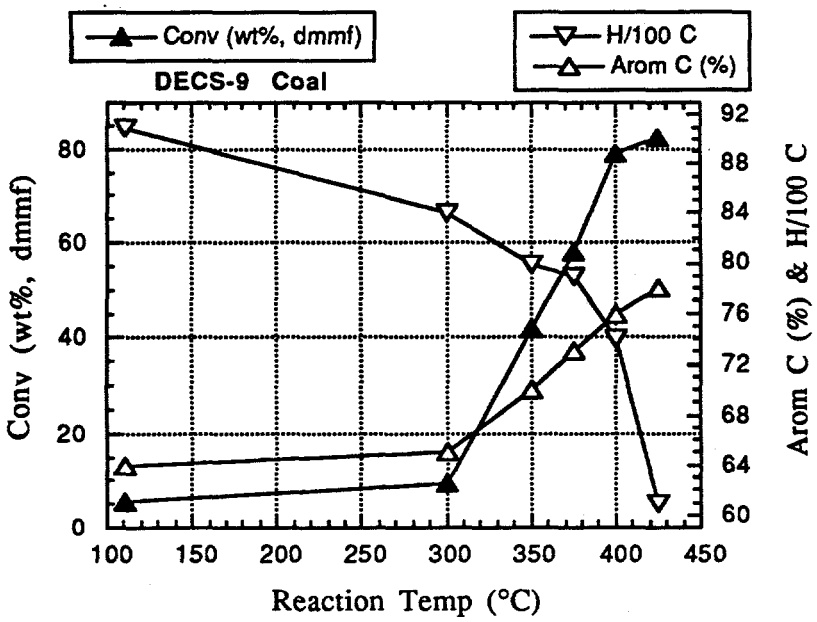

Figure 6.4. Conversion of Montana coal and changes in aromaticity (Arom C, %) and No. of H atoms/100 C in the residues versus final temperature of liquefaction (TPL) in tetralin.

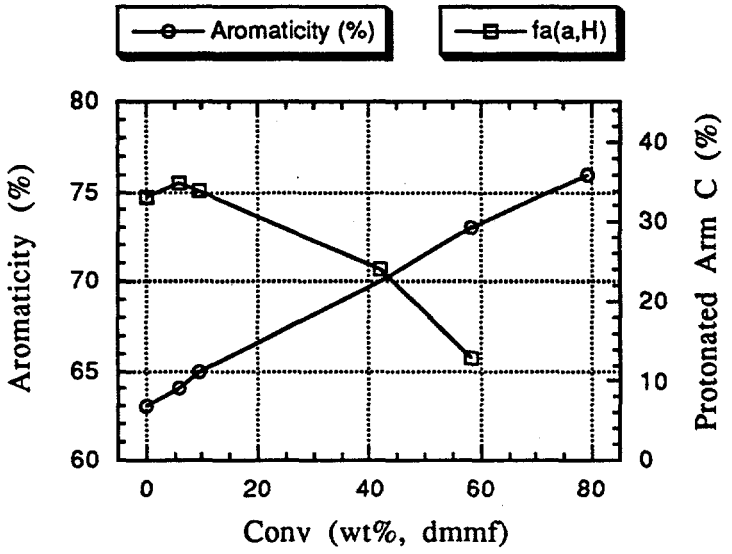

Figure 6.5. Change of aromaticity and percentage degree of protonation of aromatic carbons [fa(a,H)] in the residues versus conversion of DECS-9 Montana coal in TPL with tetralin.

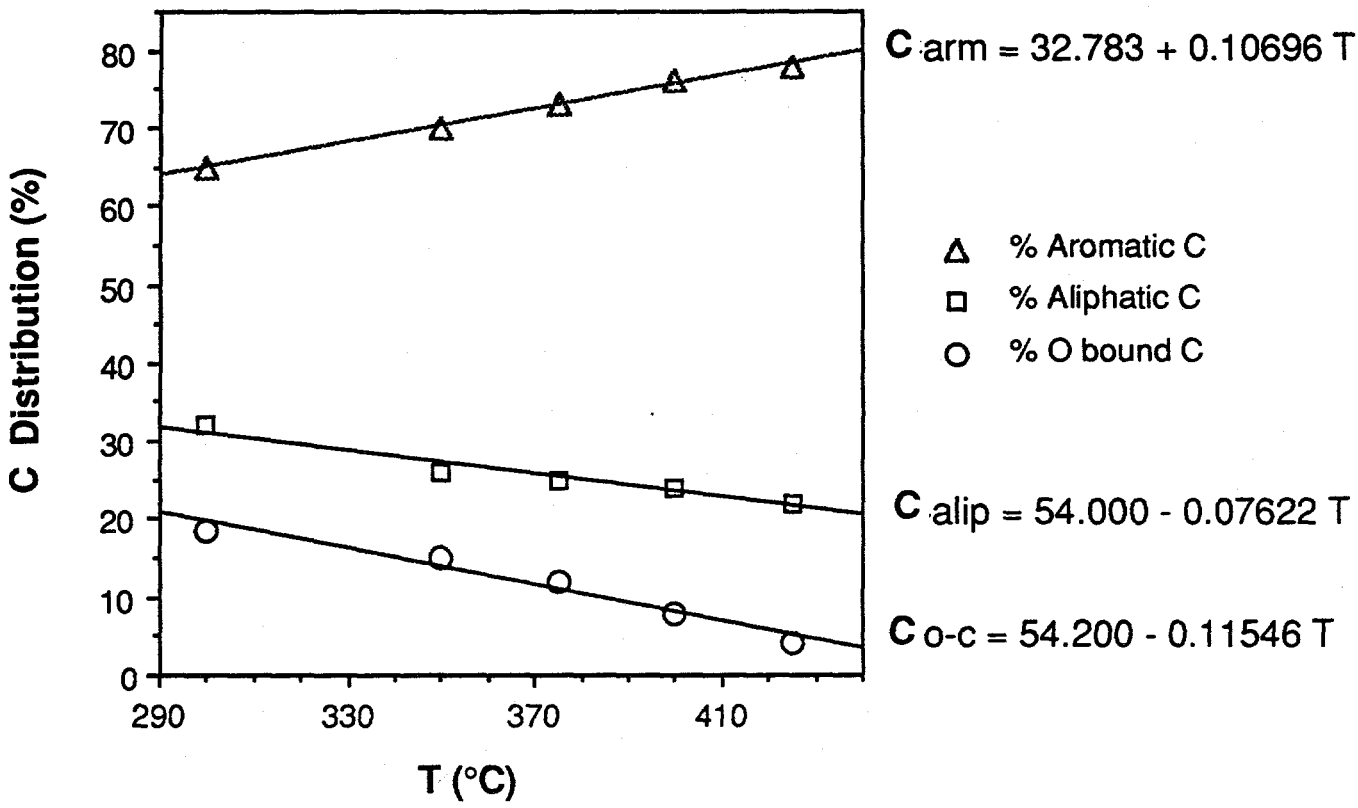

Figure 6.6. The changes in the aromatic, aliphatic, and oxygen-bound carbons of the residues

Characterization of Residues from Catalytic Liquefaction at 350°C

We also performed CPMAS and DDMAS ^{13}C NMR analysis of THF-insoluble residues derived from non-catalytic and catalytic liquefaction of Wyodak subbituminous coal at 350°C for 30 min under 6.9 MPa (cold) H_2 pressure. Table 6.2 shows the results of carbon aromaticities determined by CPMAS ^{13}C NMR, and the degree of protonation of aromatic carbons determined by DDMAS ^{13}C NMR. Reactions at 350°C can be viewed as pretreatments or low-severity liquefaction. For the sake of convenience, we will call all the reactions as liquefaction.

The coal conversion data have been reported in a recent paper (Song et al., 1994). Briefly, in the absence of catalyst, coal conversion at 350°C into THF-solubles plus gas was 12.5 wt% (dmmf) without solvent, 18.3 wt% with 1-methylnaphthalene solvent, and 25.9 wt% with tetralin. The use of ATTM increased coal conversion to 29.8 wt% (dmmf) without solvent, 31.1 wt% with 1-methylnaphthalene solvent, and 36.4 wt% with tetralin.

The data in Table 6.2 shows that using dispersed catalyst (in situ generated from impregnated ammonium tetrathiomolybdate, ATTM) not only improved coal conversion, but also resulted in small but consistent decrease in carbon aromaticity of the residues. This suggests the occurence of hydrogenation on some aromatic rings in the residues in the presence of dispersed molybdenum sulfide catalyst. These results are consistent with our recent work on the CPMAS NMR analysis of residues from DECS-1 Texas Big Brown subbituminous coal (Huang et al., 1993).

Compared to the THF-extracted but unreacted coal, the degree of protonation of aromatic carbons (f_a^{aH}) is higher with the residues from non-catalytic liquefaction. It should be mentioned that the amount of THF-soluble materials in the raw coal was about 8.5 wt% (dmmf), and the coal conversion into THF-solubles plus gas in the solvent-free non-catalytic run at 350°C was 12.5 wt% (dmmf). Therefore, on the basis of dmmf coal, the THF-extracted coal sample has about 4 wt% more organic material compared to the residue from solvent-free non-catalytic run. Since the latter has higher aromaticity (0.63) than the former (0.57), the higher f_a^{aH} value (0.40) could be due to the higher proportion of aromatics in the latter.

Some of the aromatics were probably formed from dehydrogenation of hydroaromatic ring via hydrogen abstraction by thermally-derived radicals, which account for the simultanesous increase of f_a and f_a^{aH} values. If this is true, then the use of hydrogen-donor solvent should suppress the increase of f_a^{aH} value, because the reactive radicals would be stablilized by the hydrogen donation of solvent molecules. In fact, this is the case. The f_a^{aH} value decreased from 0.40 to 0.33 when a hydrogen-donor solvent, tetralin, was used, as shown in Table 6.2. When a hydrogen-donor solvent was replaced by a non-donor vehicle, 1-methylnaphthalene solvent, f_a^{aH} value increased from 0.33 to 0.37.

Table 6.2. NMR-Derived Carbon Aromaticity (f_a) and Degree of Protonation of Aromatic Carbons (f_a^{aH}) of THF-insoluble Residues from Liquefaction of DECS-8 Wyodak Coal at 350°C for 30 min under 6.9 MPa (cold) H_2 Pressure

Sample	Temp, °C	Solvent	Catalyst	CPMAS NMR[a] fa	DDMAS NMR fa^{aH}
THF-extracted but unreacted coal				0.57	0.29
Residue	350°C	No	No	0.63	0.40
Residue	350°C	No	ATTM[b]	0.62	0.31
Residue	350°C	Tetralin	No	0.62	0.33
Residue	350°C	Tetralin	ATTM[b]	0.61	0.30
Residue	350°C	1-MN	No	0.68	0.37
Residue	350°C	1-MN	ATTM[b]	0.60	0.30

a) Integration of signal intensity between 95 and 165 ppm.
b) Ammonium tetrathiomolybdate, 1 wt% Mo on dmmf coal.

Table 6.3. CPMAS ^{13}C NMR-Derived Carbon Distribution for THF-insoluble Residues from Liquefaction of DECS-8 Coal at 350°C for 30 min under 6.9 MPa (cold) H_2 Pressure

Sample	Temp, °C	Solvent	Cat.	Arom C 95-165 ppm	Alip C 0-60 ppm	C-O C 170-230 ppm	Ar C-O 140-165 ppm	O/100 C
THF-ext. coal	raw coal	no	no	57.0	34.9	8.3	15.3	23.6
Residue	350°C	No	No	63.0	28.0	6.0	12.0	18.0
Residue	350°C	No	ATTM	62.0	29.7	7.0	10.0	17.0
Residue	350°C	Tetralin	No	62.0	27.0	8.0	12.5	20.5
Residue	350°C	Tetralin	ATTM	61.0	29.0	7.0	11.0	18.0
Residue	350°C	1-MN	No	68.0	22.0	6.0	12.0	18.0
Residue	350°C	1-MN	ATTM	60.0	28.0	6.0	10.0	16.0

a) Integration of signal intensity between 95 and 165 ppm.
b) Ammonium tetrathiomolybdate, 1 wt% Mo on dmmf coal.

Table 6.4. CPMAS ^{13}C NMR-Derived O-bound Carbon Distribution for THF-insoluble Residues from Liquefaction of DECS-8 Coal at 350°C for 30 min under 6.9 MPa (cold) H_2

Sample	Temp, °C	Solvent	Cat.	Phenolic ArOH	Catechol Ar(OH)2	Carboxyl COOH	Carbonyl C=O
THF-extracted DECS-8 coal	raw coal	no	no	8.0	7.0	4.3	4.0
Residue	350°C	No	No	7.0	5.0	3.0	3.0
Residue	350°C	No	ATTM[b]	6.5	3.5	2.8	3.2
Residue	350°C	Tetralin	No	12.5	0	5.1	2.9
Residue	350°C	Tetralin	ATTM[b]	11.0	0	3.0	4.0
Residue	350°C	1-MN	No	12.0	0	3.3	2.7
Residue	350°C	1-MN	ATTM[b]	10.0	0	3.0	3.0
THF-extr. DECS-9 coal[c]	raw coal	no	no	10.0	5.0	2.1	1.0

a) Integration of signal intensity between 95 and 165 ppm.
b) Ammonium tetrathiomolybdate, 1 wt% Mo on dmmf coal.
c) Data for DECS-9 Montana subbituminous coal, for comparison.

Interestingly, DDMAS ^{13}C NMR of the residues revealed that the degree of protonation of aromatic carbons (f_a^{aH}) is lower with the residues from catalytic liquefaction than that from non-catalytic reaction, as can be seen from Table 6.2. These results were surprising to us initially, as f_a^{aH} values usually decrease with increasing degree of condensation. However, if this is the case, this decrease should be accompanied by the increase in f_a values. It is possible that, relative to the residues from non-catalytic runs, the lower f_a^{aH} values for residues from catalytic runs were due to hydrogenation of the aromatic rings to form hydroaromatic rings.

Table 6.3 shows the carbon distribution data, and Table 6.4 gives the distribution of oxygen-bound carbon for the residues from DECS-8 coal. It should be noted that these data are very useful for comparison purpose, but we do not know how accurate the absolute values are. Generally, all the residues from runs at 350°c contain more aromatic and less aliphatic carbon as compared to the THF-extracted but unreacted coal. Among the residues from 350°C runs, the samples from catalytic runs, although they contain less organic materials due to higher comversion, have higher content of aliphatic carbon, but lower content of aromatic carbon (Table 6.3), and lower contents of oxygen-bound aromatic carbons such as phenolic C, and less carboxyl carbon (Table 6.4). These data suggest that the chemical composition of even the unconverted residue in the catalytic runs is different from that remained in the non-catalytic runs. In other words, the catalytic pretreatment at 350°C does induce smal but important structural changes. These data are also consistent with the above discussion on DDMAS and CPMAS data.

REFERENCES

Alemany, L.B.; Grant, D.M.; Alger, T.D.; Pugmire, R.J. J. Am. Chem. Soc., 1983, 105, 6697.

Franco, D.V.; Gelan, J.M.; Martens, H.J.; Vanderzande, D.-J.-M. Fuel, 1991, 70, 811-817.

Hatcher, P.G. Org. Geochem., 1987, 11 (1), 31-39.

Hatcher, P.G. Energy & Fuels, 1988, 2 (1), 48-58.

Hatcher, P.G.; Lerch III, H.E.; Kotra, R.K.; Verheyen, T.V. Fuel, 1988, 67, 1069-1075.

Hatcher, P.G.; Wilson, M.A.; Vassallo, A.M.; Lerch III, H.E. Int. J. Coal Geol., 1989, 13, 99-126.

Huang, L.; Song, C.; Schobert, H.H. Am. Chem. Soc. Div. Fuel Chem. Prepr., 1993, 38 (3), 1093-1099.

Saini, A. K.; Song, C.; Schobert, H. H.; Hatcher, P. G. Am. Chem. Soc. Div. Fuel Chem. Prepr., 1992, 37 (3), 1235-1242.

Saini, A. K.; Song, C. Am. Chem. Soc. Div. Fuel Chem. Prepr., 1994, 37 (3-4), in press.

Pan, V.H.; Maciel, G.E. Fuel, 1993, 72 (4), 451-468.

Song, C.; Schobert, H.H.; Hatcher, P.G. Energy & Fuels, 1992, 6 (3), 326-328.

Song, C.; Schobert, H.H. Am. Chem. Soc. Div. Fuel Chem. Prepr., 1992, 37 (2), 976-983.

Song, C.; Hou, L.; Saini, A.K.; Hatcher, P.G.; Schobert, H.H. Fuel Processing Technol., 1993, 34 (3), 249-276.

Song, C.; Saini, A.K.; Schobert, H.H. Energy & Fuels, 1994, 8 (2), 301-312.

Fatemi-Badi, S.M.; Swanson, A.J.; Sethi, N.K.; Roginski, R.T. Am. Chem. Soc. Div. Fuel Chem. Prepr., 1991, 36 (2), 470-480.

Wenzel, K.; Hatcher, P. G.; Cody, G. D.; Song, C. Am. Chem. Soc. Div. Fuel Chem. Prepr., 1993, 38 (2), 571-576.

Wilson, M.A.; Pugmire, R.J.; Karas, J.; Alemany, L.B.; Woolfenden, W.R.; Grant, D.M. Anal. Chem., 1984, 56, 933-943.

Yoshida, T.; Maekawa, Y., Fuel Processing Technol. 1987, 15, 385-395.

CHAPTER 7. TGA and Pyrolysis-GC-MS Analysis of Raw and Thermally Treated Bituminous Coals

INTRODUCTION

For the low-temperature pretreatment, it is important to know the thermal reactivity of coals. Therefore, we have examined the thermal reactivity by thermogravimetric analysis (TGA), and studied the structural changes of coal under pyrolytic conditions but at different temperatures using pyrolysis/gas chromatography/mass spectrometry (Py-GC-MS). TGA of three bituminous coals has revealed the differences in their devolatilization behavior. Py-GC-MS of these coals at different pyrolysis temperatures and the Py-GC-MS of thermally pretreated samples provided some new information on their structures and structural transformations.

EXPERIMENTAL

Samples

In this work we characterized two bituminous coals, DECS-6, Blind Canyon, and DECS-12, Pittsburgh #8, and one subbituminous coal, DECS-7, Adaville #1. Their characterization was carried out using thermogravimetric analysis (TGA), pyrolysis-GC-MS, and solid-state NMR.

TGA Analysis

The Perkin-Elmer Series 7 Thermal Analysis System was used for TGA experiments under inert atmosphere. Thermogravimetric analyses were preformed on coals DECS-7, Adaville #1, DECS-6, Blind Canyon, and DECS-12, Pittsburgh #8. This thermal method of analysis measures percent weight loss of material (devolatilization) upon heating in an inert (N_2) atmosphere. The yields of volatile components, moisture, and reactivity of the coals can be determined with this technique. Prior to analysis the coals were dried in a vacuum oven at 45 ^{o}C for twenty four hours. Fifteen to nineteen milligrams of coal were weighted directly in a crucible in the furnace of a Perkin -Elmer TGA 7 thermogravimetric analyzer. The coal was heated from 30 ^{o}C to 750 ^{o}C-800 ^{o}C at a rate of 5 ^{o}C/min.

Pyrolysis/Gas Chromatography/Mass Spectrometry

Flash Py/GC/MS procedures are the same as those explained in Song et al., (1993). A

series of four Py/GC/MS experiments were preformed on the Adaville #1 and the Blind Canyon coals with pyrolysis temperatures starting at 310° C and increasing to 610° C at 100° C increments . Sample weights ranged from 0.5 mg to 1.0 mg.

Thermal Treatment

The thermal pretreatments of the raw coals, DECS-7, DECS-6, and DECS-12 were carried out at 400° C. Four grams of coal were placed in a 25 ml microautoclave and pressurized with H_2 to 1000 psi. The coals were heated for 30 minutes. After the reaction, the products were separated by sequential extraction with hexane, toluene and THF. After the extraction the THF-insoluble residues were washed first in acetone and then in pentane in order to remove the THF, followed by drying at 110° C for 24 hours under vacuum (Song et al., 1992). The residue was then analyzed by PY/GC/MS.

RESULTS AND DISCUSSION

TGA Results

Figures 7.1, 7.2, and 7.3 show the TGA-derived weight loss curves vs time for each of the coal samples. All three coals show the same general trend. Initially there is an immediate weight loss which is due to water, carbon dioxide, and argon which still remains in the coal even after drying. The percent weight loss curve then levels off after 16 minutes (110° C) and remains relatively flat until release of the volatile components of the coal. Devolatilization starts a few degrees above 320° C for both the Adaville #1 and the Pittsburgh #8 coals but starts 40° C lower, 280° C for the Blind Canyon coal. This early weight loss in Blind Canyon is due to a devolatilization of resinite which constitutes a significant maceral component of the coal. This maceral volatilizes at a lower temperature than the other macerals. Pyrolysis GC/MS data discussed below confirms this conclusion. Between 500° C and 525° C the rate of weight loss slowly levels off until the end of the experiment. Table 5 shows the results of the TGA experiments.

Table 5 TGA analysis of selected coals

Coals	% MOISTURE	DEVOLATILIZATION TEMPERATURE	% VOLATILES	% RESIDUE
DECS-7	8.7	~317°	36.7	54.6
DECS-6	2.7	~280°	41.8	55.5
DECS-12	0.9	~315°	33.5	65.6

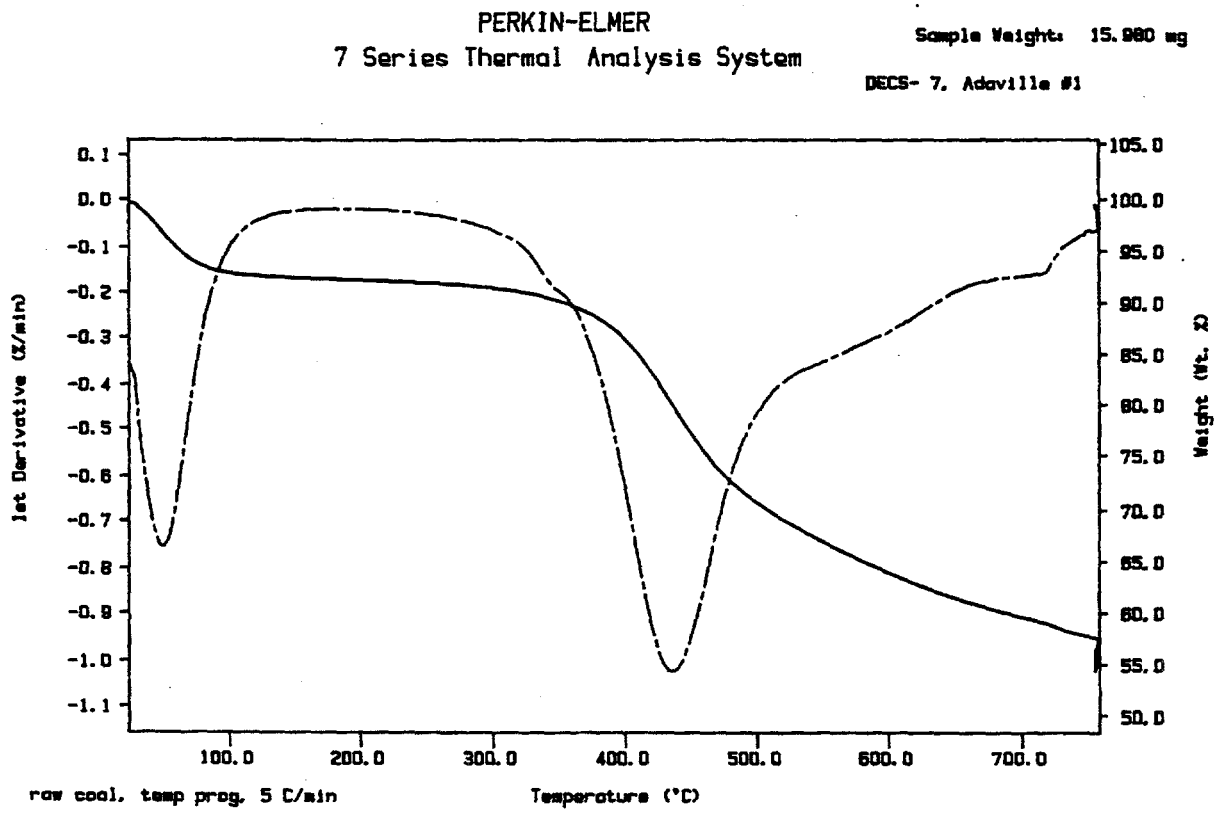

Figure 7.1. TGA and DTG plots of the Adaville #1 coal.

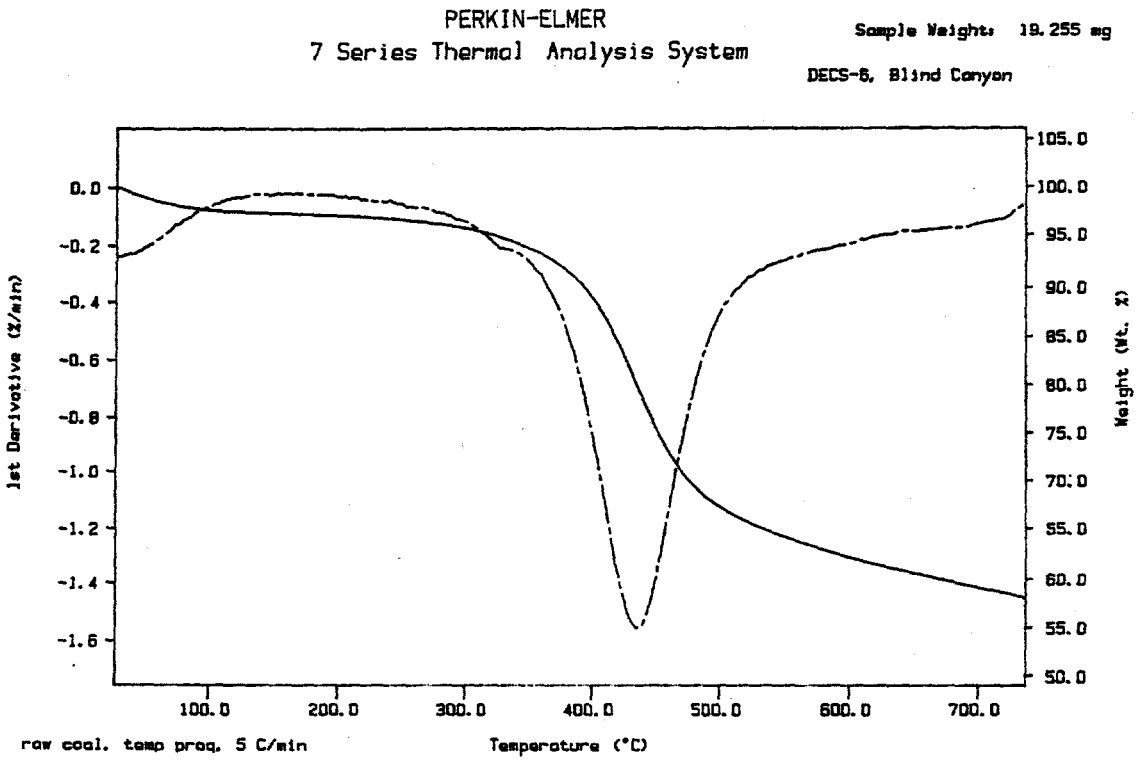

Figure 7.2. TGA and DTG plots of the Blind Canyon coal.

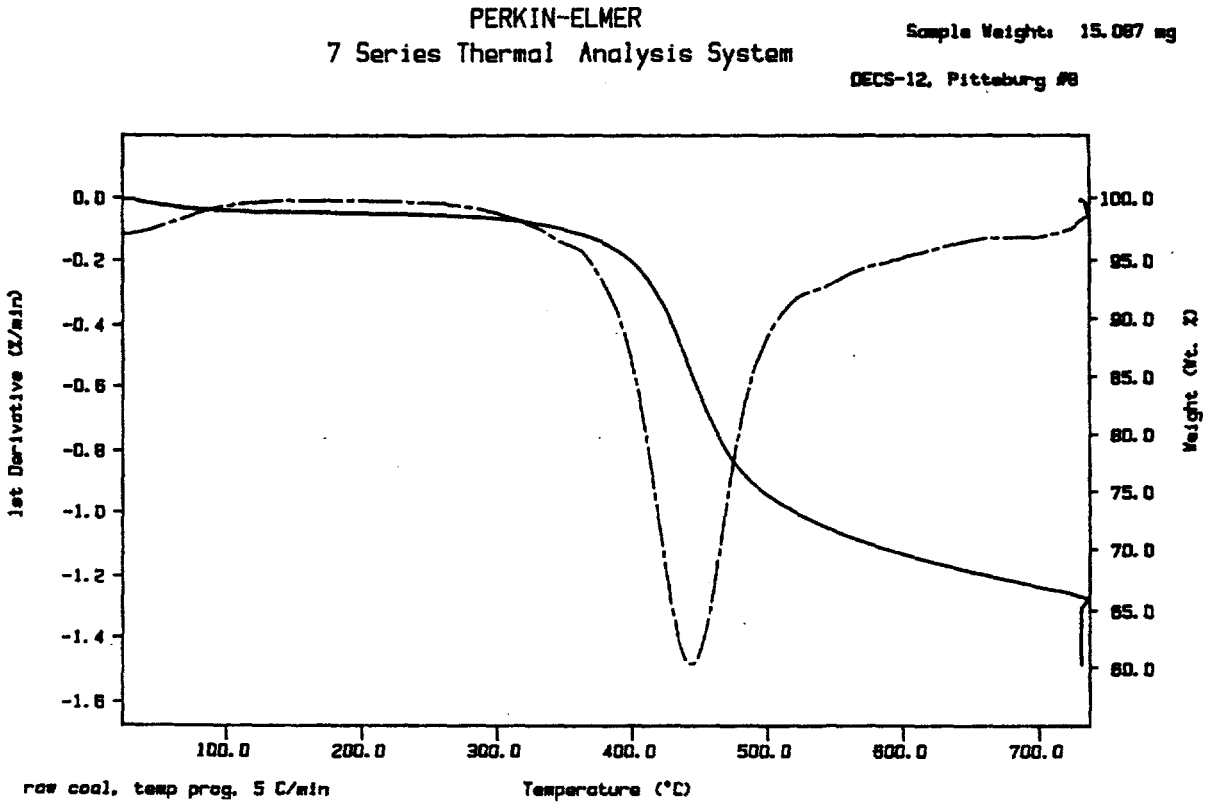

Figure 7.3. TGA and DTG plots of the Pittsburgh #8 coal.

Pyrolysis-GC-MS

Figure 7.4 shows the chromatogram of DECS-7 run at 310° C. This temperature is insufficient to pyrolyze the sample, but the temperature is high enough to thermally desorb the coal. Duplicate experiments yielded between seven and nine percent desorbed material. The volatiles consisted of sulfur compounds, mostly SO_2 and a trace of COS, and high molecular weight biomarkers, pentacyclic triterpenoids and aromatized triterpenoids. Also released but not shown in Figure 7.4 was bound water, CO_2, and argon.

Figure 7.5 shows a series of chromatograms run at 310° C, 410° C, 510° C and 610° C. There is little difference between the 310° C and 410° C pyrograms except for a trace of the alkene Prist-1-ene. At 510° C an increase in volatile pyrolysis products is observed indicating that significant pyrolysis of the coal occurs at this temperature. An abundant amount of Prist-1-ene and some straight chain alkanes, C19 through C31, are released. Not until 610° C does major pyrolysis of the coal occur. Released at this temperature are the homologous series of alkanes/alkenes, C4 through C31, phenols and alkyl phenols (C1 through C3) and benzene and alkylbenzenes (C1 through C4). Single ion chromatograms for the alkane/alkenes (m/z 71, 69), benzene compounds (m/z 78, 92, 106, 120), and phenol compounds (m/z 94, 108, 122) are shown in Figures 7.6, 7.7, and 7.8, respectively. Figure 7.9 is a plot of the volatile yield vs pyrolysis temperature. This plot shows that as temperature increases the amount of volatile material released increases from 7 percent at 310° C to 33 percent at 610° C.

A similar set of experiments was run on the Blind Canyon coal with different results, Figure 7.10. At 310° C the major products released were the bicyclic sesquiterpenoids, C20 to C30 straight chain alkanes, and sesquiterpenoids and triterpenoids. Again little change occurs at 410° C but also little change occurs at 510° C with only a slight increase of the high molecular weight alkanes. Just as in the DECS-7 experiments, pyrolysis of all the major compounds does not occur until 610° C. Figure 7.11 shows with increasing temperature the amount of volatile product also increases just as with the Adaville #1 coal.

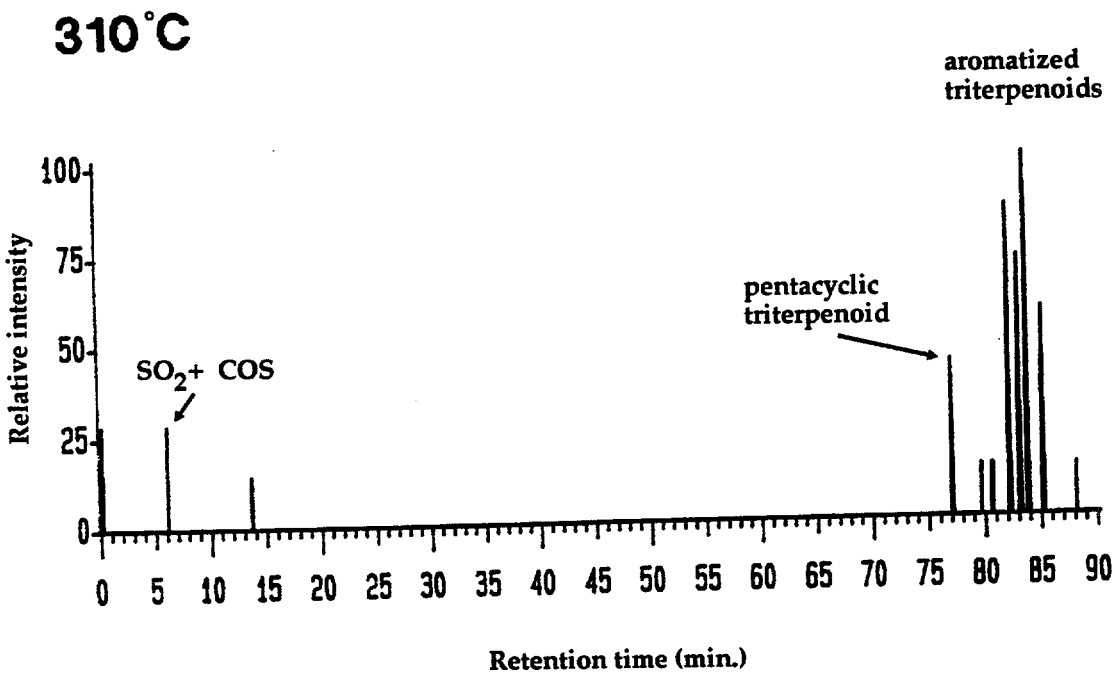

Figure 7.4. Pyrolysis-GC-MS chromatogram of DECS-7 Adaville #1 coal (pyrolysis at 310°C, representing thermally desorbed materials)

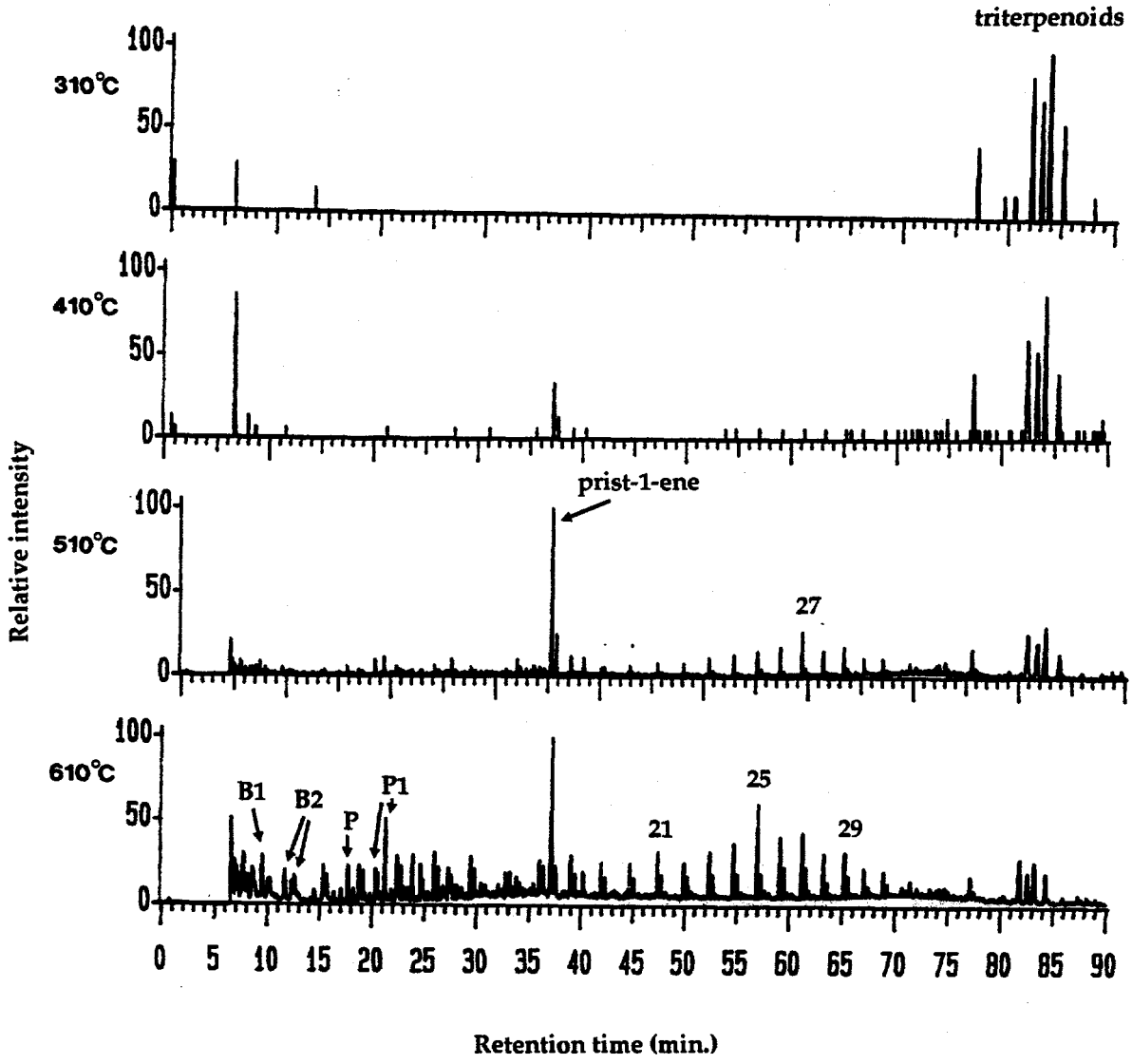

Figure 7.5. Pyrolysis-GC-MS chromatogram of DECS-7 Adaville #1 coal (pyrolysis at 310°C, 410°C, 510°C and 610°C).B1= toluene, B2= xylene, P= phenol, P1= cresol, numbered peaks are alkane/alkene pairs.

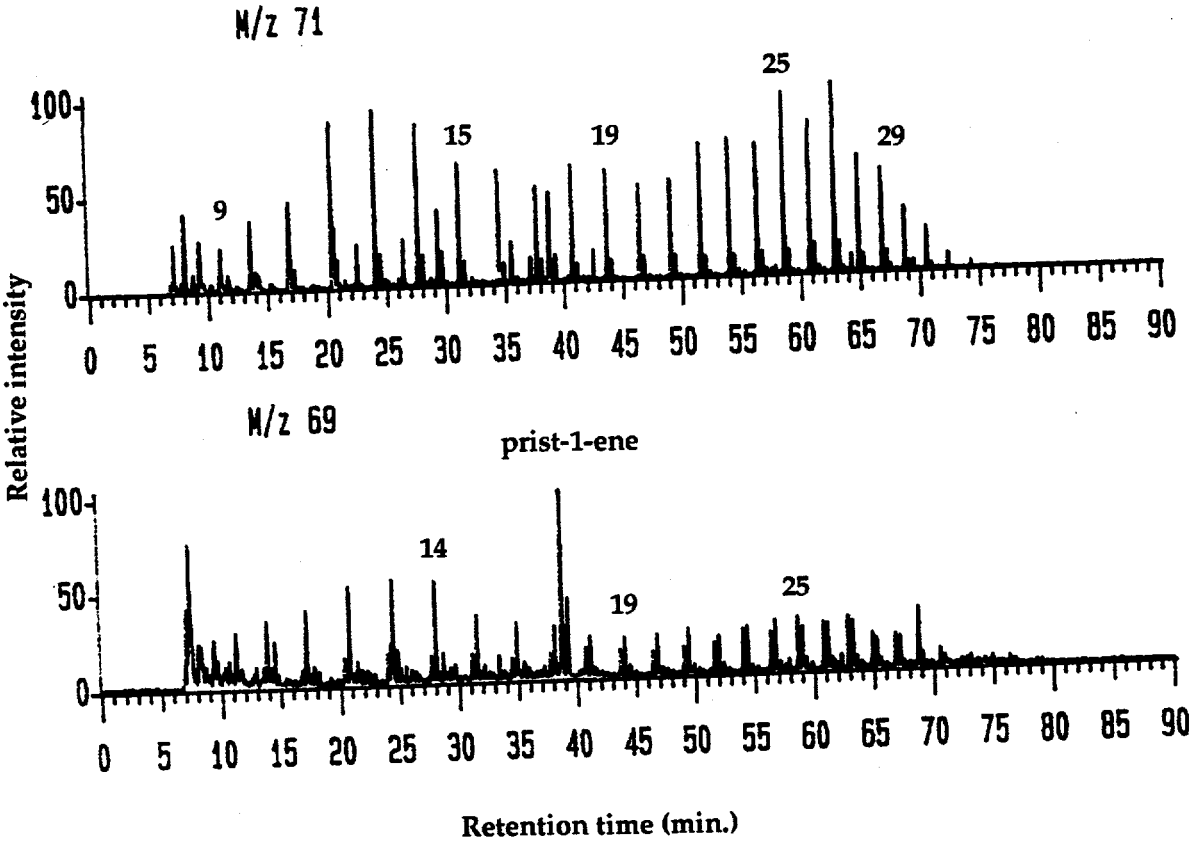

Figure 7.6. Single ion chromatograms from pyrolysis-GC-MS of DECS-7 Adaville #1 coal (representing the homologous series (numbers) of alkanes (m/z 71) and alkenes (m/z 69).

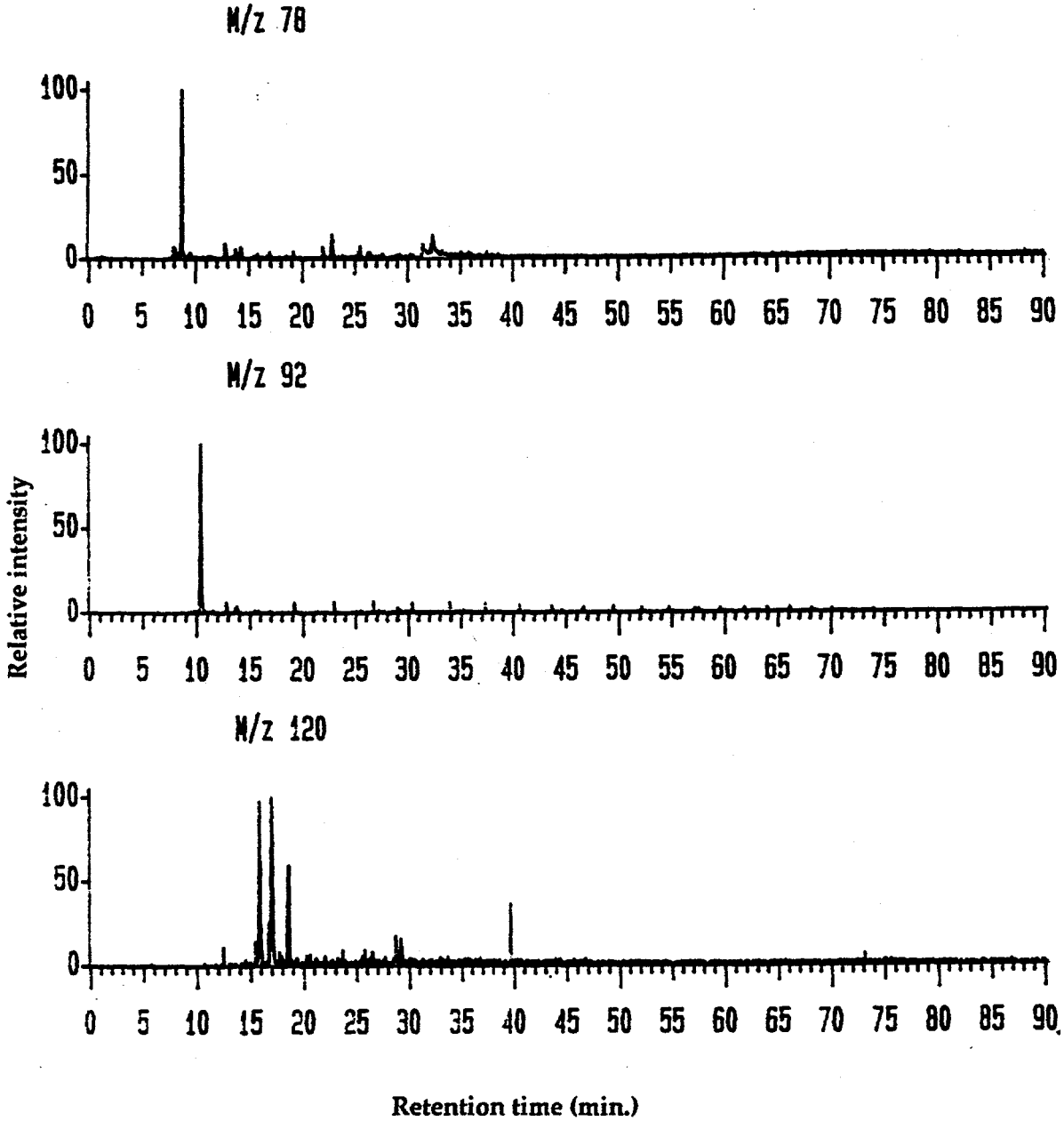

Figure 7.7. Single ion chromatograms from pyrolysis-GC-MS of DECS-7 Adaville #1 coal (representing benzene (m/z 78), toluene (m/z 92) and C_3-benzenes (m/z 120).

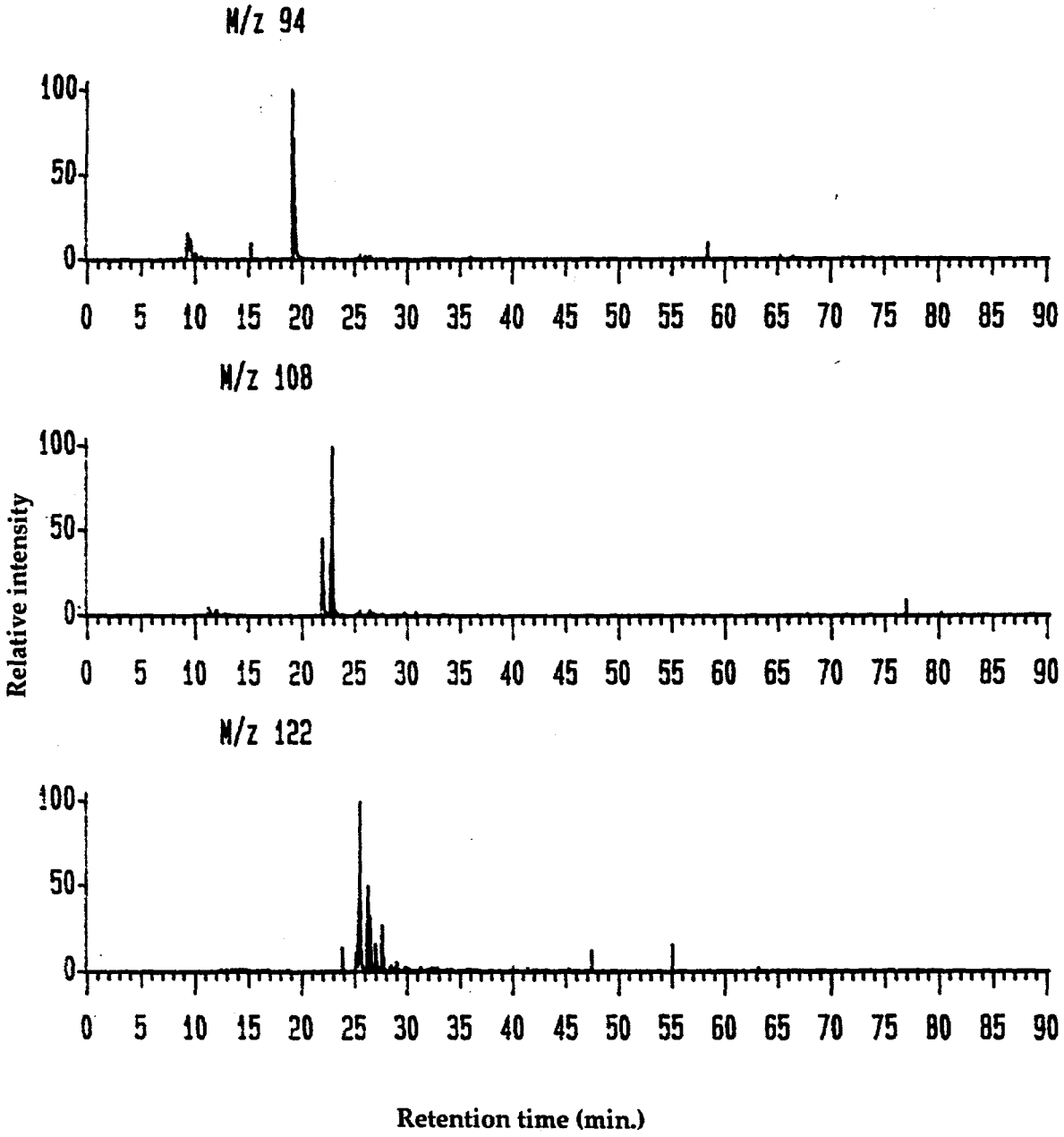

Figure 7.8. Single ion chromatograms from pyrolysis-GC-MS of DECS-7 Adaville #1 coal (representing phenol and alkylphenol).

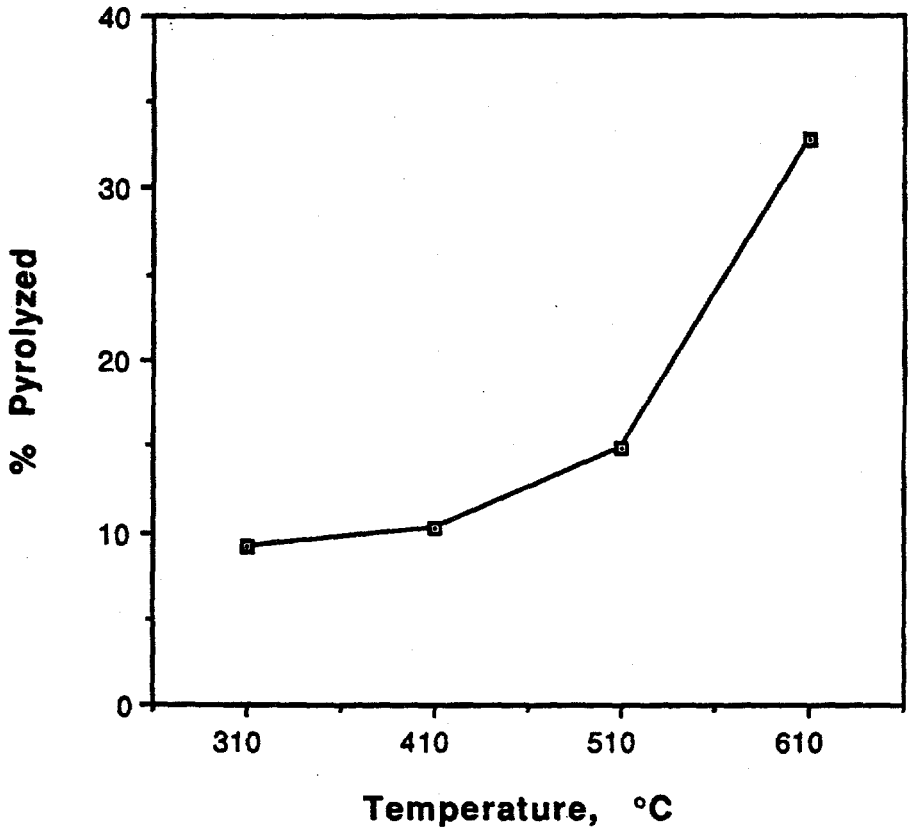

Figure 7.9. Percentage of the Adaville #1 coal pyrolyzed vs pyrolysis temperature.

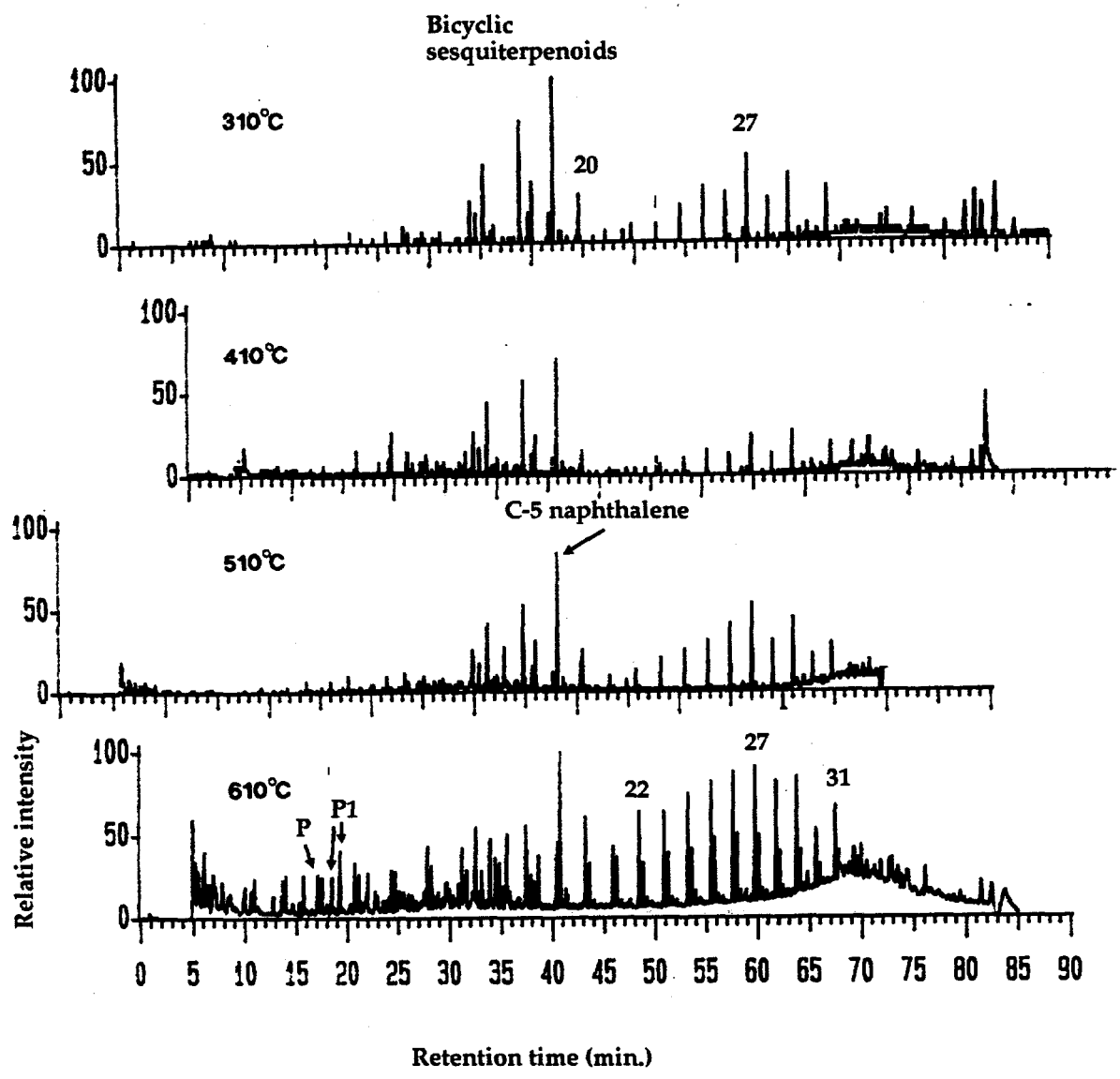

Figure 7.10. Pyrolysis-GC-MS chromatogram of the Blind Canyon coal (pyrolysis at 310°C, 410°C, 510°C and 610°C). P= phenol, P1= cresol, numbered peaks are alkane/alkene pairs.

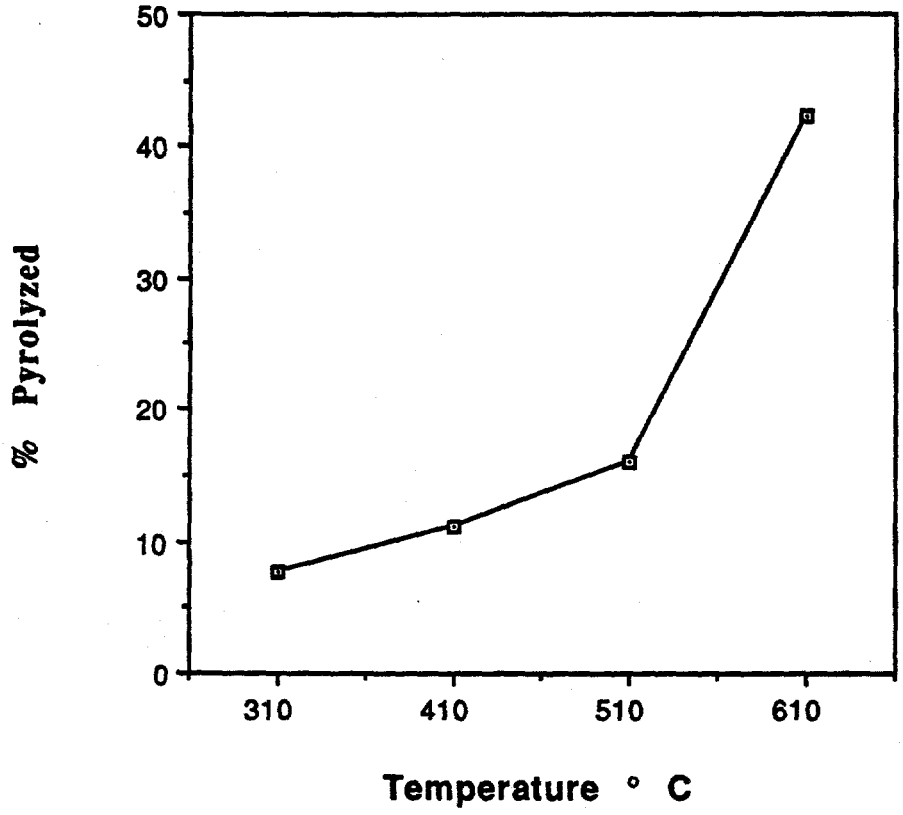

Figure 7.11. Percentage of the Blind Canyon coal pyrolyzed vs pyrolysis temperature.

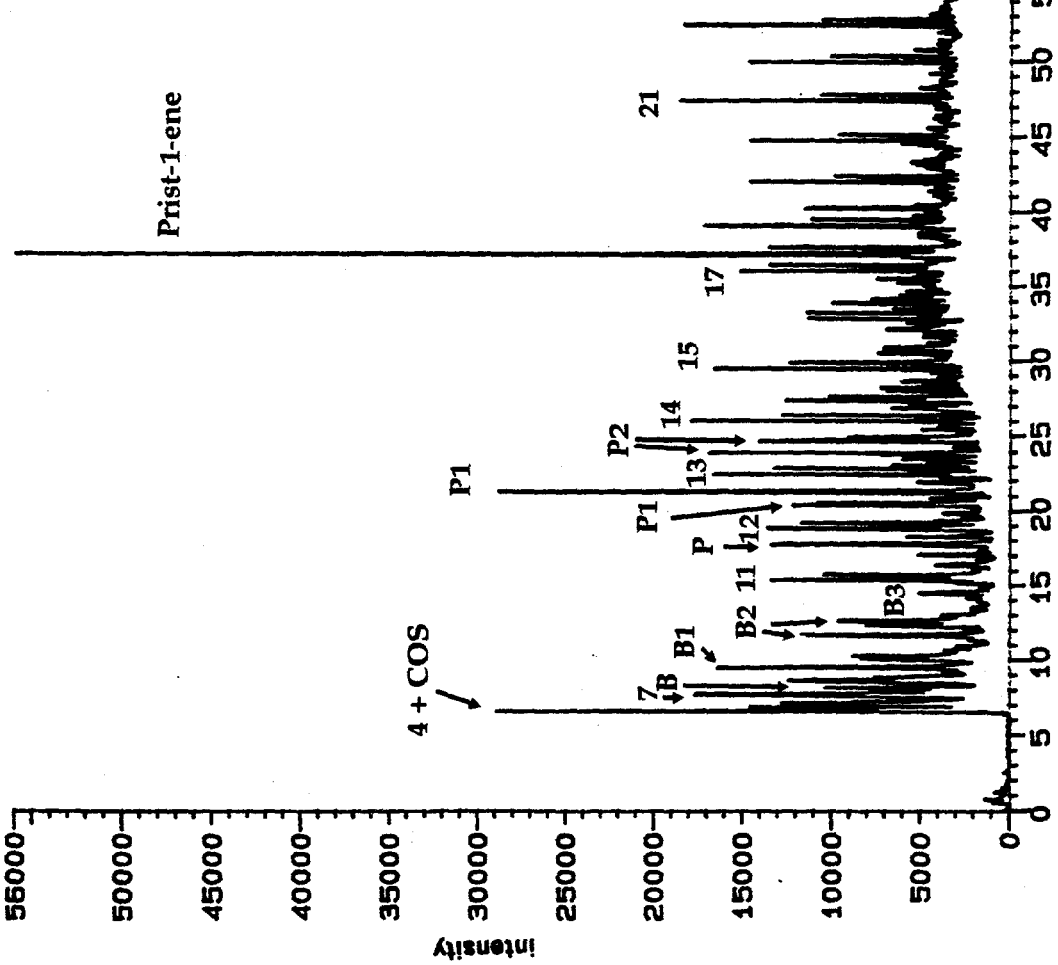

Figure 7.12. Pyrolysis-GC-MS chromatogram of the Adaville #1 coal. B= benzene,B1= toluene, B2= xylene, P= phenol, P1= cresol, P2= C-2 -phenols, numbered peaks are alkane/alkene pairs.

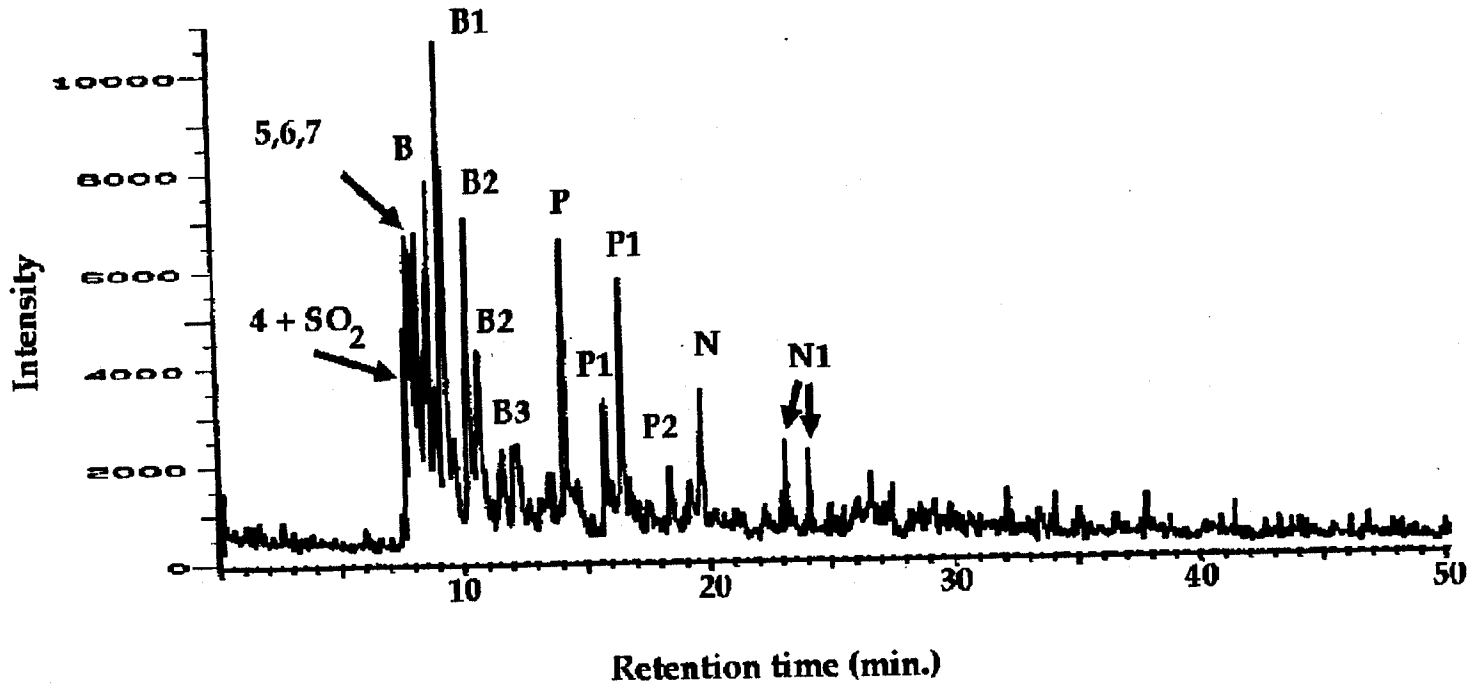

Figure 7.13. Pyrolysis-GC-MS chromatogram of the residue from Adaville #1 coal (after thermal pretreatment and extraction). B= benzene, B1= toluene, B2= xylene, B3= C-3-benzenes, P= phenol, P1= cresol, P2= C-2-phenols, N= naphthalene, N1= methylnaphthalenes, numbered peaks are alkane/alkene pairs.

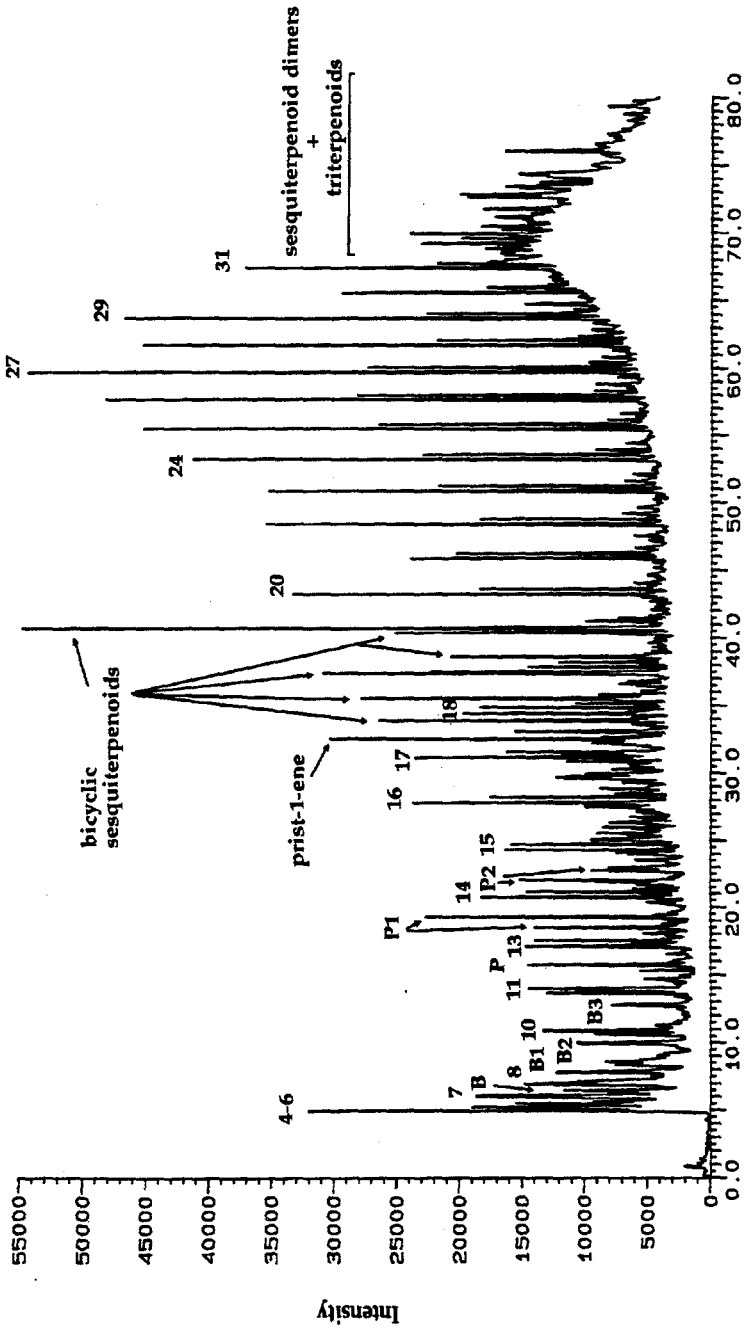

Figure 7.14. Pyrolysis-GC-MS chromatogram of the Blind Canyon coal. B= benzene, B1= toluene, B2= xylene, B3= C-3-benzenes, P= phenol, P1= cresol, P2= C-2-phenols, numbered peaks are alkane/alkene pairs.

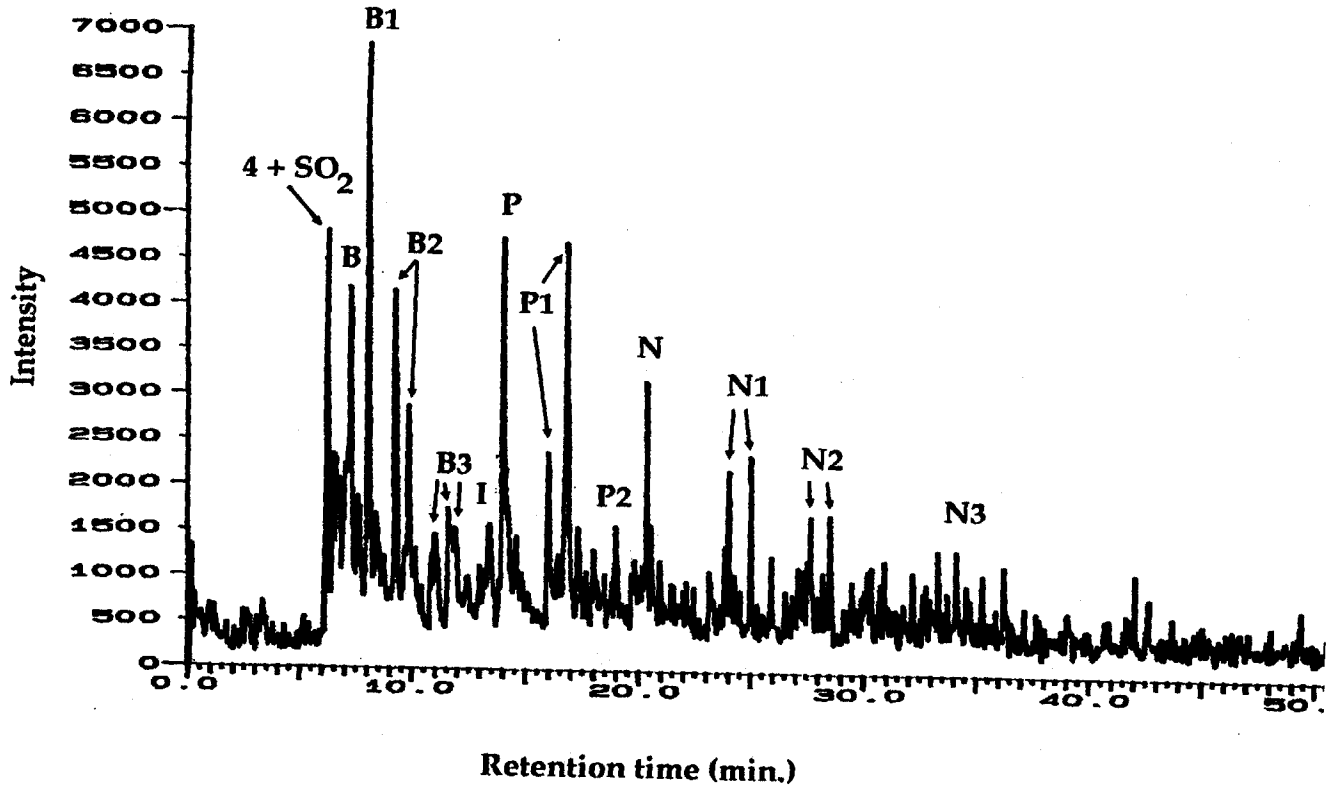

Figure 7.15. Pyrolysis-GC-MS chromatogram of the residue from Blind Canyon coal (after thermal pretreatment and extraction). B= benzene, B1= toluene, B2= xylene, B3= C-3-benzenes, I= indene, P= phenol, P1= cresol, P2= C-2-phenols, N= naphthalene, N1= methylnaphthalenes, N2= C-2-naphthalenes, N3= C-3-naphthalenes, numbered peaks are alkane/alkene pairs.

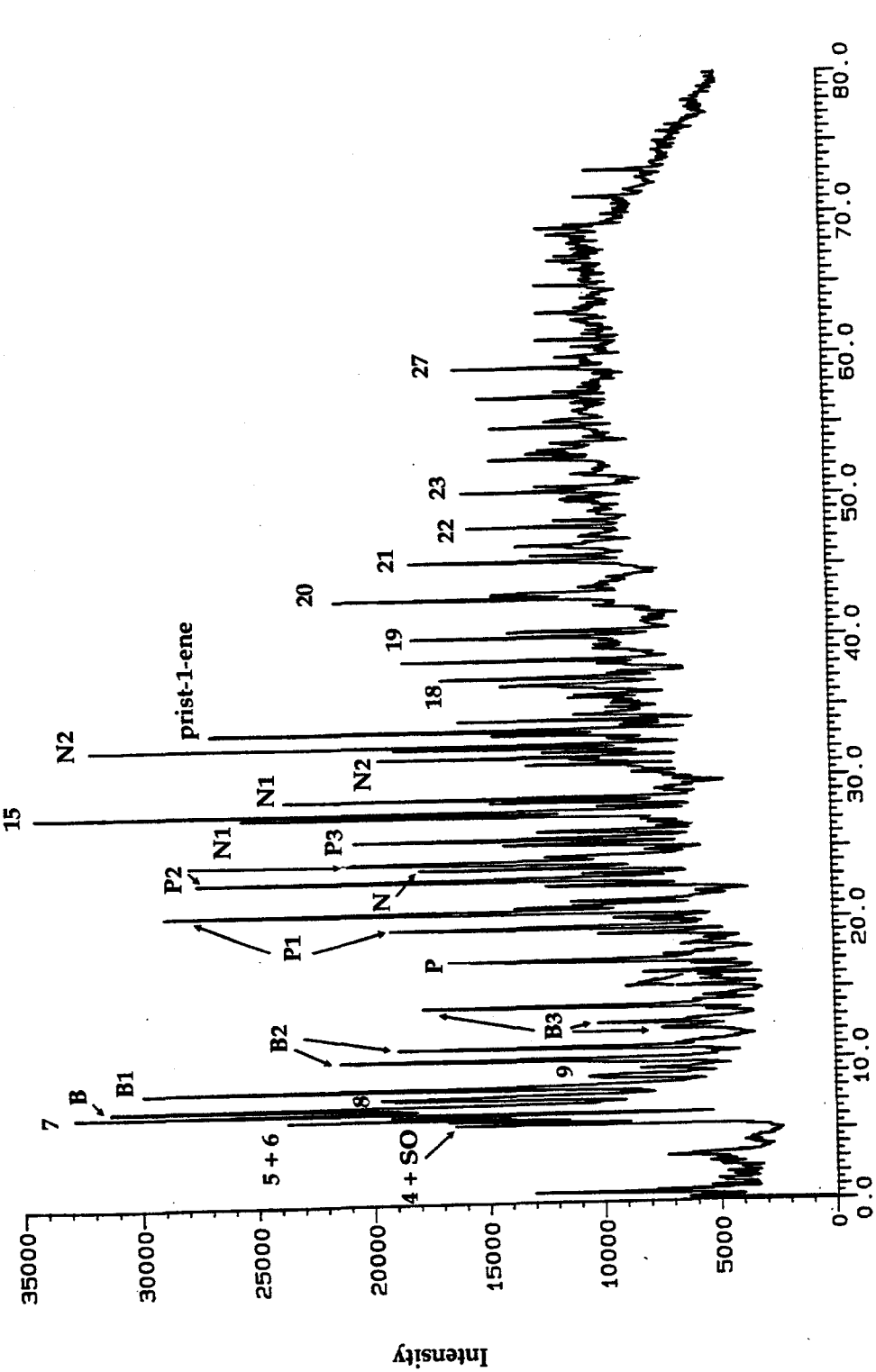

Figure 7.16. Pyrolysis-GC-MS chromatogram of the Pittsburgh #8 coal. B= benzene, B1= toluene, B2= xylene, B3= C-3-benzenes, P= phenol, P1= cresol, P2= C-2-phenols, N= naphthalene, N1= methylnaphthalenes, N2=C-2-napthalenes, numbered peaks are alkane/alkene pairs.

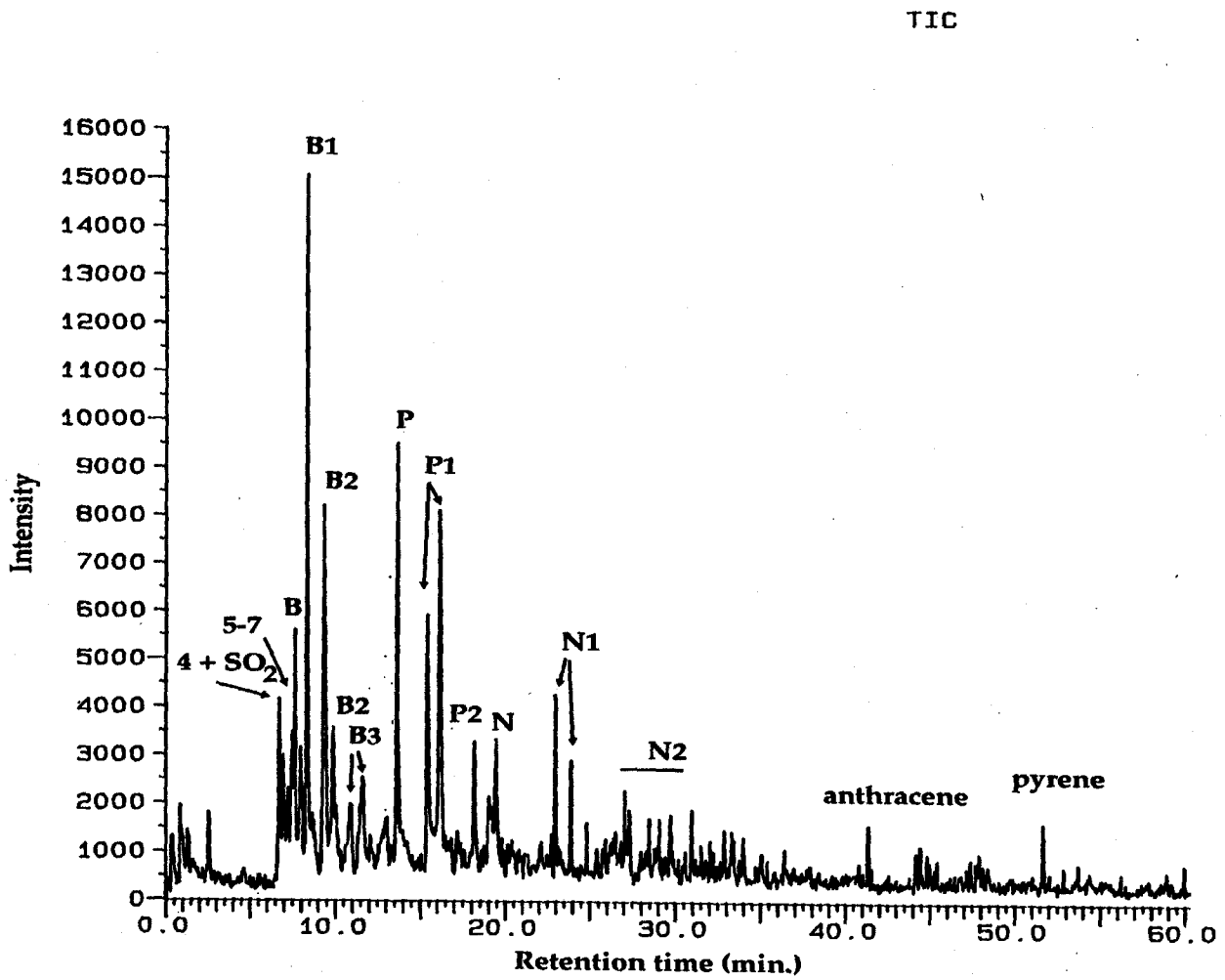

Figure 7.17. Pyrolysis-GC-MS chromatogram of the residue from Pittsburgh #8 coal (after thermal pretreatment and extraction). B= benzene, B1= toluene, B2= xylene, B3= C-3-benzenes, P= phenol, P1= cresol, P2= C-2-phenols, N= naphthalene, N1= methylnaphthalenes, numbered peaks are alkane/alkene pairs.

Characterization of Thermally Treated Bituminous Coals

Figure 7.12 shows the pyrolysis-GC-MS total ion chromatogram for the unreacted Adaville #1 coal, and Figure 7.13 shows the chromatogram for the thermally treated Adaville #1 coal. A comparison of these two pyrograms shows a strikingly different pyrolyzates. Prist-1-ene, the alkane/alkenes series, and the high molecular weight biomarkers are completely missing from the reacted Adaville #1. Other changes that have occurred to the treated coal are the addition of naphthalene and alkyl naphthalenes in the pyrograms and an increase in the phenol concentration relative to the C_1 phenols. These differences indicate the macromolecular structure of the Adaville #1 coal has been thermally altered during the heating experiment (400° C).

Figure 7.14 shows the chromatogram for the unreacted Blind Canyon coal and Figure 7.15 shows the chromatogram for the thermally treated Blind Canyon coal. Again there is a significant difference between the unreacted and the reacted coal's. There is a complete loss of the alkane\alkene series, the bicyclic sesquiterpenoids, and the triterpenoids as compared to the unreacted coal. The addition of naphthalene and alkyl naphthalenes and the increase in the phenol concentration relative to the C1 phenols has also occurred. Severe heating has caused the same changes to occur in the Blind Canyon coal as has occurred in the Adaville #1 coal.

Figure 7.16 and Figure 7.17 are pyrograms of the Pittsburgh #8 unreacted coal and heat treated coal, respectively. Here a comparison between the two coal shows that the differences in the chromatograms are not as great as what has occurred in the previous two heating experiments. There is only a loss of the alkane/alkenes and an addition of anthracene and pyrene.

References

Hatcher, P.G. Org. Geochem., 1987, 11 (1), 31-39.

Hatcher, P.G. Energy & Fuels, 1988, 2 (1), 48-58.

Song, C.; Hou, L.; Saini, A.K.; Hatcher, P.G.; Schobert, H.H. Fuel Processing Technol., 1993, 34 (3), 249-276.

Chapter 8. Characterization of Three Bituminous Coals and Their Products and Residues from Solvent-Free Thermal Liquefaction at 400°C

Introduction

The liquefaction behavior of three bituminous coals with a carbon content ranging from 77% to 85% was evaluated spectroscopically by ^{13}C NMR and pyrolysis/gas chromatograpy/mass spectrometry to delineate the structural changes that occur in the coal during liquefaction. Complementary data includes ultimate and proximate analysis, along with optical microscopy for maceral determinations. Even though these are all bituminous coals they exhibit quite different physical and chemical characteristics. The coals vary in rank, ranging from HvC b to HvA b, in petrographic composition, different maceral percentages, and in chemical nature, percent of carbon and of volatiles. It is these variations that govern the products, their distribution, and conversion percentages. Some of the products formed can be traced to a specific maceral group.

Experimental

Samples

Three bituminous coals (DECS-7, DECS-6, and DECS-12) were obtained from the DOE/Penn State Coal Sample Bank. They were thermally reacted and then analyzed by ^{13}C NMR and py/GC/MS. A summary of their important properties is found in Table 8.1. The Adaville coal (DECS-7) has the highest vitrinite (a low hydrogen, high carbon content maceral) content and the lowest liptinite (a high hydrogen, low carbon content maceral) content. It also has the lowest carbon content by ultimate analysis of the three coals . The Blind Canyon has the lowest vitrinite content and the highest liptinite content. Pittsburgh #8 maceral composition is intermediate between these two coals. Its carbon content is the highest, though. As it will be shown these are important parameters in determining which products are formed and in which extracted fraction they are found.

The three coals were extracted in hexane, toluene, and THF to determine the amount of mobile constituents in the samples. The results are also shown in Table 8.1. The THF extracted residues were pyrolyzed for comparison with the raw coals and reacted residues.

Liquefaction Experiments

Thermal reaction of four grams of raw coal was preformed on the three bituminous coals in 32 ml tubing bombs pressurized to 1000 psi H_2. The reactors were placed in a 400° C sandbath and heated for 30 minutes. After cooling the reactor , the products were separated using a procedure by which the reactor was opened, the gas volume measured, then the reacted residue extracted in solvents so the oil, asphaltenes, preasphaltenes and residue could be analyzed. A detailed description of the procedure can be found in Song et al. (1992).

Table 8.1. Physical and Chemical Properties of the Selected Coals

Coal	DECS-7	DECS-6	DECS-12
	Adaville #1	Blind Canyon	Pittsburgh #8
Maceral group dmmf, vol %			
Vitrinite	94.7	69.1	83
Liptinite	3.2	17	8.9
Inertinite	2.1	13.9	8.1
Rank	HvC Bit.	HvB Bit.	HvA Bit.
% C dmmf	77.45	81.72	84.75
% volatiles	38.11	42.4	35.16
% THF extracted from Raw coal dmmf wt%	12.2	14.2	8.9

CPMAS ^{13}C NMR Spectroscopy

A Chemagnetics M-100 NMR spectrometer was used to collect spectra on the raw coals, Adaville #1, Blind Canyon, and Pittsburgh # 8, their unreacted THF-insoluble residues and their thermally reacted THF-insoluble residues. All samples used the same experimental procedures. The rotor was filled with the sample to be analyzed, inserted into the NMR probe and spun at about 3.5 kHz with a magic angle of 54.7°. Acquisition of 30,000 scans was required to assure a

good signal-to noise ratio. Acquisition parameters were contact time equalled 1 μs with a pulse delay of 1 s, tau equalled 400 ms and line broadening equalled 29.9 Hz. See Hatcher et al. (1989) for further details concerning NMR data for coals.

Pyrolysis-GC-MS

Flash Py/GC/MS procedures are the same as those explained in Song et al., 1992. Analyses were preformed on DECS-7, DECS-6, and DECS-12, the raw coals, the reacted residues and the THF-insoluble unreacted residues. Thermal desorption experiments were also performed on all three bituminous coals. Samples were weighed in a capillary quartz tube and then placed between the heating coils of a CDS 1000 pyroprobe. The probe was then inserted into the injection port of the Dupont GC/MS. Injection port temperature is held at 280° C. The probe was heated to 300° C for 30 seconds. This temperature is insufficient to cause pyrolysis (Song et al., 1992) but is high enough to drive off any mobile volatile material that has migrated into the coal's pores or that has been generated in situ. Flash pyrolysis experiments were also performed on the THF-insoluble residues generated during the thermal liquefaction experiments.

GC/MS

After rotoevaporating the solvent from the hexane soluble fraction (oil) of the reacted residues, the oil was analyzed by injecting a sample into a Hewlett Packard 5890 gas chromatograph coupled to a Hewlett Packard 5971A mass spectrometer. Injector temperature was 250 °C and the temperature program started at 40°C with a three minute delay and increased at 5°C/min to a final temperature of 280°C.

Results and Discussion

Thermal Liquefaction

Heating the coals to 400° C under 1000 psi H_2 caused a significant redistribution in material. DECS-7 lost 30% of its mass while both DECS-6 and DECS-12 lost almost 40% of their mass on a dry mineral matter free basis. DECS-12 had the highest overall conversion with 39.9% but also had the highest amounts asphaltene and preasphaltene. DECS-6 had the greatest oil yield with 22.5% with almost as good total conversion. See Table 2 for conversion data.

CPMAS ^{13}C NMR

CPM ^{13}C NMR data can be used to identify the structural changes induced by thermal pretreatment of the three bituminous coals under study. The spectra for the raw coals are shown in Figure 8.1. For all the coals and residues the spectra can be divided into three regions. The

first region (0-60 ppm) represents the aliphatic carbons, the second region (80-170 ppm) represents the aromatic carbons, and the third region (170-225 ppm) represents the carboxyl and carbonyl carbons. The differences seen in the spectra can be related to the differences in rank between the three coals. The NMR data shows as the rank of the coals increases the aliphatic content decreases, the aromaticity increases, and the oxygen content decreases. Oxygen loss is accomplished through the loss of carboxyl (180 ppm) and carbonyl (200 ppm) functional groups. Another important mechanism for oxygen removal is the dehydration of the hydroxyl group from phenols (153 ppm).

Table 1.2. Thermal Liquefaction Data of Raw Bituminous Coals

Coal	DECS-7	DECS-6	DECS-12
products			
dmmf wt %			
Gas + Oil	13.8	22.5	16.5
Asphaltene	8.9	7.3	9.1
Preasphaltene	7.7	9.2	12.8
Total Conversion	30.4	39	39.9
THF insol.	69.6	61	60.1

Figures 8.2 (DECS 7), 8.3 (DECS 6), and 8.4 (DECS 12) show the spectra for the raw coal versus the THF-insoluble residue of the thermally reacted coal. All three coals show the same trends. There is a major loss of aliphatics with a corresponding increase in aromaticity. Carboxyl and carbonyl functional groups are completely removed. Most catechols are lost and the phenols are diminished. The THF-insoluble residues from the reacted coals show strikingly similar spectra (Figure 8.5) even though the starting coals are so different, both chemically and physically.

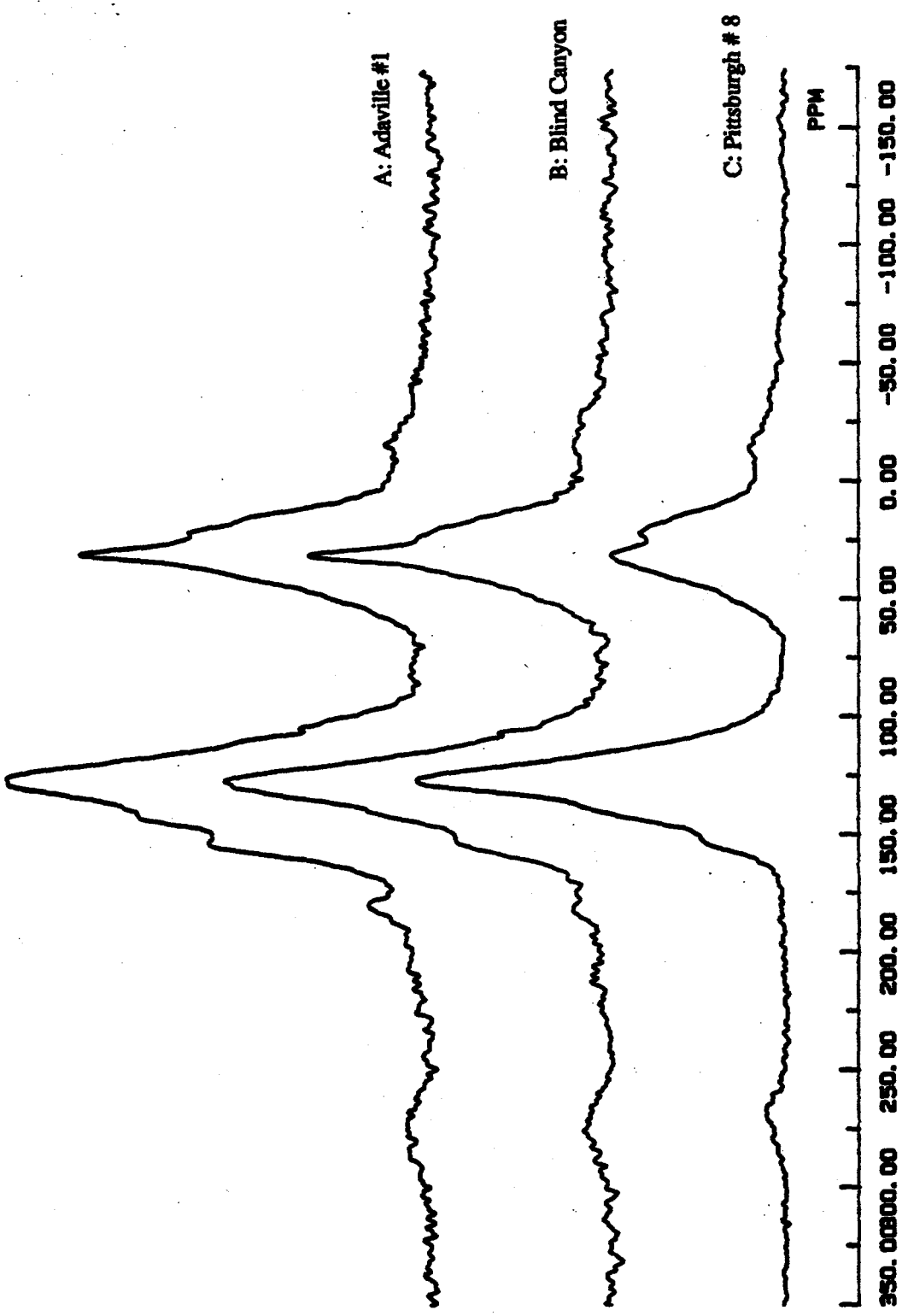

Figure 8.1 CPMAS ^{13}NMR spectra of the raw coals (A) DECS-7, (B) DECS-6, (C) DECS-12.

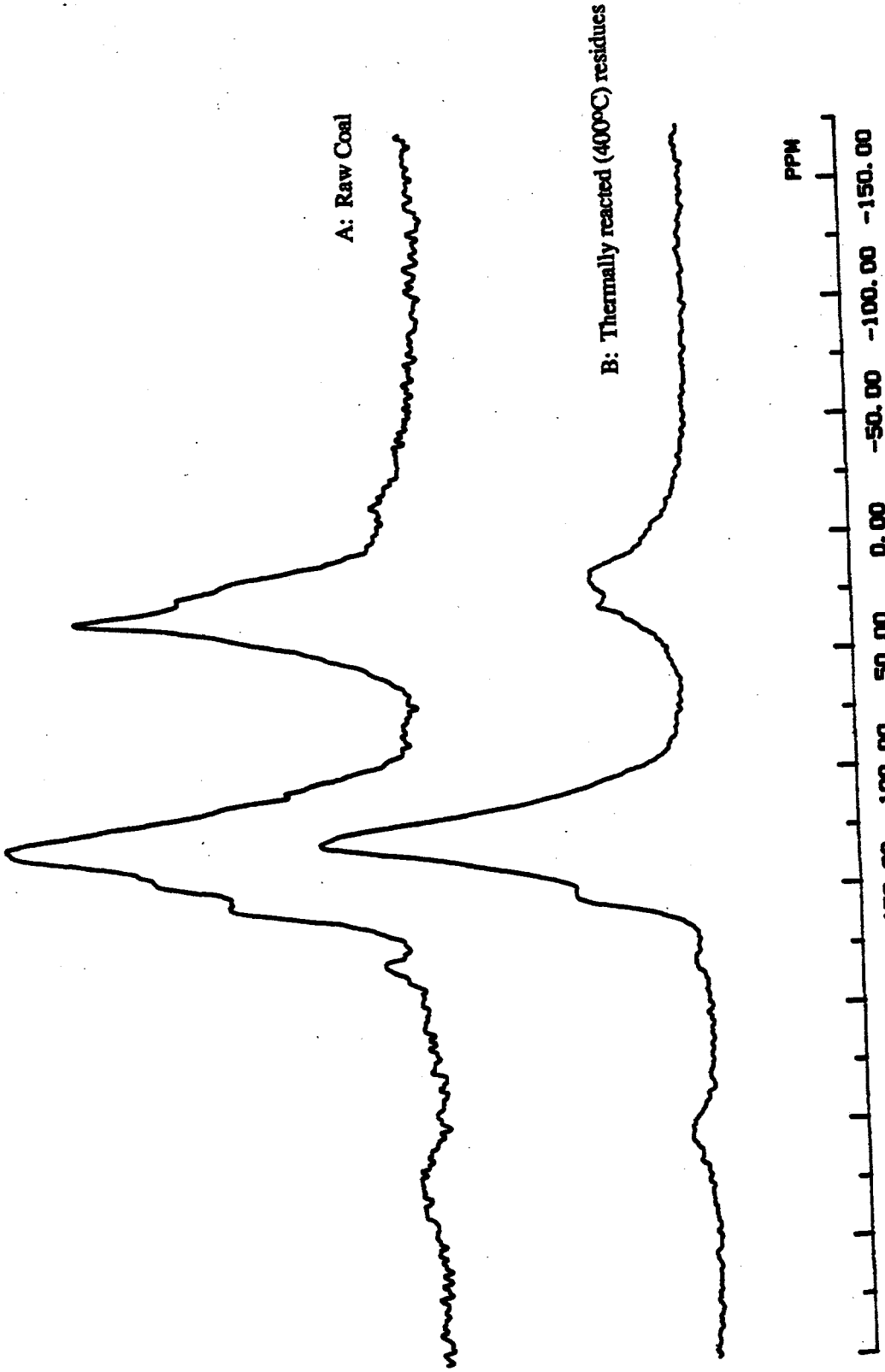

Figure 8.2 . CPMAS ^{13}NMR spectra of DECS-7 (A) raw coal, (B) THF-insoluble residue of the reacted coal.

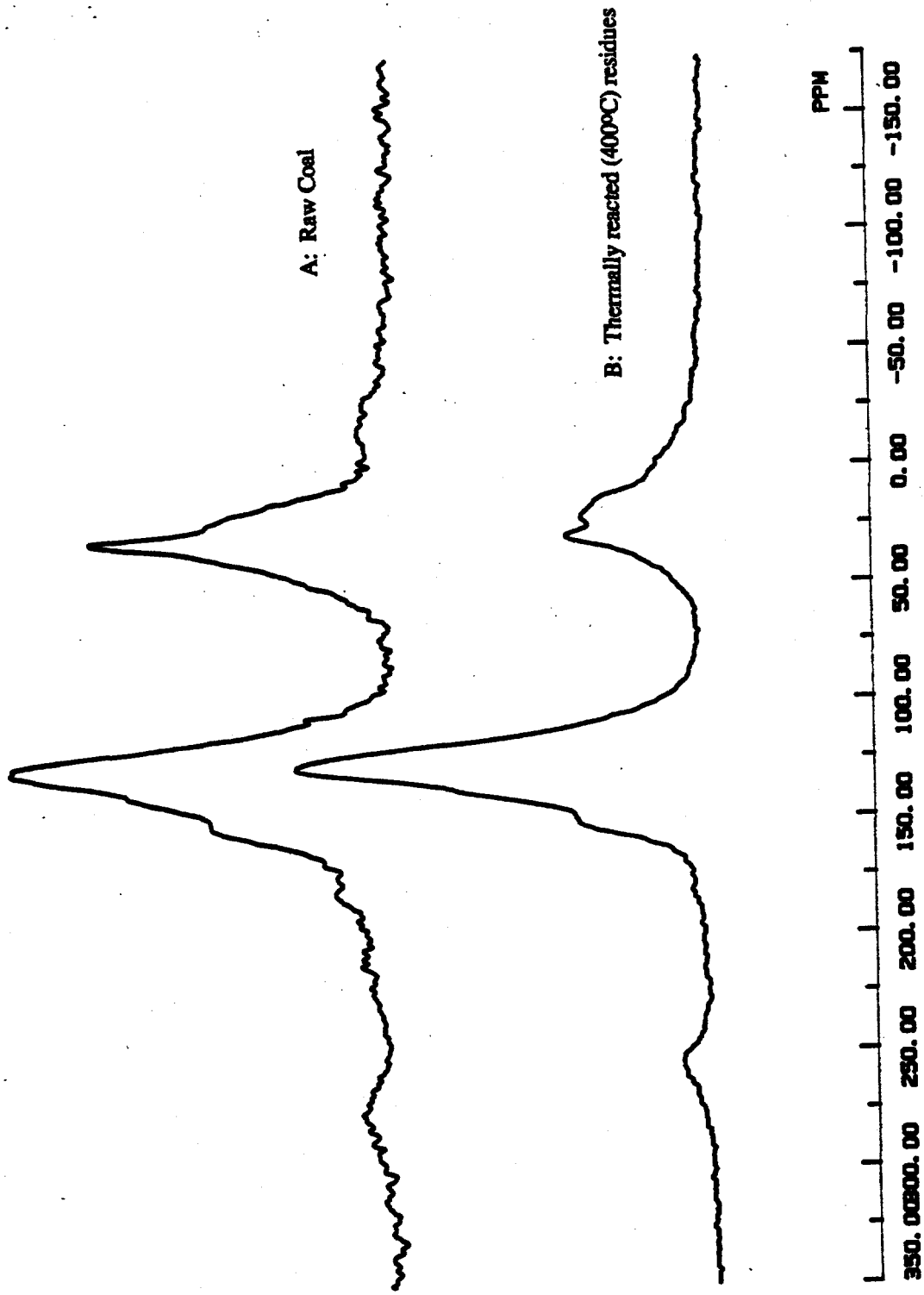

Figure 8.3 . CPMAS ^{13}NMR spectra of DECS-6 (A) raw coal, (B) THF- insoluble residue of the reacted coal.

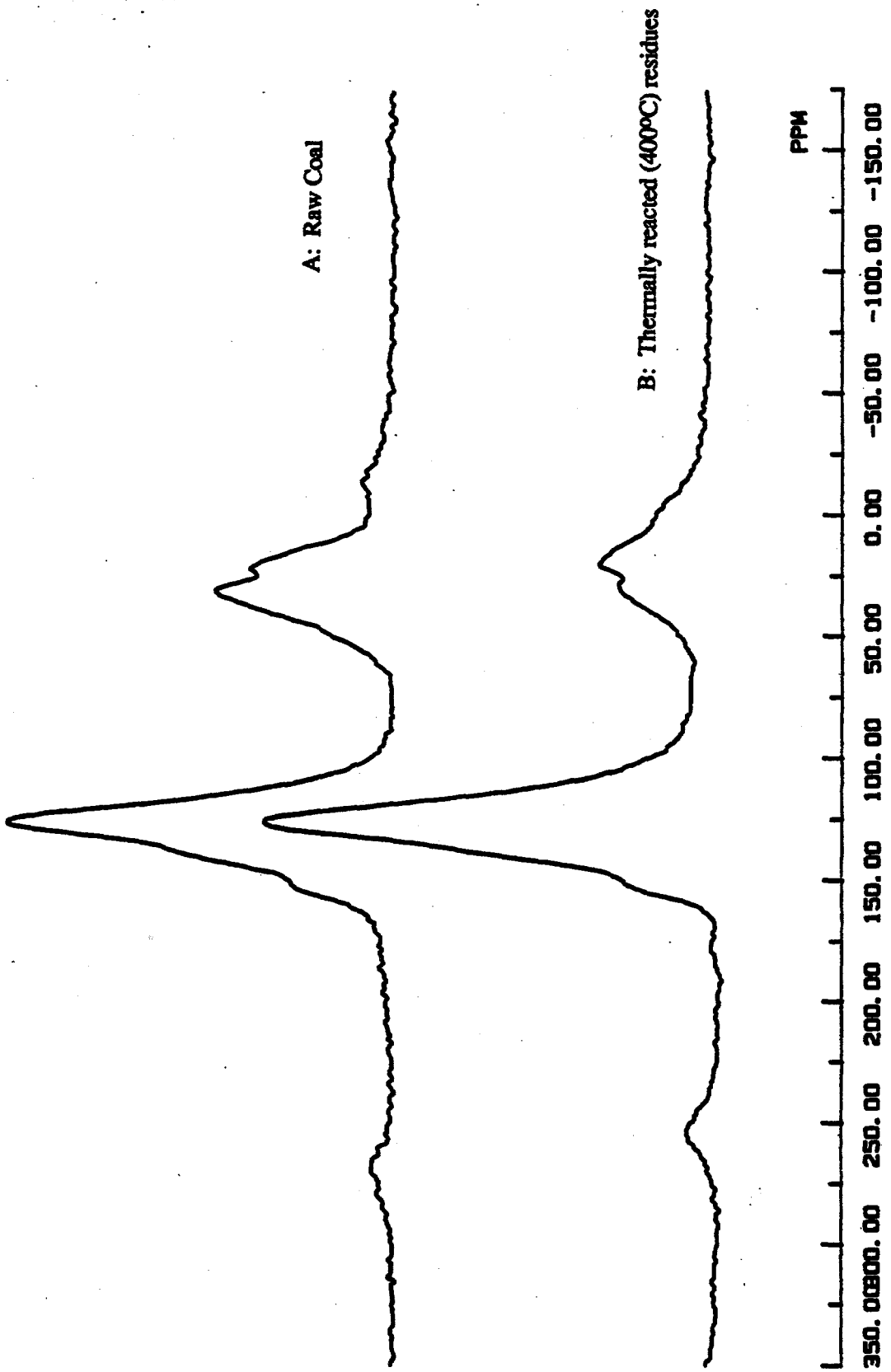

Figure 8.4. CPMAS ^{13}NMR spectra of DECS-12 (A) raw coal, (B) THF- insoluble residue of the reacted coal.

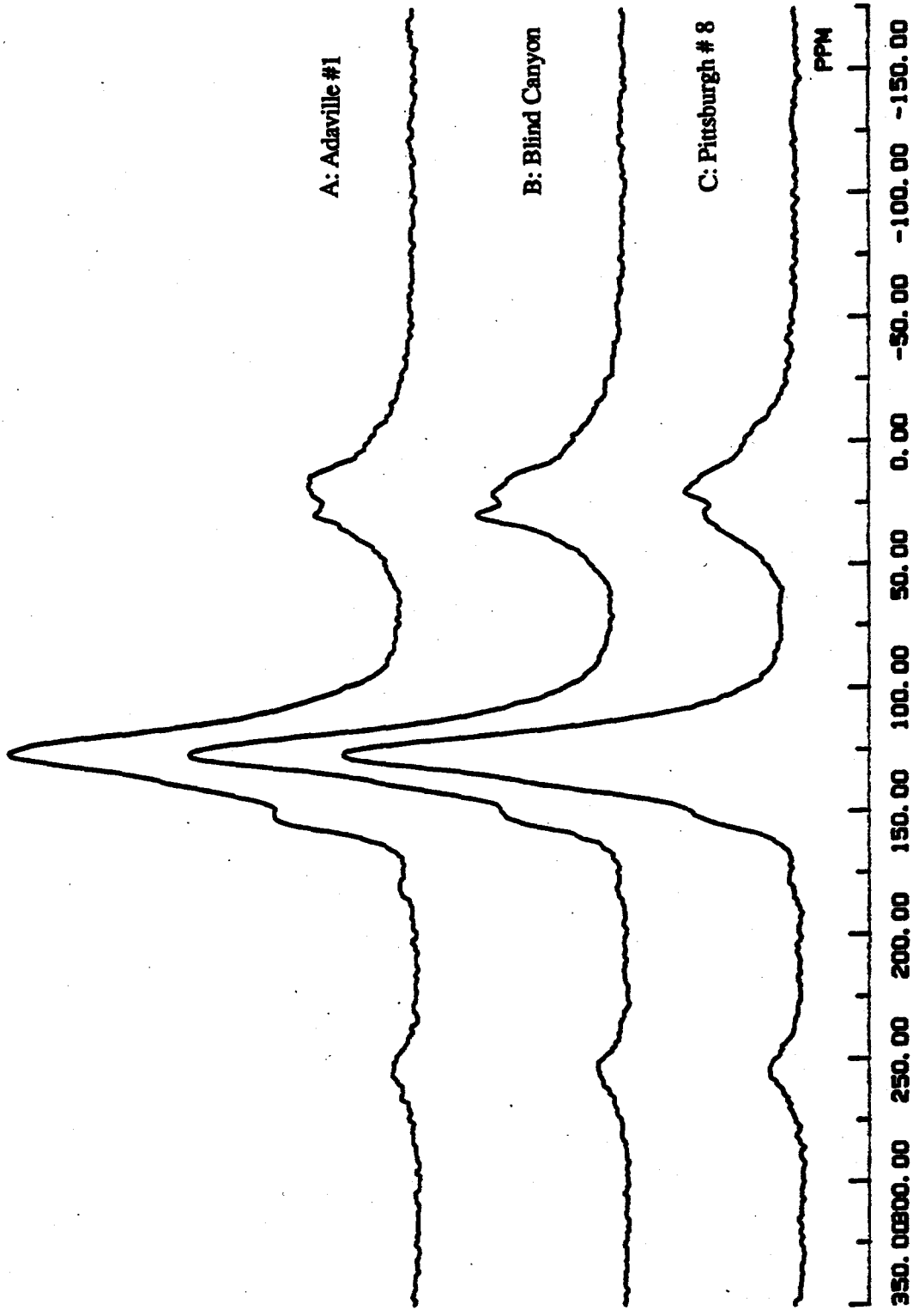

Figure 8.5. CPMAS 13NMR spectra of the reacted residues (A) DECS-7, (B) DECS-6, (C) DECS-12.

Pyrolysis GC/MS

Pyrolysis of the coals and their reacted residue yields a complex mixture of aliphatic, phenolic, naphthalene compounds. As stated in a previous report (Song et al, 1992) the exact composition is directly related to the rank, maceral content of the particular coal analyzed. Table 8.3 lists the major peaks identified by number for all the pyrograms. Figure 8.6 is the chromatogram of DECS-7. Comparing this chromatogram with the chromatogram of an unreacted THF extracted sample (Figure 8.7) of DECS-7 shows a few interesting differences. There is a drastic reduction in prist-1-ene. The high molecular weight n-alkanes (greater than C_{22}) are preferentially reduced over the low molecular weight alkanes. More importantly though, there is a reduction in phenol and both isomers of cresol. These are the backbone components that compose the macromolecular structure of vitrinite, the dominant maceral in all three of these bituminous coals. A reduction of these components in the pyrolyzate indicates that THF may be altering the macromolecular structure of the Adaville coal. A pyrogram (Figure 8.8) of a thermally desorbed sample of the Adaville coal does not show this similar result.

Figure 8.9 shows the py-gc-ms profile of the residue from the thermally treated Adaville. Identification numbers correspond to those shown in Table 3. It should be noted that only a small percent (10%) of the residue pyrolyzed indicating that much of the structure condensed into nonvolatile components during liquefaction. The pyrolyzate is dominated by benzene, p-xylene, phenol, and p-cresol. Toluene is a remnant of the solvent used to extract the asphaltene fraction from the residue. The percentage of naphthalene and phenanthrene/anthracene in the residue increased relative to the amount found in the raw coal, also indicating condensation reactions taking place. Thermal prereatment removed most but not completely all the alkanes. It also significantly reduced the amount of alkyl substituted benzenes, phenols, and naphthalenes. Not found in the original coal but identified in the residue was biphenyl, fluorene, and dihydroinden-1-one.

Figure 8.10 shows the pyrogram of DECS-6. Figure 8.11 is the pyrogram of the THF extracted sample of the Blind Canyon. Here again significant changes occurred. Again as with DECS-7 the high molecular weight n-alkanes were reduced. The resinite components were also extracted. Missing are cadalene and the tetrahydronaphthalenes that originate from resinite. Prist-1-ene was reduced but not as drastically as in the Adaville. The amount of C_1, C_2, and C_3 naphthalenes decreased. Unlike DECS-7 the phenol components seem to be uneffected. Again the thermally desorbed pyrogram (Figure 8.12) of DECS-6 does not show these changes. What effect THF has on the structure of these coals needs to be investigated further.

The chromatogram of the residue form the thermally treated Blind Canyon coal is shown in Figure 8.13. Again only a small percentage pyrolyzed. The same trends that were seen happening in the Adaville are occuring with the Blind Canyon. The benzene and phenol group

of compounds dominate, naphthalene and phenanthrene/anthracene increased along with the addition of fluorene, dihydroinden-1-one, but not biphenyl. Fluoranthene was also identified as a new product.

Table 8.3. Identified Peaks in TICs from PY-GC-MS of Bituminous Coals and Residues

Peak No.	MW	Compound *	Peak No.	MW	Compound *
1	56	C_4 alkene	39	266	C_{19}, prist-1-ene
2	70	C_5 alkene	40	170	C_3 naphthalene
3	86	C_6	41	184	C_4 naphthalene
4	100	C_7	42	254	C_{18}
5	78	benzene	43	182	naphthol
6	114	C_8	44	268	C_{19}
7	92	toluene	45	198	Cadalene
8	128	C_9	46	282	C_{20}
9	106	p-xylene	47	296	C_{21}
10	142	C_{10}	48	178	phenanthrere/anthracene
11	106	o-xylene	49	306	quaterphenyl
12	120	propyl benzene	50	310	C_{22}
13	120	ethyl methyl benzene	51	192	C_1 phen/anth
14	156	C_{11}	52	324	C_{23}
15	120	trimethyl benzene	53	206	C_2 phen/anth
16	134	C_4 benzene	54	338	C_{24}
17	106	benzaldehyde	55	220	C_3 phen/anth
18	94	phenol	56	352	C_{25}
19	118	indane	57	366	C_{26}
20	170	C_{12}	58	380	C_{27}
21	132	C_1 indane	59	394	C_{28}
22	108	o-cresol	60	408	C_{29}
23	108	p-cresol	61	422	C_{30}
24	184	C_{13}	62	320	C_1 quaterphenyl
25	122	2-ethyl phenol	63	436	C_{31}
26	122	2,4-dimethyl phenol	64	450	C_{32}
27	122	C_2 phenol	65	464	C_{33}
28	122	4-ethyl phenol	66	468	C_{34}
29	128	naphthalene	67	154	biphenyl
30	122	C_2 phenol	68	68	fluorene
31	198	C_{14}	69	106	benzaldehyde
32	136	ethyl methyl phenol	70	256	dimethyl benzophenanthrene
33	136	C_3 phenol	71	188	tetramethyl dihydronaphthalene
34	212	C_{15}	72	202	dimethyl methyl-ethyl dihydronaphthalene
35	142	C_1 naphthalene	73	132	dihydroindn-1-one
36	226	C_{16}	74	178	methylene fluorene
37	156	C_2 naphthalene	75	202	fluoranthene
38		C_{17}			

* C_6 - repesents carbon number of alkane/alkene doublet, alkene MW = alkane-2

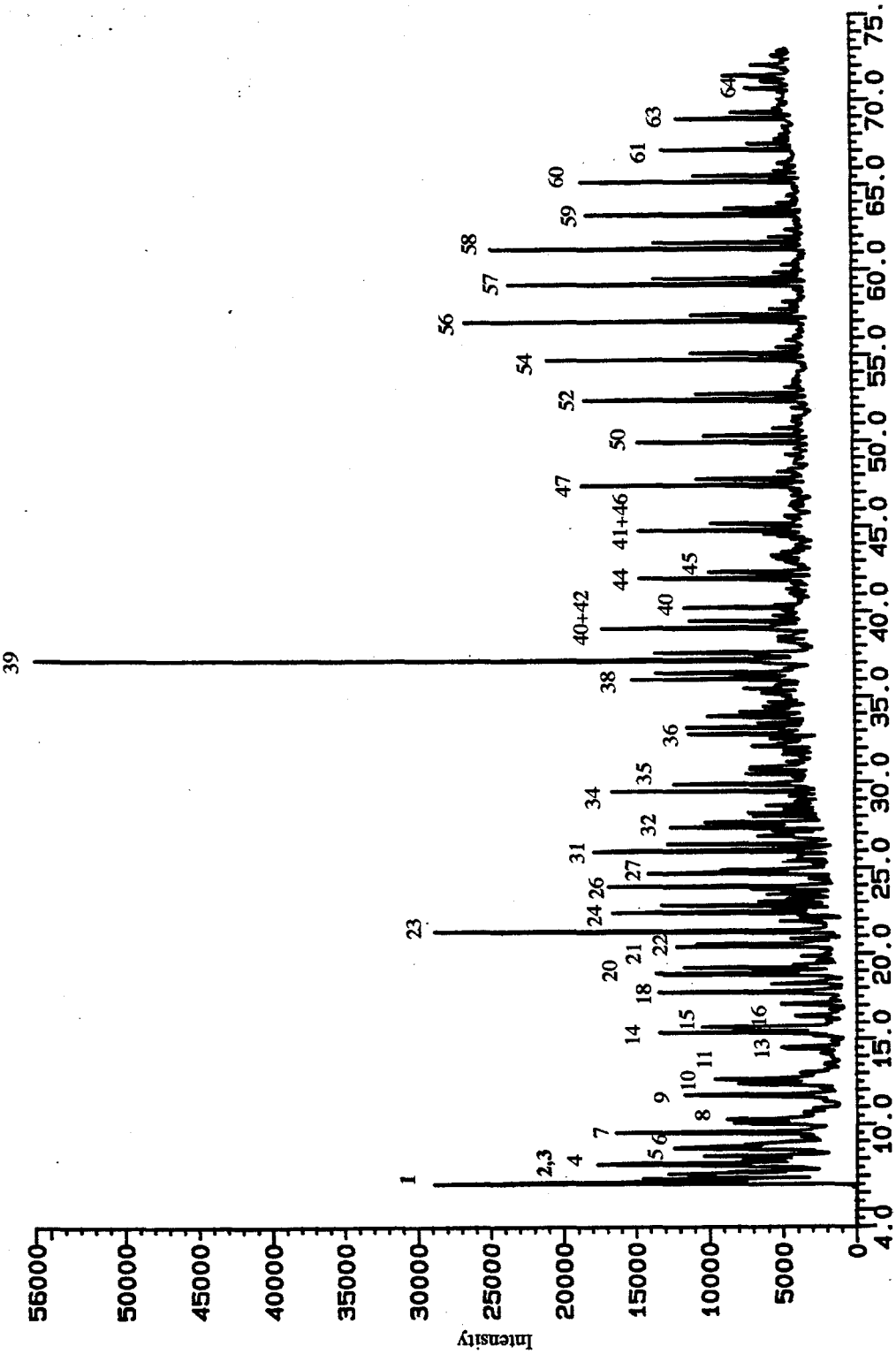

Figure 8.6. Py-GC-MS chromatogram of DECS-7, TIC.

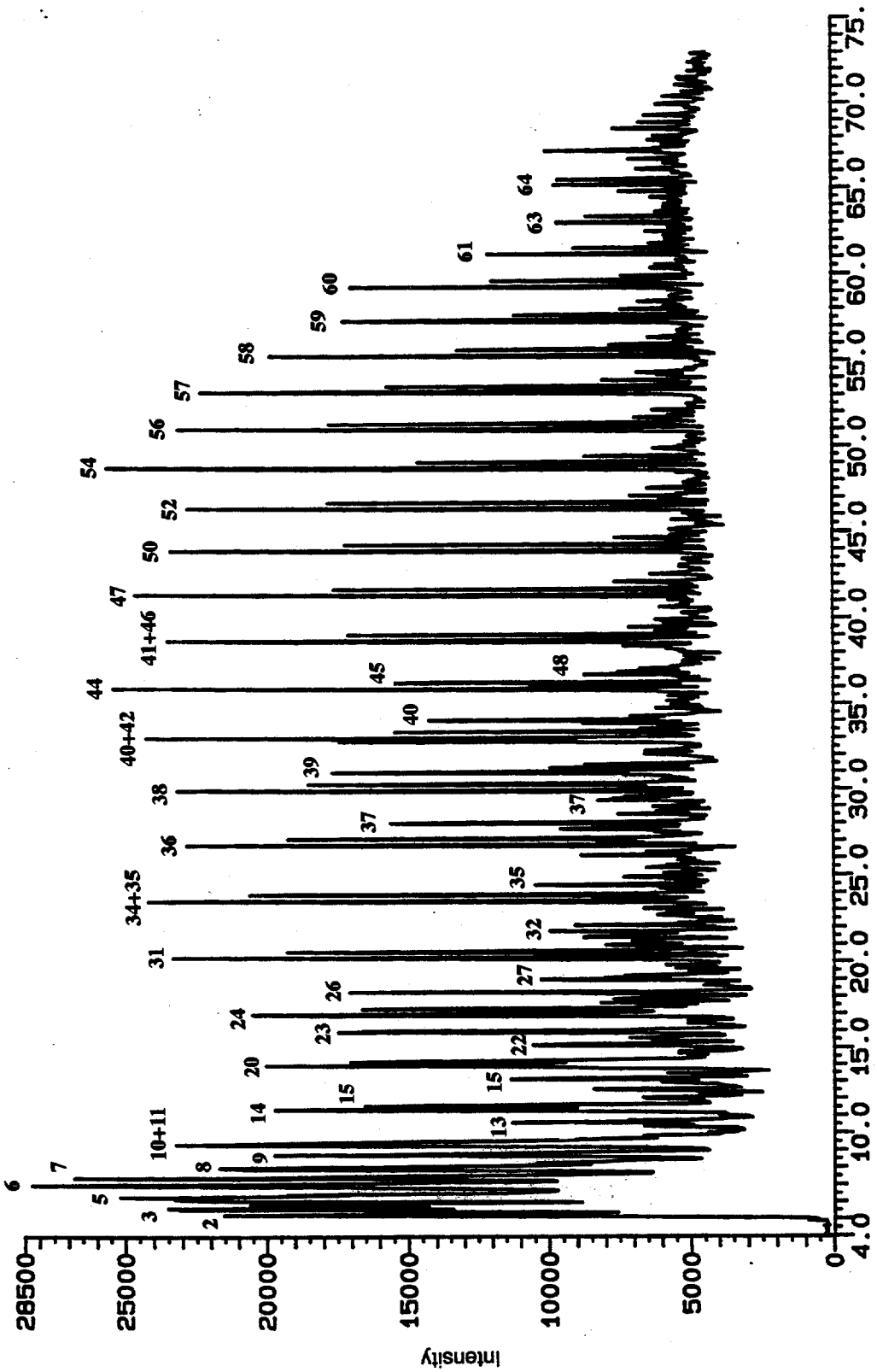

Figure 8.7. Py-GC-MS chromatogram of THF extracted unreacted DECS-7.

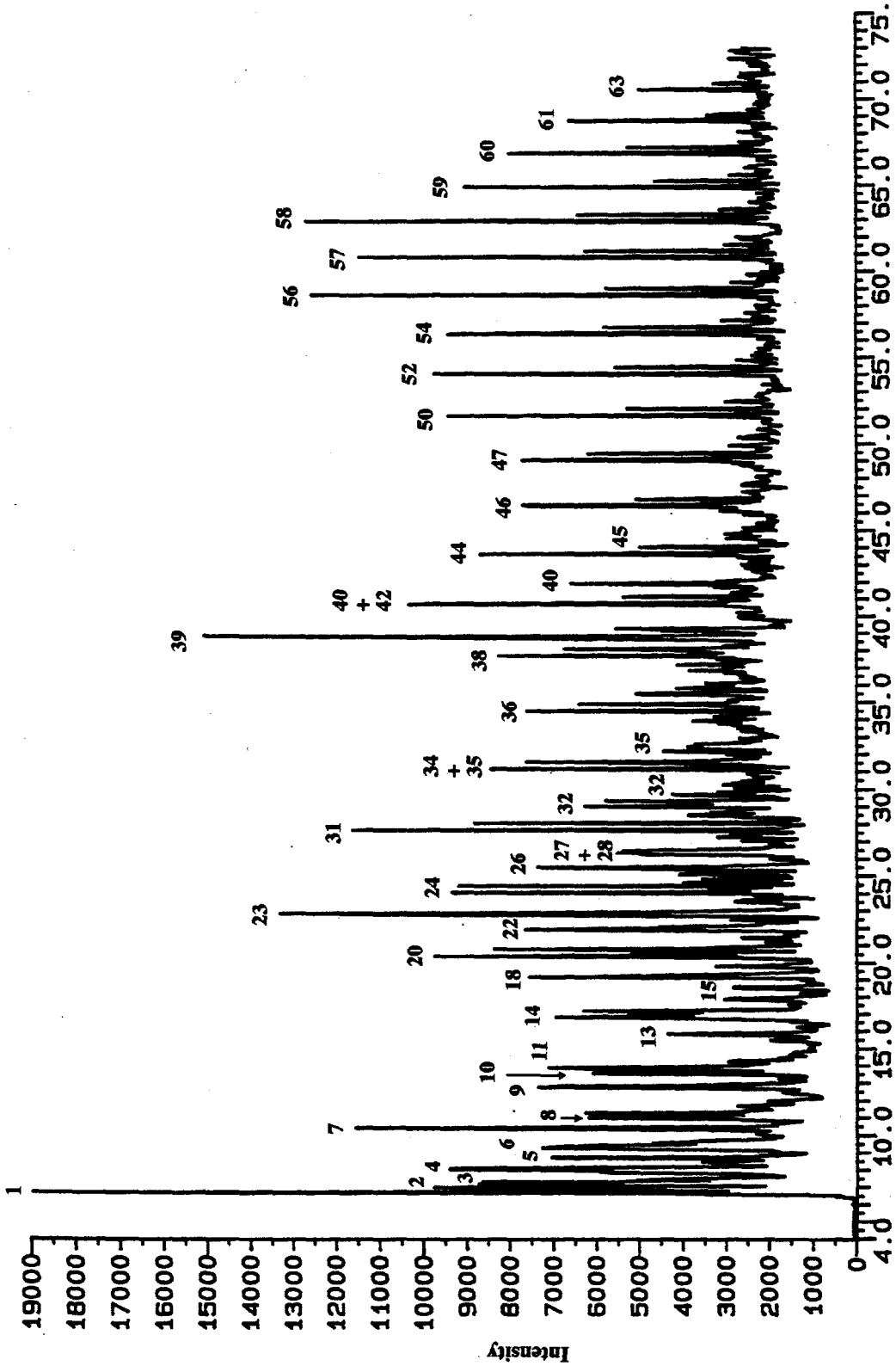

Figure 8.8. Py-GC-MS chromatogram of thermally desorbed DECS-7.

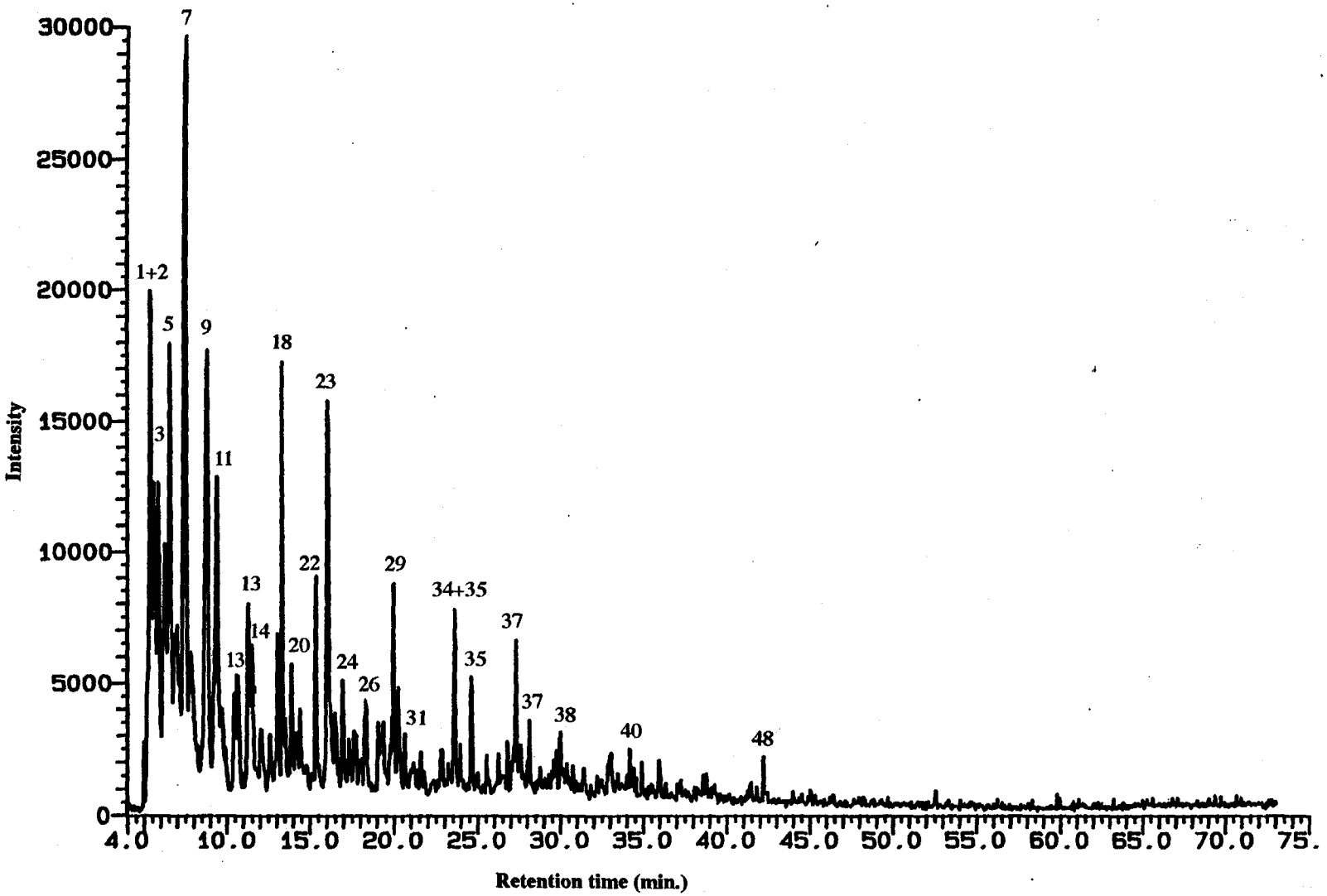

Figure 8.9. Py-GC-MS chromatogram of DECS-7 thermally reacted THF-insoluble residue.

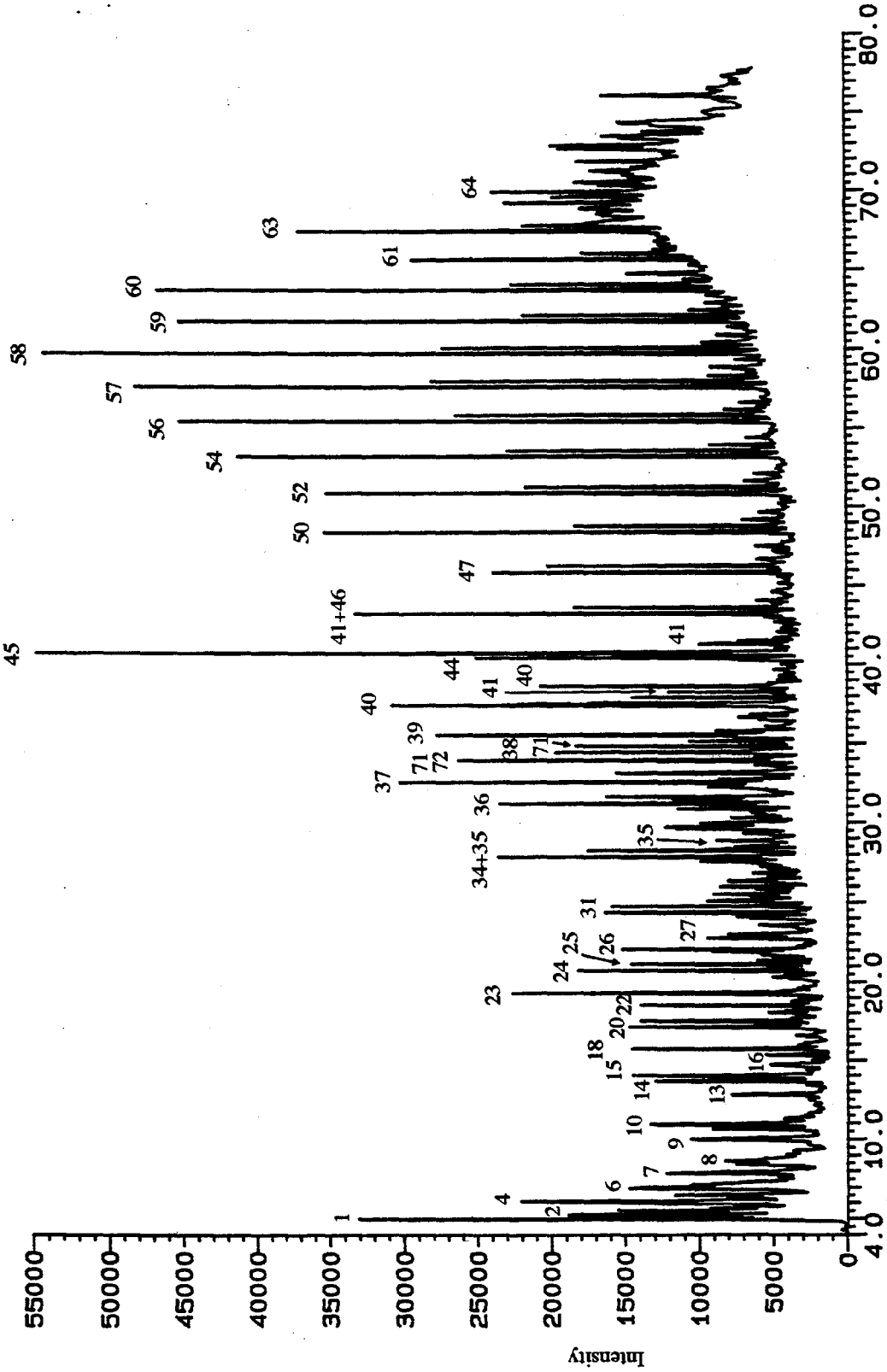

Figure 8.10 Py-GC-MS chromatogram of DECS-6, TIC.

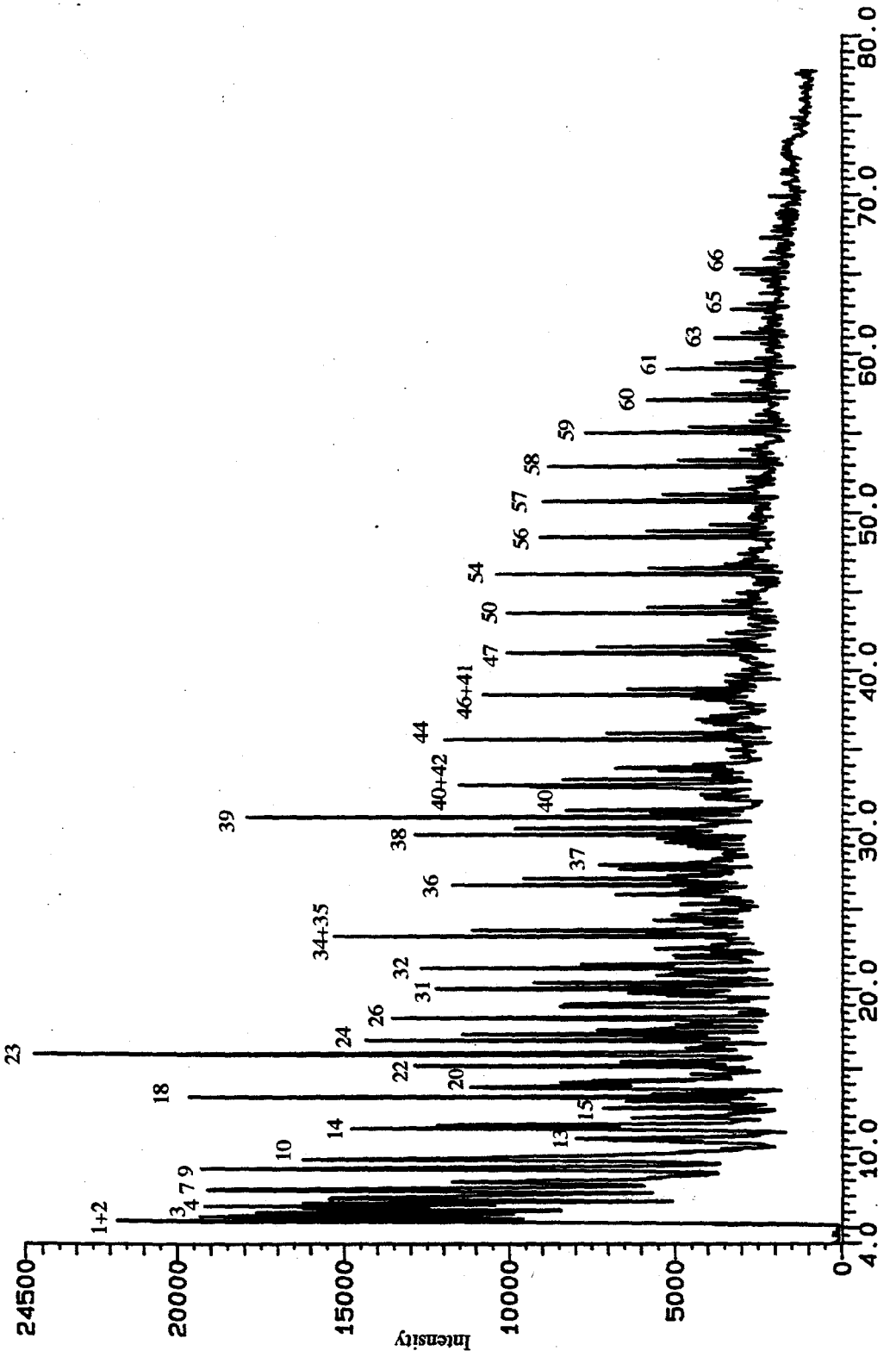

Figure 8.11. **Py-GC-MS chromatogram of THF extracted unreacted DECS-6.**

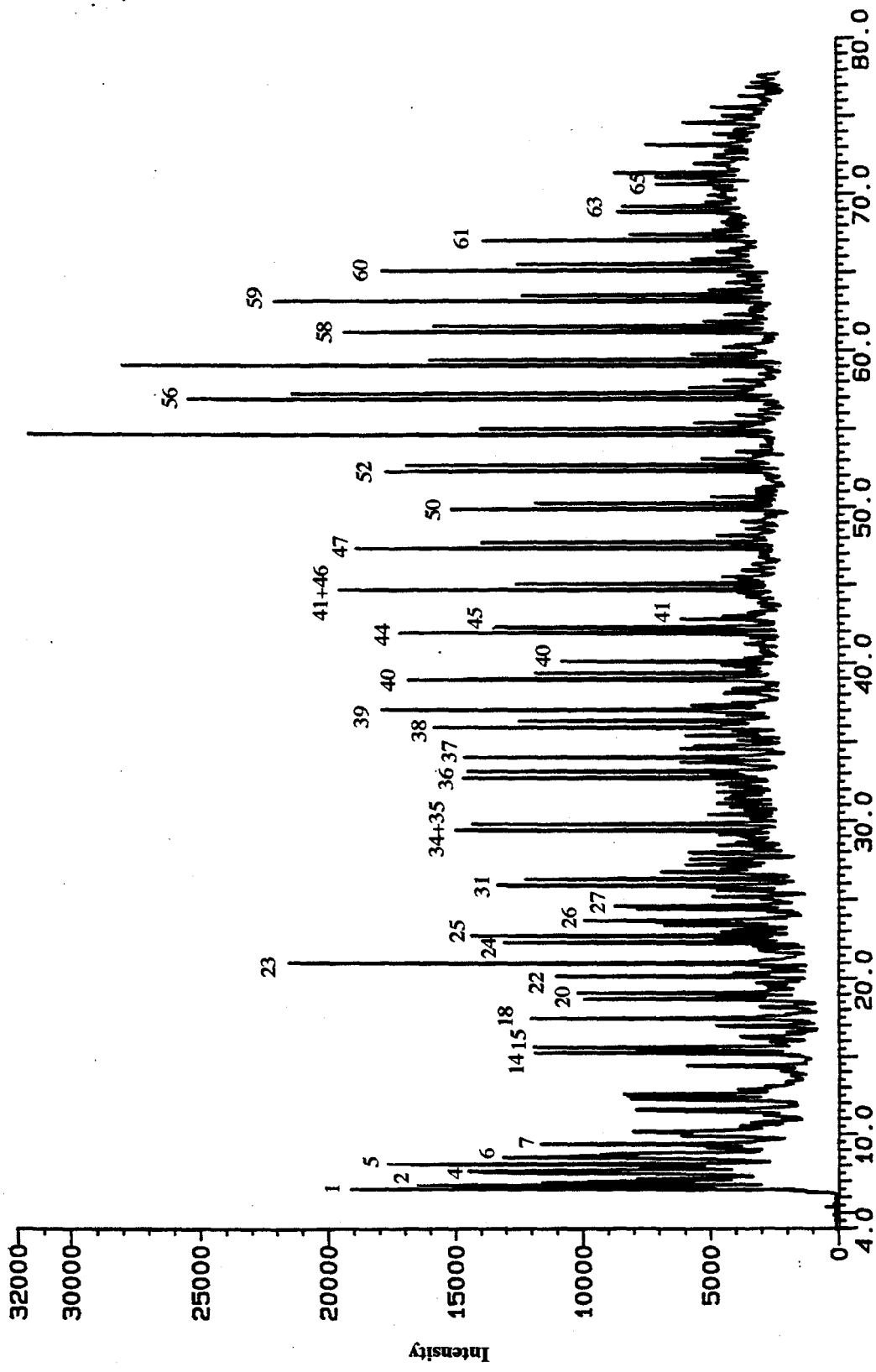

Figure 8.12. Py-GC-MS chromatogram of thermally desorbed DECS-6.

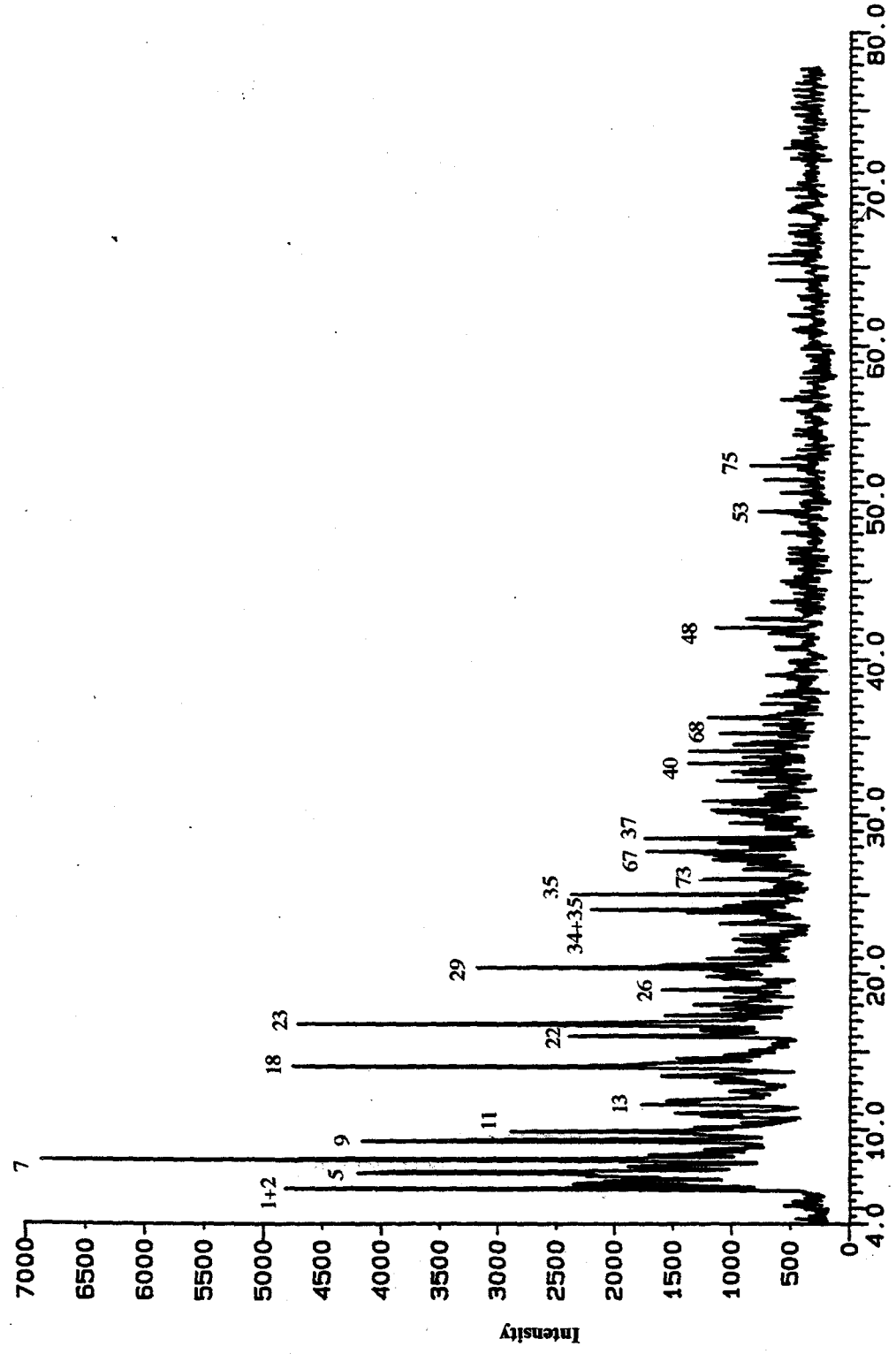

Figure 8.13. Py-GC-MS chromatogram of DECS-6 thermally reacted THF-insoluble residue.

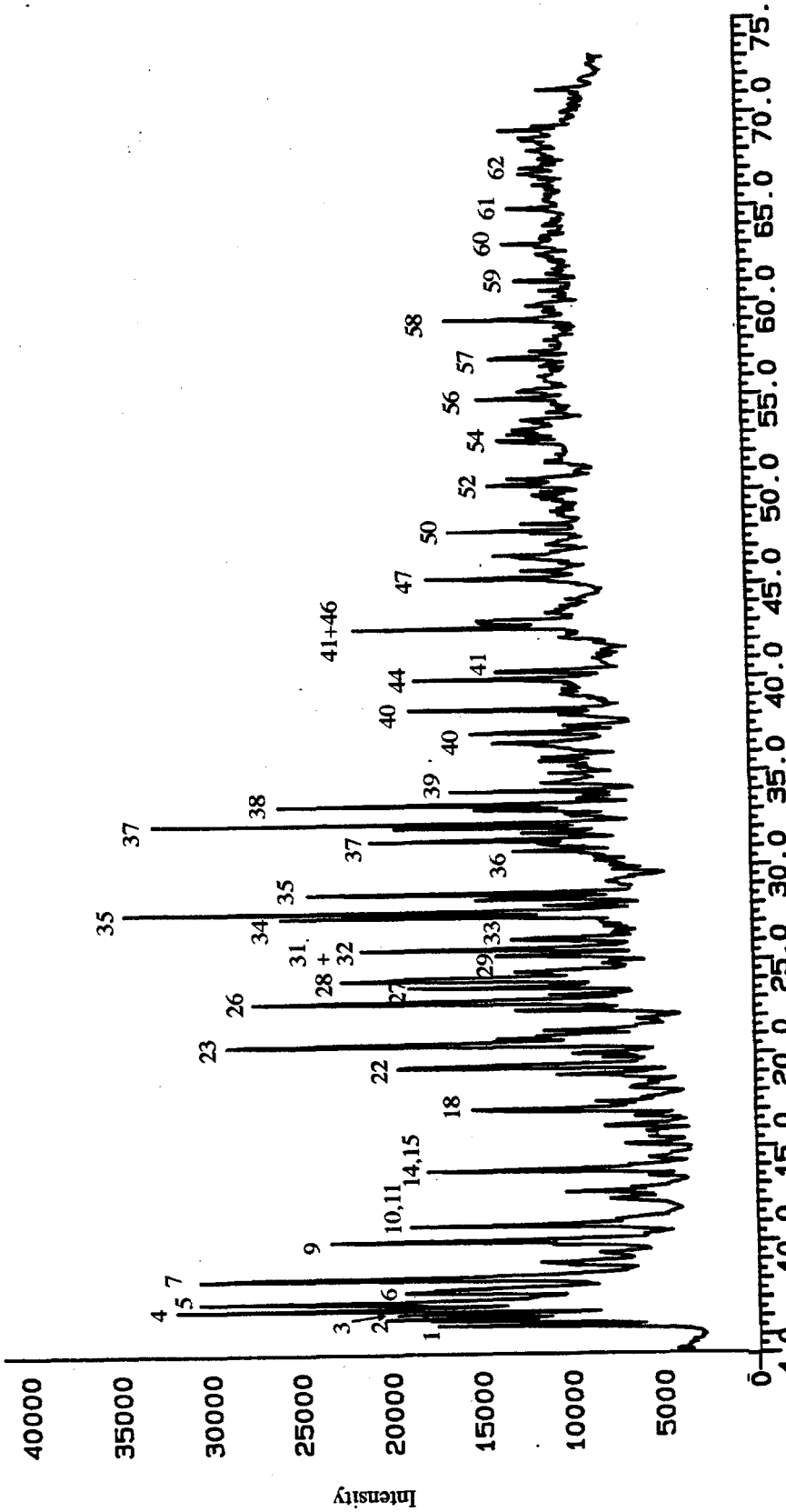

Figure 8.14. Py-GC-MS chromatogram of DECS-12, TIC.

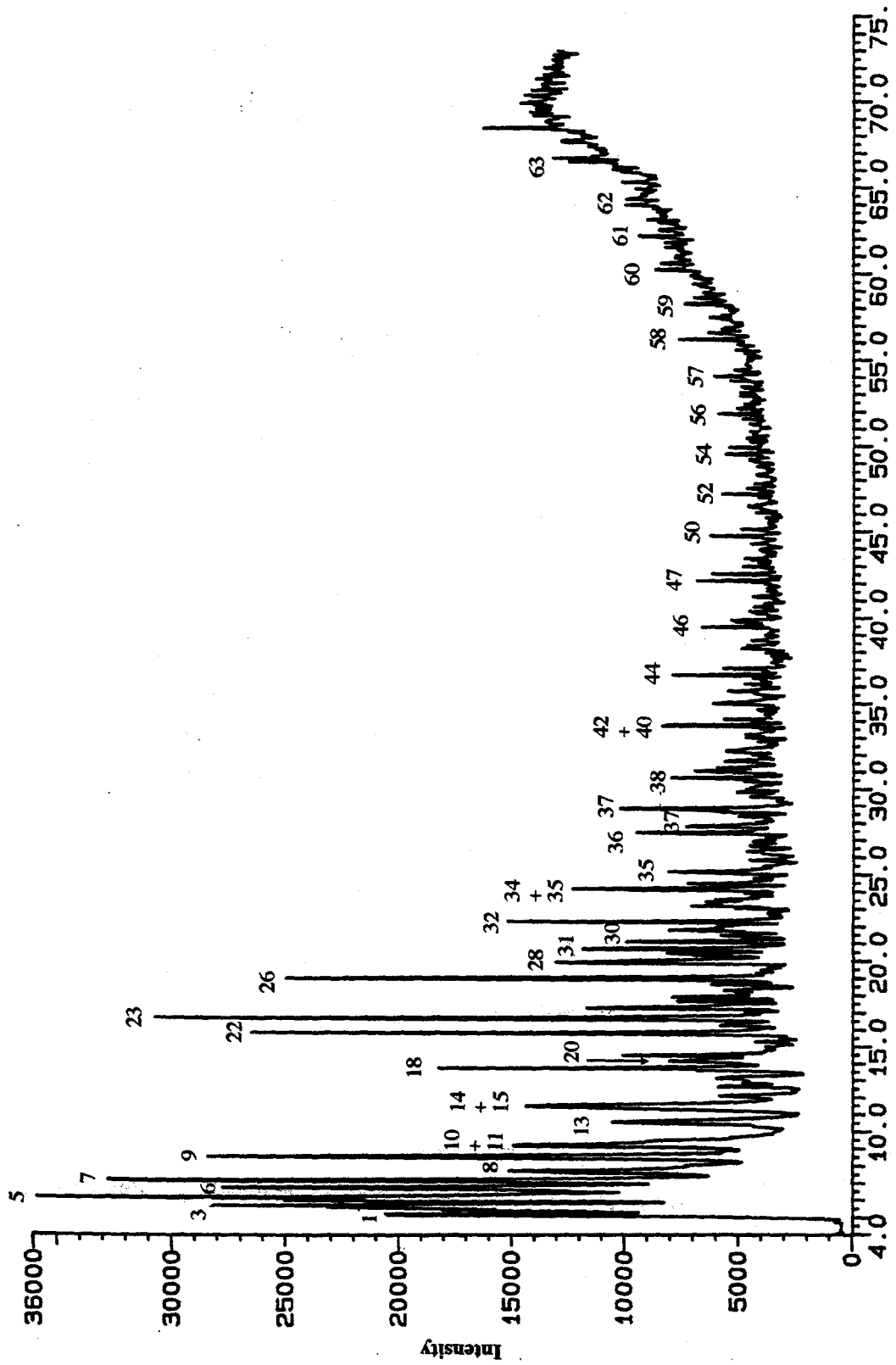

Figure 8.15. Py-GC-MS chromatogram of THF extracted unreacted DECS-12.

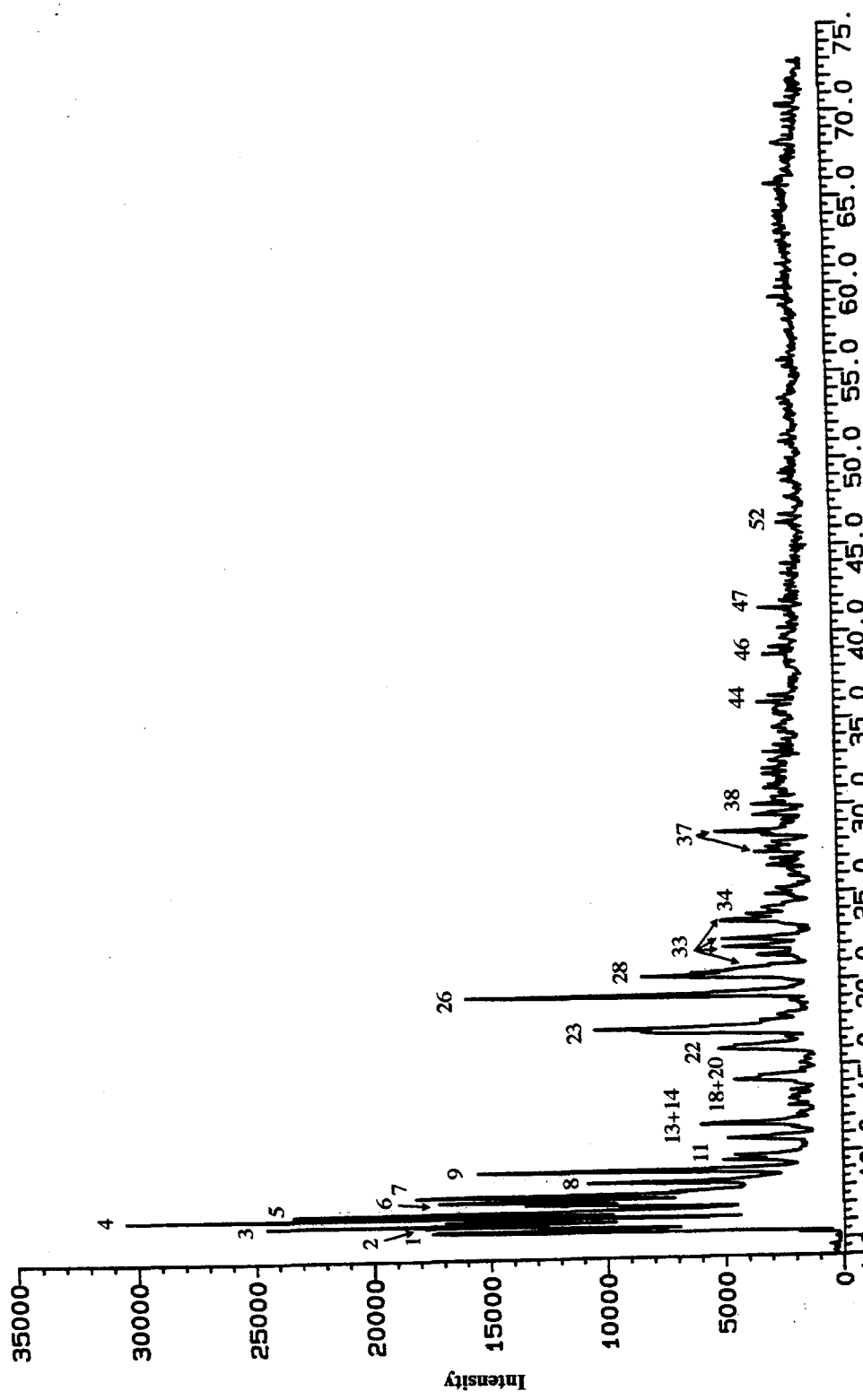

Figure 8.16. Py-GC-MS chromatogram of thermally desorbed DECS-12.

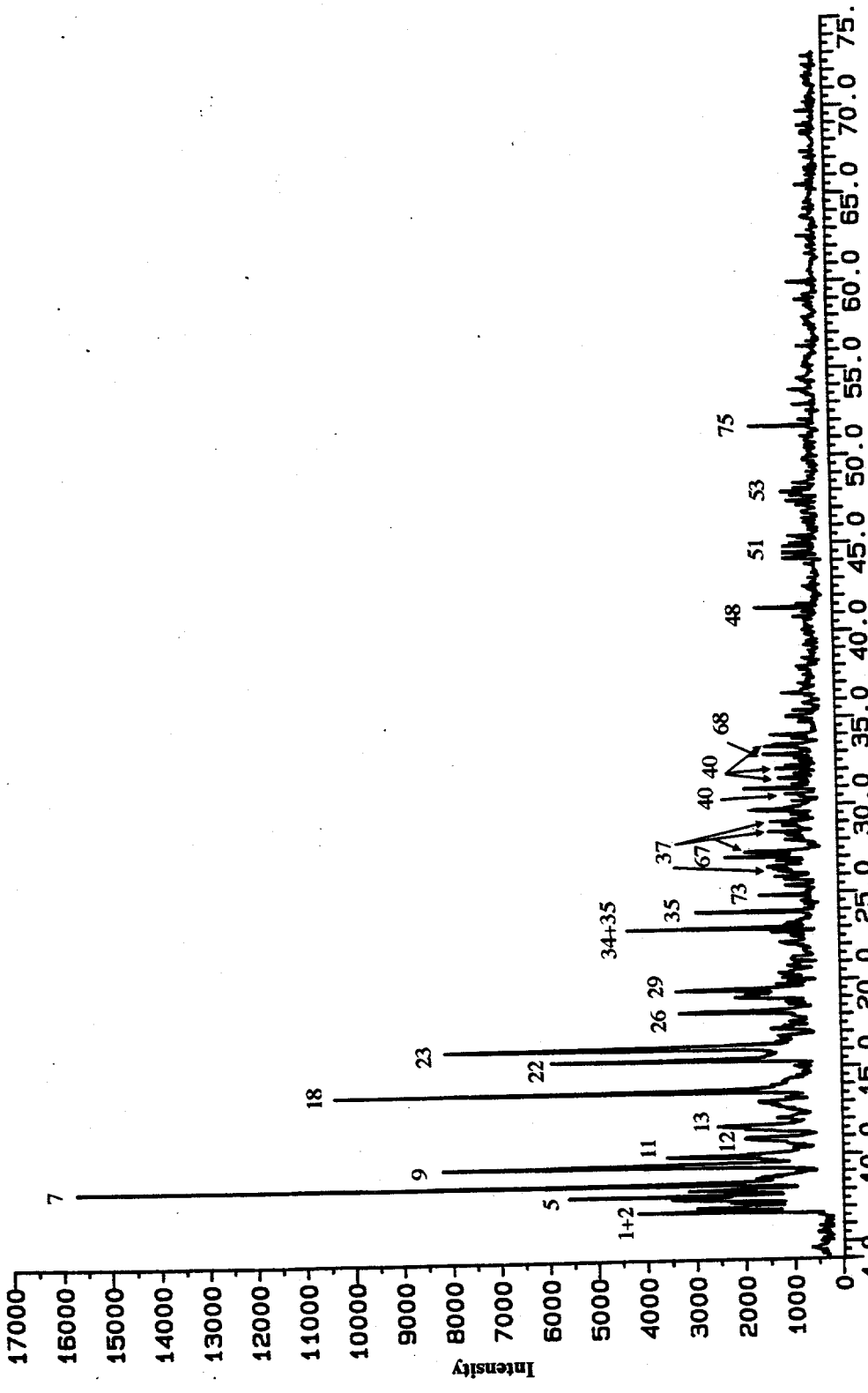

Figure 8.17. Py-GC-MS chromatogram of DECS-12 thermally reacted THF-insoluble residue.

Comparing the raw coal pyrogram of DECS-12, Figure 8.14, with the pyrograms of the THF extracted DECS-12, Figure 8.15,and the thermally desorbed pyrogram, Figure 8.16, structural changes do not seem to occur. Both reactions show similar features. The straight chain hydrocarbons are lost along with a reduction of alkylated naphthalenes. 2, 4-Dimethyl phenol does seem to be enhanced, though.

Figure 8.17 is the chromatogram of the reacted THF-insoluble residue for DECS-12. It too is dominated by benzene and alkyl benzenes, phenol and cresols like the residues from the other reacted coals. Naphthalene and C_1 and C_2 naphthalene are also present. Biphenyl, fluorene, fluoranthene, and C_1 phenanthrene/anthracene and C_2 phenanthrene/anthracene have been formed in the reaction process.

GC/MS

Figures 8.18, 8.19, and 8.20 are the total ion chromatograms of the oil generated during liquefaction of DECS-7, DECS-6, and DECS-12, respectively. Table 8.4 lists the major peaks identified by number. All three oils contained the same groups of compounds: alkanes, benzene, alkylated benzenes, indan, alkylated indane, phenol, alkylated phenols, naphthalene, alkylated naphthalenes, phenanthrene/anthracene, and alkylated phenanthrene/anthracenes. The different coals chromatographic signatures are quite distinctive, though. The Adaville coal is dominated by phenols, cresols, and C_2 phenols. These are derived from the degradation of vitrinite, the dominate maceral (94.7%) in this coal. Figures 8.21 through 8.26 are single ion chromatograms representing the above named groups of compounds for DECS-7. Table 8.5 lists a few of the isomers identified by number for the C_2 and C_3 phenols. These show the degree of alkylated side chains on each class of compounds. Combined these groups represent over ninety percent of the compounds in all three oils. Even though some isomers are not very abundant they do show a compete mix of species. The Blind Canyon is dominated by compounds derived from the maceral resinite. The resinite in this coal in composed of bicyclic sesquiterpenoids and diterpenoids. Upon degradation these compounds produce alkylated two ring compounds such as cadalene, propyl (C_3) naphthalene, and dimethyl (C_2) naphthalene. Figures 8.27 through 8.32 are single ion chromatograms for DECS-6. Naphthalene is the major compound in the Pittsburgh #8 coal. It has no dominant group, though. The alkanes, benzenes, phenols and naphthalenes all contribute about equally. Figures 8.33 through 8.38 are single ion chromatograms for DECS-12.

Table 8.4. Identified Peaks in TICs from GC-MS of the Hexane Soluble Fraction (Oil)

Peak No.	MW	Compound*	Peak No.	MW	Compound*
1	114	C_8 branched	34	142	C_1 naphthalene
2	114	C_8 branched	35	188	C_4 indan-one
3	92	toluene	36	226	C_{16}
4	128	C_9	37	156	C_2 naphthalene
5	106	p-xylene	38	156	C_2 naphthalene
6	142	C_{10}	39	268	C_{19} branched
7	106	o-xylene	40	240	C_{17}
8	120	ethyl methyl benzene	41	266	C_{19} alkene
9	156	C_{11}	42	188	C_4 indan-one
10	120	trimethyl benzene	43	266	C_{19} alkene
11	134	C_4 benzene	44	170	C_3 naphthalene
12	120	trimethyl benzene	45	254	C_{18}
13	94	phenol	46	170	C_3 naphthalene
14	118	indane	47	170	C_3 naphthalene
15	170	C_{12}	48	268	C_{19}
16	184	C_{13} branched	49	184	C_4 naphthalene
17	132	C_1 indane	50	198	Cadalene
18	108	o-cresol	51	184	C_4 naphthalene
19	108	p-cresol	52	282	C_{20}
20	132	C_1 benzofuran	53	184	C_4 naphthalene
21	184	C_{13}	54	296	C_{21}
22	122	2-ethyl phenol	55	178	phen/anth
23	122	2,4-dimethyl phenol	56	310	C_{22}
24	122	C_2 phenol	57	324	C_{23}
25	122	4-ethyl phenol	58	338	C_{24}
26	122	C_2 phenol	59	352	C_{25}
27	198	C_{14}	60	366	C_{26}
28	136	ethyl methyl phenol	61	380	C_{27}
29	136	ethyl methyl phenol	62	394	C_{28}
30	226	C_{16} branched	63	408	C_{29}
31	136	C_3 phenol	64	422	C_{30}
32	212	C_{15}	65	436	C_{31}
33	142	naphthalene			

Table 8.5. List of Phenol Isomers

No.	MW	Compound	No.	MW	Compound
1	122	2-ethyl phenol	5	122	dimethyl phenol
2	122	2,4-dimethyl phenol	6	136	ethyl methyl phenol
3	122	dimethyl phenol	7	136	propyl phenol
4	122	4-ethyl phenol	8	136	trimethyl phenol

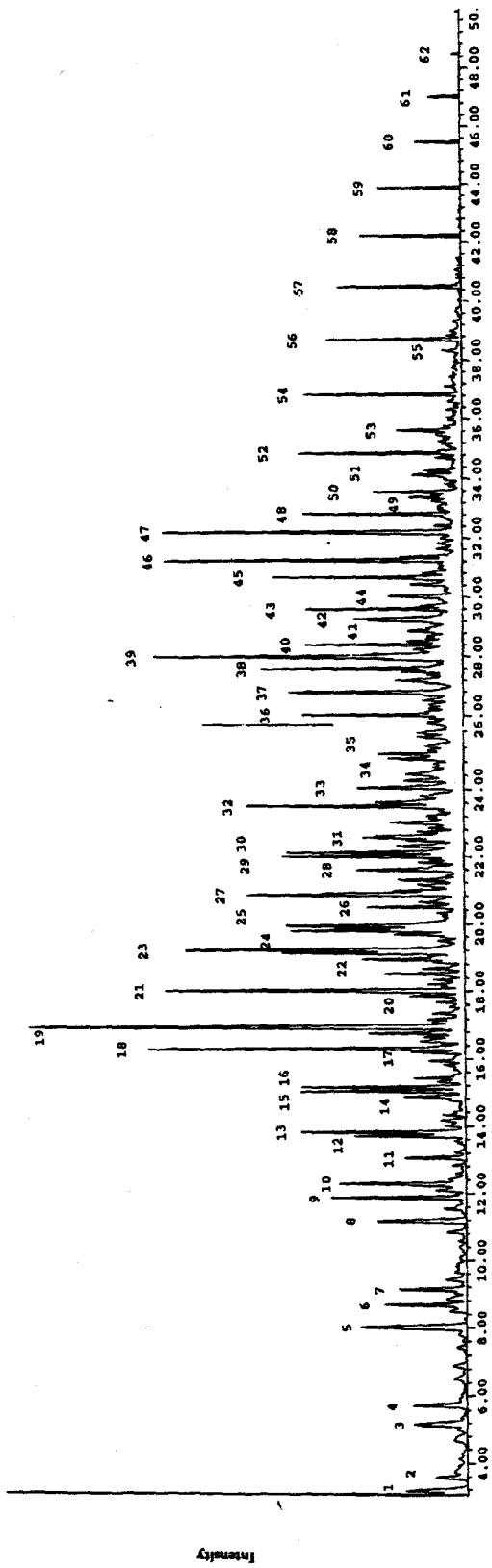

Figure 8.18. GC/MS chromatogram of the oil fraction of the reacted residue, DECS-7

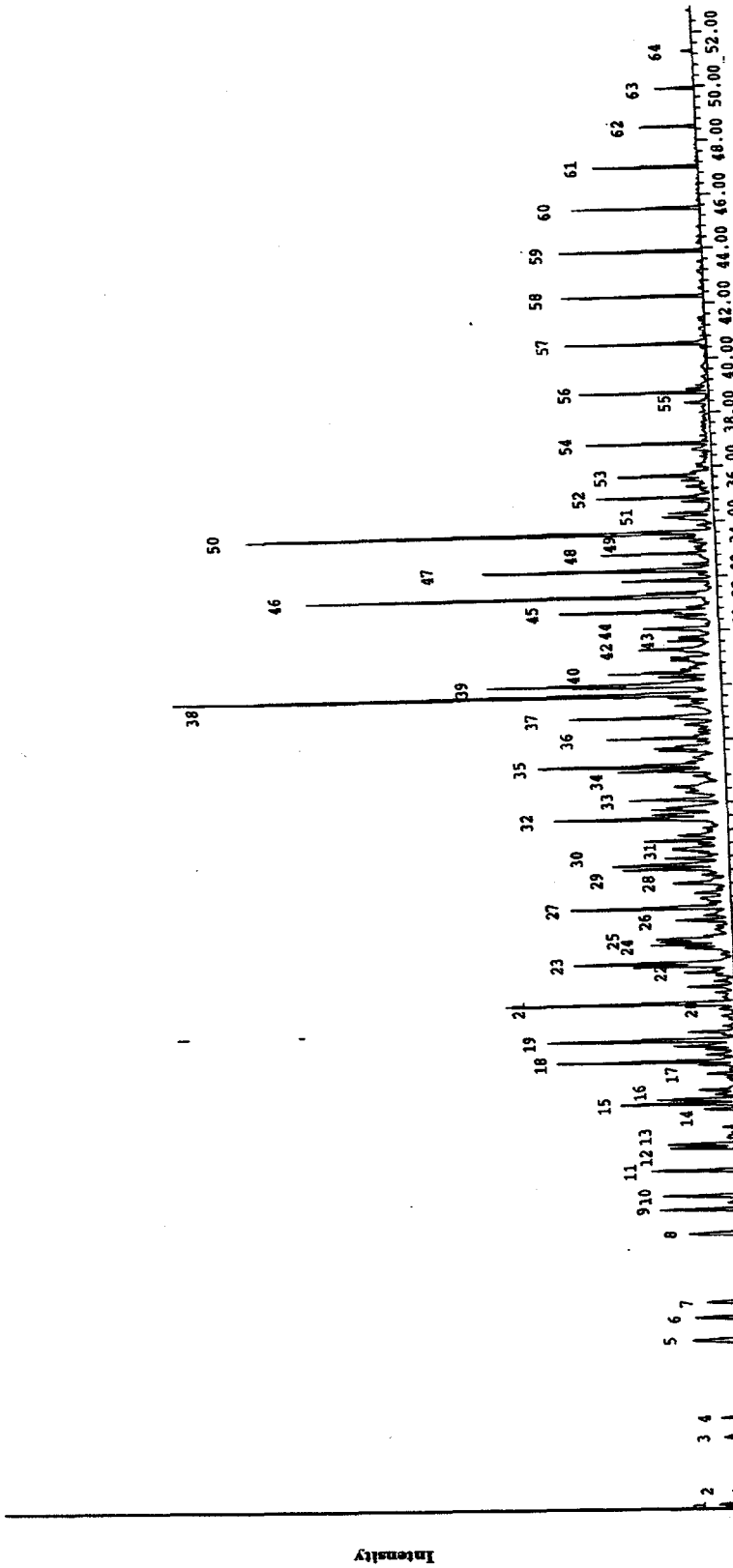

Figure 8.19. GC/MS chromatogram of the oil fraction of the reacted residue, DECS-6

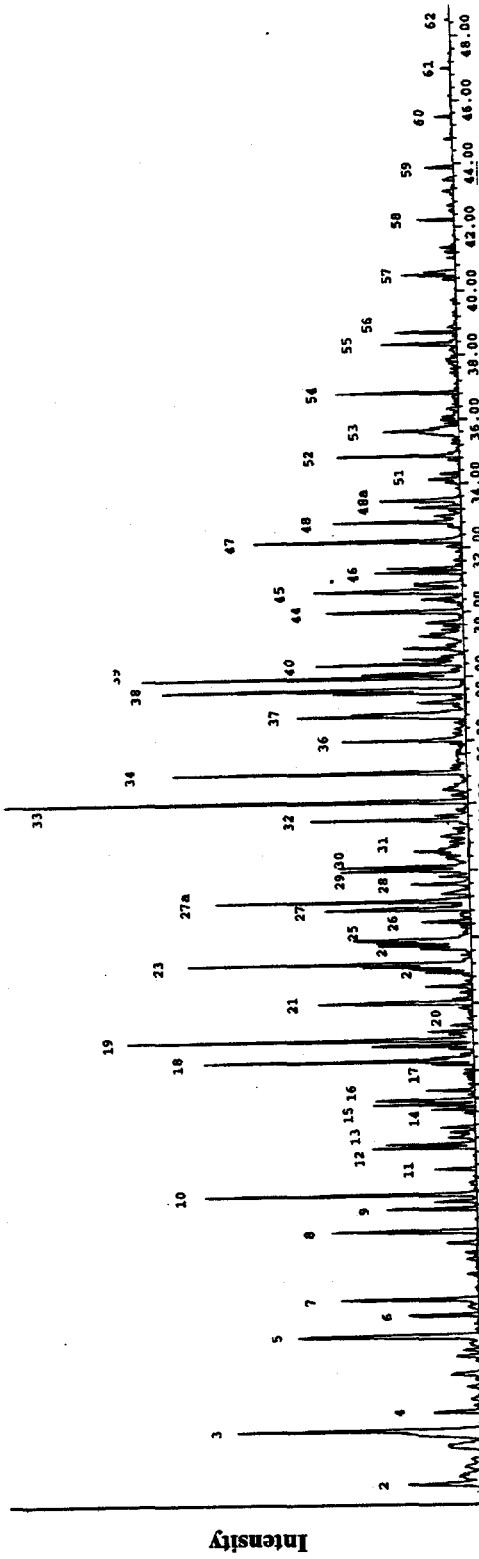

Figure 8.20. GC/MS chromatogram of the oil fraction of the reacted residue, DECS-12

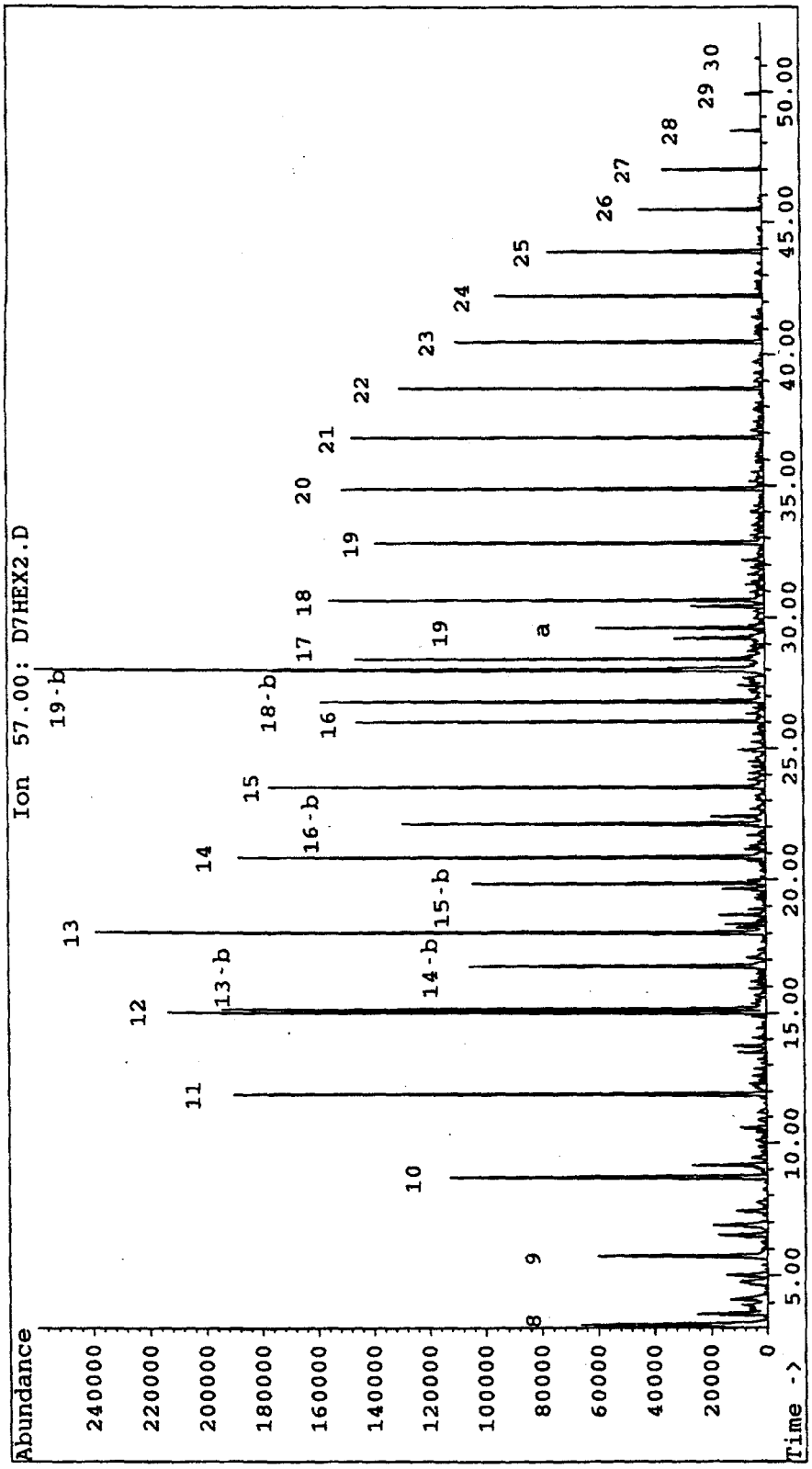

Figure 8.21. GC/MS single ion chromatogram of DECS-7,
(representing alkanes)
8=carbon chain length
b=branched chain

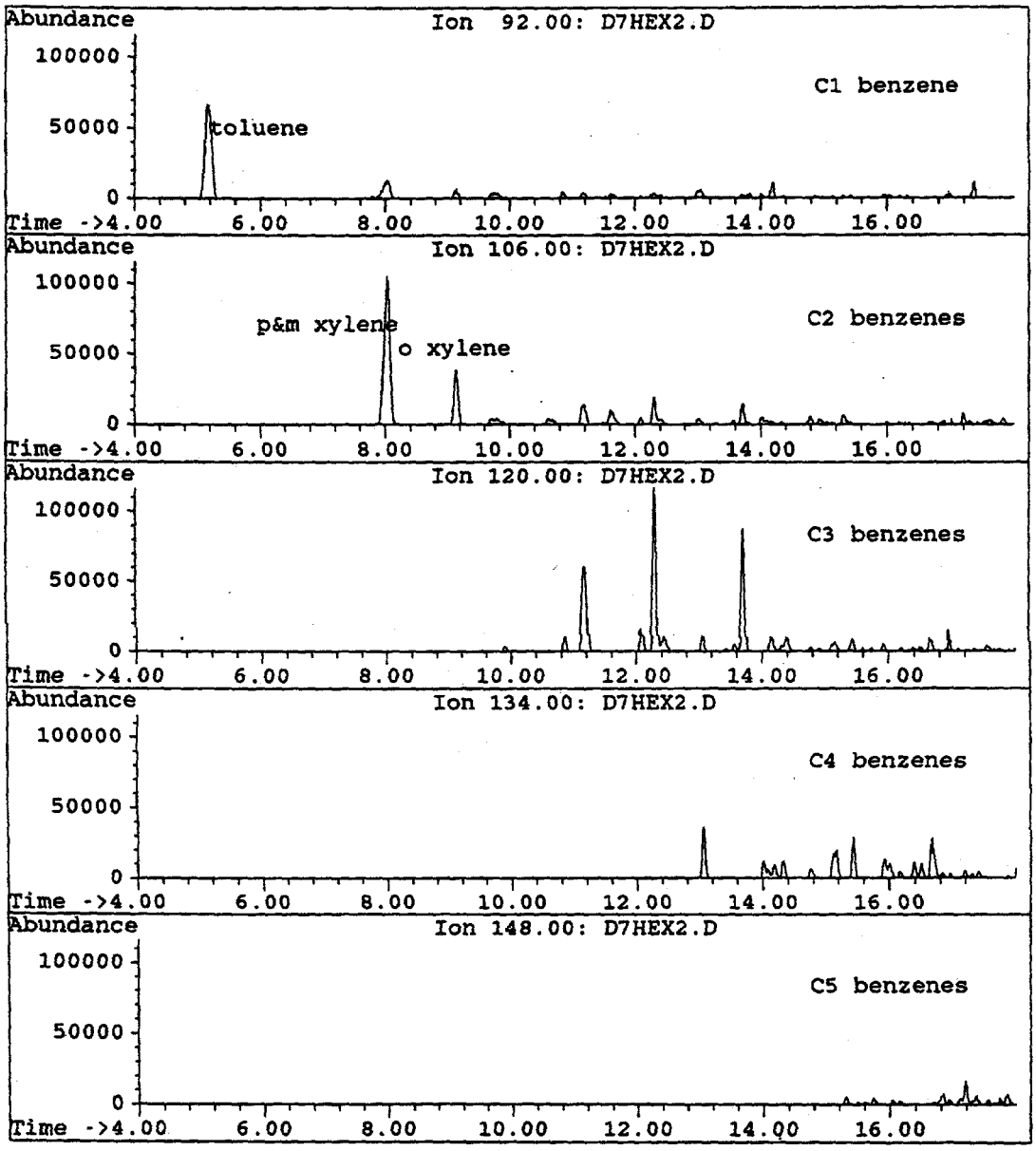

Figure 8.22. GC/MS single ion chromatogram of DECS-7, (representing benzene and alkyl benzenes)

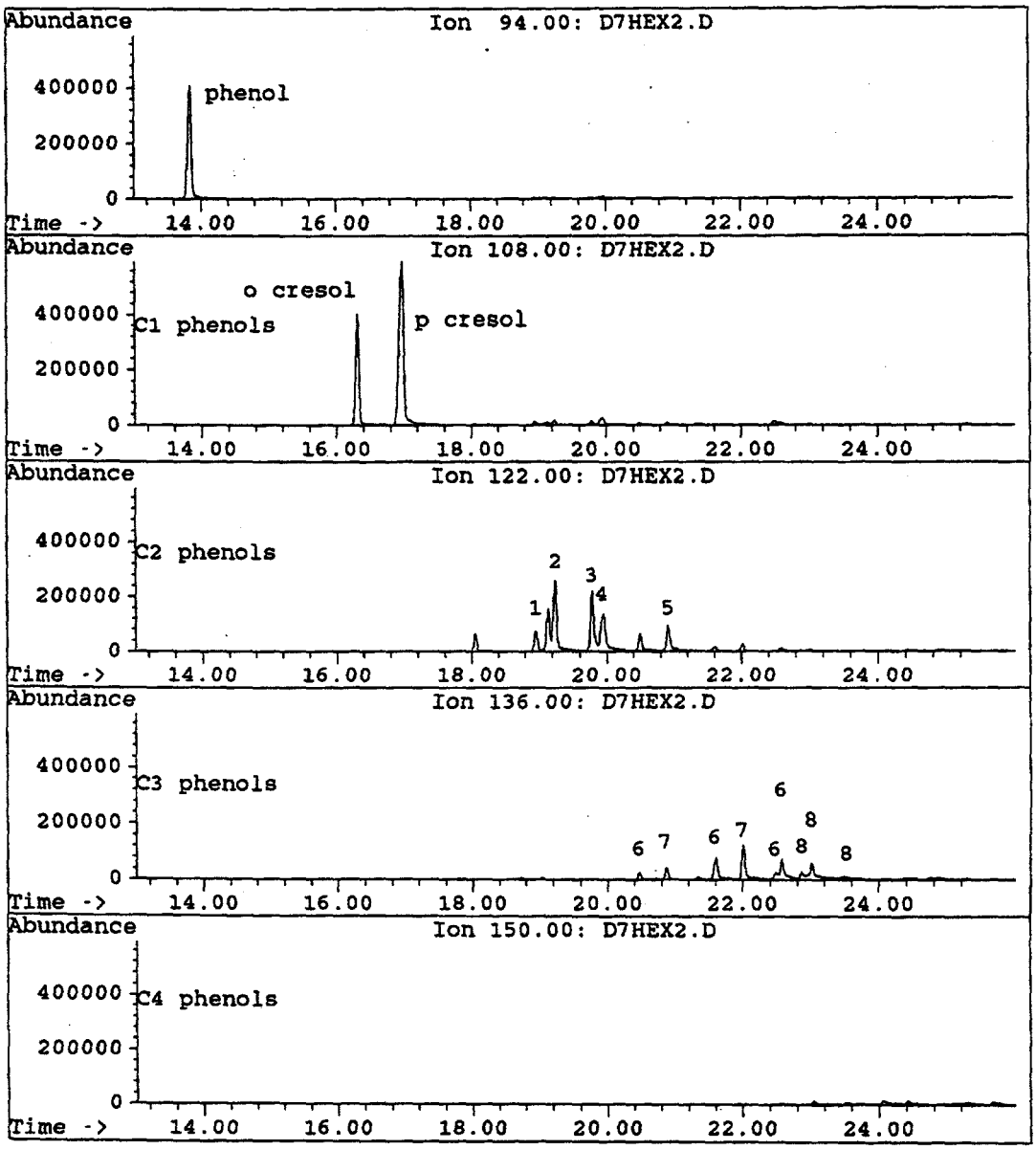

Figure 8.23. GC/MS single ion chromatogram of DECS-7, (representing phenol and alkyl phenols)

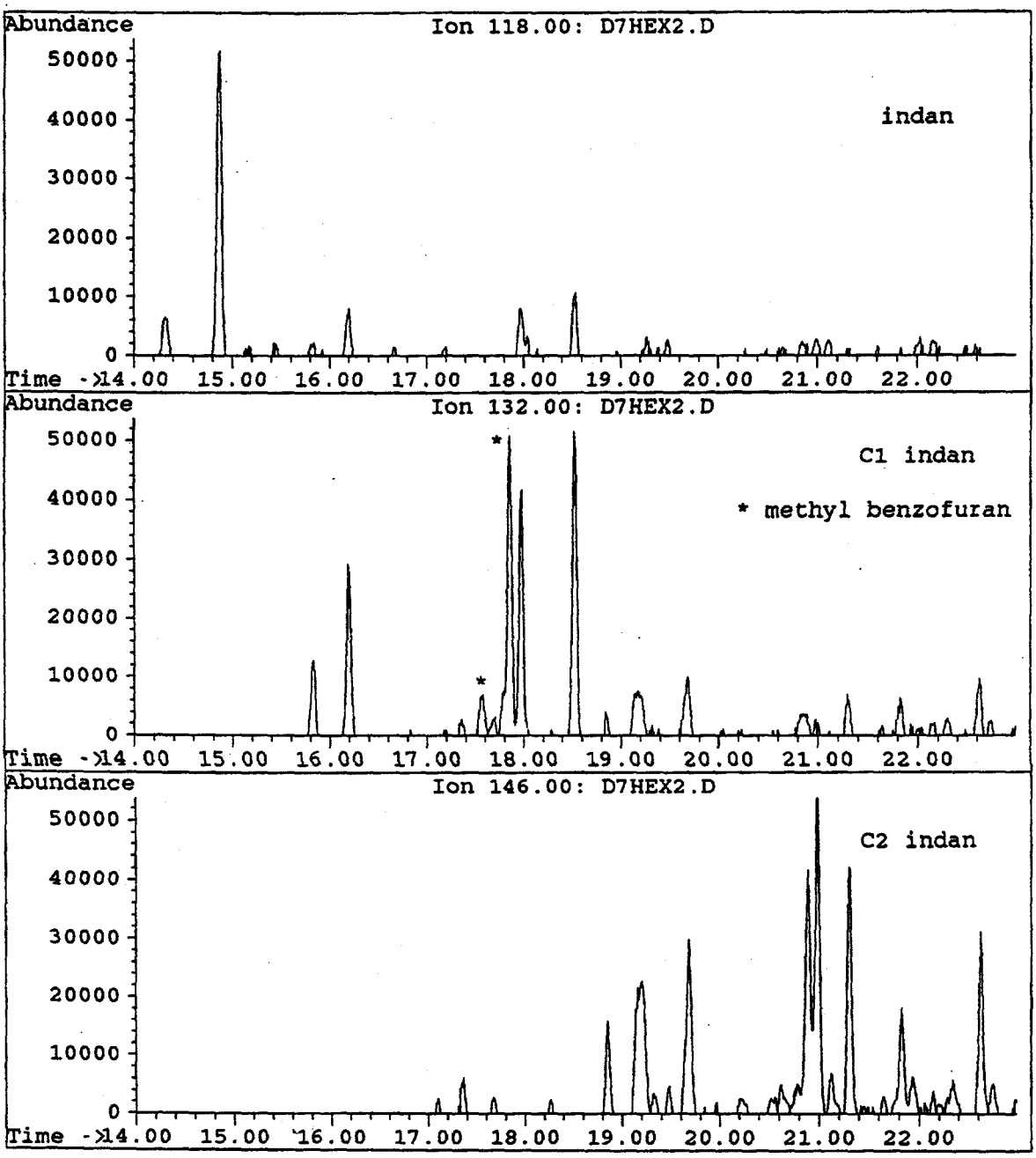

Figure 8.24. GC/MS single ion chromatogram of DECS-7, (representing indan and alkyl indan)

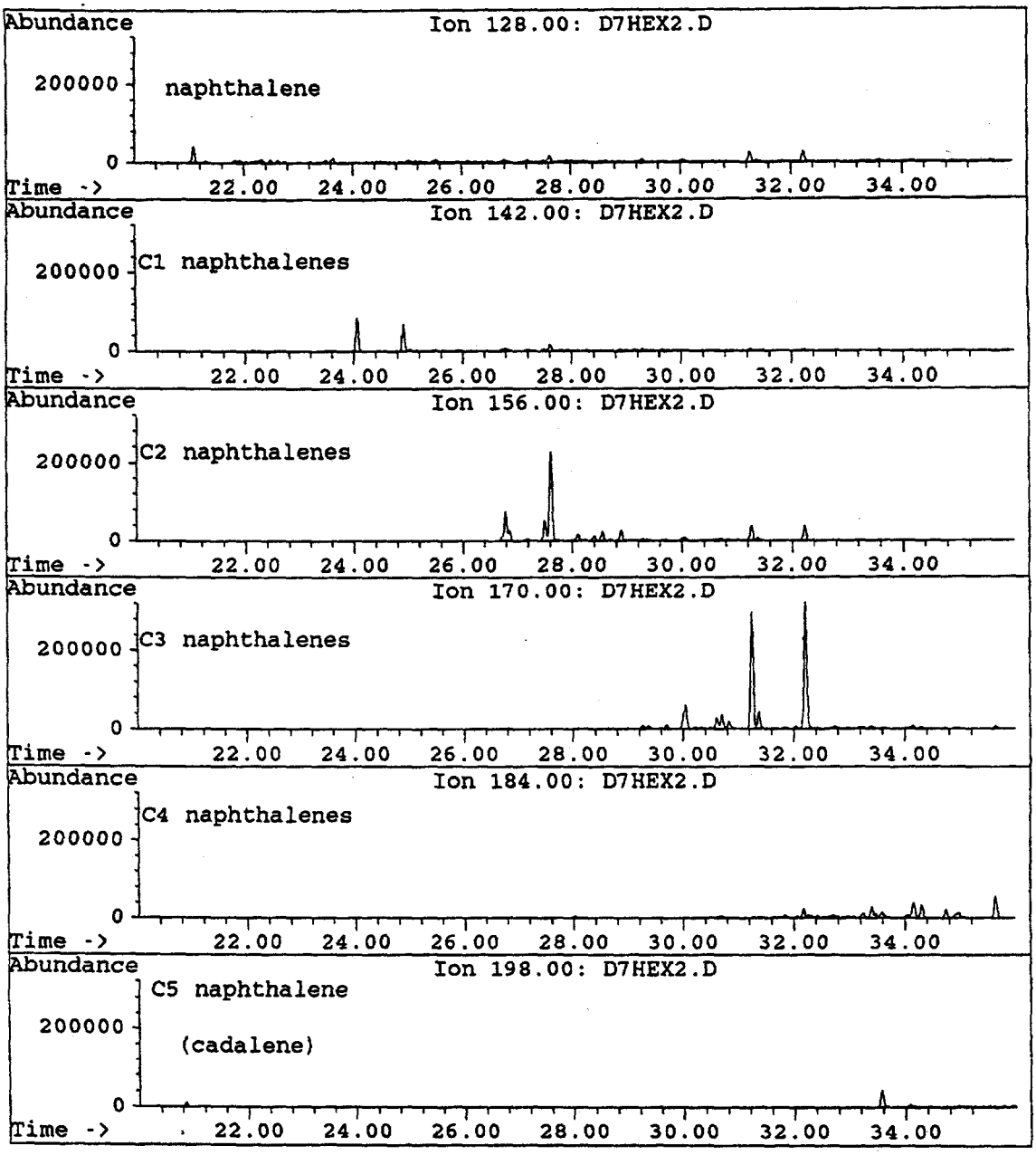

Figure 8.25. GC/MS single ion chromatogram of DECS-7, (representing naphthalene and alkyl naphthalenes)

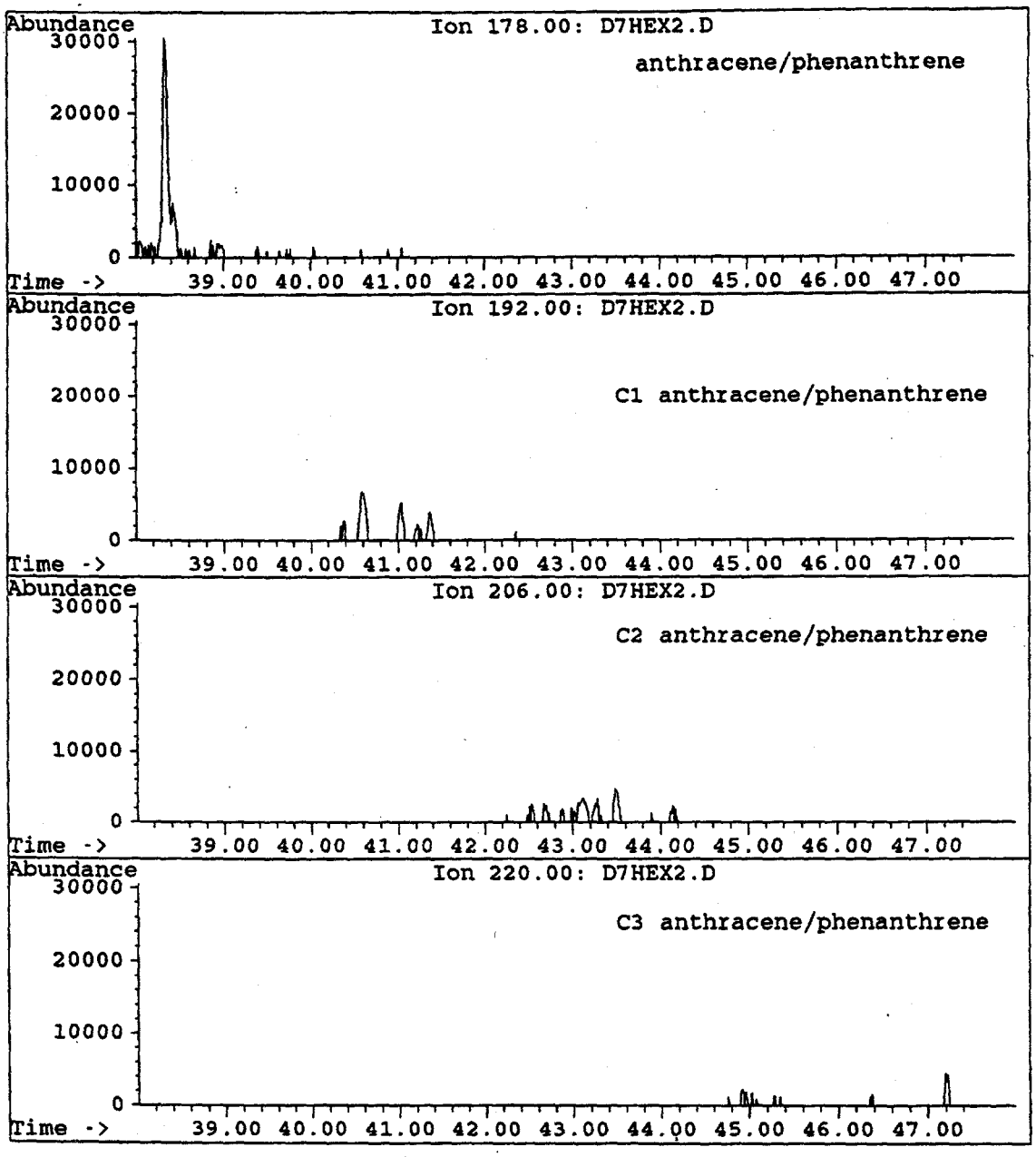

Figure 8.26. GC/MS single ion chromatogram of DECS-7,
(representing phenanthrene/anthracene and alkyl phen/anth)

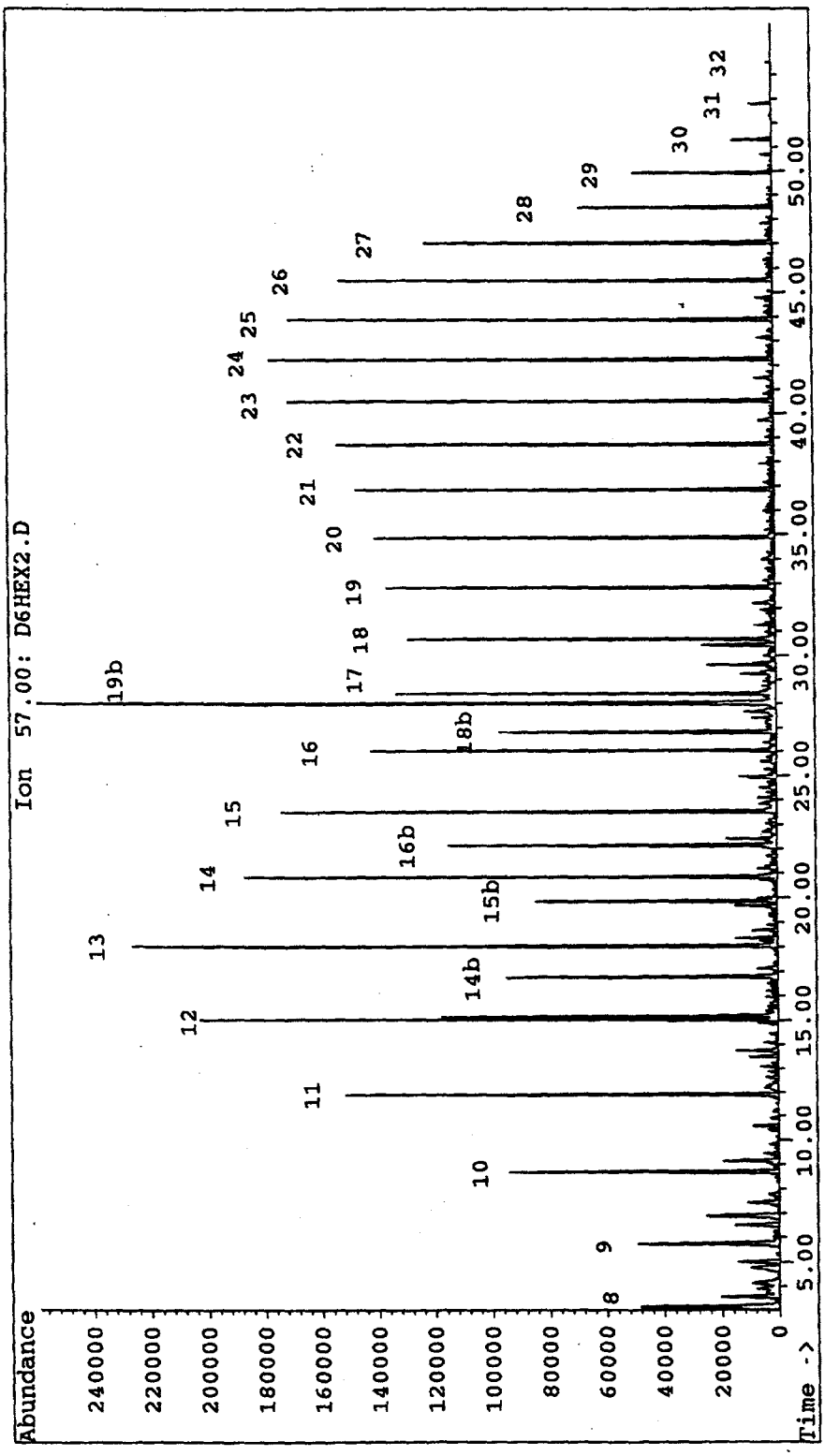

Figure 8.27. GC/MS single ion chromatogram of DECS-6,
(representing alkanes)
8=carbon chain length
b=branched chain

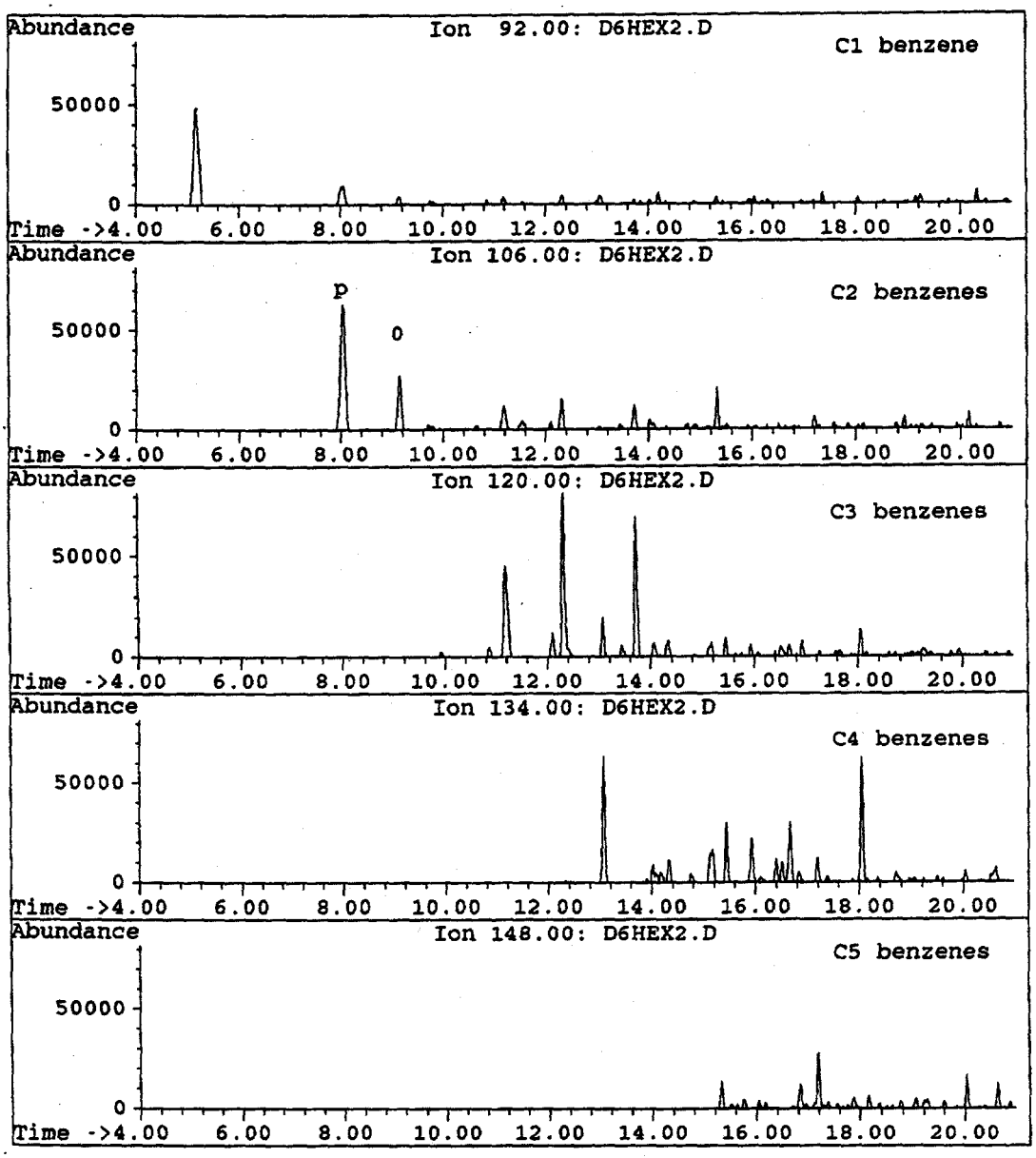

Figure 8.28. GC/MS single ion chromatogram of DECS-6, (representing benzene and alkyl benzenes)

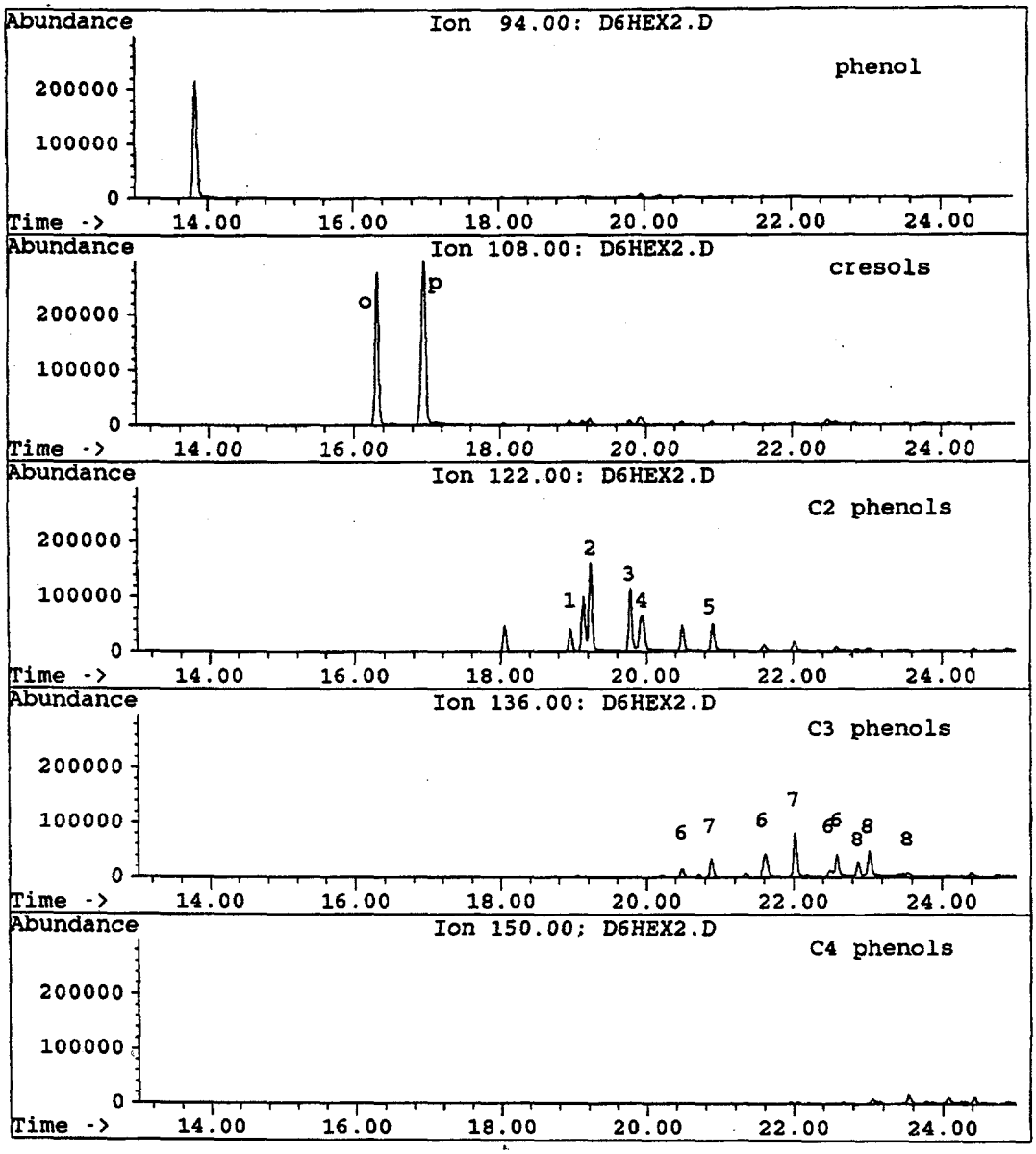

Figure 8.29. GC/MS single ion chromatogram of DECS-6, (representing phenol and alkyl phenols)

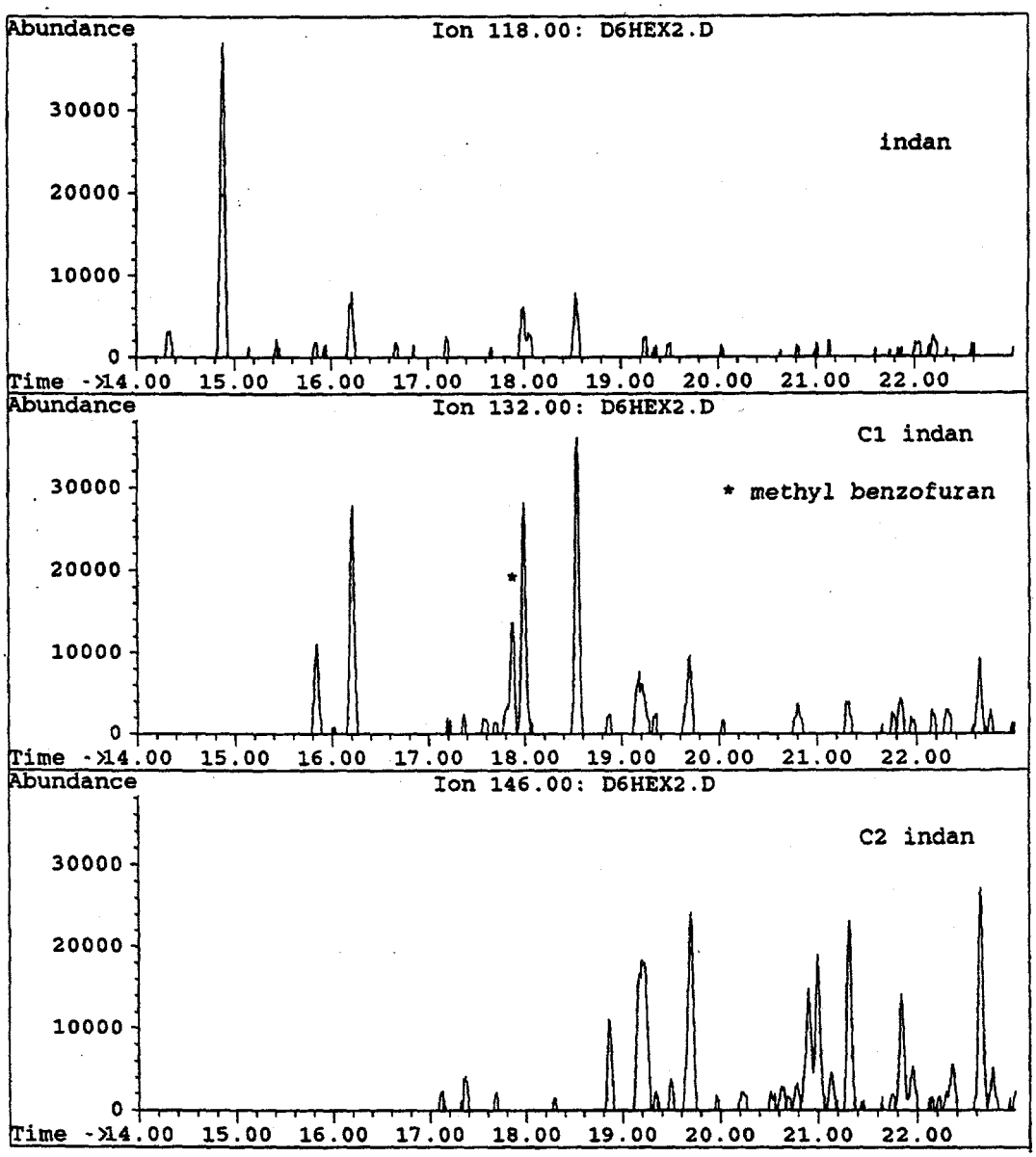

Figure 8.30. GC/MS single ion chromatogram of DECS-6, (representing indan and alkyl indan)

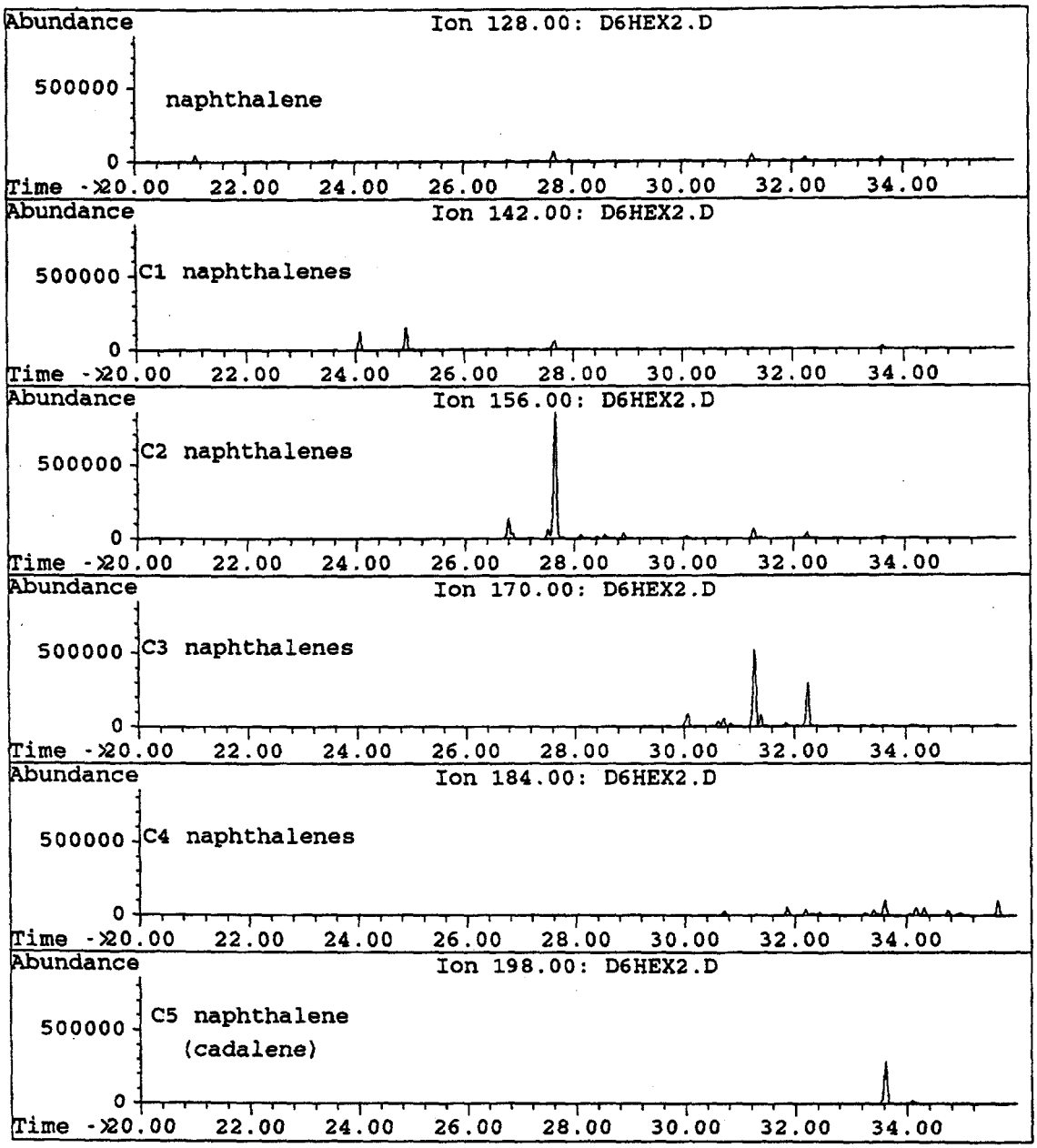

Figure 8.31. GC/MS single ion chromatogram of DECS-6 (representing naphthalene and alkyl naphthalene)

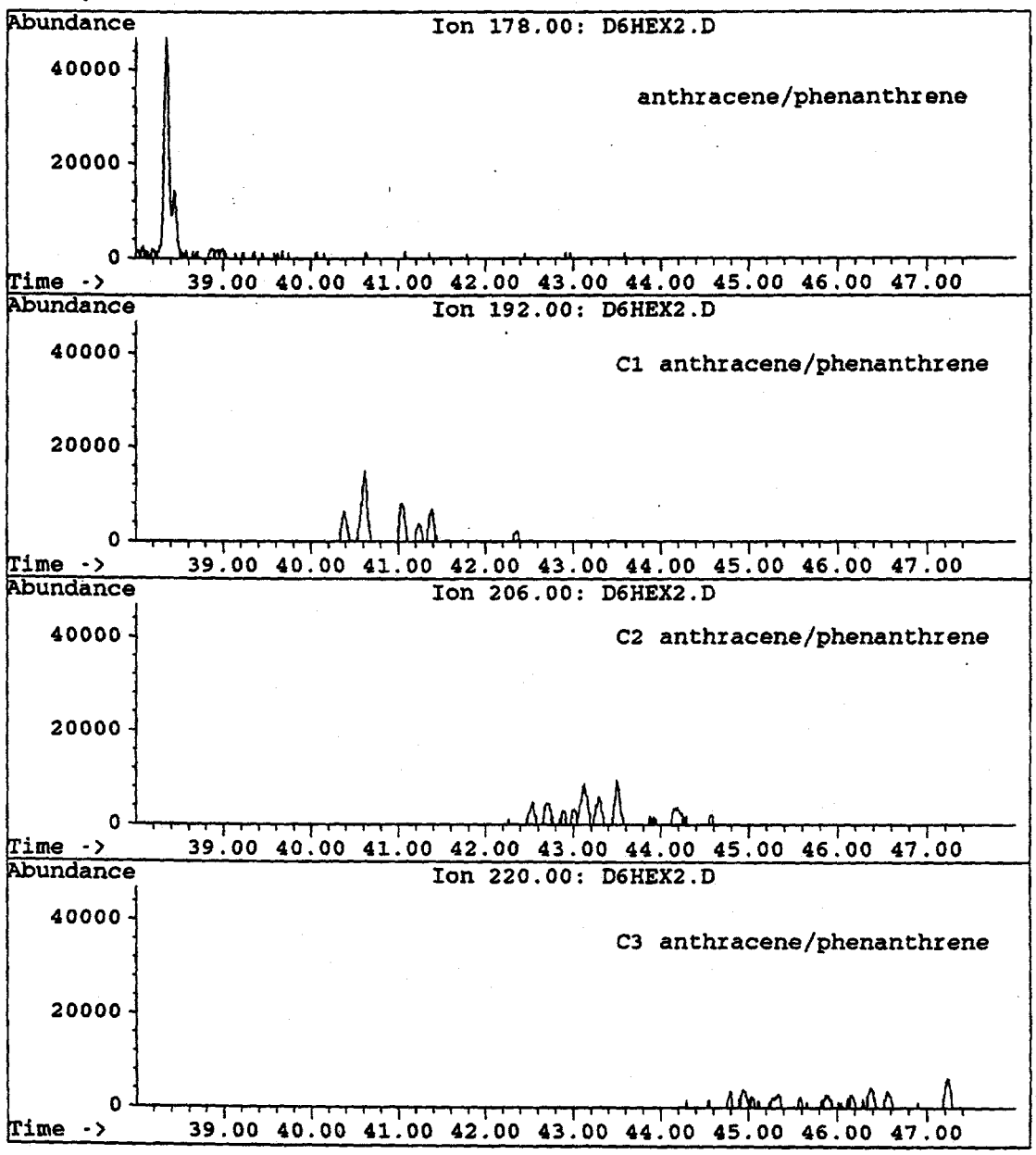

Figure 8.32. GC/MS single ion chromatogram of DECS-6,
(representing phenanthrene/anthracene and alkyl phen/anth)

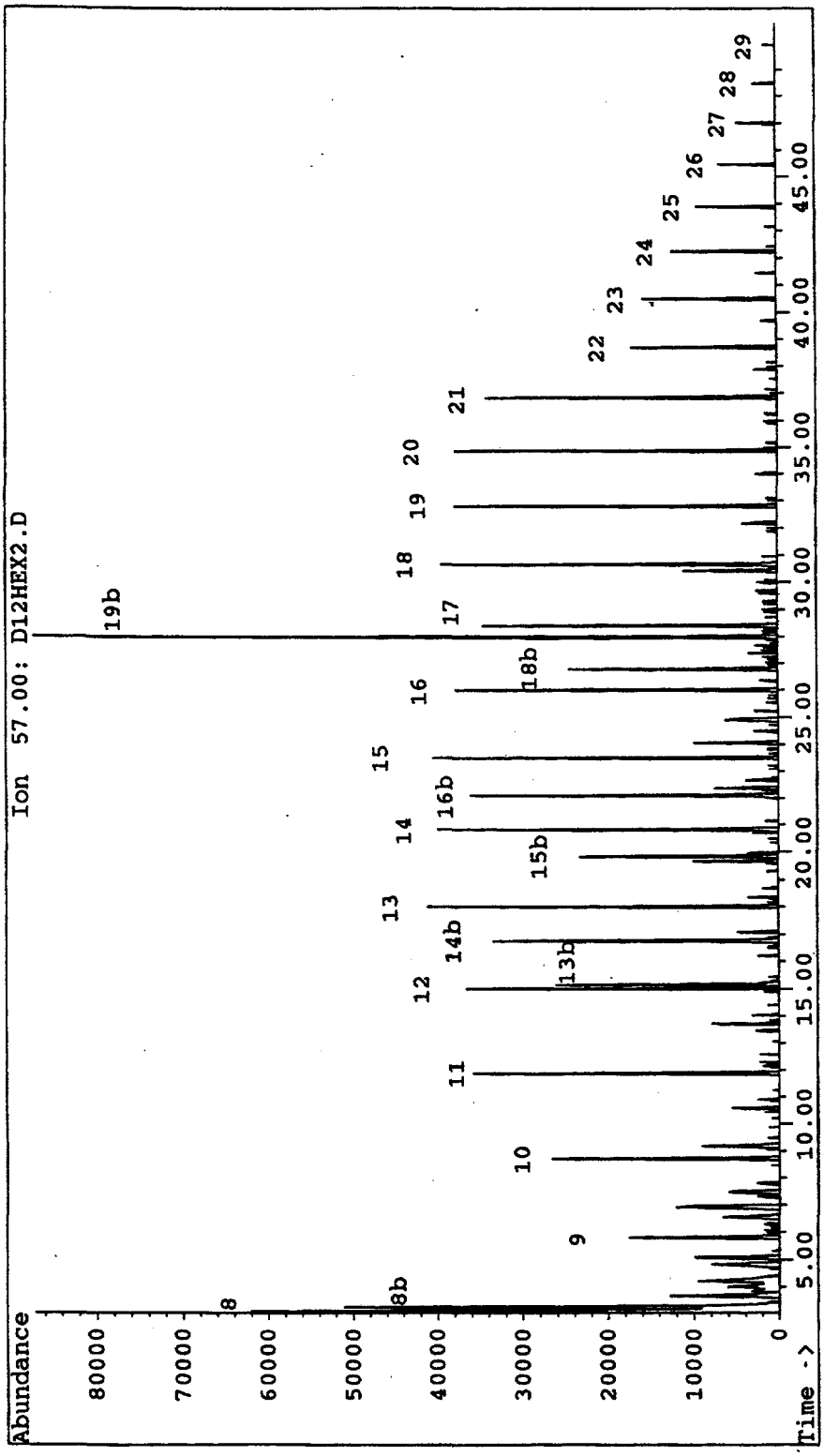

Figure 8.33. GC/MS single ion chromatogram of DECS-12,
(representing alkanes)
8=carbon chain length
b=branched chain

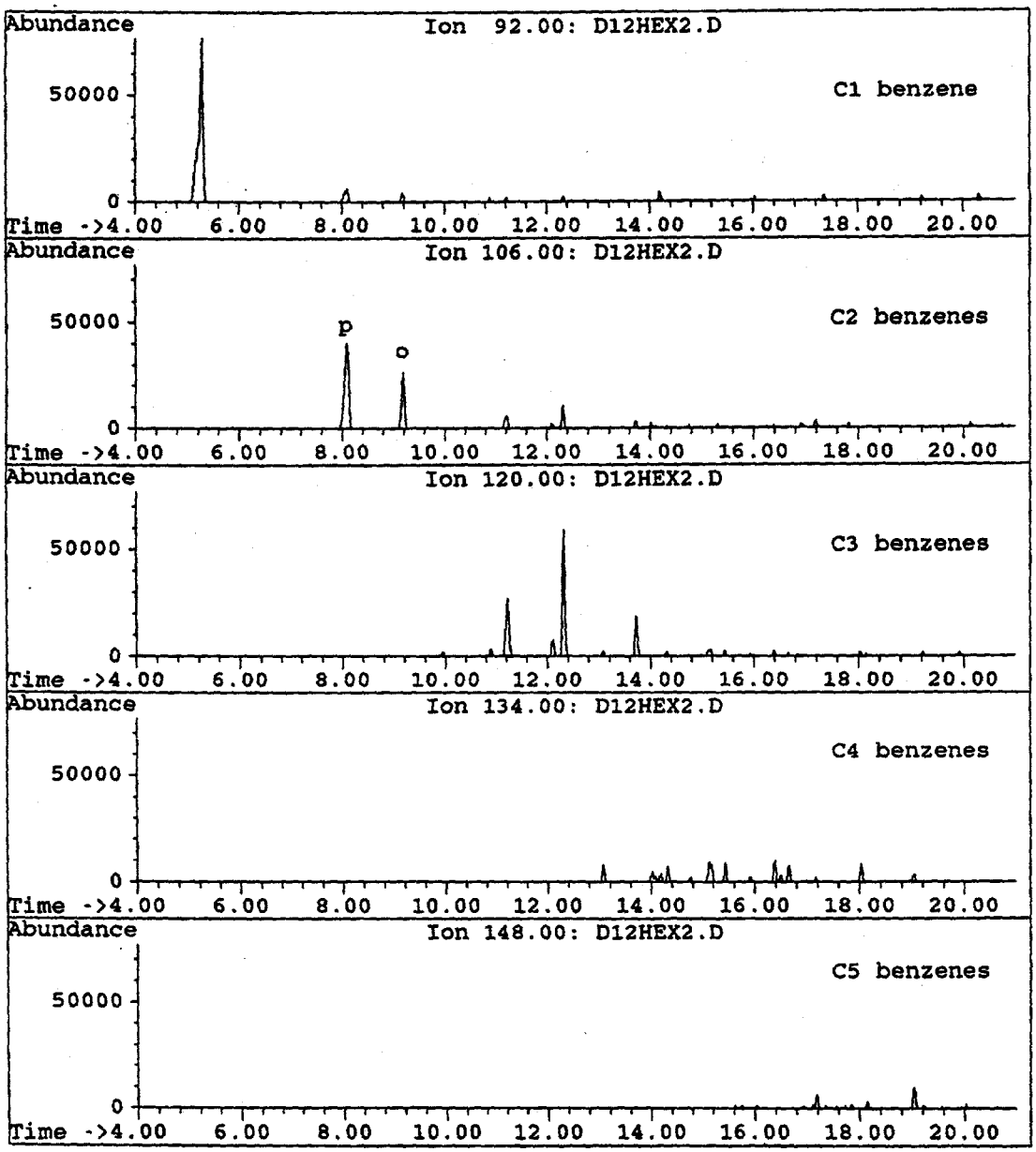

Figure 8.34. GC/MS single ion chromatogram of DECS-12, (representing benzene and alkyl benzenes)

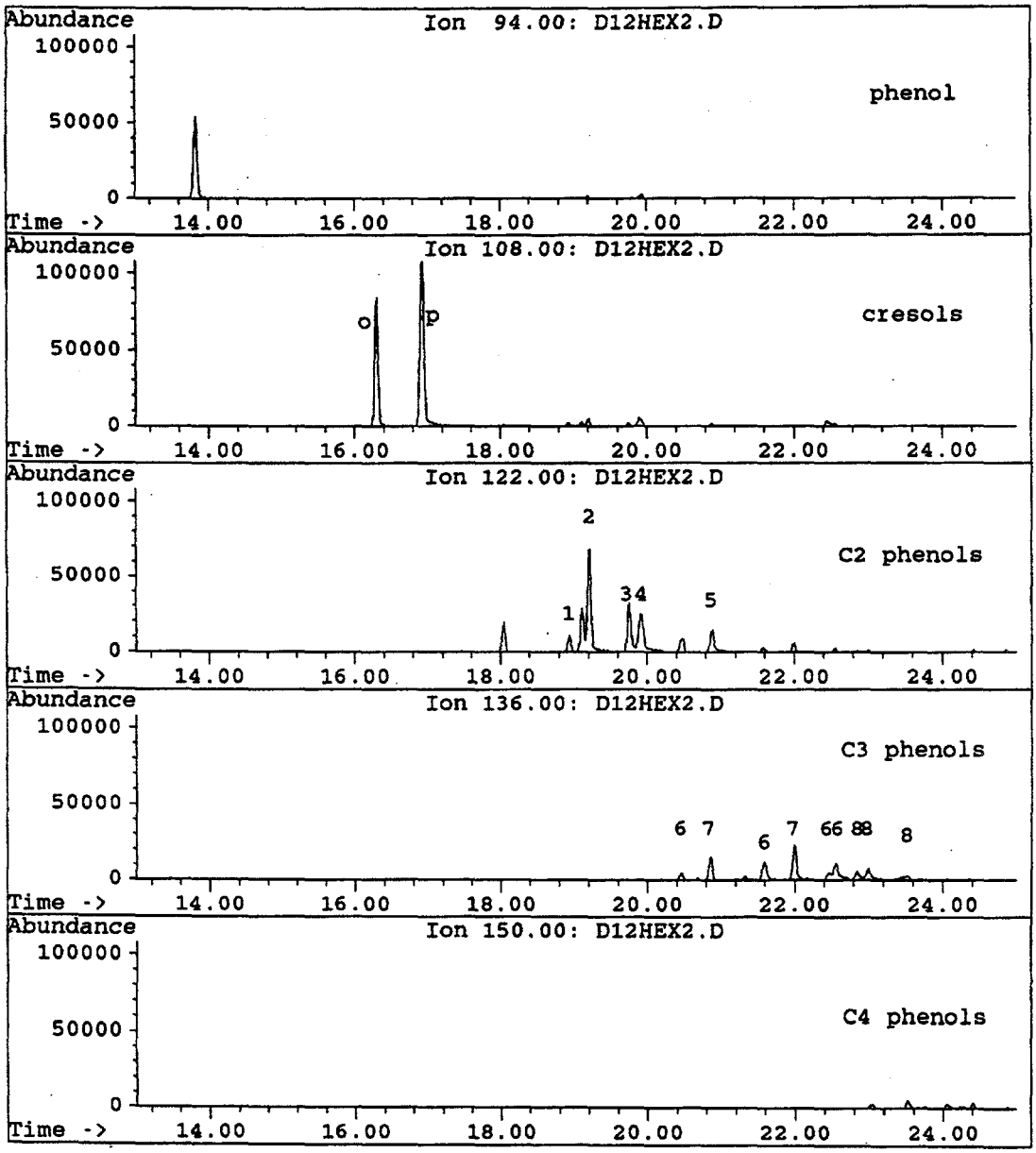

Figure 8.35. GC/MS single ion chromatogram of DECS-12, (representing phenol and alkyl phenols)

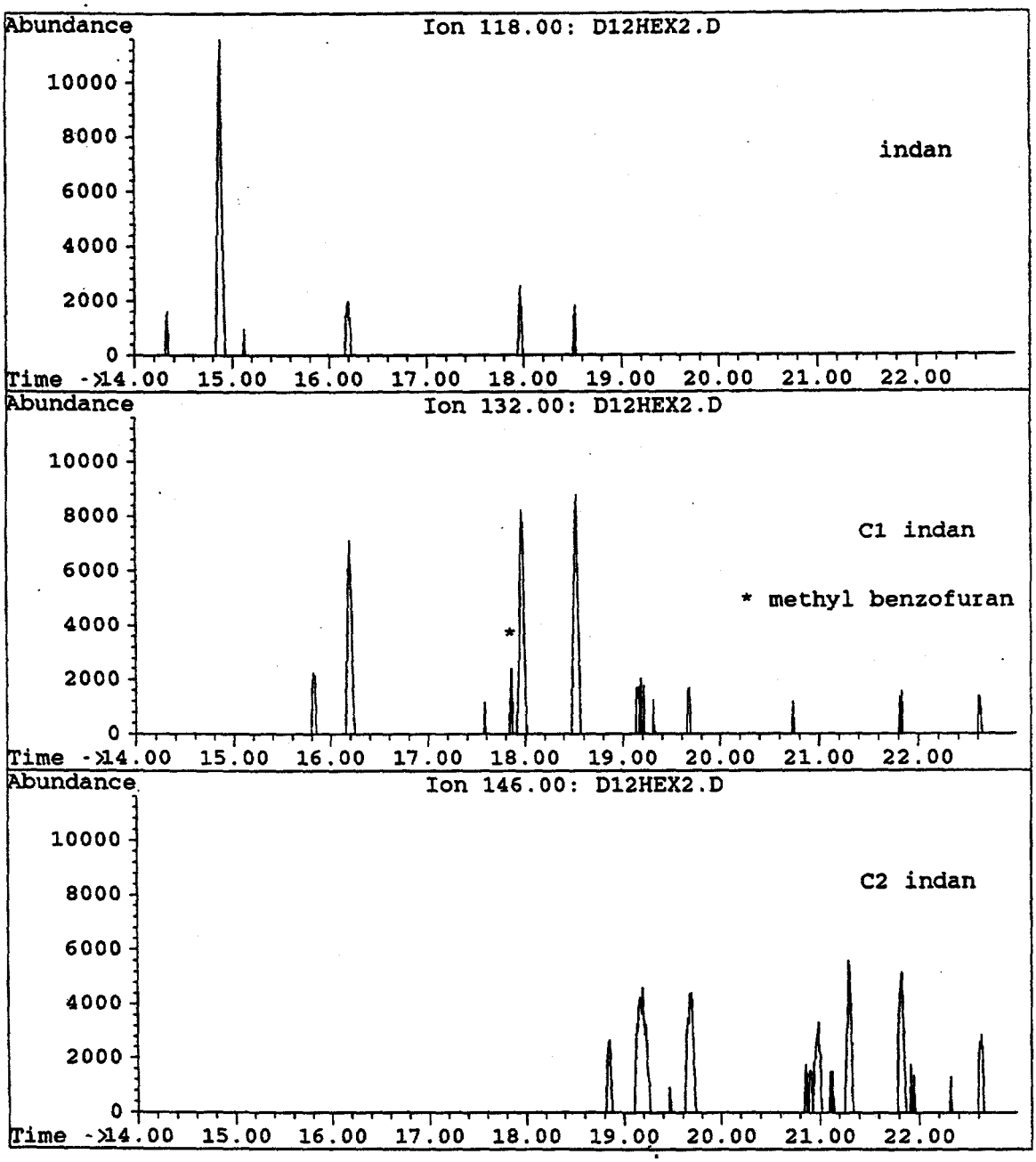

Figure 8.36. GC/MS single ion chromatogram of DECS-12, (representing indan and alkyl indan)

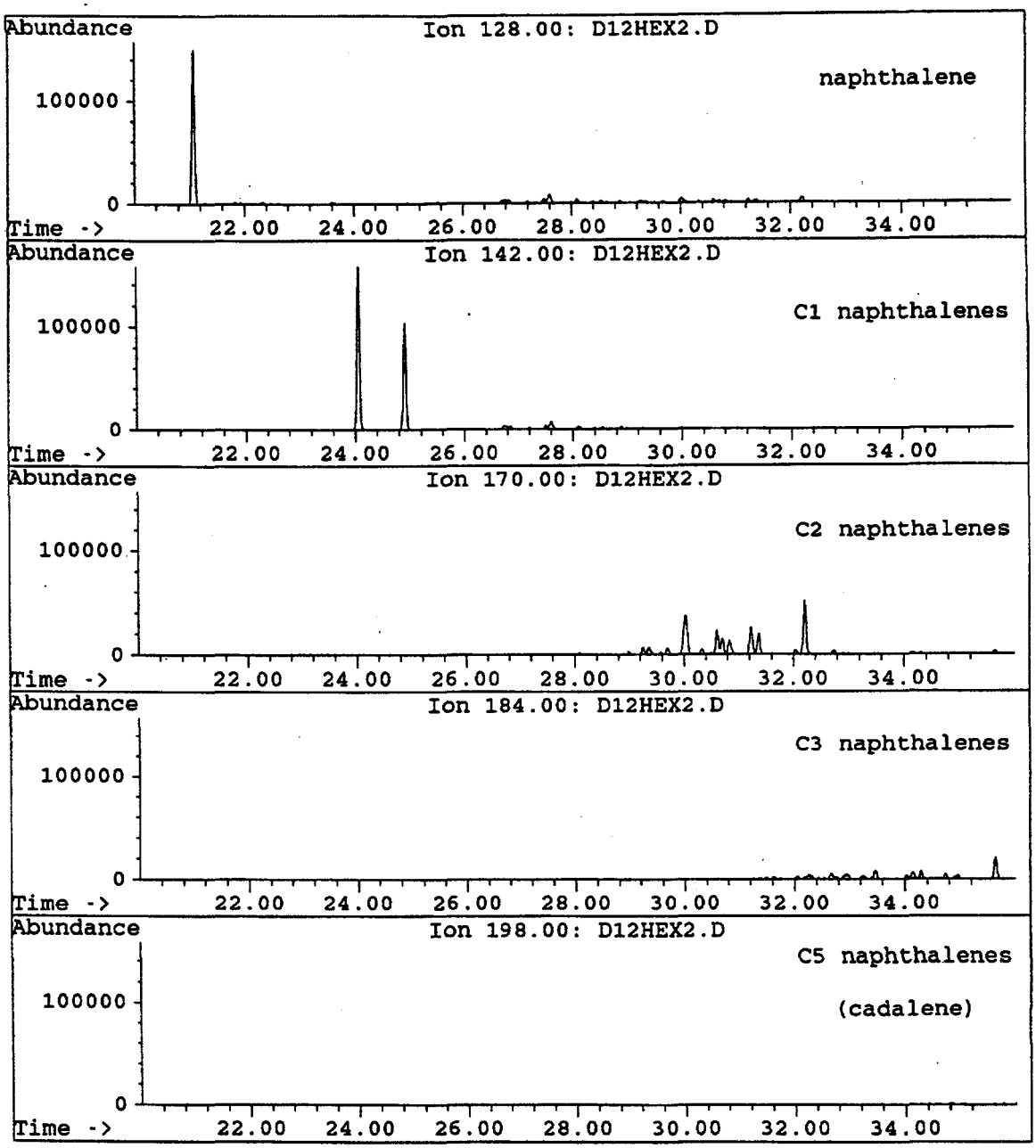

Figure 8.37. GC/MS single ion chromatogram of DECS-12, (representing naphthalene and alkyl naphthalene)

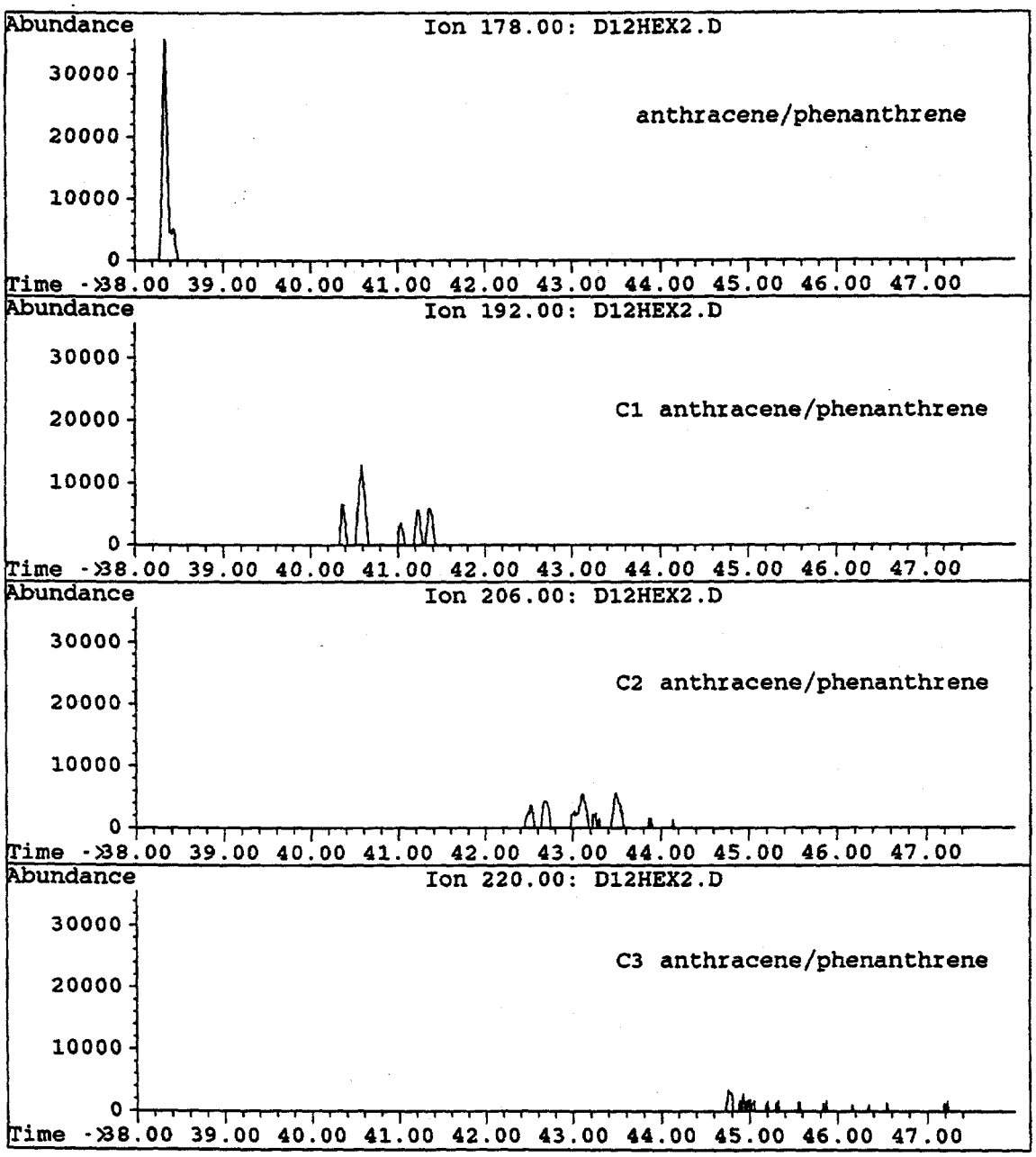

Figure 8.38. GC/MS single ion chromatogram of DECS-12, (representing phenanthrene/anthracene and alkyl phen/anth)

Temperature-programmed Liquefaction and Product Analysis

We also performed temperature-programmed liquefaction (TPL) of the three bituminous coals, with an attempt to examine how low-temperature thermal pretreatment affect coal conversion at higher temperature. The temperature-programmed liquefaction was conducted by heating the reactor rapidly into 200°C, held there fore 15 min, then programmed heating to 400°C at about 7°C/min, followed by final holding at 400°C for 30 min. The TPL are shown in Table 8.6, together with those for single stage liquefaction (SSL) and those of raw coal extraction. The results show that TPL runs give significantly higher conversion than conventional SSL runs.

In order to see if there is any beneficial effect in performing programmed heating from 200 to 400°C in TPL runs, we conducted several tests which uses rapid heating from 200 to 400°C by using two preheated sand baths in one experiment. We call these experiments as temperature-staged liquefaction (TSL: r.t. to 200°C, held there fore 15 min, rapid heating to 400°C, then held there for 30 min) to distinguish these run from TPL runs. The results are also shown in Table 8.6. The results are surprising in that TSL runs gave even lower conversion than SSL runs. These results suggest that the controlled or programmed heat up from a low to a high temperature in TPL runs is important. However, it must be noted that these experiments should be repeated in the future because there was leak during TSL run of DECS-7 and asphaltene spill during product recovery in the TSL run of DECS-12.

The oil products from TPL runs were also analyzed by using GC-MS. Figure 8.39 and Figure 8.40 show the GC-MS total ion chromatograms of oils from TPL of DECS-7 adaville coal and DECS-12 Pittsburgh #8 coal, respectively. The oils from TPL runs have different compositions as compared to the oils from corresponding SSL runs (Figure 8.39 vs. Figure 8.18; Figure 8.40 vs. Figure 8.20).

The above results are interesting in that TPL runs, even in the absence of any solvents and without a catalyst, can not only improve coal conversion for the bituminous coal, but also alter the product distribution and composition. However, it should be mentioned, that these TPL and SSL runs were not yet duplicated for the three bituminous coals. For coal conversion experiments, it is important to check the reproducibility. Therefore, further confirmation of these data is needed before making reliable comparison, and meaningful discussion.

Table 8.6 Results of Temperature-Programmed and Single Stage Solvent-free Non-Catalytic Liquefaction of Three Bituminous Coals at 400°C under 6.9 MPa (Cold) H_2

Coal ID/Name	Run Mode	Conv, dmmf wt%	Preasphaltene	Asphaltene	Oil+Gas
Solvent Extraction					
DECS-7 / Adville#1	B.P. Extract	12.2			
DECS-6 / Blind Can	B.P. Extract	14.2			
DECS-12/ Pitt #8	B.P. Extract	8.9			
Single Stage Liqu					
DECS-7 / Adville#1	400°C-SSL	31.2	7.7	8.9	14.6
DECS-6 / Blind Can	400°C-SSL	38.8	9.1	7.3	22.4
DECS-12/ Pitt #8	400°C-SSL	46.1	12.8	9.1	24.2
Temp Program Liqu					
DECS-7 / Adville#1	400°C-TPL	47.1	6.9	3.5	36.7
DECS-6 / Blind Can	400°C-TPL	58.6	8.8	9.2	40.6
DECS-12/ Pitt #8	400°C-TPL	64.1	23.0	10.2	30.9
Temp Staged Liqu					
DECS-7 / Adville#1	400°C-TSL[a]	21.2	5.8	3.6	11.8
DECS-6 / Blind Can	400°C-TSL	30.9	23.1	3.2	4.6
DECS-12/ Pitt #8	400°C-TSL[b]	31.1	12.4	7.5	11.2

SSL: r..t. to 400°C, then held there for 30 min.

TPL: r.t. to 200°C, held there fore 15 min, programmed heating to 400°C at about 7°C/min, then held there for 30 min.

TSL: r.t. to 200°C, held there fore 15 min, rapid heating to 400°C, then held there for 30 min.

a) There was a major reactor gas leak during this run. b) There was a product spill.

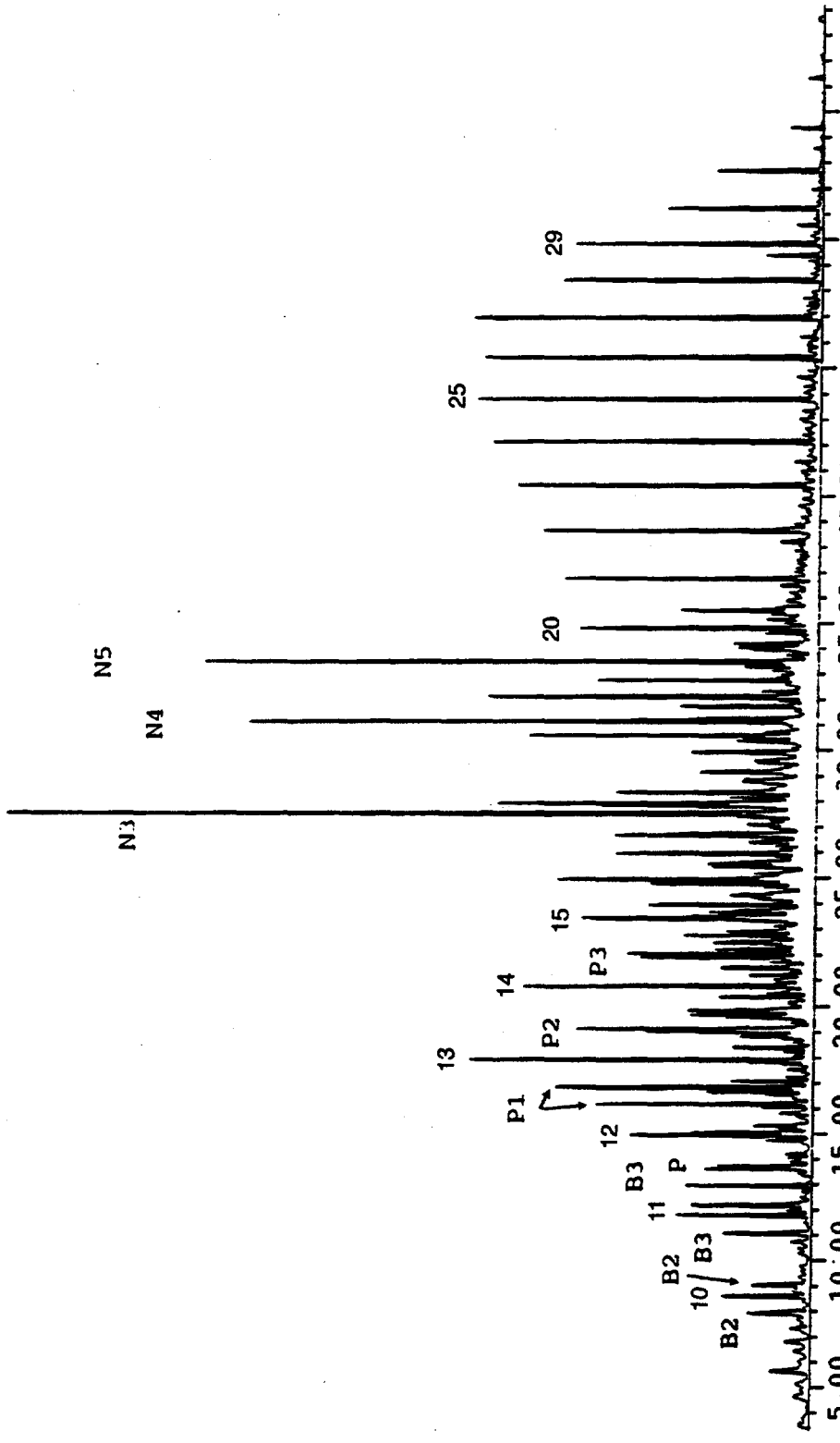

Figure 8.39. Temperature programmed liquefaction, DECS-7, hexane fraction (oil)

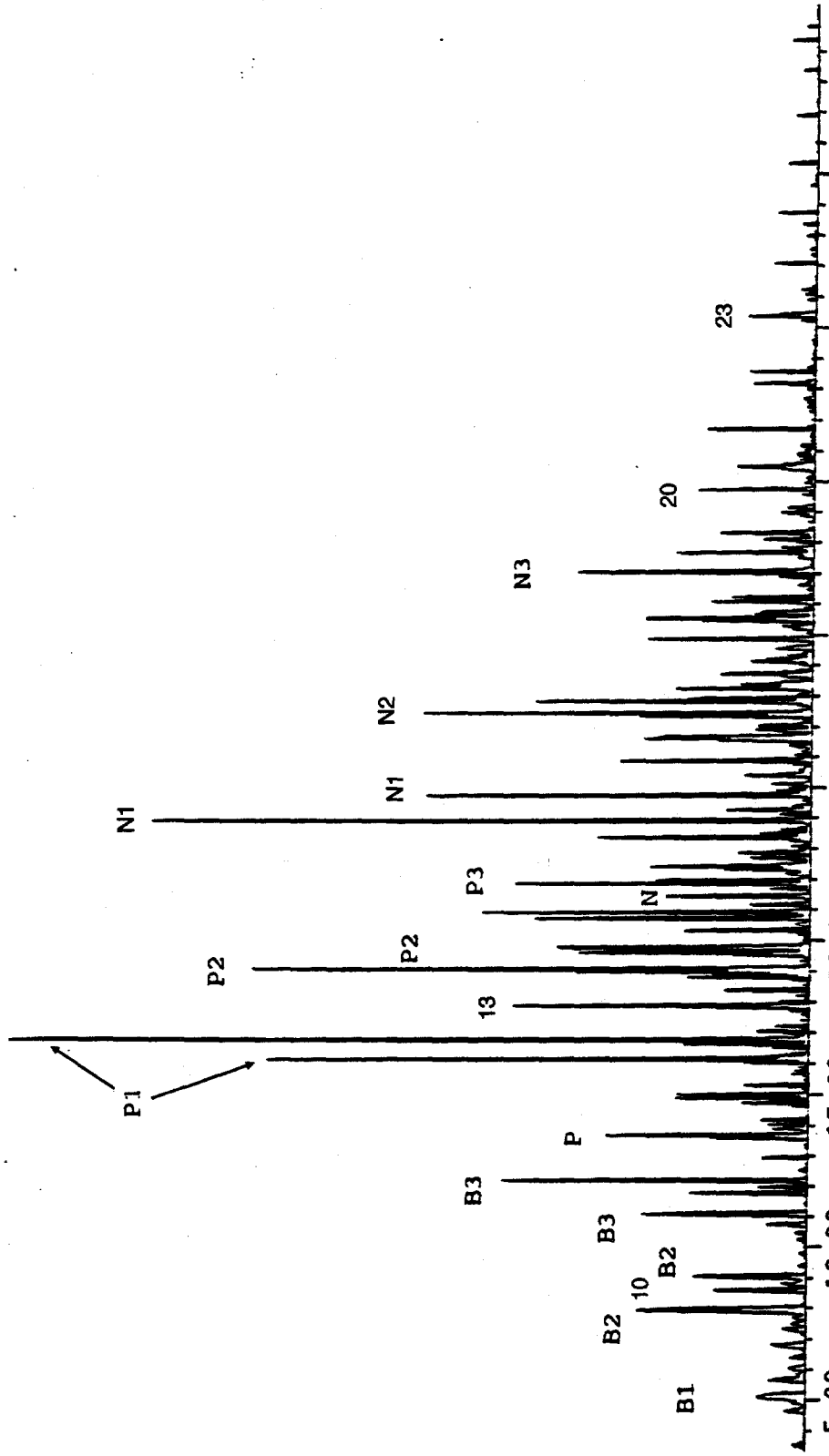

Figure 8.40. Temperature programmed liquefaction, DECS-12, hexane fraction (oil)

Conclusions

Liquefaction of this suite of bituminous coals at 400°C provided conversions between 30 and 40 percent. The higher the liptinite content the higher the oil and gas yields. The aliphatic components of these coals are being redistributed into all the products: gas, oil, asphaltenes and preasphaltenes. Whereas, high concentrations of vitrinite yielded lower quantities of a phenolic based oil. Preasphaltene concentrations increased slightly, from seven to thirteen percent, with increasing carbon content (increasing rank). The asphaltene content was roughly the same (8%) for three coals.

NMR data revealed a loss of aliphatic carbon with a corresponding increase in aromatic carbon, which corresponds with the product distribution; aliphatic hydrocarbons were in all product class. There is also a decrease in oxygen content, most likely through the generation of CO, and CO_2, but also through the generation of H_20 through dehydration reactions Aromaticity is increasing, most likely by retrogressive reactions. Py/GC/Ms data suggest the reacted residue is a low volatile highly condensed char, low in oxygen and hydrogen functional groups. Most likely some of the hydrogen being abstracted to cap the radicals formed due to thermal cracking of the aliphatic compounds found in the liptinite macerals causes further condensation. Also some of the hydrogen is lost with the generation of water.

By combining modern spectroscopic techniques, ^{13}C NMR and pyrolysis/gas chromatograpy/mass spectrometry with proven analytical techniques, optical microscopy and elemental data, a more detailed understanding of the relationship between the physical and chemical composition, and structure of coal can be achieved. By using these same techniques to characterize the products generated during liquefaction experiments a better understanding of the conversion processes and reaction pathways should be revealed. Work is continuing along these lines, as well as new work with single-staged liquefaction and temperature-programmed liquefaction experiments with and without solvents and catalysts on these three bituminous coals.

1.5 References

Hatcher, P.G. et al., Org. Geochem., 1989, 14, 145.

Song, C.; Saini, A.K.; Huang, L.; Wenzel, K.; Hatcher, P.G.; Schobert, H.H.; "Effects of Low-Temperature Catalytic Pretreatments on Coal Structure and Reactivity in Liquefaction", Technical Progress Report for the period April - July 1992, DE-AC22-91PC91042-TPR-3, U.S. DOE/PETC, August 1992.

Song, C. et al., ACS Fuel Chem. Preprint., 1992, 37 (2), 976.

CHAPTER 9. Effects of Catalytic and Thermal Pretreatments on Conversion and Structural Changes of Wyodak Subbituminous Coal. Spectroscopic Characterization by Solid-State ^{13}C NMR, Pyrolysis-GC-MS, and FTIR

INTRODUCTION

Coal conversion into liquids is an extremely complex process and involves both chemical and physical transformations. The dissolution of coal requires homolytic cleavage of bonds to yield free radicals and their immediate stabilization with hydrogen, otherwise they may recombine or crosslink to form more refractory materials. The rate of thermal fragmentation is mainly determined by coal reactivity and reaction conditions, particularly temperature and heating rates. The conventional concept for high-severity conversion of coal is that coal must be heated to high temperatures (400-450°C) causing thermal cleavage of bonds in organic matrix of coal to yield free radicals, which are capped by hydrogen to form low-molecular-weight products. However, recent fundamental research in coal liquefaction and pyrolysis has revealed that coal is more reactive than had been thought previously. The thermally initiated reactions of coal can take place very rapidly (1,2) and especially for low-rank coals, can occur at lower temperatures (3,4). The previous work in our laboratory has demonstrated that more bonds in low-rank are thermally broken at lower temerature as compared to bituminous coals, and a concept of bond energy distribution has been developed from temperature-programmed pyrolysis (3,4).

It has been also demonstrated that the combination of low-temperature catalytic reaction followed by the high-temperature catalytic reaction using dispersed molybdenum catalyst significantly enhanced coal conversion (5-12). The work presented here is concerned with the effects of low-temperature catalytic pretreatment on coal structure and reactivity in liquefaction. Recently, we have demonstrated that the combined use of solid-state NMR and pyrolysis-GC-MS has the potential to reveal the major and minor structural changes in the macromolecular network of coal induced by liquefaction (13, 14). The specific objectives of the present work are to identify the basic changes in coal structure induced by catalytic and thermal pretreatments by using modern analytical techniques, including pyrolysis-GC-MS, solid-State ^{13}C NMR and FTIR.

In this Chapter we report 1) structural characterization of raw and THF-extracted raw coal;

2) low-temperature catalytic and thermal pretreatments at 300 and 350°C in the absence of any solvent and in the presence of hydrogen-donor tetralin or non-donor 1-methylnaphthalene; and 3) structural characterization of the THF-insoluble part (residue) of the pretreated coal samples.

EXPERIMENTAL

The coal used was a Wyodak subbituminous coal provided by the Penn State Sample Bank (DECS-8). The characteristics of this coal are as follows: 32.4% volatile matter, 29.3 % fixed carbon, 9.9% ash and 28.4% moisture, on a as-received basis; 75.8% C, 5.2% H, 1.0% N, 0.5% S and 17.5% O, on a dmmf basis. The coal was dried in a vacuum oven at 100°C for 2 h before use.

Pretreatment

The pretreatments (or low-temperature liquefaction) of coal were carried out at 300 and 350°C with and without catalyst (ammonium tetrathiomolybdate, 1 wt% of molybdenum of the dmmf coal) and solvents. The solvents used were tetralin, a known H-donor, and 1-methyl-naphthalene (1-MN), a non-donor. Liquefaction was carried out in 25 ml microautoclaves using 4 g of coal and 4g of solvent, under 1000 psi H_2 (cold) pressure. The reaction time was 30 minutes plus 3 minutes for the heat-up time for autoclave to attain the reaction temperature. After the reaction, the liquid and solid products were separated by sequential extraction with hexane, toluene and THF. After the extraction the THF-insoluble residues were washed first with acetone and then with pentane in order to remove all the THF, followed by drying at 110°C for 6 h under vacuum.

Residue Analysis

The residues were analyzed by pyrolysis-GC-MS (Py-GC-MS), cross-polarization and magic angle spinning (CPMAS) solid state ^{13}C NMR and FTIR techniques. The advantages of CPMAS and Py-GC-MS and the experimental details have been described in recent papers (Hatcher et al., 1989; Song et al., 1992b).

Solid-State NMR. The NMR spectra were acquired on a Chemagnetics M-100 NMR spectrometer by using the combined high power proton decoupling, cross-polarization and magic-angle-spinning (CPMAS) techniques. The measurements were carried out at a carbon

frequency of 25.1 MHz. About 0.4-0.6 g of a sample was packed in a bullet-type Kel-F rotor (0.4 ml capacity); the spinning speed of the rotor was about 3.5 kHz. The experimental conditions for all the samples are as follows: a cross-polarization contact time of 1 ms and a pulse delay time of 1 s. An instrumental calibration test was performed with the rotor containing hexamethylbenzene, which was adjusted to the magic angle (54.7°) to give the correct chemical shifts. To assure good spectra with high signal-to-noise ratios, the number of pulses accumulated for obtaining a spectrum was at least 10,000, and most of the spectra were obtained with numbers of scans between 20,000 to 35,000.

Py-GC-MS Analysis. Py-GC-MS analysis was performed on a Du Pont 490B GC-MS system fitted with a 30 m x 0.25 mm i.d. capillary column DB-17 coated with 50% phenylmethylsilicone stationary phase with a film thickness of 0.25 um, and interfaced to a Chemical Data Systems Pyroprobe-1000 pyrolyzer. Helium was used as a carrier gas. The data acquisition and data processing were controlled through a computer-aided system. Prior to the start of data acquisition, the samples were flash-pyrolyzed at 610°C for 10 seconds, during which the pyrolysates (pyrolysis products) were retained in the close-to-inlet part of the capillary column by cooling with liquid nitrogen. The column temperature was programmed from 30°C (or 40°C) to 280°C at a rate of 4°C/min. The mass spectrometer was operated in the electron impact mode at 70 eV. In order to derive information related to the macromolecular network, the low molecular weight species in the coal and coal liquefaction products were removed by THF extraction prior to Py-GC-MS analysis.

FT-IR. The FT-IR analysis of the samples was performed on a Digilab FTS 60 FTIR spectrometer. The samples were analyzed as KBr pellets. A accurately weighed amount (approximately 3 mg) of the vacuum dried samples were ground with a pre-weighed amount of KBr (approximately 300 mg). The pellets were pressed under a pressure of 10 tons. The pellets were dried at 100°C under vacuum for 24 h before recording their infrared spectra.

RESULTS AND DISCUSSION

Characterization of DECS-8 Wyodak subbituminous coal

Figure 9.1 shows the CPMAS ^{13}C NMR spectra of raw DECS-8 coal and THF-extracted DECS-8 raw coal. The NMR spectrum shows two major very broad bands between 0-60 ppm and 90-165 ppm. The first band (0-60 ppm) is due to aliphatic carbons and may also include aliphatic ether carbons. The second region (90-165) is identified as an aromatic region. This band consists of three types of aromatic carbons: an intense peak around 130 ppm (aromatic C), first shoulder at 142 ppm (catechol-like C) and another at 152 ppm (phenolic or aromatic ether C). The other weak and broad bands at 181 and 212 ppm are attributed to carboxylic and ketonic carbons, respectively. The THF-extracted coal did not show any noticeable difference as compared to that of the unextracted raw coal in terms of aromaticity and functionality. THF-extraction, which resulted in the loss of 8% of organic materials from DECS-8 coal, did not produce any apparent changes in its NMR spectrum. This may not be true for some coals; the THF-extracted sample may display a substantially different spectrum for certain coals.

The FTIR spectrum of the THF-extracted raw coal was also recorded and compared with that of the unextracted raw coal, as shown in Figure 9.2. There was no significant difference between the two samples, except that the intensity of hydroxyl band around 3400 cm^{-1} is higher with the raw coal than with the THF-extracted and dried coal. Pre-drying in vacuum prior to THF extraction did not cause any significant changes in the NMR and FT-IR spectra, as can be seen from Figure 9.1 and Figure 9.2, respectively.

Figure 9.3 shows the total ion chromatogram (TIC) from Py-GC-MS of the THF-extracted raw coal up to the retention time 30 minutes, which is a part of the total pyrogram, and the specific ion chromatograms which are indicative of specific compounds. Low-rank coals are known to have higher oxygen functionalities, but the O-containing structural features are not clearly established. As can be seen from Figure 9.3, phenol (m/z 94), alkylphenols (m/z 108 for methylphenol, m/z 122 for ethyl- and dimethylphenol), catechol (m/z 110) and methylcatechol (m/z 124) are the most intense peaks in the pyrogram of the THF-extracted Wyodak subbituminous coal. The other minor oxygen-containing compounds identified are indanol, alkyl-indanol and

hydroxyindene.

There are several intense peaks between 0-2 min (RT) of the pyrogram (Figure 9.3). These peaks are C_5-C_8 alkanes plus alkenes which coelute. There are many more peaks over the whole pyrogram, and selective ion monitoring at m/z 71 indicates that they are long chain alkanes and alkenes. There is another quite intense peak around 25 minutes (RT); it is prist-1-ene, a branched alkene with m/z 266. Overall, Py-GC-MS of the THF-extracted raw coal indicates that Wyodak subbituminous coal contains significant amount of oxygen containing structures including phenol, alkylphenols, catechol and other benzenediols as well as indanols. These observations are consistent with our earlier findings for another subbituminous coal, DECS-9 (13,14).

All the major structural units produced by the flash pyrolysis of the coal other than the alkanes and alkenes are listed in Table 9.2. Among the most abundant hydrocarbons other than alkanes and alkenes are toluene, xylenes and C_3-benzenes. Indene, alkyl indene, dihydroindene, alkyldihydroindene and alkyl naphthalenes are also identified in minor amounts.

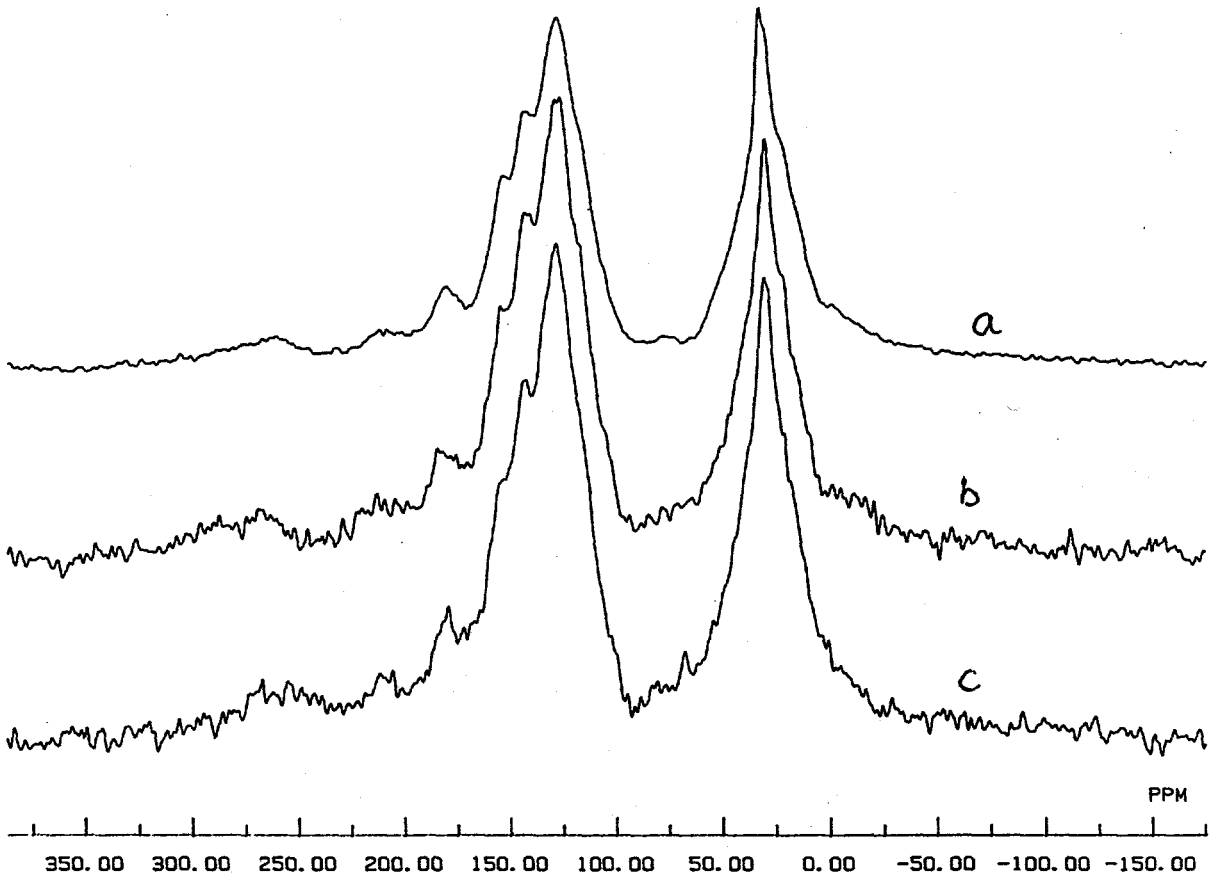

Figure 9.1 CPMAS ^{13}C NMR spectra of the;
a) raw coal;
b) undried and THF-extracted raw coal;
c) dried and THF-extracted raw coal.

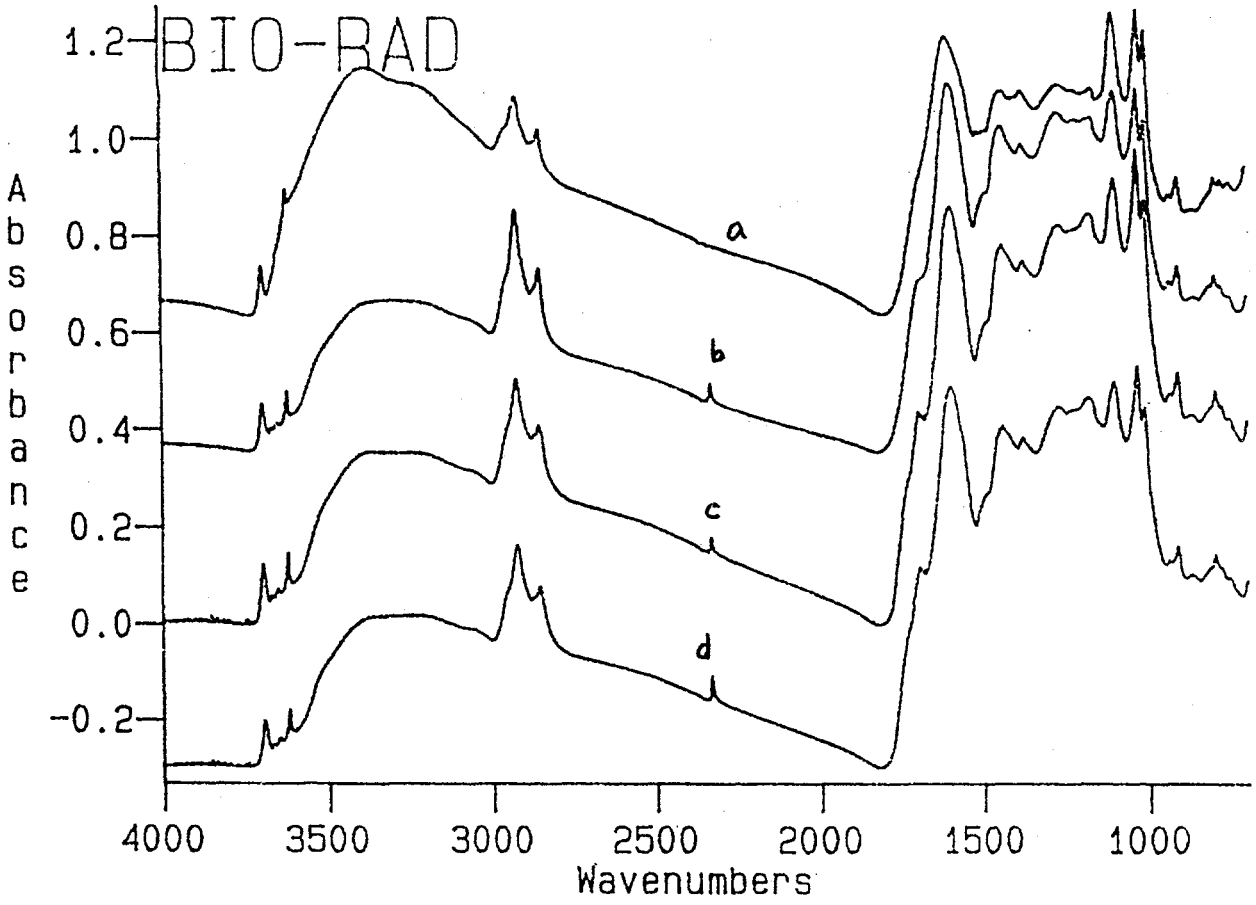

Figure 9.2 FTIR spectra of
a) Undried and unextracted raw coal;
b) Dried and Unextracted raw coal;
c) Undried and THF-extracted raw coal;
d) Dried and THF-extracted raw coal.

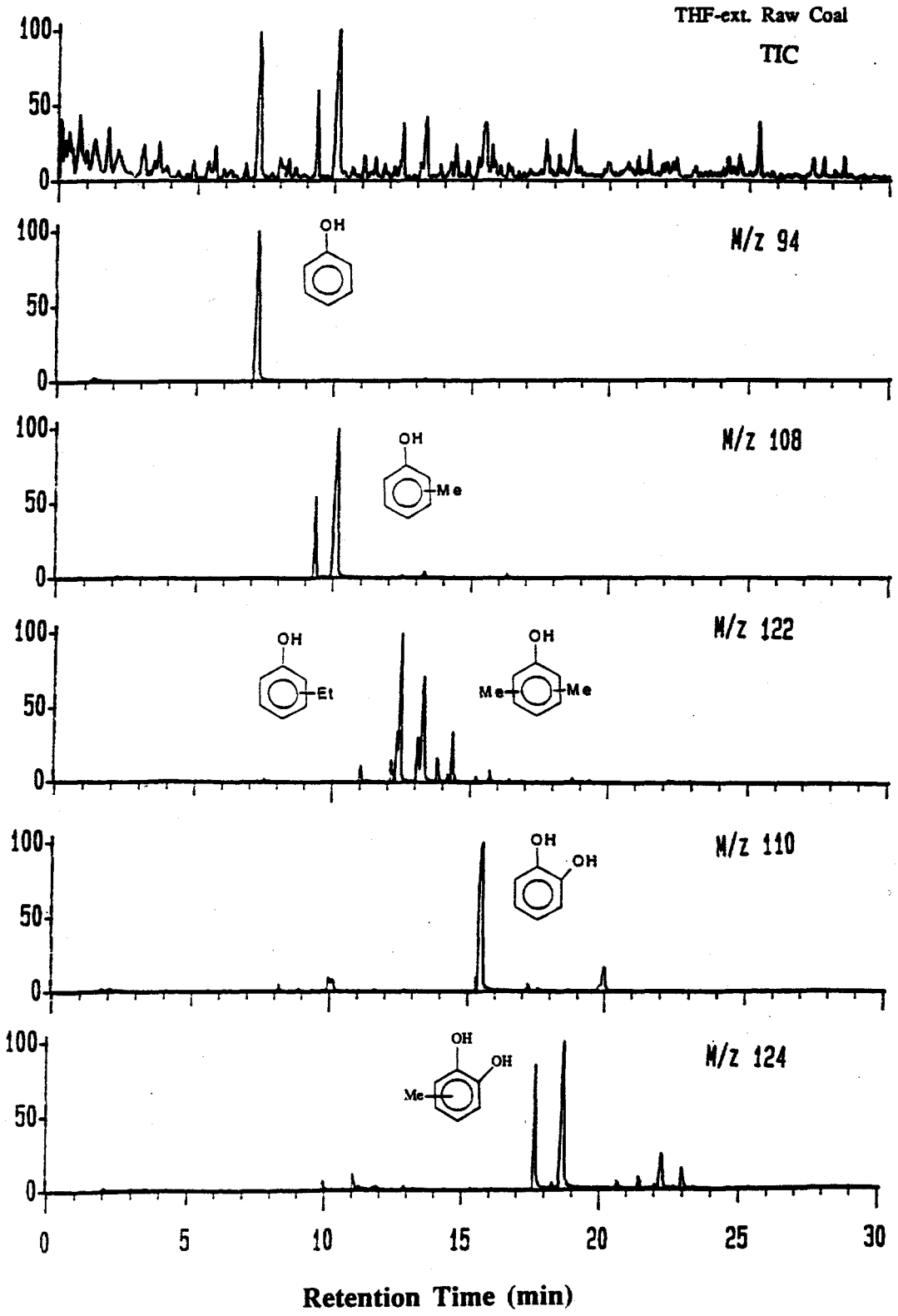

Figure 9.3 Total ion chromatogram (TIC) and specific ion chromatograms (SIC) from Py-GC-MS of the THF-extracted raw DECS-8 wyodak coal.

Low-Temperature Thermal and Catalytic Reactions

Table 9.1 presents the coal conversion data for THF extraction of unreacted coal and pretreatments (low-severity liquefaction) at 300 and 350°C. For the unreacted coal, THF extraction removed about 8 wt% organic materials. The pretreatment at 300°C (with H_2, solvent and no catalyst) gives a very small conversion (11-15%). This conversion is not very significant as compared to the total THF-soluble materials (8%) extracted from the raw coal. The presence of solvents (tetralin or 1-methylnaphthalene) seems to have no appreciable effect on the conversions. The use of catalyst also did not cause any appreciable increase in the conversion at 300°C, because at low temperature ATTM is less likely to decompose into catalytically active phase.

When the pretreatment temperature was increased to 325°C, the use of ATTM impreganted on the coal begin to afford considerable increase in coal conversion (Table 9.1). According to literature, the decomposition of ATTM proceeds by a two-step process, as shown in equations 1-3, which involves first the formation of an amorphous MoS_3 (equation 1), followed by the evolution of sulfur from the intermediate (equation 2) with the more or less simultanesous crystallization (equation 3) of the sulfide (15,16).

$$(NH_4)_2MoS_4 = 2\ NH_3 + H_2S + MoS_3 \qquad 1)$$

$$MoS_3 = MoS_2\ (\text{amorphous}) + S \qquad 2)$$

$$MoS_2\ (\text{amorphous}) = MoS_2\ (\text{crystalline}) \qquad 3)$$

On the other hand, Vasudevan (16b) stated that thermal decomposition of ATTM in inert gas atmosphere is known to produce Mo sulfide containing excess sulfur according to the equation 4; however, thermal decomposition of supported ATTM in hydrogen produces molybdenum sulfide having a valence state lower than 4 according to equation 5.

In inert gas: $(NH_4)_2MoS_4 = 2NH_3 + H_2S + (3\text{-}y)\ S + MoS_y$ 4)

In H_2 gas: $(NH_4)_2MoS_4 + y\ H_2 = (NH_4)_2S + y\ H_2S + MoS_{3\text{-}y}$ 5)

Table 9.1 Non-Catalytic and Catalytic Treatment of DECS-8 Wyodak Coal at 300-375°C for 30 min under 6.9 MPa H_2

Expt	Coal	Dis.	Temp	Solvent	CO	CO_2	C_1-C_4	Oil[a]	Asphal.	Preasp.	Tot. Conv.	H from[a]	H from[a]
No.		Catalyst	(°C)				dmmf	wt%			dmmf wt%	H_2 Gas	Tetralin
3/240	raw	n/a	n/a	n/a	--	--	--	2.5(1.5)[b]	1.8	3.8	8.1	--	--
3a	dried	n/a	n/a	n/a	--	--	--	2.6(1.6)[b]	2.2	3.7	8.5	--	--
4	dried	none	300°C	none	0.18	1.9	0.03	2.1	2.6	2.8	11.3	0.19	
5	dried	none	300°C	Tetralin	0.10	1.4	0.04	1.8	2.9	4.2	13.4	0.16	
6	dried	none	300°C	1-MN	0.08	1.4	0.04	4.9	3.8	4.7	13.8	0.21	
13	dried	ATTM	300°C	none	0.15	1.3	0.04	2.4	1.2	6.1	10.6	0.20	
14	dried	ATTM	300°C	Tetralin	0.06	1.1	0.04	4.0	2.7	4.0	11.6	0.20	
15	dried	ATTM	300°C	1-MN	0.06	1.1	0.05	4.4	2.0	5.1	12.5	0.17	
238	dried	ATTM	325°C	Tetralin	0.08	2.4	0.17	11.0	6.5	7.2	29.8	0.30	
7/16/172	dried	none	350°C	none	0.20	4.3	0.2	2.1	2.6	4.5	14.5	0.22	
173	dried	none	350°C/N_2	none/N_2	0.14	3.8	0.2				14.7		
8/17/22	dried	none	350°C	Tetralin	0.19	4.1	0.2	4.1	7.6	10.0	25.9	0.29	0.41
9/18/23	dried	none	350°C	1-MN	0.16	4.3	0.2	1.1	5.8	7.4	18.3	0.45	
10/19/227	dried	ATTM	350°C	none	0.19	2.3	0.3	10.0	5.4	10.0	29.8	1.92	
11/20/24	dried	ATTM	350°C	Tetralin	0.13	2.6	0.3	10.2	12.9	10.6	36.4	1.35	0.08
12/21/25	dried	ATTM	350°C	1-MN	0.11	3.4	0.3	6.1	10.1	12.3	31.1	1.00	
228	dried	ATTM	375°C	none	0.12	7.1	1.3	15.3	15.6	10.3	48.4	1.81	

a) H consumption, wt% based on dmmf coal.

b) The amount of physically recovered hexane-soluble oils is indicated in parenthesis.

b) Raw (fresh, as-received) coal, which contains moisture, was directly used for liquefaction.

Previous work (17,18) in this laboratory and the present work indicated that under H_2 pressure, ATTM decomposition at ≥ 325°C begin to produce catalytically active species for coal conversion. As can be seen from Table 9.1, the run using impregnated ATTM at 325°C produced higher coal conversion and oil yield than the non-catalytic runs at 350°C. This shows that ATTM has decomposed, at least partially, into some catalytically active species at 325°C. The results from the pretreatment or low-severity liquefaction at 350°C, given in Table 9.1, show an appreciable effect of catalyst and solvent on the total conversion and quality of the products. In the non-catalytic pretreatment, the variation in the total conversion with the solvent is quite significant, with a maximum conversion observed in the presence of tetralin.

The total conversions in a solvent-free run and the run with 1-MN are not much different from that at 300°C but with tetralin as a solvent the difference is significant. The presence of catalyst (ATTM) in the run at 350 °C shows a drastic increase in the total conversion with or without solvent. The larger increase in conversion is in the solvent-free liquefaction, though the total conversion is maximum in the presence of tetralin.

Characterization of the Pretreated Coal

CPMAS ^{13}C NMR

Figure 9.4 compares the CPMAS ^{13}C NMR spectra for the THF-extracted raw DECS-8 coal and the coal after thermal pretreatment at 300°C without any catalyst. Figure 9.5 compares the CPMAS ^{13}C NMR spectra for the THF-extracted raw DECS-8 coal and the coal after catalytic pretreatment at 300°C using ATTM. The residue from the reaction at 300°C displays a spectrum very much similar to that of the residue from the raw coal. The residues produced after the pretreatments at 300°C in the absence and presence of solvents with and without catalyst share the same CPMAS ^{13}C NMR spectral features with those of the THF-extracted raw coal. The only apparent difference is that the catecholic shoulder around 142 ppm is smaller with the pretreated coal than with the raw coal. Integration of the spectrum gives only a slight increase in the aromaticity in the case of pretreated coal. This increase was relatively less when catalyst was used in the pretreatment reaction.

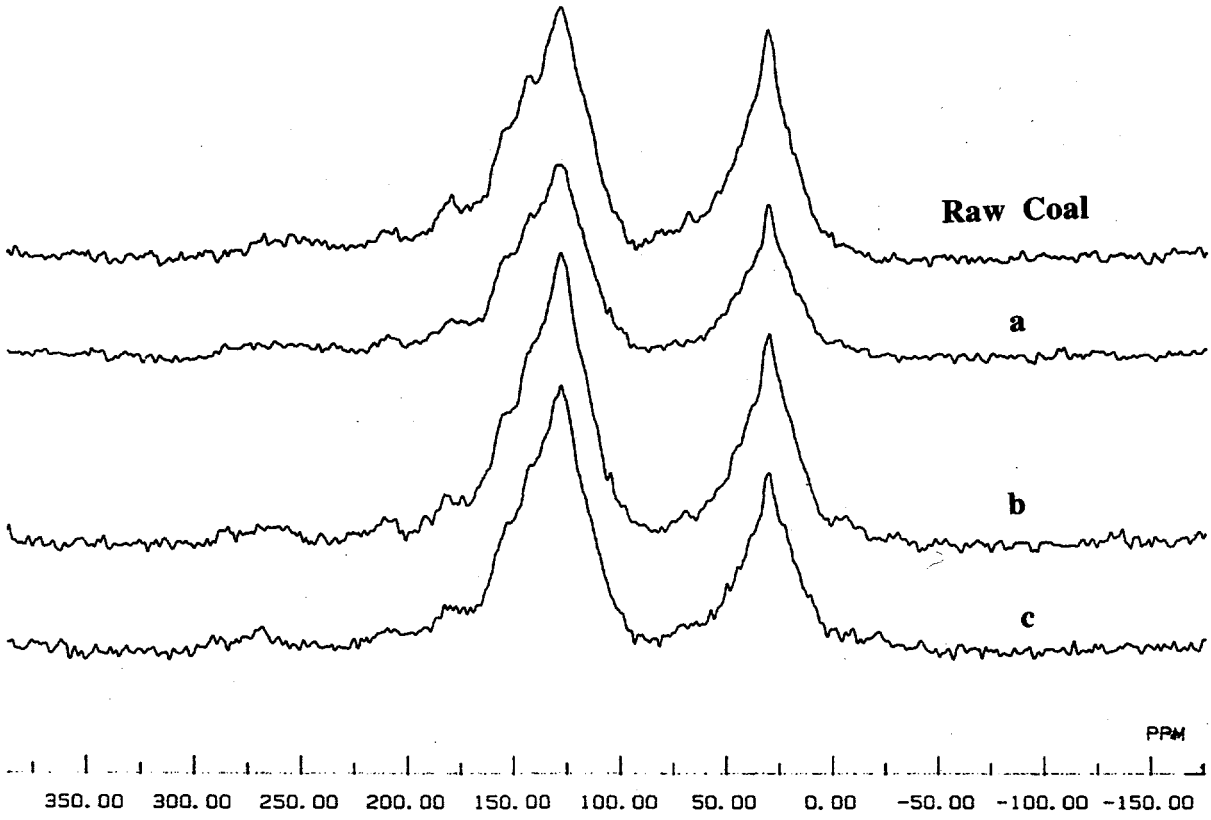

Figure 9.4 CPMAS ^{13}C NMR spectra of THF-insoluble residues from preliquefaction of coal at 300 °C without catalyst
a) solvent free;
b) with tetralin as solvent;
c) with 1-methylnaphthalene as solvent.

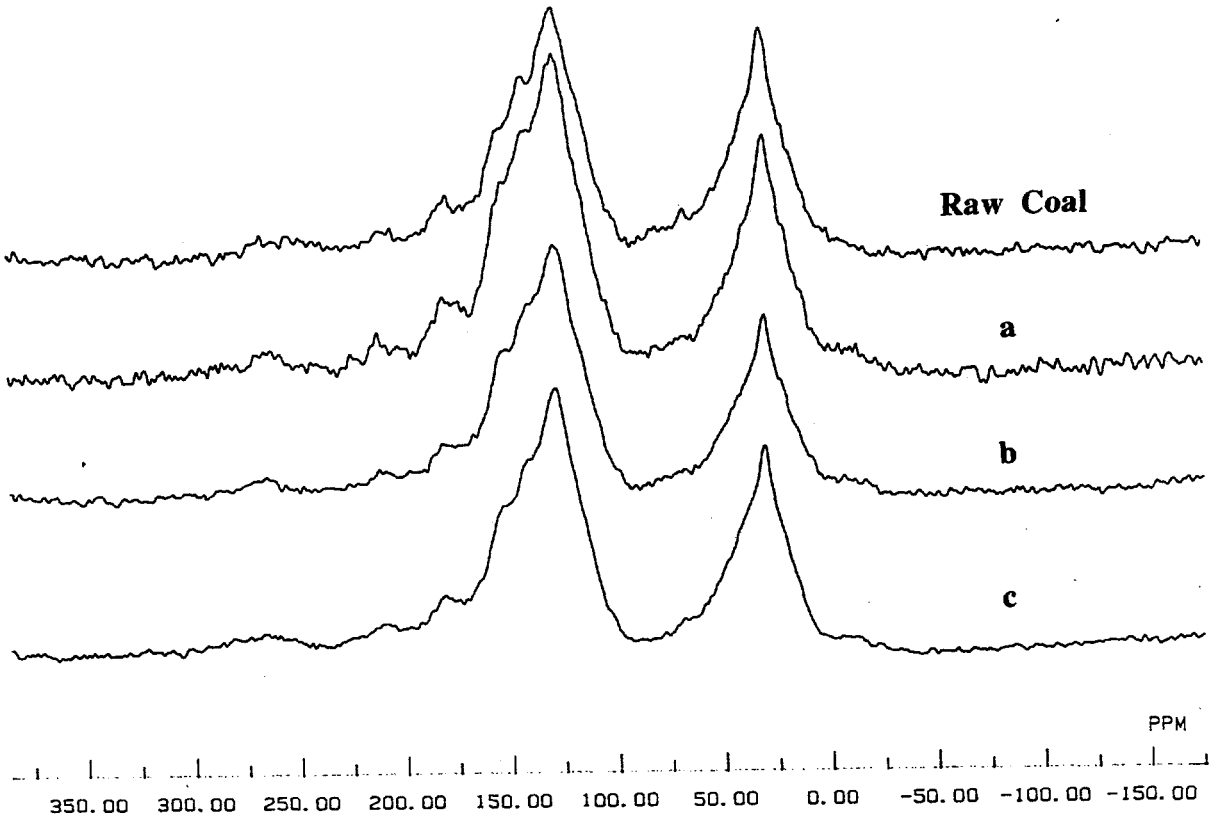

Figure 9.5 CPMAS ^{13}C NMR spectra of THF-insoluble residues from preliquefaction of coal at 300 °C in presence of ATTM;
a) solvent free;
b) with tetralin as solvent;
c) with 1-methylnaphthalene as solvent.

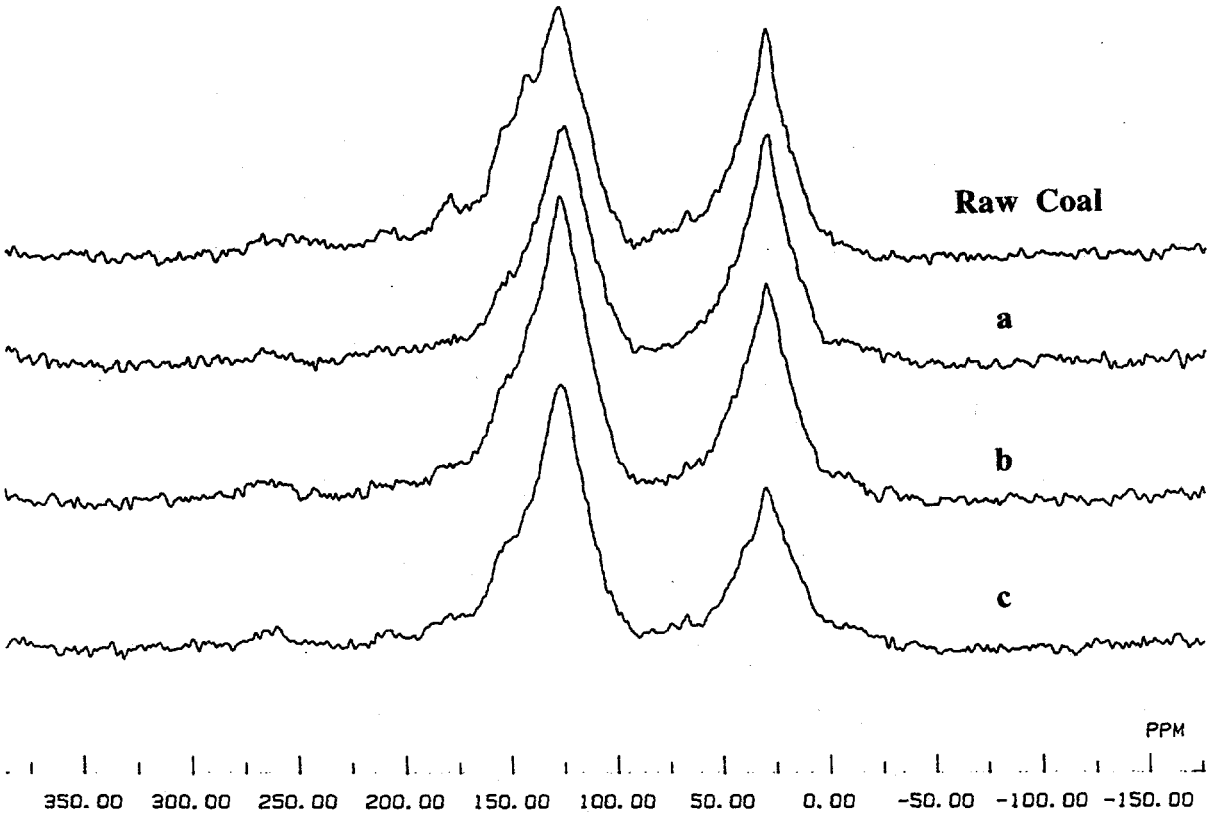

Figure 9.6 CPMAS ^{13}C NMR spectra of THF-insoluble residues from preliquefaction of coal at 350 °C without catalyst
a) solvent free;
b) with tetralin as solvent;
c) with 1-methylnaphthalene as solvent.

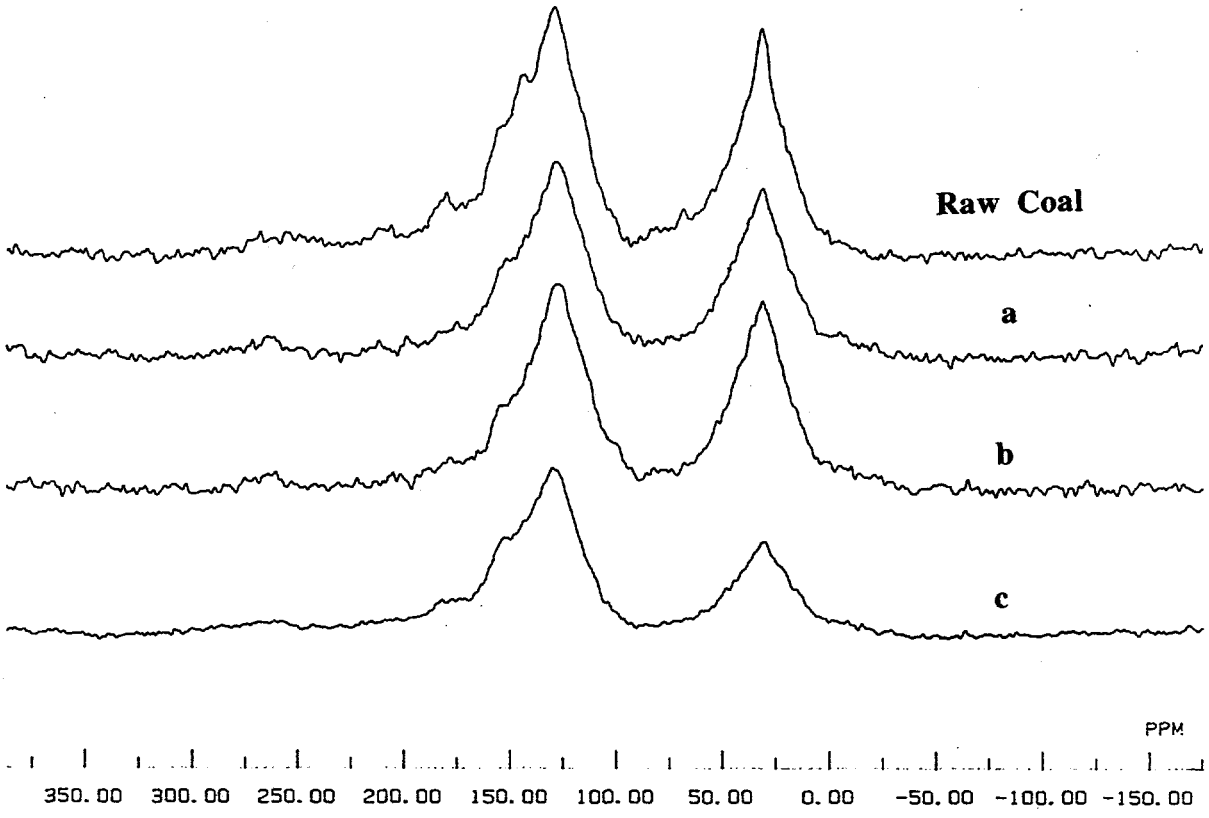

Figure 9.7 CPMAS ^{13}C NMR spectra of THF-insoluble residues from preliquefaction of coal at 350 °C in presence of ATTM;
a) solvent free;
b) with tetralin as solvent;
c) with 1-methylnaphthalene as solvent.

Figure 9.6 and Figure 9.7 show the CPMAS ^{13}C NMR spectra for the THF-insoluble parts of thermally (non-catalytically) and catalytically pretreated DECS-8 coal, respectively. The residues from runs at 350°C show different spectra as compared to the raw coal. The catecholic (142 ppm) and carboxylic (181 ppm) bands almost disappeared after the run at 350°C and there is a slight decrease in the intensity of the phenolic (152 ppm) band. The residues obtained from the liquefaction at 350 °C in presence of a solvent (tetralin or 1-MN) were also characterized by NMR. As compared to that of the solvent-free run, the residue from the run with tetralin shows slightly more of catechol-like carbons, but less intense than that of the THF-extracted raw coal. Also a decrease in the aliphatic band is observed. With 1-MN as a solvent the decrease in the aliphatic band is very prominent but the aromatic region shows similar functionality to that of the residue from solvent-free run.

We have seen that the presence of catalyst improves the total conversion at 350°C. However, CPMAS NMR spectra of the samples from catalytic runs appear to be similar to those from thermal runs. Integration of the NMR spectra reveals that the the residues from catalytic runs have slightly lower aromaticity values than those from non-catalytic runs.

FTIR Spectroscopy

Figure 9.8 and Figure 9.9 show the FT-IR spectra of the THF-insoluble residues from thermally and catalytically pretreated DECS-8 coal, respectively, at 300°C. The analysis of the residues produced from pretreatment at 300°C showed no marked changes in the FTIR spectrum as compared to that of the THF-extracted raw coal, except a slight decrease in the aliphatic band in the 2950 cm^{-1} region. Using a solvent during the liquefaction also did not cause any appreciable difference in the FTIR spectra of the residues.

The residue produced after the liquefaction in presence of catalyst showed a slight decrease in the ether region (1110-1300 cm^{-1}). This becomes more apparent with the comparison of relative intensity of peaks in the ether region (1110-1300 cm^{-1}) with those of mineral matter peaks (at 1010, 1033, and 1100 cm^{-1}). Moreover, relative to the mineral matter peaks, the intensity of the C=C strecting band at 1600 cm^{-1} is always lower with the catalytically treated samples than with the thermally treated samples.

Figure 9.10 shows the FTIR spectra of the residues from pretreatment at 350°C (solvent-free) with and without catalyst, along with that of the THF-extracted raw DECS-8 coal. Figure 9.11 and Figure 9.12 show the FT-IR spectra of the THF-insoluble residues from thermally and catalytically pretreated DECS-8 coal, respectively, at 350°C. There are some changes apparent in the FT-IR spectra of coal after pretreatment at 350°C. There is a decrease in the carbonyl band at 1700 cm^{-1} (presumably due to carbonyl loss) and hydroxyl region at 3400 cm^{-1}. In the presence of catalyst, which improves the total conversion at 350°C, the effect on the ether region is significant. The residue produced after the pretreatment at 350°C in presence of catalyst showed a slight decrease in the ether region (1110-1300 cm^{-1}), as also observed in the case of 300°C runs. It thus appears that catalyst has enhanced the cleavage of the ether bonds in the coal network. The FT-IR difference spectra between the catalytically treated and thermally treated samples also indicate that using a Mo sulfide catalyst also increased the content of aliphatic groups, as reflected by the increased intensity of the apilphatic band centered around 2950 cm^{-1} region. These results indicated that the catalytic pretreatment at 350°C not only improves coal conversion, but also induce structural changes in the unconverted organic materials, such as less ether linkages and more aliphatic groups.

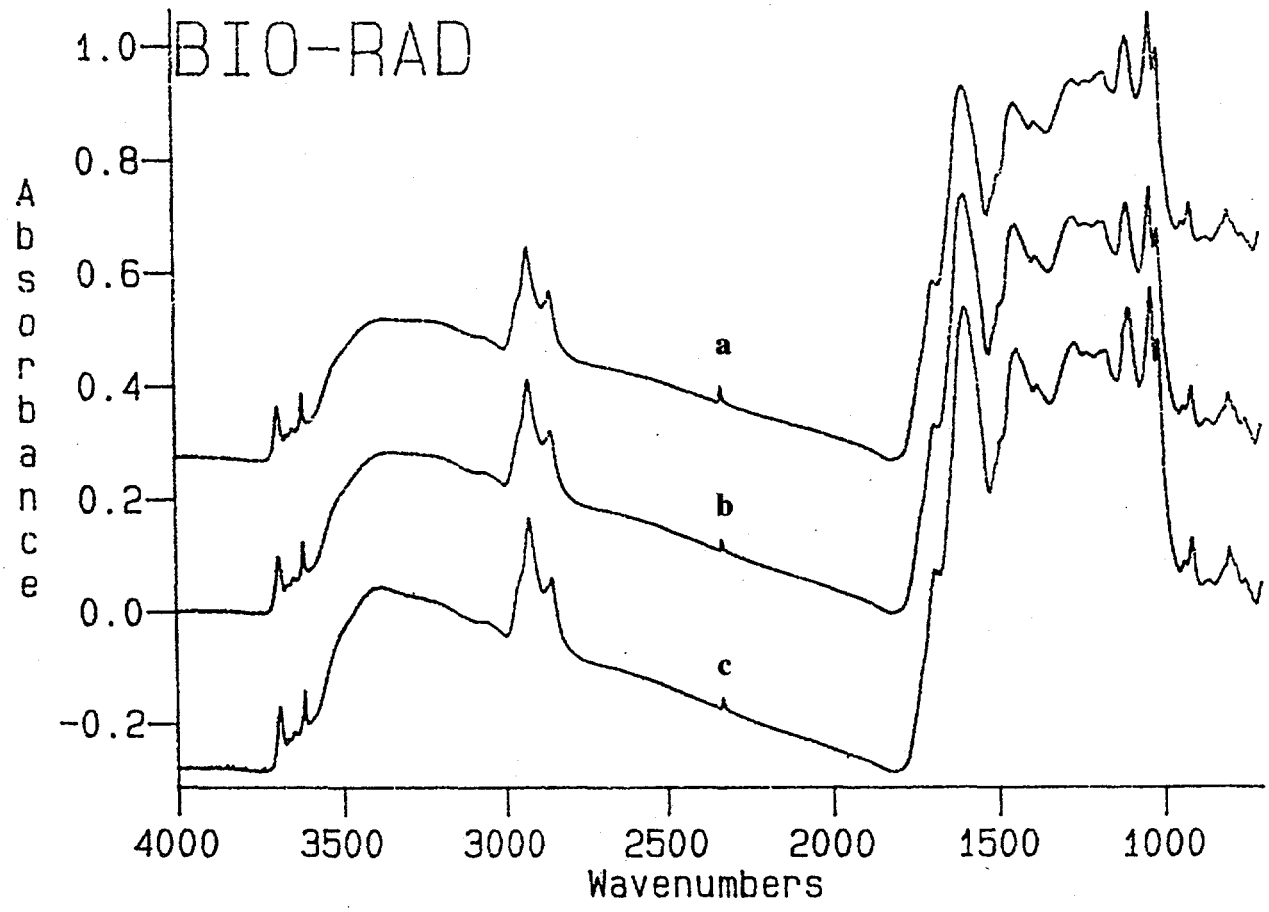

Figure 9.8 FTIR spectra of the THF-extracted coal preliquefied coal at 300 °C without catalyst;
a) solvent free;
b) with tetralin as solvent;
c) with 1-methylnaphthalene as solvent.

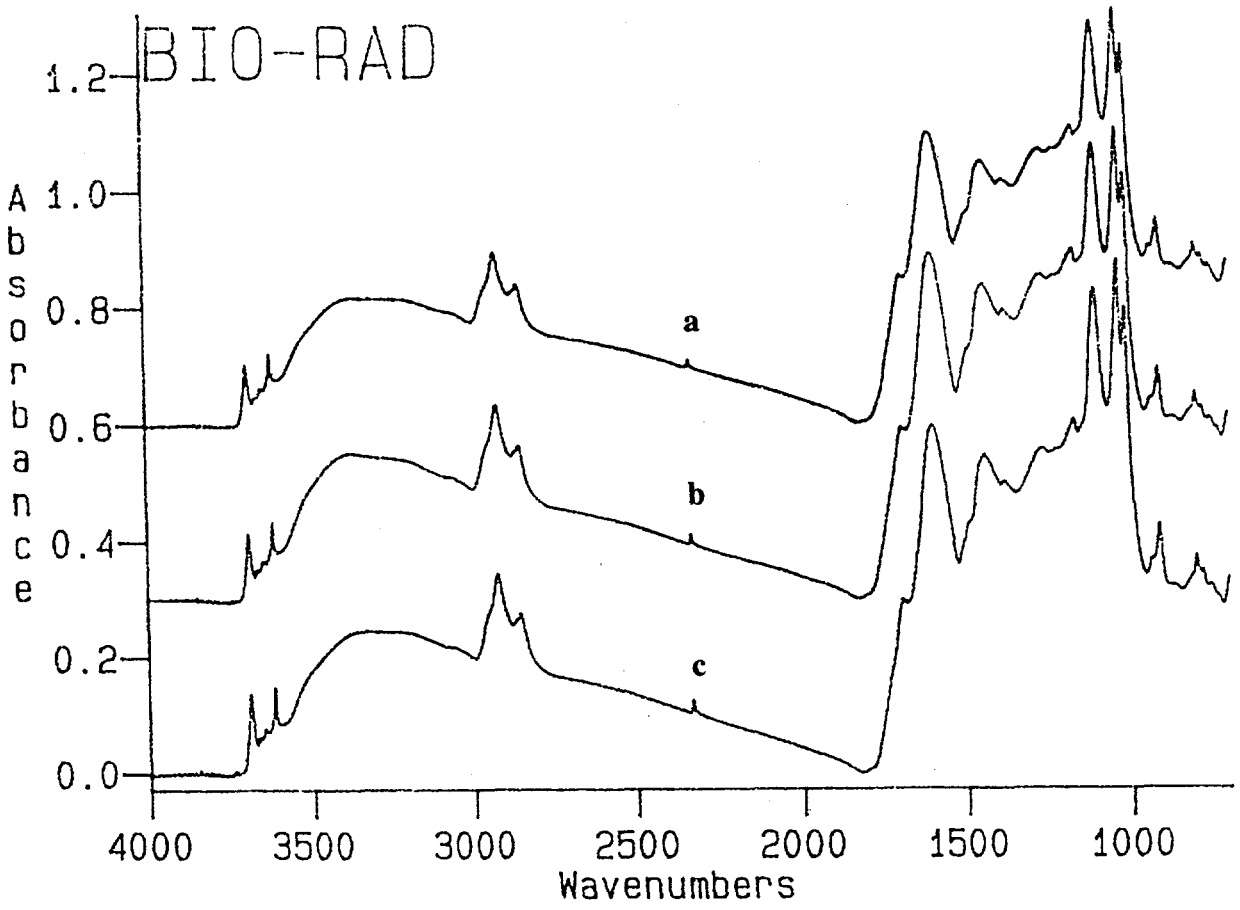

Figure 9.9 FTIR spectra of the THF-extracted coal preliquefied at 300 °C in presence of ATTM;
a) solvent free;
b) with tetralin as solvent;
c) with 1-methylnaphthalene as solvent.

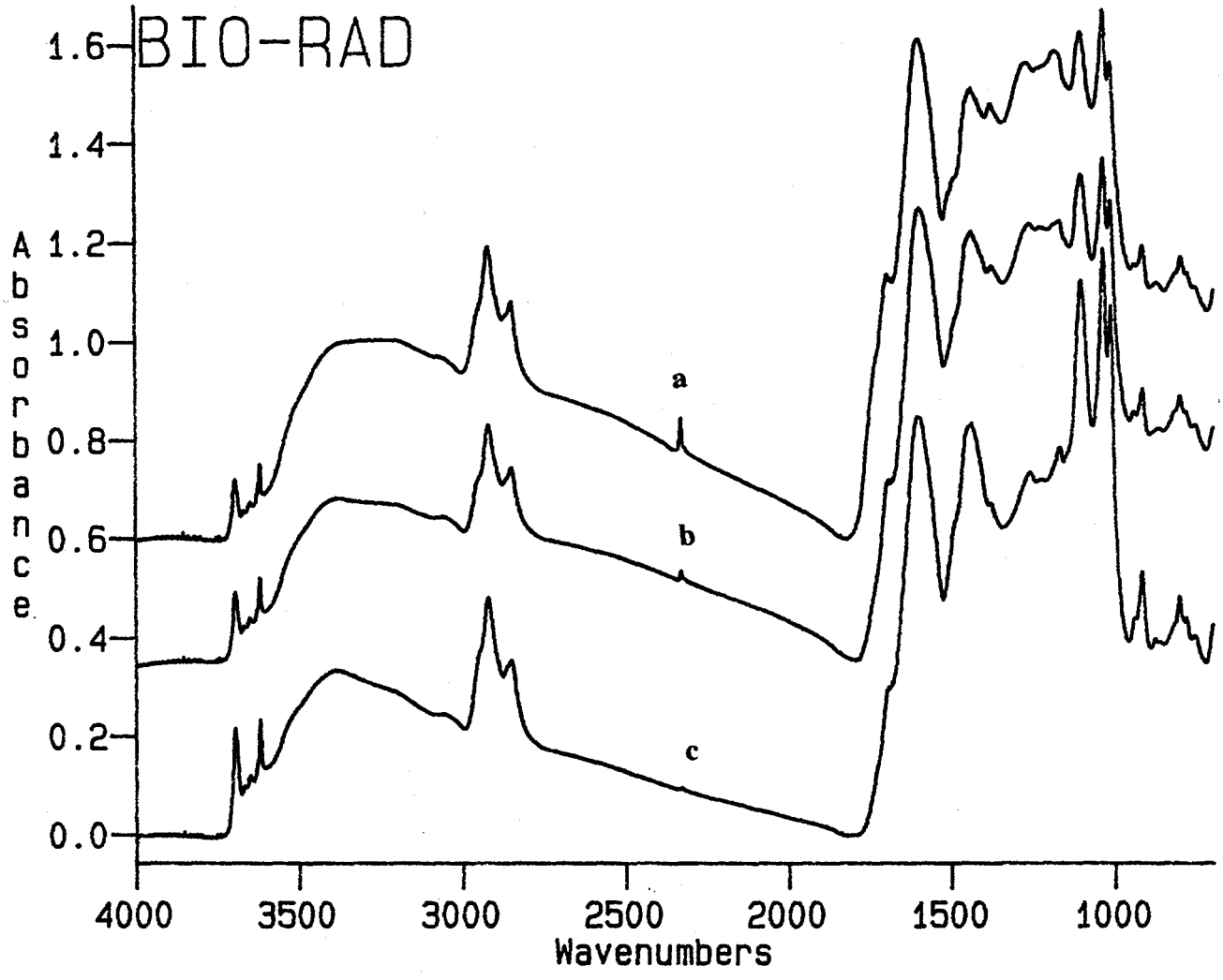

Figure 9.10 FTIR spectra of (a) THF-extracted raw coal and the residues from the solvent-free, (b) thermal, and (c) catalytic liquefactions at 350°C

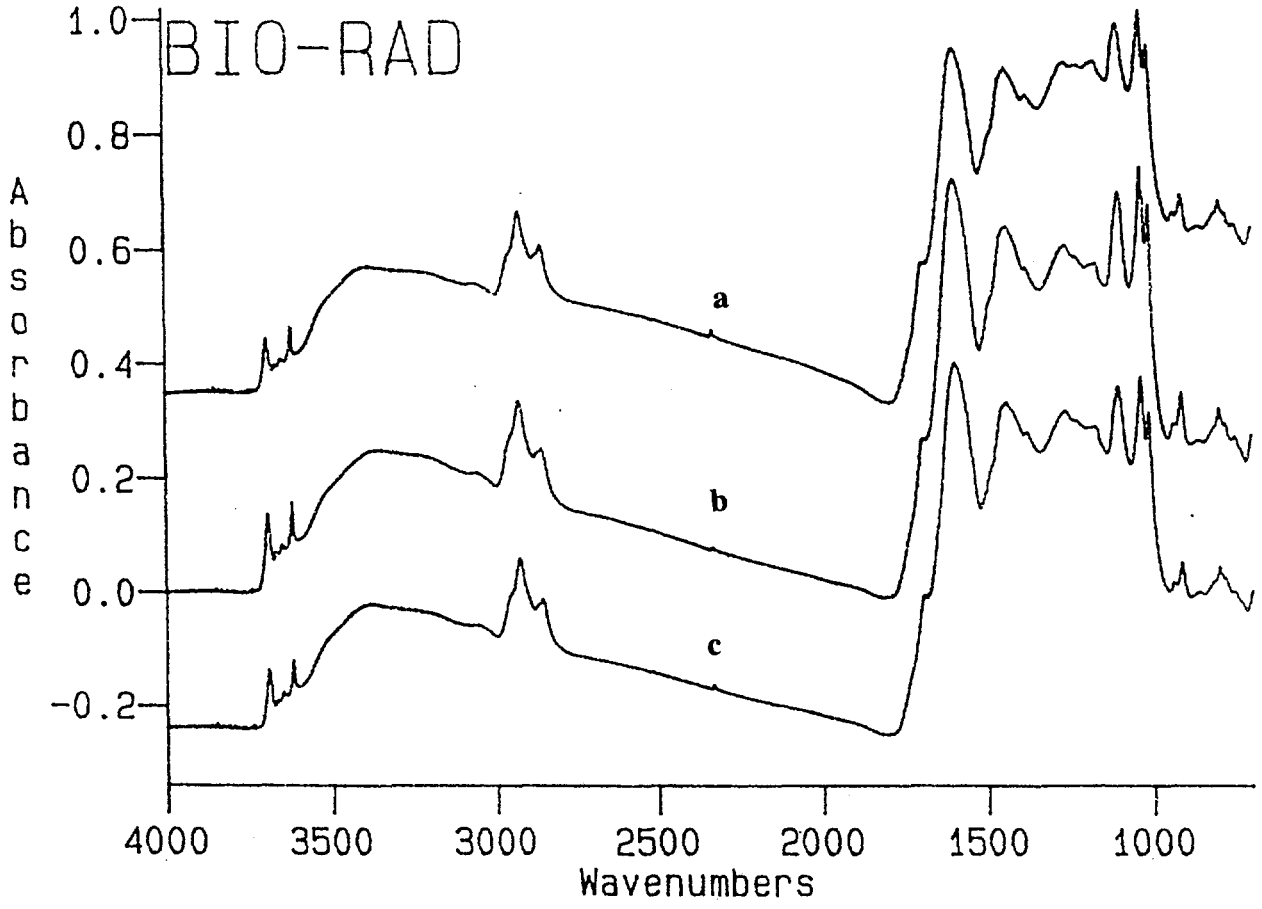

Figure 9.11 FTIR spectra of the THF-extracted coal preliquefied at 350 °C without catalyst;
a) solvent free;
b) with tetralin as solvent;
c) with 1-methylnaphthalene as solvent.

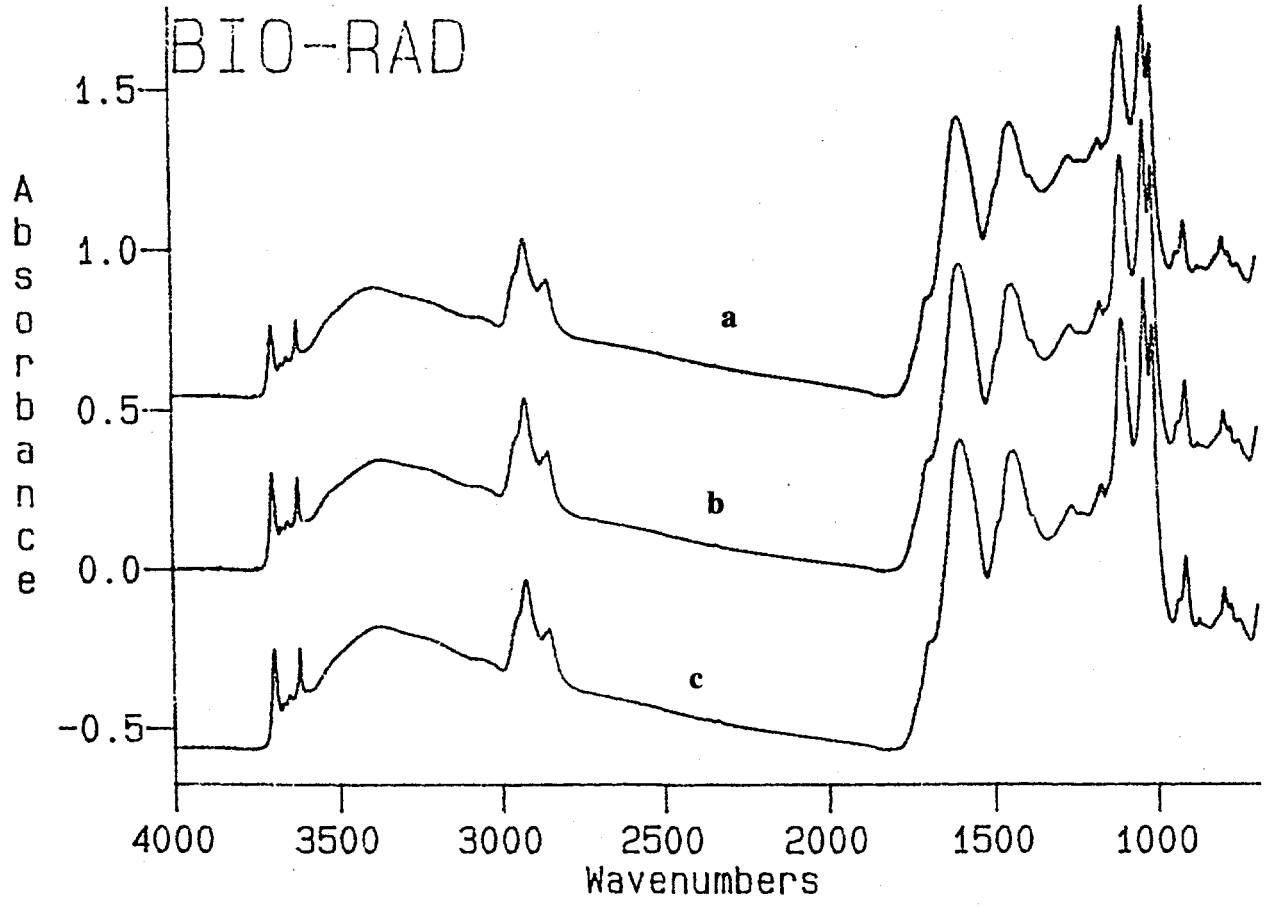

Figure 9.12 FTIR spectra of the THF-extracted coal preliquefied at 350 °C in presence of ATTM;
a) solvent free;
b) with tetralin as solvent;
c) with 1-methylnaphthalene as solvent.

PYROLYSIS-GC-MS

Figure 9.13 shows the selected retention time region of the Py-GC-MS total ion chromatogram (TIC) of the residues from the liquefaction at 300 and 350°C (solvent- and catalyst-free), together with that of the THF-extracted raw DECS-8 coal. Table 9.2 lists the major peaks which are identified in the TIC. Compared to the pyrogram of the THF-extracted raw coal, all the major species such as phenol, alkylphenols, alkylbenzenes, as well as alkanes and alkenes, are formed from the pyrolysis of the residues from the liquefied coal, but there are apparent differences. A substantial decrease in the intensity of the catechol and alkylcatechol peaks in the pyrogram of the residue from the run at 300°C, and the disappearance of these peaks from the pyrogram of the residue from 350°C run, are the most significant. This change in the residue from the 300°C run is not apparent from NMR, but after liquefaction at 350°C the shoulder at 142 ppm in the CPMAS ^{13}C NMR spectrum disappears completely. From this it is clear that reaction at 300°C did cause some structural changes in the coal network.

The residues from the liquefaction experiments at 300 and 350°C in presence of solvents and with and without catalyst were also characterized by Py-GC-MS. The pyrogram of the residues from liquefaction at 300 and 350 °C in presence of tetralin as solvent (with and without catalyst) are shown in Figure 9.14. The peaks identified are given in Table 9.2.

Table 9.3 shows the relative ratios of the oxygen-containing units to the alkylbenzenes before and after liquefaction. For oxygen-containing species the areas of the phenol, alkylphenols and catechol peaks were added, and for alkylbenzenes, toluene, xylenes and C_3-benzenes were used. As compared to that for raw coal, the ratio decreased for the sample from solvent-free run at 300°C, and the sample from the run at 350 °C with 1-MN or without solvent. There ratios show that the presence of solvent does make a difference in the loss of specific type of species from the coal network and it is independent of the catalyst. In solvent-free reaction and with non-donor solvent (1-MN), more oxygen-containing species are lost during liquefaction. In presence of tetralin during the liquefaction, this ratio did not decrease much from that of the raw coal and is highest as compared to the others.

The peaks marked with a letter in the pyrograms in Figure 9.14 are the new peaks observed after liquefaction in presence of a solvent, as also indicated in Table 9.2. When tetralin was used in the pretreatment, an intense naphthalene peak was observed in the residues obtained from both non-catalytic and catalytic runs at either 300 or 350°C. Although not as intense as naphthalene

peak, 2- and 1-methylnaphthalene peaks also appear to be bigger in the runs with tetralin than in the solven-free runs.

Table 9.2. Major identified peaks in pyrograms

No.	MW	Identified Compounds
1	92	Toluene
2	106	p-Xylene
3	106	o-Xylene
4	120	C_3-benzene
5	120	C_3-benzene
6	120	C_3-benzene
7	94	Phenol
8	118	Indane
9	116	Indene
10	108	o-Cresol
11	108	m-+p-Cresol
12	132	Methylindane
13	130	Methylindene
A*	132	Tetralin
14	122	Ethylphenol
B*	130	Dihydronaphthalene
15	122	Ethylphenol
16	122	Dimethylphenol
C*	128	Naphthalene
17	146	Dimethylindene
18	122	Dimethylphenol
19	136	C_3-Phenol
20	110	Catechol
21	136	C_3-Phenol
22	144	Dimethylindene
23	136	C_3-Phenol
24	124	Methylcatechol
25	124	Methylcatechol
D*	142	2-Methylnaphthalene
E*	142	1-Methylnaphthalene
26	110	1,3-Benzenediol
27	134	Indanol
28	134	Indanol
39	132	Hydroxyindene
30	138	C_2-Catechol
31	156	C_2-Naphthalene
32	170	C_3-Naphthalene

* The compounds identified in Py-GC-MS profiles (Figure 4) of the residues from the liquefactions in presence of tetralin.

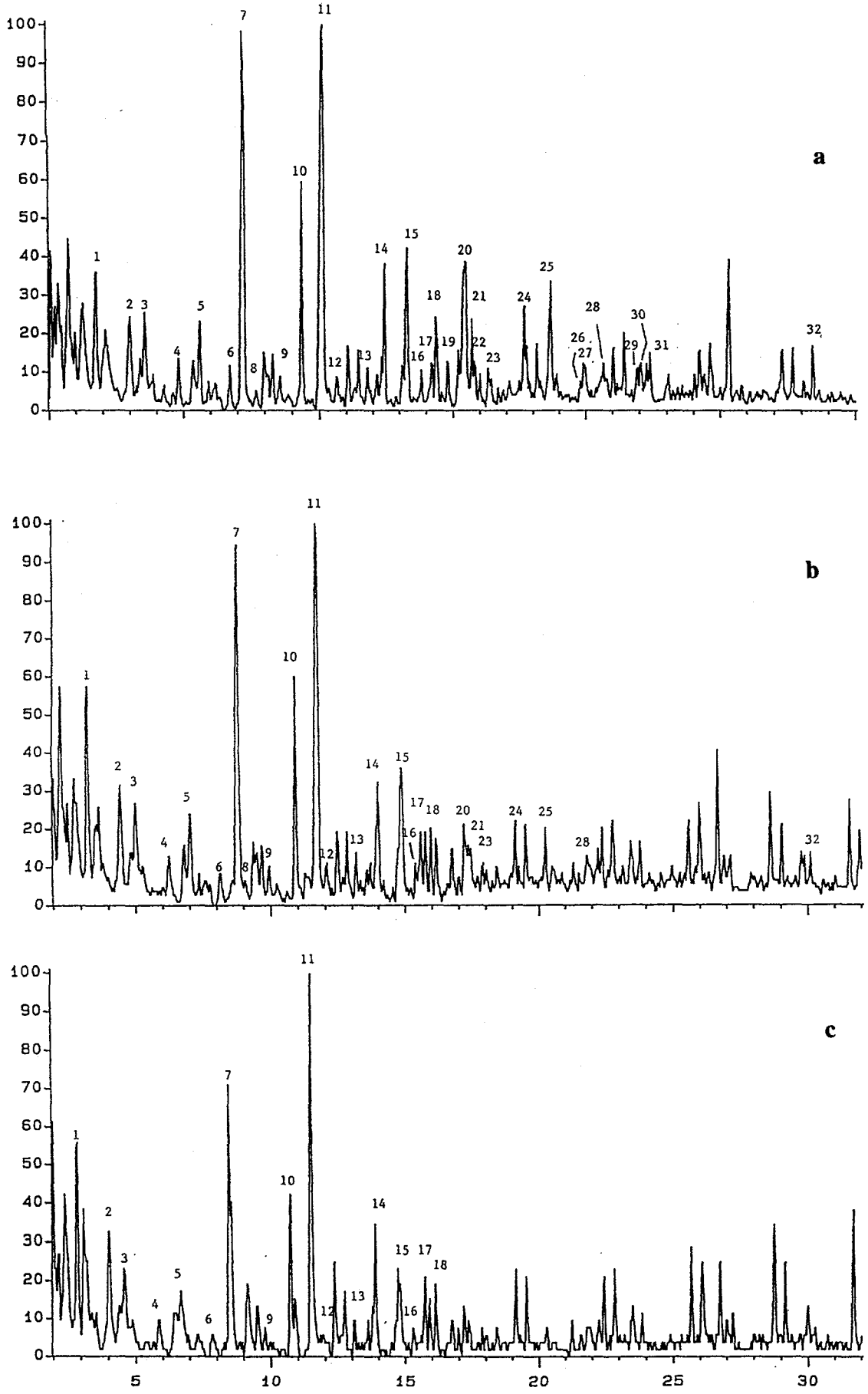

Figure 9.13 Py-GC-MS profiles of (a) THF-extracted raw coal and the residues from the thermal liquefactions at (b) 300°C, and (c) 350 °C.

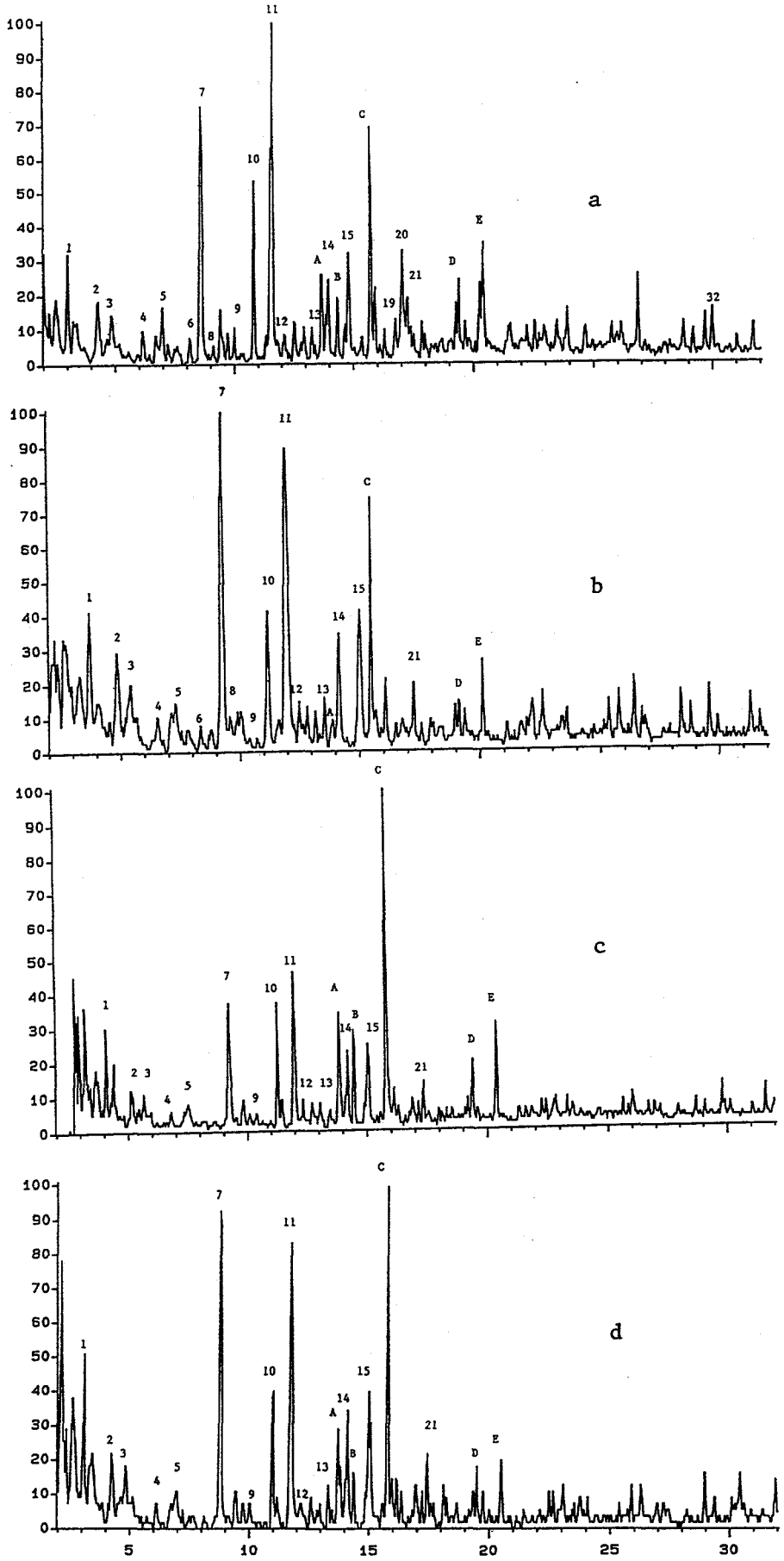

Figure 9.14 Py-GC-MS profiles of the residues from the liquefactions in presence of tetralin, (a) thermal, (b) catalytic at 300°C, and (c) thermal, (d) catalytic at 350°C.

Table 9.3. Ratios of the amount of the oxygen-containing units to the alkylbenzene units.

Temperature (°C)	Solvent	Ratio Phenolic/Alkylbenzenes	
		Thermal	Catalytic
Raw Coal		3.6	
300	none	2.4	2.5
300	Tetralin	3.5	3.1
300	1-MN	3.6	3.2
350	none	2.3	2.4
350	Tetralin	3.2	3.1
350	1-MN	1.9	2.3

The methylnaphthalene peak observed here was also seen in the case of a solvent-free run, but with a very low intensity. These new peaks appear to have come from the adduction of solvent because they were not observed in the Py-GC-MS profiles of the residues from the solvent-free runs. When 1-methylnaphthalene was used as solvent, the tetralin and dihydronaphthalene peaks were not observed and the 1-methylnaphthalene peak was very intense, showing that it is due to the solvent . The naphthalene peak was relatively weak in presence of 1-methylnaphthalene, as compared to that in the presence of tetralin. Since the residue was extracted with THF for 24 h and dried, the solvent remaining in the residue must be either chemically bound or physically entraped in the solvent-inaccessible micropores, or both, as also noted in an earlier work (14).

In the residue from the liquefaction in the presence of catalyst and solvent, the adduction of solvent was decreased, as shown by the decreased intensity of the solvent peak in the pyrogram. The reason for the decreased adduction of solvent molecules could be due in part to the formation of reduced number of free radicals from the solvent molecules in presence of catalyst. This is also supported by the decreased amount of hydrogen transfer from tetralin and increased amount of hydrogen gas consumption during liquefaction in presence of catalyst compared to that of the catalyst-free experiment.

Nature of Solvent Incorporation Examined by Using Tetralin-d_{12}

As mentioned above, we observed solvent incorporation in the pretreatment using a solvent. Figure 9.15 illustrates this trend with tetralin and 1-methylnaphthalene (1-MN) solvent. To clarify whether the peaks due to solvent can be attributed to physically trapped or chemically bound solvent molecules, we performed a pretreatment of vacuum-dried (100°C-2h) DECS-8 coal using deuterium-labled compound, tetralin-d_{12} (0.5 g coal, 0.5 g tetralin-d12, 350°C, 30 min, 6.9 MPa H_2). Although the peaks due to solvent appears to be dominant in the pyrograms in Figure 9.15, it is estimated that the solvent incorporation can not be more than a few percent based on coal. This is based on the fact that the CPMAS NMR spectra and FT-IR spectra of the residues from solvent-free runs and the corresponding runs with either tetralin or 1-MN solvent are relatively similar to each other.

Figure 9.16 shows the TIC from Py-GC-MS of the THF-insoluble residue obtained from the pretreatment. The most intense peak in the TIC is naphthalene. The expanded retention time window for naphthalene between 14-16 min, the corresponding SIC at m/z 135 and m/z 136, and the mass spectra for the peak are also given in Figure 9.16. Pure naphthalene shows one single most intense peak at m/z 128 for non-deuterated compound, and at m/z 136 for completely deuterated compound. They have M-1 peak but its intensity is much lower than that of molecular ion. The naphthalene peak in Figure 9.16 consists of two components. One is completely deuterated naphthalene-d_8 (m/z 136), and in the other, one of the deuterium in naphthalene-d_8 is replaced by hydrogen (m/z 135). The mass spectra at both positions **a** and **b** in Figure 9.16 are mixture of two components, with more m/z 136 at position **a** but more m/z 135 at position **b**.

Since completely deuterated solvent tetralin-d12 was used, the peak of naphthalene-d_8 with m/z 136 can be attributed to physically imbibed solvent (tetralin) molecules or the converted (H-consumed) solvent (naphthalene) molecules. The peak component of naphthalene-d_7 with m/z 135, however, may be attributable, at least in part, to the chemically bonded solvent molecules to the coal organic material.

Figure 9.17 illustrates our mechanistic consideration for the formation of components with m/z 136 and m/z 135 from tetralin-d_{12} with m/z 144. When tetralin is used, the coal-derived radicals can abstract H from the hydroaromatic ring to give a relative stable 1-tetrallyl radical, which reacts with another radical to form 1,2-dihydronaphthalene (DHN). DHN can readily react in a step wise manner with two radicals to form naphthalene. Most of these products can be

extracted and recovered after the reaction. However, a small portion of these solvent molecules are trapped into the small pores, which upon cooling shrink further and become inaccessible by the extraction solvent molecules, not even with THF solvent. This explains the peak component of naphthalene-d_8 with m/z 136 observed.

A question that arises is, if the trapping is the mechanism, why the naphthalene peak is much higher than tetralin ? This can be explained by considering the diffusion limitation. There are tetralin molecules in the bulk liquid in excess. However, only a limited amount of tetralin diffues into the pore where reactions occur that consumes tetralin to form naphthalene.

The above discussion is concerned with physical aspects of the solvent incorporation. However, solvent incorporation through chemical reaction also occurred during runs at 350°C. This is a consequence of H-abstraction reaction, since tetralin alone is very stable even at 450°C (19). When the H-abstraction from tetrallyl or dihydronaphtyl radicals does not proceed in time, these radicals seek self stabilization by cross-linking into coal organic material or by coupling with other molecular fragments.

Two types of cross-linking are possible: attack of the solvent-derived radical on the aromatic ring systems in coal, and coupling of the solvent-derived radical with the coal-derived immobilized radical. Thus one deuterium in the solvent molecule is replaced by a C-C bond, which breaks down upon pyrolysis to generate a free radical whose abstraction of H leads to naphthalene observed in the pyrograms.

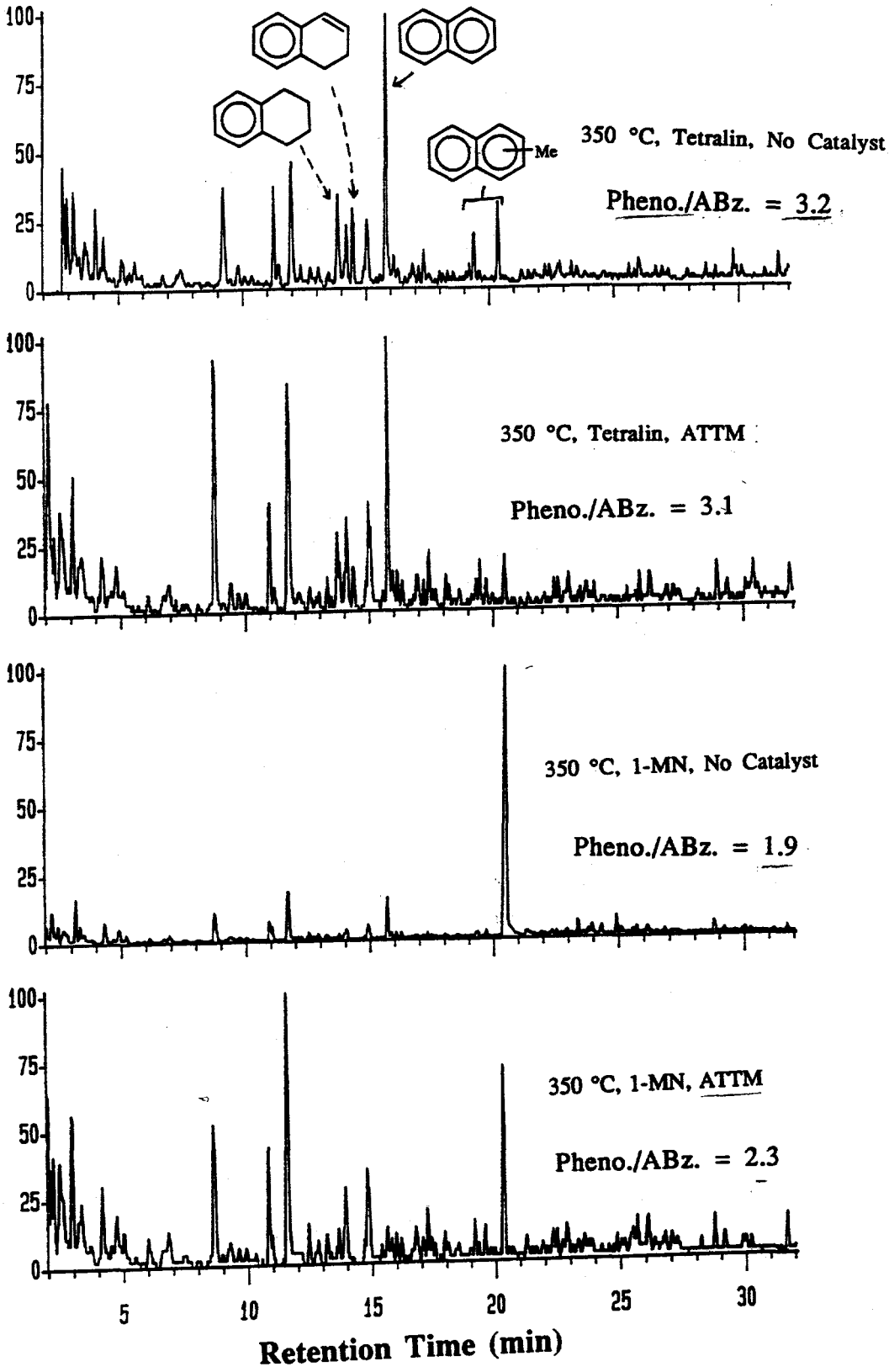

Figure 9.15 Total ion chromatograms from Py-GC-MS of THF-insoluble residues from pretreatments at 350°C with tetralin and 1-MN solvents.

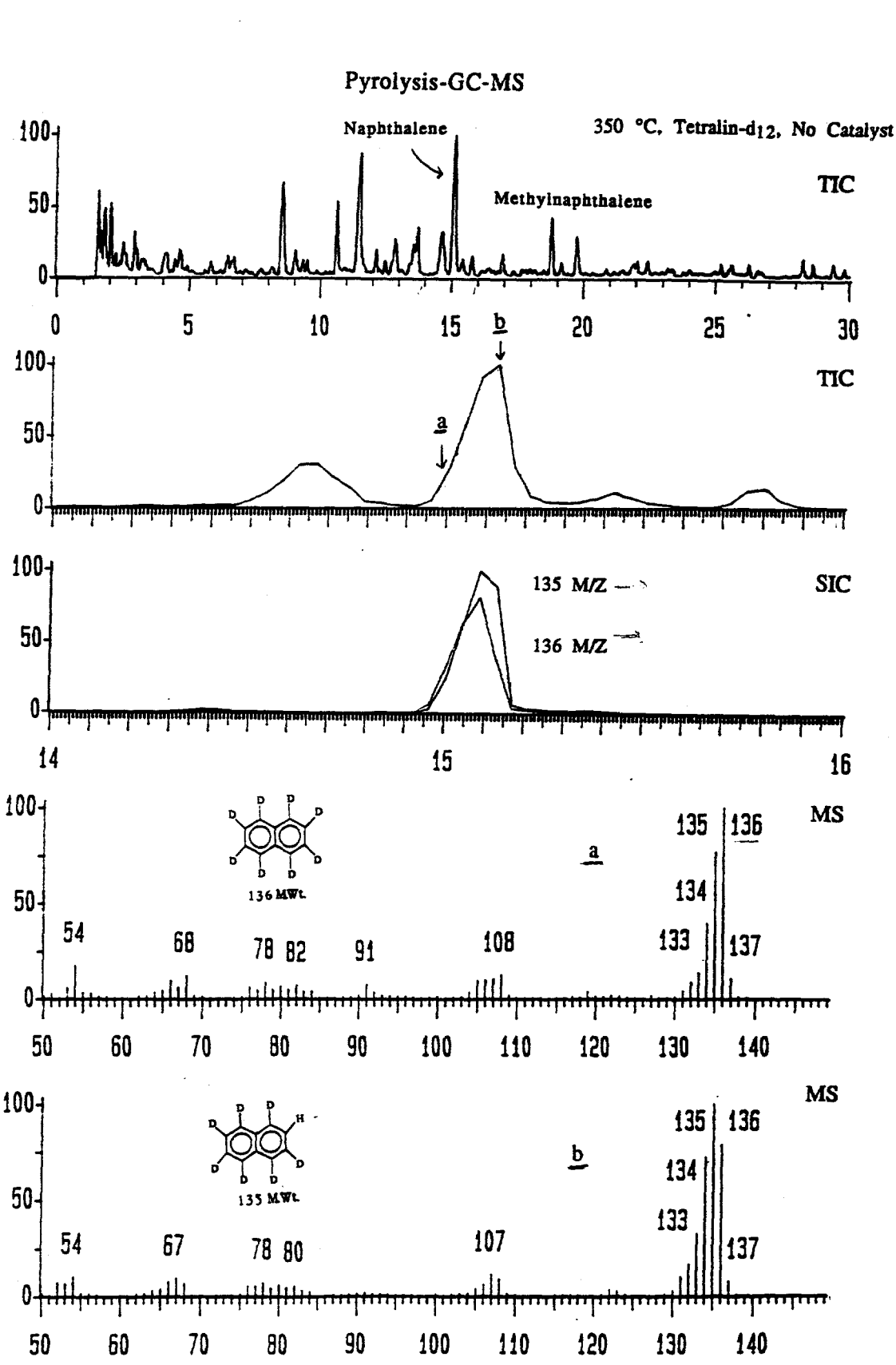

Figure 9.16 TIC and SIC at m/z 135 and m/z 136 from Py-GC-MS of the THF-insoluble residue from the non-catalytic pretreatment of DECS-8 with tetralin-d12 at 350°C.

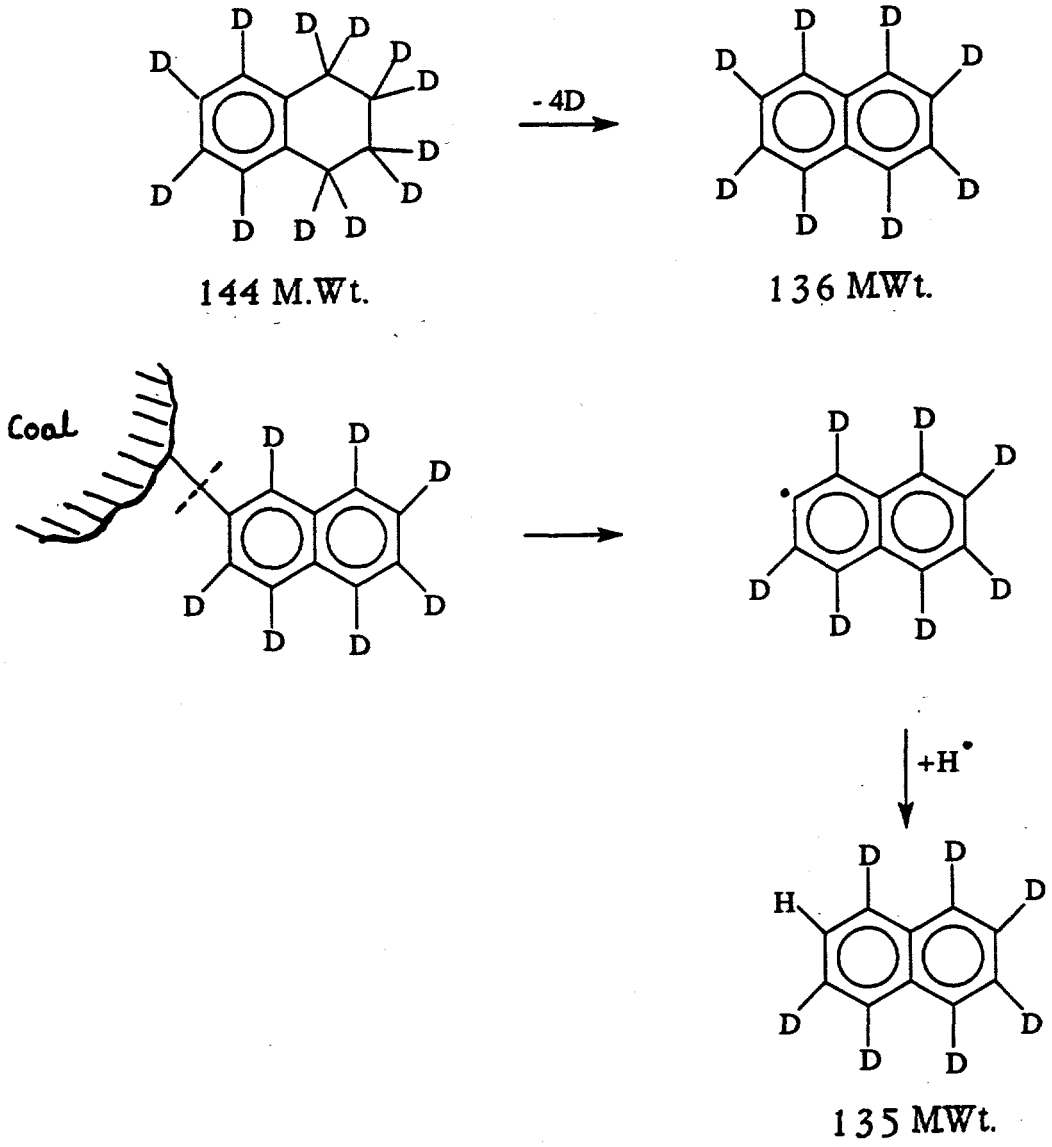

Figure 9.17 Possible modes of reactions leading to m/z 136 and m/z 135 from tetralin-d_{12}.

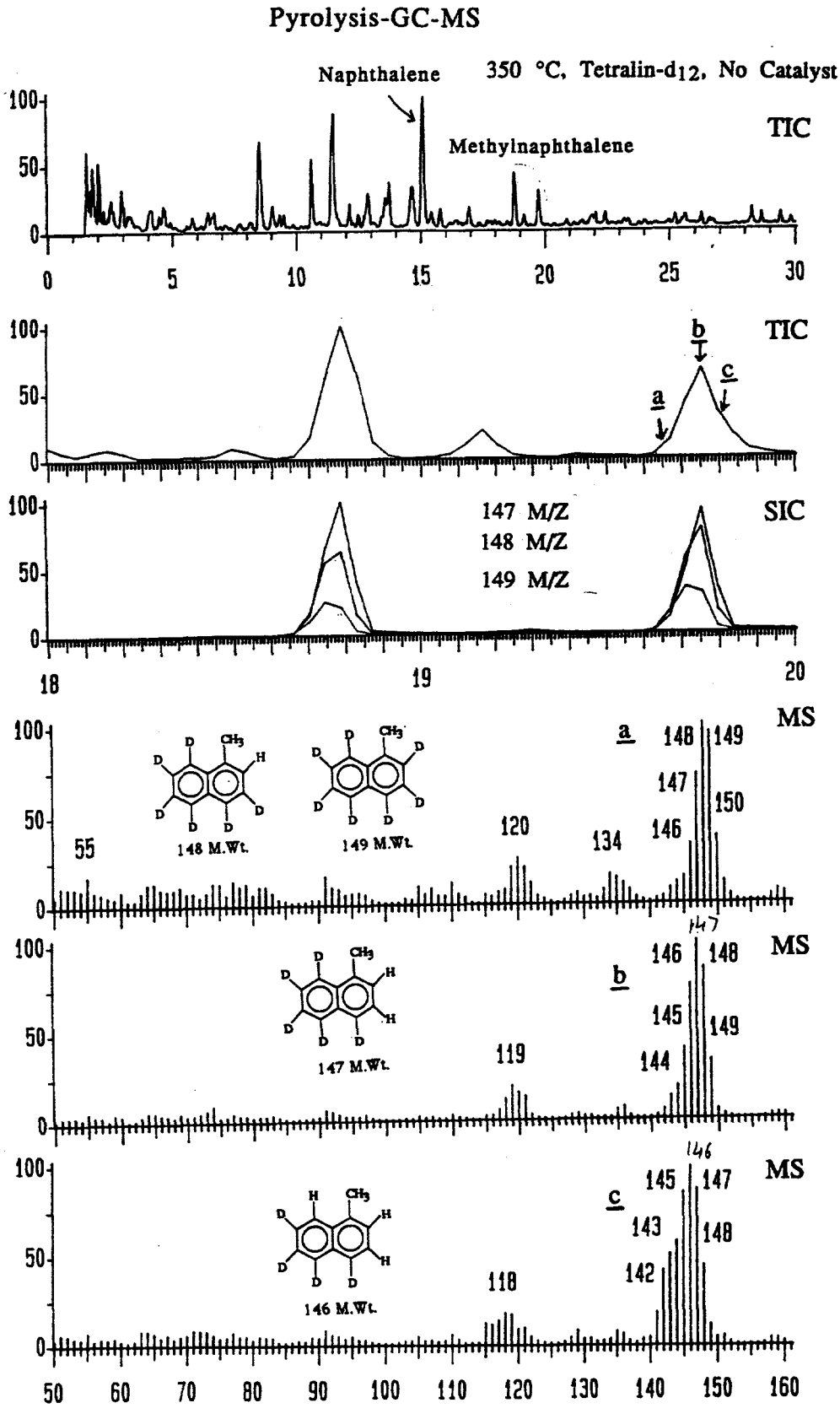

Figure 9.18 TIC and SIC at m/z 147, 148, and 149 from Py-GC-MS of the THF-insoluble residue from the non-catalytic pretreatment of DECS-8 with tetralin-d12 at 350°C.

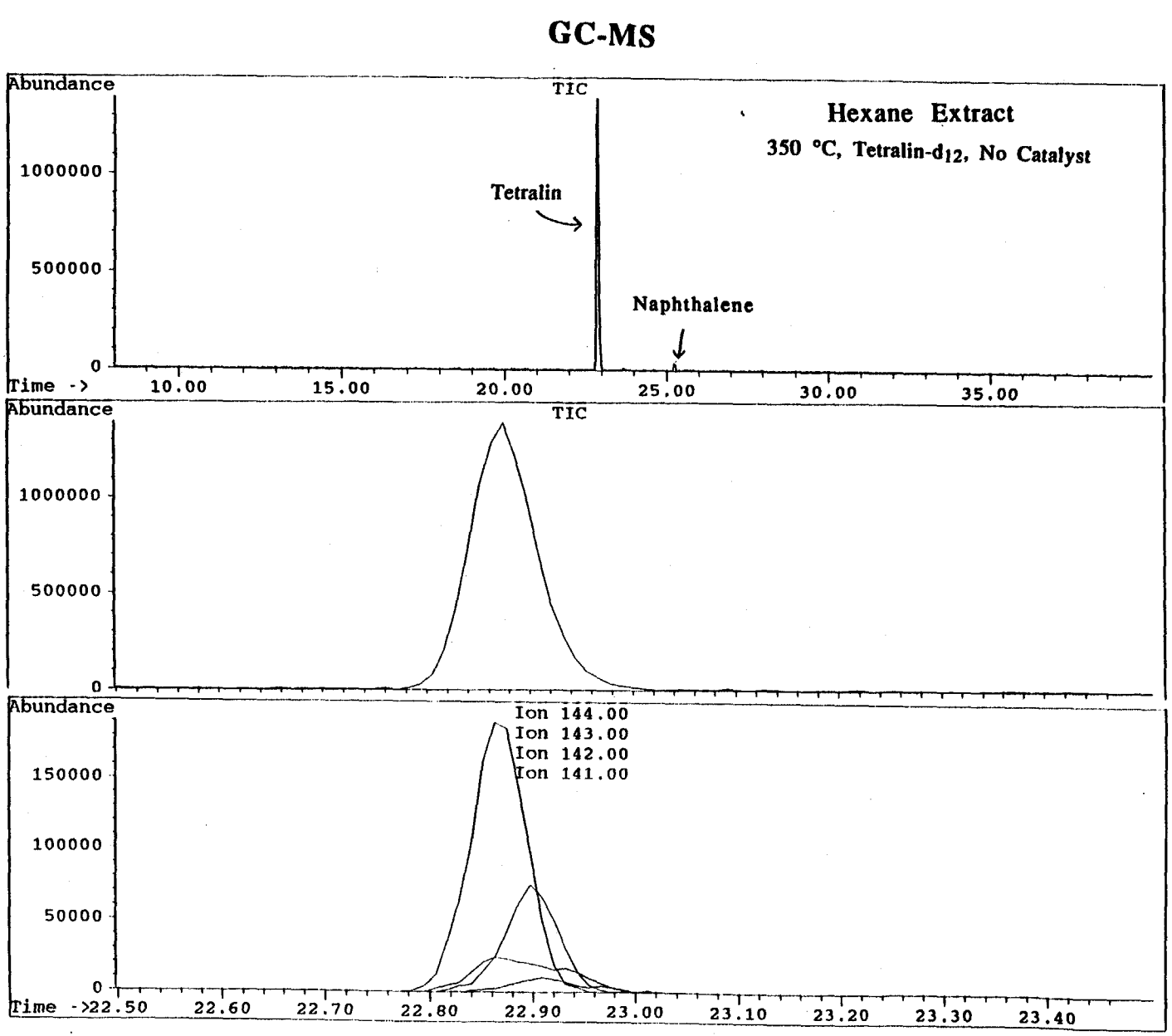

Figure 9.19 TIC and SIC at m/z 141, 142, 143, and 144 from GC-MS of the hexane-soluble products from the non-catalytic pretreatment of DECS-8 with tetralin-d12 at 350°C.

GC-MS

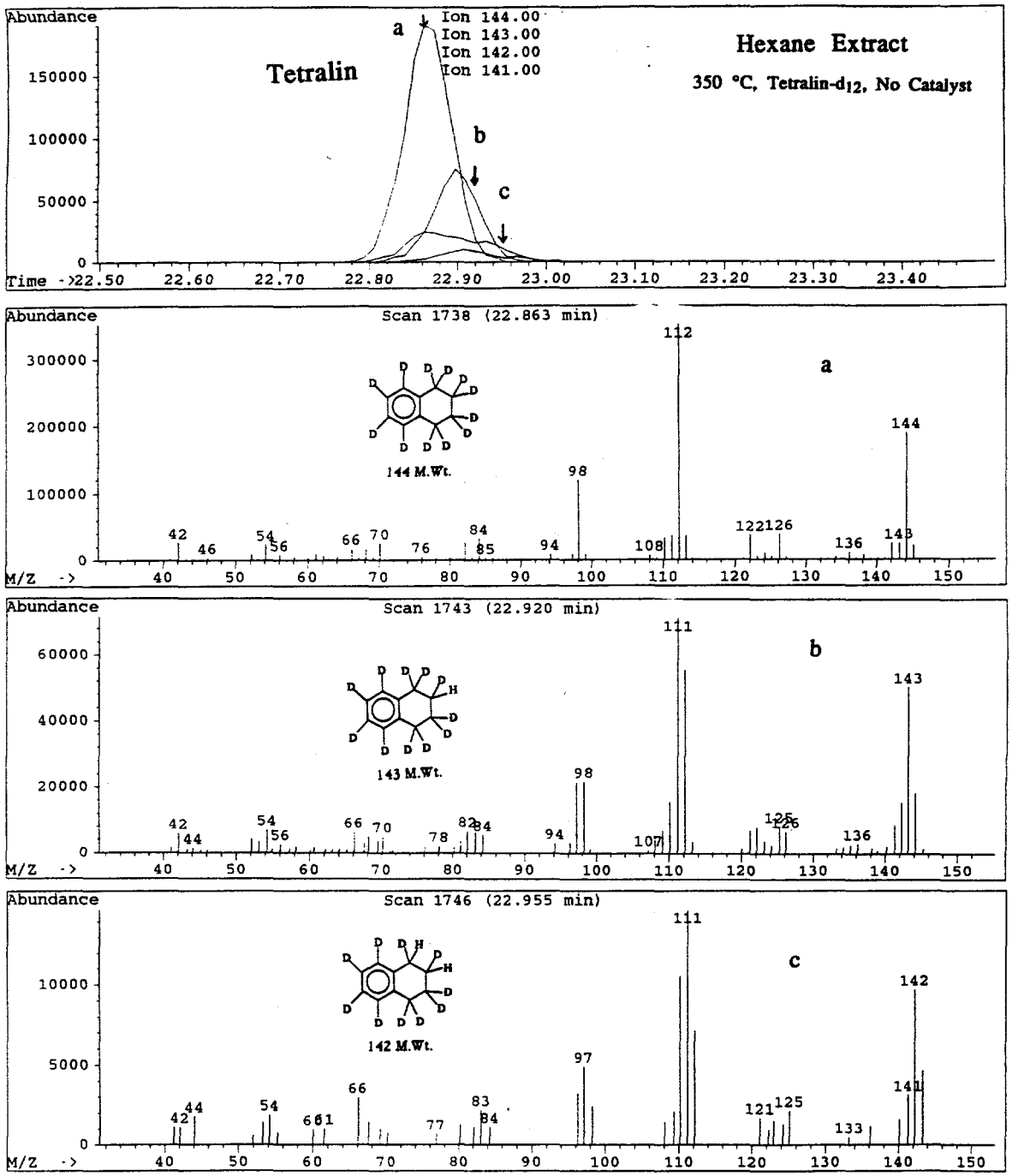

Figure 9.20 SIC at m/z 141, 142, 143, and 144 from GC-MS RT window for tetralin in the hexane-soluble products from the non-catalytic pretreatment of DECS-8 with tetralin-d12 at 350°C.

GC-MS

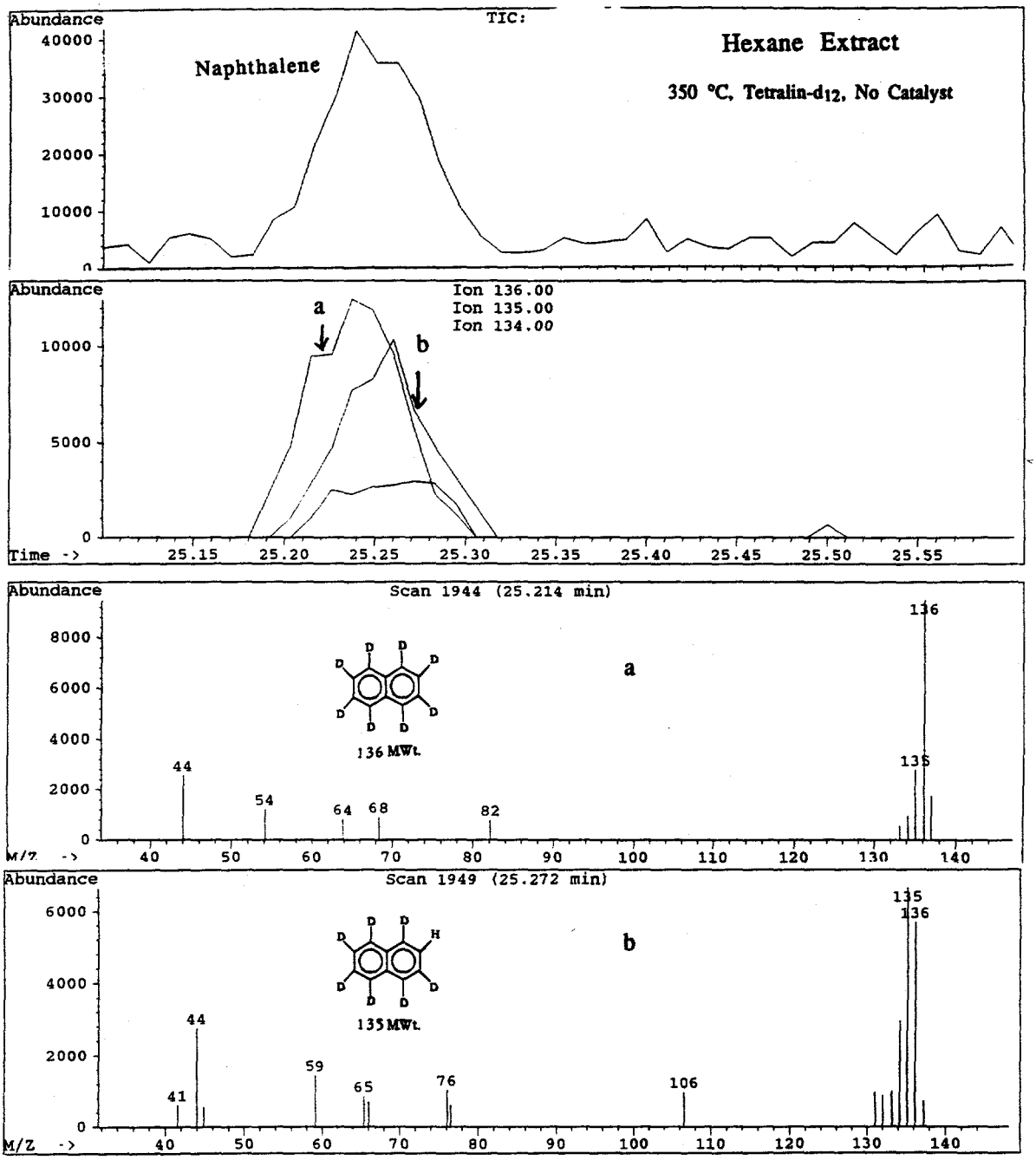

Figure 9.21 SIC at m/z 134, 135, and 136 from GC-MS RT window for naphthalene in the hexane-soluble products from the non-catalytic pretreatment of DECS-8 with tetralin-d12 at 350°C.

Supporting evidence for the chemical bonding also comes from the analysis on the methynaphthalene peak. Figure 9.18 shows the TIC and SIC at m/z 147, 148, and 149 from Py-GC-MS of the THF-insoluble residue from the non-catalytic pretreatment of DECS-8 with tetralin-*d12* at 350°C. Pure methylnaphthalene or methylphenanthrene shows a characteristic M-1 peak in its mass spectrum due to the formation of fused-ring tropylium ion (20,21). Another major peak in the mass spectra of methylnaphthalene is the M-27 peak, which is due to acetylene loss (loss of 26 mass units) from the metastable $[C_{11}H_9]^+$ ion, the so-called M-1 ion (20). Since tetralin-d_{12} was used, the methyl group was due to the reaction with coal or coal-derived fragments. This provides the direct evidence of chemical reaction of solvent molecules, other than the H-donation. The $C_{10}D_7CH_3$ peak with m/z 149 may be formed through bond cleavage of chemically bonded solvent molecules. It is apparent that both 2-methyl and 1-methylnaphthalene were originated from the reaction of solvent molecules with coal species during the pretreatment.

It may be argued that some of the partially deuterated solvent molecules observed in the pyrolysis products were due to H-D exchange reactions. To clarify this issue, we also analyzed the "free" solvent molecules in the hexane soluble products. It is assumed the extent of H replacement might provide a qualitative measure of H-D exchange during the reaction. Figure 9.19 shows the TIC and SIC at m/z 141, 142, 143, and 144 from GC-MS of the hexane-soluble products from the non-catalytic pretreatment of DECS-8 with tetralin-d_{12} at 350°C. It can be seen that most tetralin remain unconverted, as the most dominant peak is tetralin, and the only other very minor peak is due to naphthalene.

Figure 9.20 shows the SIC at m/z 141, 142, 143, and 144 from GC-MS RT window for tetralin in the hexane-soluble products from the non-catalytic pretreatment of DECS-8 with tetralin-d12 at 350°C. From the relative intensity of m/z 144 (tetralin-d_{12}) to those with m/z 143 and m/z 142, it is estimated that about 70% of the recovered tetralin is completely deuterated tetralin. The other 30% is partially "H-exchanged" deuterated tetralin. Figure 9.21 gives the SIC at m/z 134, 135, and 136 from GC-MS RT window for naphthalene in the hexane-soluble products from the non-catalytic pretreatment of DECS-8 with tetralin-d_{12} at 350°C. Both completely deuterated naphthalene and partially "H-replaced" deuterated naphthalene are present. However, the former is considerably more than the latter.

Characterization of Pretreated but Unextracted Wyodak Coal

The above results were obtained from pretreated and THF-extracted coal samples. The structural changes observed in the residues may not directly reflect all the changes due to pretreatment. To see what changes are brought about as a whole by thermal pretreatment, we also performed FT-IR analysis of the unfractionated coal samples after pretreatment at 350°C under either H_2 or N_2 pressure. The general experimental procedures and analytical methods used for these tests are essentially the same to those described in our recent paper (22).

In addition, it was observed in some experiments that gas-phase molecular H_2 reacts with coal faster or in preference to hydrogen from H-donors such as tetralin at low temperatures such as 350°C (23). Since these are supported by some experimental observations, they suggest the existence of non-radical pathways for hydrogen incorporation (23). It was suggested that 1,3- and 1,4-dihydroxy benzene and 2-naphthol are the possible representative structures that could participate in some concerted reactions, in which they are converted to ketones (23). In other words, such structures might be able to add H_2 through a concerted pathway, forming enols which then convert to ketones. The characterization of pretreated but unfractionated coal may also contribute to testing this idea, as we used a reaction temperature of 350°C and DECS-8 Wyodak coal, which is relatively rich in phenolic structures.

Due to the need to obtain the whole, unfractionated product for FT-IR characterization and the need to check the consistency or reproducibility of the coal conversion data with earlier runs, we designed a somewhat special procedures for this part of work. The pretreatment (low-severity liquefaction) reactions were conducted as usual. After the reaction, the gaseous products were collected and analyzed by GC. However, the liquid+solid products, which have solid-like appearance, were divided into two parts. The first part was saved for the subsequent preparation of KBr pellet samples for FT-IR analysis. The other part was subjected to THF extraction, with the intention to obtain both coal conversion data and the THF-soluble and insoluble products for later characterization. (We have also tried to analyze the THF-extracts but it was difficult to make the KBr pellet, because the extract was sticky. For the same reason it was difficult to do solid-state NMR analysis of the extract.)

Runs with Vacuum-dried DECS-8 Wyodak Coal. Table 9.3 shows the low-temperature non-catalytic conversion of DECS-8 Wyodak coal at 350°C for 30 min under an initial pressure of 1000 psi H_2 or N_2 (cold), where all the yield data are wt% based on dmmf coal. We did a FT-IR analysis of the unfractionated liquid+solid products from the run at 350°C under

Table 9.3. Low-Temperature Non-catalytic Conversion of DECS-8 Wyodak Coal at 350°C for 30 min under 1000 psi H_2 or N_2 (Cold) (all the yield data are wt% based on dmmf coal).

Coal	Expt ID #	Solvent /gas	Gas (diff.) wt%	Hex Sol wt%	Toluene Sol wt%	THF Sol wt%	**Conv** dmmf wt%	CO dmmf wt%	CO2 dmmf wt%	CH4 dmmf wt%	C2H6	C3H8	C4H10	**H_2** Consum wt%	**H** from Tetralin wt%
VD2h	7/16	no/H_2	3.3	2.1	2.6	4.5	**12.5**	0.24	4.5	0.10	0.02	0.03	0.04	**0.20**	
VD2h	8/17/22	tetralin /H_2	4.2	4.1	7.6	10.0	**25.9**	0.19	4.1	0.09	0.03	0.02	0.01	**0.29**	**0.41**
VD2h	9/18/23	1-MN /H_2	4.0	1.1	5.8	7.4	**18.3**	0.16	4.34	0.09	0.03	0.03	0.01	**0.45**	
VD2h	172	no/H_2	FT-IR				**16.5**[a]	0.16	4.09	0.10	0.03	0.03	0.01	**0.24**	
VD2h	173	no/N_2	FT-IR				**14.7**[a]	0.14	3.80	0.10	0.03	0.05	0.02	**n/a**	
Raw	51/63 /93	no/H_2	7.7	5.4	2.8	9.1	**25.0**	0.37	8.90	0.12	0.04	0.05	0.01	**0.61**	
Raw	52/64 /94	tetralin /H_2	7.7	15.8	9.3	12.4	**43.3**	0.21	8.95	0.11	0.05	0.04	0.01	**0.63**	**0.31**
Raw	53/65 /95	1-MN /H_2	6.4	15.9	6.6	11.4	**39.9**	0.16	8.88	0.10	0.04	0.04	0.01	**0.58**	

H_2. As shown in Figure 9.22, the FT-IR difference spectrum between the whole product and the vacuum-dried but unreacted coal indicates that the reaction involved the loss of hydroxyl groups (3300-3600 cm^{-1}) and increase of aliphatic C-H groups (2920 and 2850 cm^{-1}). Interestingly, we also observed the decrease in carbonyl groups (1600, 1700 cm^{-1}).

At first glance, this seems to be against what might be expected (increase in carbonyl) according to the possible conversion of some phenolics (such as 2-naphthol-type and 1,3- and 1,4-dihydroxy-type aromatics) into their corresponding ketones. However, the decrease in ketone groups in the whole products (compared to the vacuum-dried but unreacted coal) could also be due to decarbonylation at 350°C. In fact, we did detect the formation of CO at 350°C, as shown in Table 9.3.

To examine whether what we observed were due to hydrogenation or thermal reactions, we also carried out an experiment with pressurized N_2 gas (1000 psi, cold) instead of H_2, under otherwise identical conditions. The results in Table 9.3 indicate that the yields of CO, CO_2, and hydrocarbon gases produced from thermal runs under H_2 and under N_2 pressure are almost identical (within the experimental error range). The gas formation in both runs at 350°C seems to be due to thermally driven reactions. Therefore, the CO formation in the 350°C-run under H_2 does not appear to be attributable to the newly formed ketones due to non-radical H-transfer under H_2 pressure.

As shown in Figure 9.23, the FT-IR difference spectrum between the whole product from 350°C-N_2 run and the vacuum-dried but unreacted coal indicates the same trends: the loss of hydroxyl groups (3300-3600 cm^{-1}), increase in aliphatic C-H groups (2920 and 2850 cm^{-1}), and the decrease in carbonyl groups (1600, 1700 cm^{-1}). The structural changes caused by runs under H2 and under N2 were very similar, as can be seen from comparing the two difference spectra in Figure 9.24. These trends reflect the structural changes caused by thermal reactions at 350°C for 30 min.

In summary, these preliminary data largely rule out the possibility that, under the conditions used, there is significant ketone formation (which is the product of non-radical incorporation of molecular H_2 into coal). The fact that we obtained similar coal conversions under H_2 and under N_2 at 350°C also suggests that hydrogenation did not contribute much to the conversion of vacuum-dried coal into THF-solubles plus gases in the absence of any catalysts. Finally, the structural changes observed in the thermally pretreated (under H_2 and N_2) here were not caused by any added catalyst.

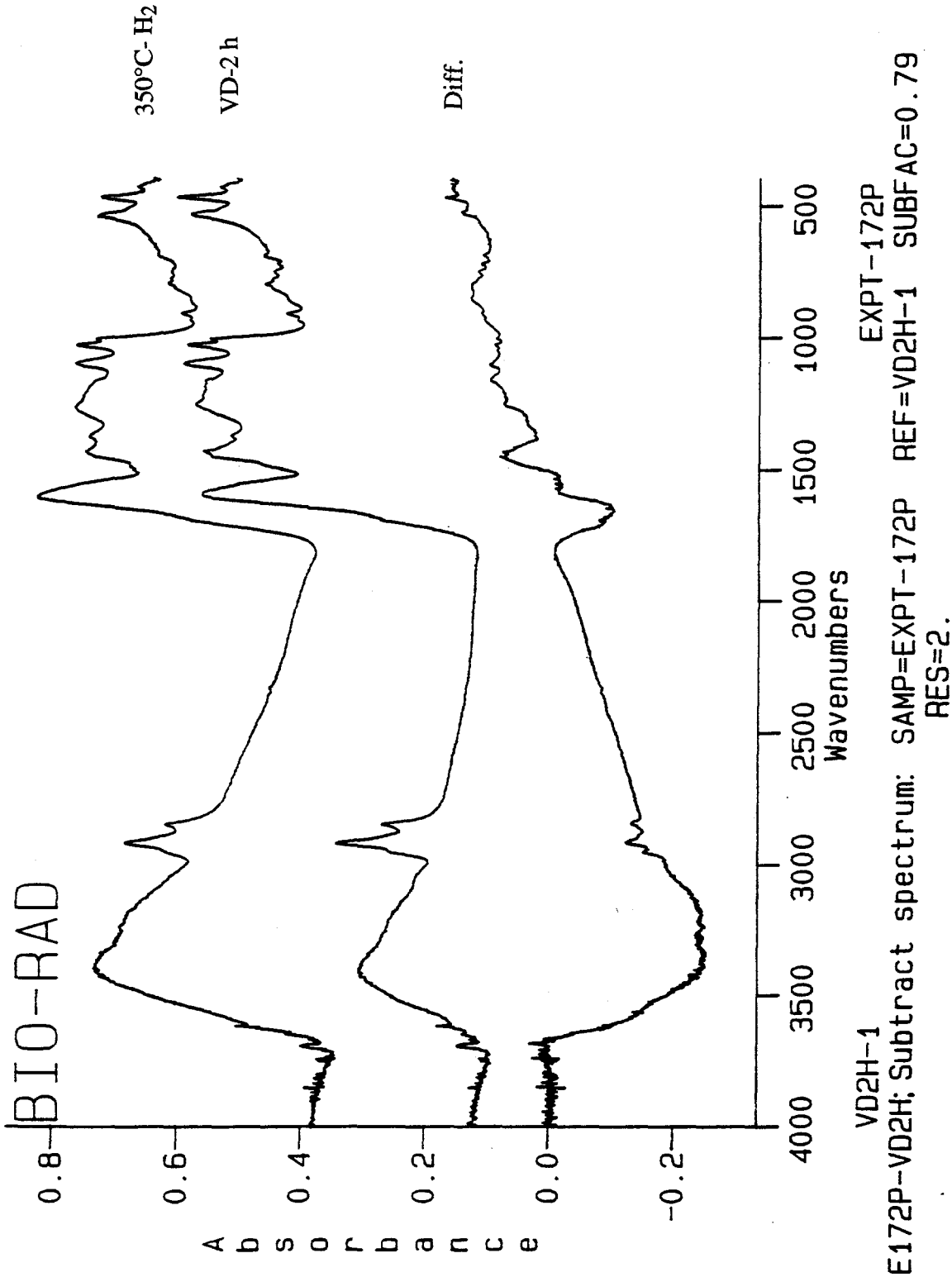

Figure 9.22. FT-IR spectra of the pretreated (350°C-30 min under H_2) but unfractionated coal and the vacuum-dried but unreacted DECS-8 coal and their difference spectrum (pretreated coal - vacuum-dried coal).

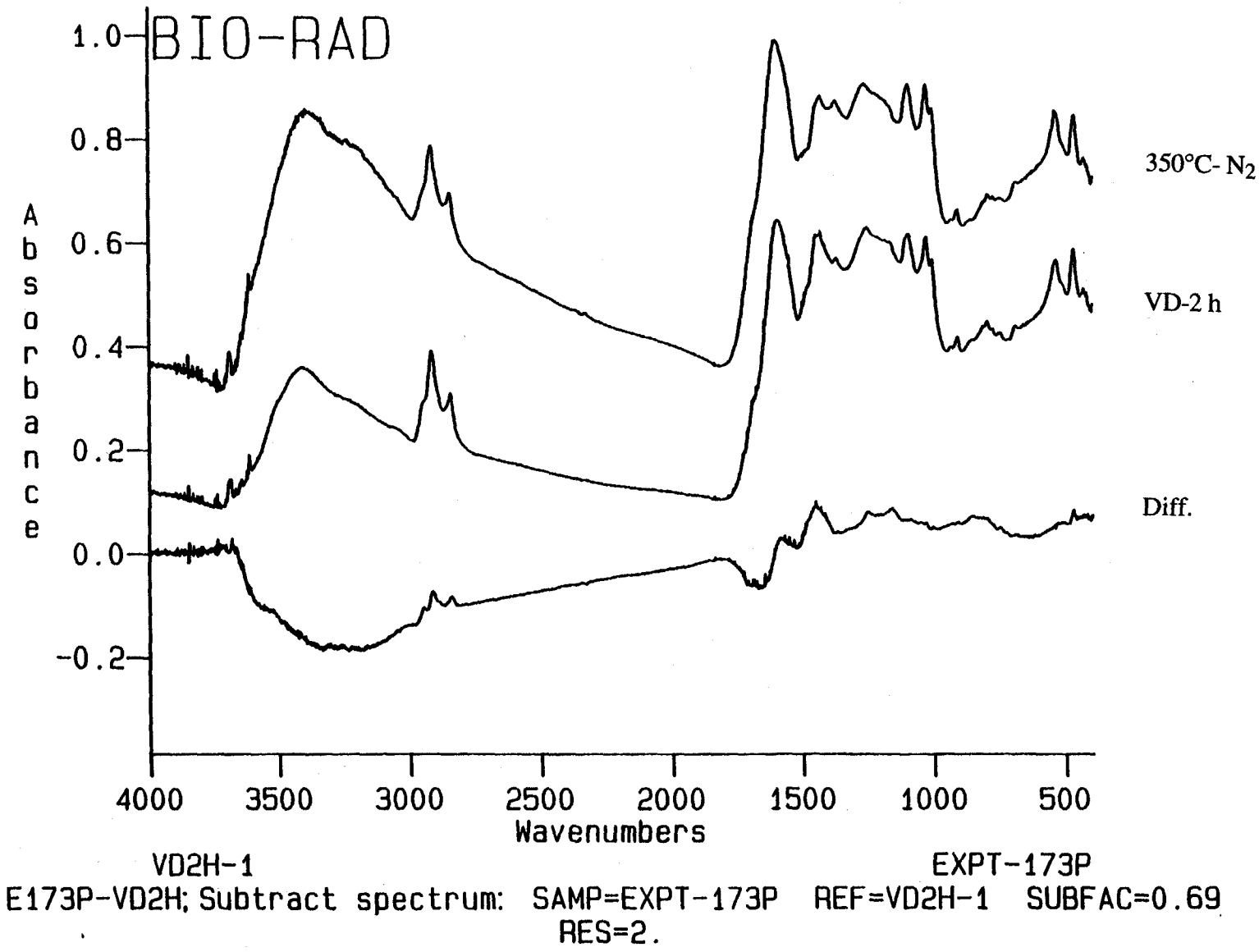

Figure 9.23. FT-IR spectra of the pretreated (350°C-30 min under N_2) but unfractionated coal and the vacuum-dried but unreacted DECS-8 coal and their difference spectrum (pretreated coal - vacuum-dried coal).

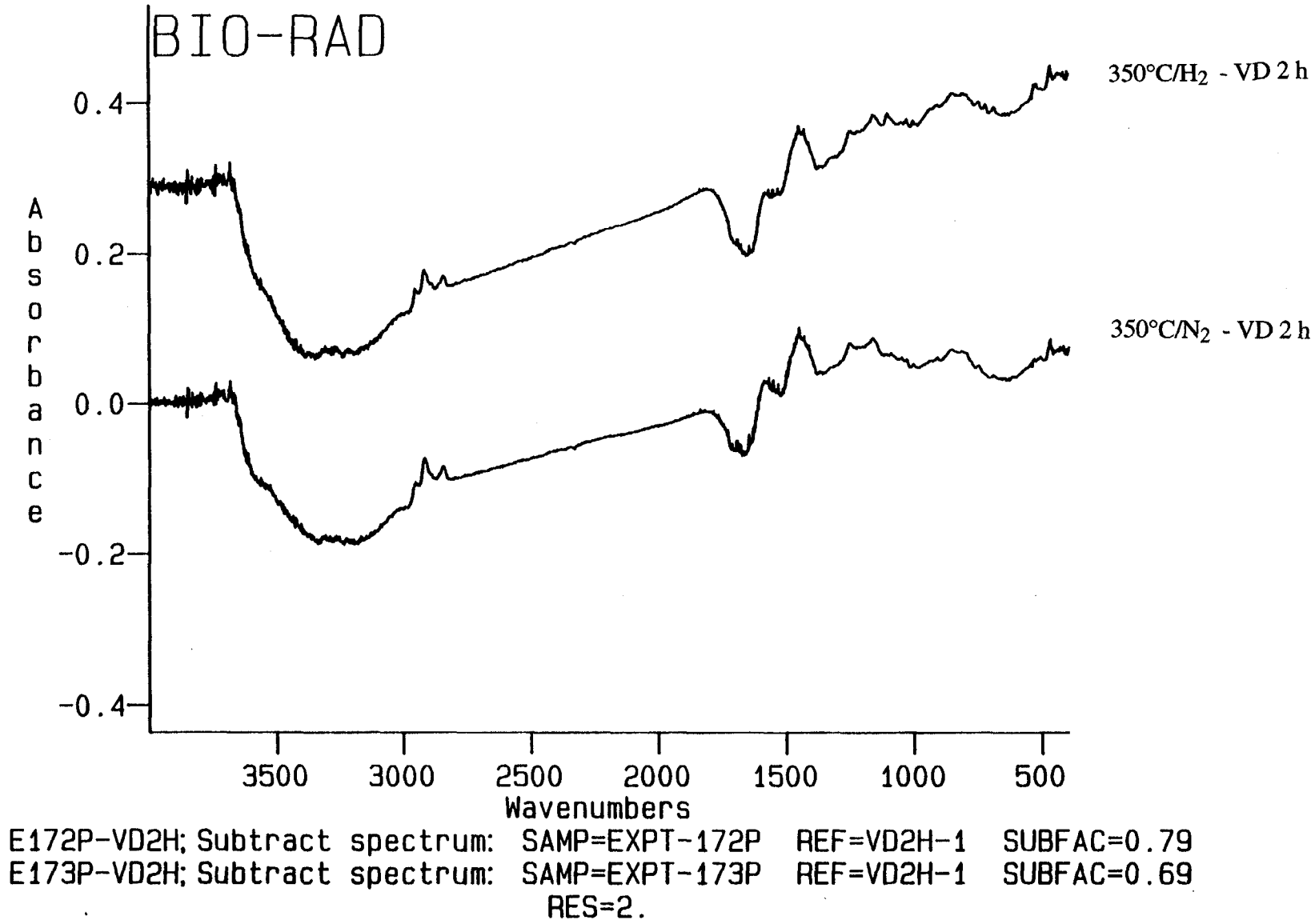

Figure 9.24. FT-IR difference spectrum between the pretreated (350°C-30 min under H_2 or 350°C-30 min under H_2) but unfractionated coal and the vacuum-dried but unreacted DECS-8 coal.

Runs with Fresh Raw Coal - Some Additional Observations. Although the above FT-IR data do not provide evidence of enhanced ketone formation, we can not rule out the possibility that there is some kind of non-radical pathway of H_2 incorporation into coal. We observed that when we used raw coal instead of vacuum-dried coal as starting material, the consumption of gas-phase H2 is almost two times the amount of net hydrogen transfer from tetralin at 350°C under 1000 psi H_2, as shown in Table 9.3. The three duplicated runs gave H_2 consumption values of 0.77, 0.62, and 0.63 wt% (based on dmmf coal) and the values of 0.26, 0.27, and 0.31 for hydrogen from tetralin.

A questions that arises is: Why the hydrogen consumption from gas-phase H_2 is higher than that from tetralin in the run of the raw coal at 350°C ? There are two possibilities. First, there are some reactions in which H_2 is more reactive or suited than tetralin, and such reactions should not be simple conventional hydrogen abstraction by free radicals. Possibility of ionic reactions or mineral matter-catalyzed reactions can not be ruled out. Second, since the raw coal pore surfaces may be more hydrophobic, diffusion of tetralin may be less favored. It is known that heating in tetralin can induce sweeling. However, when heated up, whether tetralin can induce more swelling in vacuum-dried coal than in raw coal is not clear at the present stage.

Another question from examining Table 9.3 is, why the runs of the raw coal (the presence of moisture) resulted in more consumption of gas-phase H_2 (0.61 wt% for solvent-free run; 0.63 wt% for the run with tetralin) than those of the vacuum-dried coal at 350°C (0.20-0.24 wt% for solvent-free run; 0.29 wt% for the run with tetralin) ? It may be that H_2 can diffuse more readily into coal pores with the raw coal sample, than with the vacuum-dried coal. The volumetric shrinkage of DECS-8 raw coal upon drying can be over 20% (24). The surface area of low-rank coals decrease upon drying, and this applies to both N_2 BET surface area (25) and CO_2 surface area (26,27). On the other hand, it should be noted that the N_2 and CO_2 surface area values may not be representative of the internal areas accessible by tetralin or 1-MN solvent molecules, which have much larger molecular sizes than CO_2 and N_2.

Conclusions

The above results have shown that there are significant changes in the coal structure as a consequence of the low-temperature catalytic pretreatments. The combination of the spectroscopic analyses and the conversion data indicated that the catalytic pretreatment at 350°C not only improves coal conversion, but also induce structural changes in the unconverted organic materials, such as decrease in the content of catechol groups (Py-GC-MS and CPMAS NMR), reduction in ether linkages (FT-IR), and increase in the content of aliphatic groups (FT-IR) such as those in the hydroaromatic unit (DDMAS and CPMAS NMR).

Py-GC-MS revealed that the residue from pretreatments using solvent also incorporates solvent molecules. Test using deuterium-labled compound (tetralin-d_{12}) indicated the solvent incorporation is due to both physical trapping of the solvent molecules and chemical bonding of the solvent-derived radical with coal species. Both types are equally important. It is interesting to note that the physically trapped solvent molecules were not removed by extensive solvent extraction with tolune and THF for over 24 h. However, the amounts of solvent incorporated into the residue are estimated to be within a few percent based on the weight of residue, which are small enough to give similar NMR and FT-IR spectra to those of the samples pretreated without any solvents.

REFERENCES

1. Whitehurst, D. D., "Coal Liquefaction Fundamentals", Am. Chem. Soc. Sym. Ser. 1980, 139, 132.
2. Whitehurst, D. D., Mitchell, T. O. and Farcasiu, M., "Coal Liquefaction", Academic Press, New York, 1980.
3. Song, C. and Schobert, H. H., "Temperature-Programmed Liquefaction of Low-Rank Coals in H-donor and Non-donor Solvents", Am. Chem. Soc. Div. Fuel Chem. Prepr., 1992, 37(2), 976.
4. Song, C., Nomura, M., Ono, T., Am. Chem. Soc. Div. Fuel Chem. Prepr., 1991, 36 (2), 586-596.
5. Davis, A., Derbyshire, F. J., Finseth, D. H., Lin, R., Stansberry, P. G. and Terrer, M-T., Fuel, 1986, 65, 500.
6. Davis, A., Derbyshire, F. J., Mitchell, G. D. and Schobert, H. H., "Enhanced Coal Liquefaction by Low- Severity Catalytic Reactions", U. S. Department of Energy, Final Report DOE-PC-90910-F1, July, 1989, 175p.
7. Derbyshire, F. J., Davis, A., Lin, R., Stansberry, P. and Terrer M-T., Fuel Proc. Technol., 1986, 12, 127.
8. Derbyshire, F. J., Davis, A., Epstein, M. and Stansberry, P., Fuel, 1986, 65, 1233.
9. Derbyshire, F. J., Energy and Fuels, 1989, 3, 273.
10. Stansberry, P. G., Lin, R., Terrer, M-T., Lee, C. W., Davis, and Derbyshire, F., Energy and Fuels, 1987, 1, 89.
11. Burgess, C. and Schobert, H. H., ACS Fuel Chem. Prepr., 1990, 35, 31.
12. Burgess, C., Artok, L., Schobert, H. H., ACS Fuel Chem. Prepr., 1991, 36 (2), 462.
13. Song, C., Schobert, H. H., Hatcher, P. G., Energy & Fuel, 1992, 6, 326-328.
14. Song, C.; Hou, L.; Saini, A.K.; Hatcher, P.G.; Schobert, H.H., "CPMAS ^{13}C NMR and Pyrolysis-GC-MS Studies of Structure and Liquefaction Reactions of Montana Subbituminous Coal", Fuel Processing Technology, 1993, 33, No.2, 157-196.
15) Prasad, T.P.; Diemann, E.; Muller, A. J. Inorg. Nucl. Chem., 1973, 35, 1895-1904.
16) a) Naumann, A.W.; Behan, A.S.; Thorsteinson, E.M. Proc. 4th Int. Conf. on Chemistry and Uses of Molybdenum, Golden, Colorado, USA, August 9-13, 1982, pp.313-318.
b) Vasudevan, P.T.; Zhang, F. Appl. Catal. A. General, 1994, 112, 161-173.
17) Garcia, A.B.; Schobert, H.H. Fuel, 1989, 68, 1613.
18) Artok, L.; Davis, A.; Mitchell, G.D.; Schobert, H.H. Energy & Fuels, 1993, 7, 67.
19) Song, C., Lai, W.-C.; Schobert, H. H., Ind. Eng. Chem. Res., 1994, 33, 548-557.

20) My, N. K.; Schwarz, H. Org. Mass Spectr., 1987, 22, 248-250.

21) Standley, L.J.; Hites, R.A. Org. Mass Spectr., 1989, 24, 767-782.

22) Song, C.; Saini, A.K.; Schobert, H.H. Energy & Fuels, 1994, 8, 301-312.

23) Larsen, J.W. Third Peter Given Lecture, Pennsylvania State University, Sept 18, 1992.

24) Suuberg, E. M.; Otake, Y.; Yun, Y.; Deevi, S. C. *Energy and Fuels* 1993, 7, 384.

25 Vorres, K. S.; Wertz, D. L.; Malhotra, V.; Dang, Y.; Joseph, J. T.; Fisher, R. *Fuel*, 1992, 71, 1047.

26 Swann, P. D.; Allardice, D. J.; Evans, D. G. *Fuel* 1974, 53, 85.

27 Cited in Mahajan, O. "Coal Porosity" in "Coal Structure", R. A. Meyers (Ed.), Academic Press: New York, 1982, Chap. 3, p.51.

Appendix 1

-- List of Publications Related to This Project --

Subject: Pretreatments/Liquefaction and Spectroscopic Characterization of Structural Changes

1. Song, C., H.H. Schobert, and P. G. Hatcher. "Solid State ^{13}C NMR and Pyrolysis-GC-MS Studies of Coal Structure and Liquefaction Reactions". **Am. Chem. Soc. Div. Fuel Chem. Prepr.**, Vol. 37, No.2, pp. 638-645, **1992**.

2. Saini, A. K., C. Song, H.H. Schobert, and P. G. Hatcher. "Characterization of Coal Structure and Low-Temperature Liquefaction Reactions by Pyrolysis-GC-MS in Combination with Solid-State NMR and FT-IR". **Am. Chem. Soc. Div. Fuel Chem. Prepr.**, Vol. 37, No.3, pp.1235-1242, **1992**.

3. Song, C., L. Hou, A. K., Saini, P. G. Hatcher, and H.H. Schobert. "CPMAS ^{13}C NMR and Pyrolysis-GC-MS Studies of Structure and Liquefaction Reactions of Montana Subbituminous Coal", **Fuel Processing Technology**, Vol.33, No.2, pp.157-196, **1993**.

4. Song, C., L. Hou, A. K. Saini and P.G. Hatcher. CPMAS and DDMAS ^{13}C NMR Analysis of Coal Liquefaction Residues. **Am. Chem. Soc. Div. Fuel Chem. Prepr.**, Vol. 39, No.3, pp.782-786, **1994**.

5. Saini, A. K., and C. Song. Two-Dimensional HPLC and GC-MS of Oils from Catalytic Coal Liquefaction. **Am. Chem. Soc. Div. Fuel Chem. Prepr.**, Vol. 39, No.3, pp.796-800, **1994**.

Subject: Effects of Drying & Oxidation on Coal Structure and Pretreatments/Liquefaction

1. Saini, A. K., C. Song, and H.H. Schobert. "Influence of Drying and Oxidation of Coal on Its Catalytic and Thermal Liquefaction. 1. Conversion and Product Distribution", **Am. Chem. Soc. Div. Fuel Chem. Prepr.**, Vol. 38, No.2, pp.593-600, **1993**.

2. Saini, A. K., C. Song, and H.H. Schobert. "Influence of Drying and Oxidation of Coal on Its Catalytic and Thermal Liquefaction. 2. Characterization of Dried and Oxidized Coal and Residues". **Am. Chem. Soc. Div. Fuel Chem. Prepr.**, Vol. 38, No.2, pp.601-608, **1993**.

3. Song, C., A. K. Saini, and H.H. Schobert. "Positive and Negative Impacts of Drying and Oxidation on Low-Severity Catalytic Liquefaction of Low-Rank Coal". **Proceedings of 7th International Conference on Coal Science**, Banff, Alberta, Canada, September 12-17, 1993, in press, **1993**.

4. Song, C., A. K. Saini, , H.H. Schobert. Effects of Drying and Oxidation of Wyodak Subbituminous Coal on Its Thermal and Catalytic Liquefaction. Spectroscopic Characterization and Products Distribution. **Energy & Fuels**, Vol. 8, No. 2, pp. 301-312, **1994**.

Subject: Temperature-Programmed Liquefaction (TPL) & Effects of Catalyst and Solvents

1. Song, C., H.H. Schobert, and P.G. Hatcher. "Temperature-Programmed Liquefaction of a Low Rank Coal". **Energy & Fuels**, Vol. 6, No.3, pp. 326-328, **1992**.

2. Song, C. and H. H. Schobert. "Temperature-Programmed Liquefaction of Low-Rank Coals in H-donor and Non-donor Solvents". **Am. Chem. Soc. Div. Fuel Chem. Prepr.**, Vol. 37, No.2, pp. 976-983, **1992**.

3. Huang, L., C. Song, and H. H. Schobert. Temperature-Programmed Catalytic Liquefaction of Low-Rank Coal Using Dispersed Mo Catalyst. **Am. Chem. Soc. Div. Fuel Chem. Prepr.**, Vol. 37, No.1, pp. 223-227, **1992**.

4. Huang, L., C. Song, and H. H. Schobert. Effects of Solvent and Catalyst on Liquefaction Conversion and Structural Changes of a Texas Subbituminous Coal. **Am. Chem. Soc. Div. Fuel Chem. Prepr.**, Vol. 38, No.3, pp.1093-1099, **1993**.

5. Huang, L., C. Song, and H. H. Schobert. Liquefaction of Low-Rank Coals as a Potential Source of Specialty Chemicals. **Am. Chem. Soc. Div. Fuel Chem. Prepr.**, Vol. 39, No.2, pp.591-595, **1994**.

6. Song, C., A. K. Saini, and H. H. Schobert. Retrogressive Reactions in Catalytic Coal Liquefaction Using Dispersed MoS_2. **Coal Science and Technology,** Vol. 24 (Proc. 8th Internat. Conf. on Coal Science), Oviedo, Spain, Sept 10-15, Elsevier, No. 2, pp. 1215-1218, **1995**.

7. Huang, L. and H. H. Schobert. Comparative Roles of Hydrogen Gas and Solvent in Liquefaction of Low-Rank Coals. **Coal Science and Technology,** Vol. 24 (Proc. 8th Internat. Conf. on Coal Science), Oviedo, Spain, Sept 10-15, Elsevier, No. 2, pp. 1243-1246, **1995**.

Subject: Chemical Transformation of Low-Rank Vitrinite under Hydrous Pyrolysis Conditions

1. Wenzel, K., P. G. Hatcher, G. D. Cody, and C. Song. The Structural Alteration of Huminite by Low Severity Liquefaction. **Am. Chem. Soc. Div. Fuel Chem. Prepr.**, Vol. 38, No.2, pp.571-576, **1993**.

2. Hatcher, P.G.; Wenzel, K.A.; Cody, G.D. Coalification Reactions of Vitrinite Derived from Coalified Wood. **Am. Chem. Soc. Sym. Ser.**, No. 570, pp.112-135, **1994**.

3. Hatcher, P.G., C. Song, C., K. A. Wenzel, and H.H. Schobert. Hydrous Pyrolysis of Vitrinite Derived from Coalified Wood: A Clue to Reactions of Low-Severity Pretreatment during Liquefaction. **Proceedings of US DOE Coal Liquefaction and Gas Conversion Contractors' Review Conference**, Pittsburgh, Sept 7-8, pp.239-251, **1994**.

4. Mukhopadhyay, P. K. and P. G. Hatcher. Composition of Coal. American Association of Geologists, Studies in Geology Series, **Hydrocarbons from Coal**, B.E. Law and D.D. Rice, eds., vol.38, pp. 79-118, 1993.

Subject: Promoting Effect of Water (H_2O) on Low-Severity Catalytic Coal Liquefaction

1. Song, C., A. K. Saini, and H.H. Schobert. Enhancing Low-Severity Catalytic Liquefaction of Low-Rank Coal by Adding Water. **Am. Chem. Soc. Div. Fuel Chem. Prepr.**, Vol. 38, No.3, pp.1031-1038, **1993**.

2. Song, C., A. K. Saini, L. Huang, H.H. Schobert and P.G. Hatcher. Catalytic Hydrothermal Pretreatment and Hydrogenative Pretreatment for Enhanced Coal Liquefaction over Dispersed MoS_2. **Proceedings of US DOE Coal Liquefaction and Gas Conversion Contractors' Review Conference**, Pittsburgh, Sept 27-29, Vol. I, pp.561-589, **1993**.

3. Song, C., and A. K. Saini. Using Water and Dispersed MoS_2 Catalyst for Coal Conversion into Fuels and Chemicals. **Am. Chem. Soc. Div. Fuel Chem. Prepr.**, Vol. 39, No.4, pp.1103-1107, **1994**.

4. Song, C. and A. K. Saini. Strong Synergistic Effect between Dispersed Mo Catalyst and H_2O for Low-Severity Coal Hydroliquefaction. **Energy & Fuels**, Vol. 9, No.1, pp.188-189, **1995**.

5. Song, C. Using Water and Dispersed Catalyst for Coal Liquefaction at Low Severity. **Energeia**, University of Kentucky, Vol. 6, No.2, pp.1-4, **1995**.

6. Song, C., A. K. Saini, and J. McConnie. Strong Promoting Effect of H_2O on Coal Liquefaction Using Water-Soluble and Oil-Soluble Mo Catalyst Precursors. **Coal Science and Technology,** Vol. 24 (Proc. 8th Internat. Conf. on Coal Science), Oviedo, Spain, Sept 10-15, Elsevier, No. 2, pp. 1391-1394, **1995**.